AN ARCHITECTONIC STUDY OF THREE MAMMALS: GREY SQUIRRELS (*SCIURUS CAROLINESIS*), TREE SHREWS (*TUPAIA BELANGERI*) AND GALAGOS (*OTOLEMUR GARNETTI*)

By

Peiyan Wong

Dissertation

Submitted to the Faculty of the

Graduate School of Vanderbilt University

in partial fulfillment of the requirements

for the degree of

DOCTOR OF PHILOSOPHY

in

Psychology

Dec, 2009

Nashville, Tennessee

Approved:

Professor Jon H. Kaas

Associate Professor Troy A. Hackett

Associate Professor Anna W. Roe

Professor Sohee Park

For my parents,

whom I cannot thank enough for everything they have given me.

ACKNOWLEDGEMENTS

I would like to thank my advisor, Jon Kaas, for all his advice, on work and otherwise. I am profoundly grateful for his guidance, unwavering support and inspirational passion for excellence. For their helpful counsel, I would also like to thank the members of my Dissertation Committee, Troy Hackett, Sohee Park and Anna Roe.

For the large role they have played in the research process, I thank Laura Trice and Mary Varghese for their histological expertise. My appreciation goes out to past and current members of the lab, for their help and advice. Special thanks goes out to Christina, Mary, Mark and Omar, who have, amongst many other things, taken the time to carefully proofread various portions of this thesis. For honing my histological techniques while providing an enriching cultural experience, I would like to thank Kathleen Rockland and the members of her laboratory, especially Noritaka Ichinohe.

To Zhen, Yiwen, Jiahui, June and the many friends I have made during my stay here, your friendship means a lot to me and I truly appreciate all the support you have given me. To Chris, I thank you for your encouragement and support. Finally, I am forever thankful for the unwavering support and unconditional love from my parents that have allowed me to be who I am today.

TABLE OF CONTENTS

Page

DEDICATION…… ii

ACKNOWLEDGEMENTS…… iii

LIST OF TABLES……..…….. x

LIST OF FIGURES…… xi

Chapter

I. INTRODUCTION……..……..... 1

Variability in the Neocortex…… 2
Comparative Architectonic Studies..……. 10
Research Rationale……. 15
Species Rationale…… 16
Specific Aims…….. 19
References....…….. 20

II. ARCHITECTONIC SUBDIVISIONS OF NEOCORTEX IN THE GREY SQUIRREL (SCIURUS CAROLINENSIS)…… 27

Introduction……. 27
Materials and Methods……..…….. 30
Animal subjects……. 30
Tissue preparation……...…….. 30
Zinc histochemistry..…… 31
Immunohistochemistry…….. 31
Histochemistry……. 33
Light microscopy……..…… 33
Anatomical reconstruction……...……. 34
Results……. 35
Occipital areas……... 36
Primary visual area, Area 17……..……. 36
Area 18……..…….. 44
Area 19……..…….. 45
Temporal cortex…… 46
The temporal posterior region, Tp…….. 46
The temporal mediodorsal region, Tm..…….. 48
The temporal intermediate region, Ti…….. 48

Region Ta and its subdivisions……... 49
Parietal cortex……...…… 50
Anterior parietal cortex, Pa or S1…….……. 51
Area Pm…….. 59
Pl(S2) and Pv ……. 62
The dysgranular strip (3a/dy)…....……. 63
Frontal cortex……...……. 65
Area M……..……. 67
The remaining frontal areas..…….. 68
Cingulate and Retrosplenial cortex…...…… 69
Cingulate cortex……..…… 70
Dorsal cingulate area (DCg)……...… 72
Ventral cingulate area (VCg)……...……...… 72
Rostral cingulate area (RCg)……...… 73
Retrosplenial cortex…….……... 73
Retrosplenial granular area (RSG)…….……. 74
Retrosplenial agranular area (RSA)…….……. 74
Area Prostriata (PS)…….……. 76
Perirhinal areas…….……. 77
Discussion…….…….... 80
Visual areas of occipital cortex…...……... 82
Area 17……..……. 82
Area 18……..…….. 85
Area 19……..…….. 90
Areas of the temporal cortex…….…… 91
Area Ta……..…….. 92
Area Tp…….....…….. 93
Area Ti……..…….. 94
Area Tm……...……...…….. 95
Areas of the parietal cortex……...…… 95
Area Pa(S1)..…….. 95
Area Pm…….. 99
Areas Pl(S2) and Pv ……..……. 100
Frontal cortex…… 102
Cingulate and Retrosplenial cortex…...…… 103
Cingulate cortex……..…… 103
Retrosplenial cortex…….……... 104
Perirhinal cortex…….…….…….……. 105
Insular cortex……...…… 105
Perirhinal cortex…..……... 108
Entorhinal cortex…..……...……... 106
Summary..……..……..... 106
References…….……..... 111

III. ARCHITECTONIC SUBDIVISIONS OF NEOCORTEX IN THE TREE SHREW (*TUPAIA BELANGERI)*...…….. 126

Introduction……. 126
Materials and Methods……..……...…….. 130
Animal subjects……. 131
Tissue preparation…….....…….……... 131
Histochemistry…….……. 132
Zinc histochemistry..…….…… 132
Immunohistochemistry…….. 132
Light microscopy……..…… 133
Anatomical reconstruction……...……. 133
Results……. 134
Occipital areas……... 134
Primary visual area, Area 17……..……. 135
Area 18……..……... 140
Temporal visual cortex…...……..... 141
Temporal anterior area, TA……..…….…….. 141
Temporal dorsal area, TD..……..…….. 142
Temporal posterior area, TP...……..…….. 146
Temporal inferior area, TI.....……..…….. 149
Inferior temporal cortex..…...……..... 150
Inferior temporal rostral area, ITr..……...…….. 150
Inferior temporal intermediate area, ITi.…….…….. 153
Inferior temporal caudal area, ITc.…..…….. 153
Auditory cortex.....……. 154
Primary auditory core (Ac)...……. 154
Auditory belt (Ab).....……. 157
Parietal cortex.....……. 159
Primary somatosensory area, 3b(S1)...…….. 159
Area 3a.....……. 161
Somatosensory caudal area, SC.....……..... 163
Second somatosensory, S2, and parietal ventral, Pv areas..... 164
Posterior parietal area, PP....…….……. 166
Frontal cortex.....…. 168
Primary motor cortex, M1…….……. 168
Secondary motor cortex, M2…….……. 169
Dorsal frontal cortex, DFC...…….……. 171
Orbital frontal cortex, OFC...…….……...……. 171
Medial cortex.....…. 173
Medial frontal cortex, MFC...…….……...……. 173
Cingulate ventral area, CGv...…….……...……. 174
Cingulate dorsal area, CGd....…….……...……. 174
Medial motor area, MMA.....…….……...……. 175
Infraradiata dorsal area, IRd...…….……...……. 176
Infraradiata ventral area, IRv...…….……...……..……. 176
Prostriata (PS)….…….……. 178
Retrosplenial agranular area (RSag)…...……. 179
Retrosplenial granular area (RSg)…….……. 179

Remaining cortical areas..... 180
Insular cortex..... 180
Perirhinal cortex..... 180
Discussion..... 181
Occipital cortex..... 182
Temporal visual cortex..... 186
Inferior temporal cortex..... 188
Auditory cortex..... 189
Parietal cortex..... 190
Frontal cortex..... 194
Medial cortex..... 197
Remaining cortical areas..... 200
References..... 204

IV. ARCHITECTONIC SUBDIVISIONS OF NEOCORTEX IN THE GALAGO (*OTOLEMUR GARNETTI)*..... 216

Introduction..... 216
Materials and Methods..... 219
Animal subjects..... 219
Tissue preparation..... 219
Histochemistry..... 219
Zinc histochemistry.....
Immunohistochemistry..... 220
Light microscopy..... 221
Anatomical reconstruction..... 221
Results..... 222
An overview of cortical organization based on brain sections cut parallel to the surface of flattened cortex 223
Occipital cortex..... 224
Area 17..... 224
Area 18..... 229
Area 19 dorsal (V3d) and area 19 ventral (V3v)..... 231
Dorsomedial (DM) and dorsolateral (DL) visual areas..... 233
Temporal cortex..... 236
Temporal extrastriate areas – Middle temporal visual area (MT) and the crescent of the middle temporal visual area (MTc)..... 239
The middle superior temporal area (MST) and the fundal area of the superior temporal sulcus (FST)..... 243
Inferior temporal rostral (ITr) and inferior temporal caudal (ITc) areas..... 246
Auditory associated areas – Primary auditory (A) and auditory belt (Ab) areas..... 248
Remaining temporal areas – Area temporopolaris (TG) and superior temporal dorsal area (STd)..... 253
Parietal cortex..... 255

Primary somatosensory area, 3b(S1)..... 255
Area 3a..... 262
Area 1/2..... 262
Second somatosensory (S2) and parietal ventral (Pv) areas..... 264
Posterior parietal region..... 265
Claustral cortex..... 269
Frontal cortex..... 272
Primary motor cortex (M1)..... 272
Area 6..... 274
Granular frontal posterior area (GrP)..... 275
Granular frontal anterior area (GrA)..... 275
Granular frontal medial area (GrM)..... 276
Orbital frontal dorsal area (OFd)..... 279
Orbital frontal ventral area (OFv)..... 279
Orbital frontal medial area (OFm)..... 280
Medial frontal area (MF)..... 281
Medial cortex..... 281
Paralimbic area (Para)..... 282
Area 24..... 283
Area 23..... 283
Retrosplenial agranular area (RSag)..... 284
Retrosplenial granular area (RSg)..... 285
Prostriata (PS)..... 285
Remaining cortical areas – Perirhinal area (PRh)..... 286
Discussion..... 286
Occipital cortex..... 287
Area 17..... 288
Area 18..... 291
Area 19..... 292
DM and DL..... 294
Temporal cortex..... 295
MT..... 295
MTc..... 297
FST and MST..... 298
Inferior temporal and remaining temporal areas..... 298
Auditory areas..... 300
Parietal cortex..... 301
Area 3b(S1)..... 301
Area 3a..... 301
Area 1/2..... 303
S2 and Pv..... 303
Posterior parietal cortex..... 305
Claustral cortex..... 307
Frontal cortex..... 302
Primary motor cortex..... 308
Area 6..... 309

Remaining frontal areas..... 310
Medial cortex..... 312
Medial area 7..... 312
Cingulate areas..... 312
Retrosplenial areas..... 315
Prostriata area..... 316
Perirhinal area..... 317
References..... 321

VI. CONCLUDING REMARKS..... 340

Similarities and Differences in General Cortical Organization..... 340
Similarities and Differences in Architectonic Appearances of Shared Cortical Areas..... 344
Summary and Future Directions..... 348

LIST OF TABLES

Page

Chapter II

Table 1. Abbreviations……... 109

Chapter III

Table 1. Abbreviations……... 203

Chapter IV

Table 1. Abbreviations……... 319

LIST OF FIGURES

Figure		Page
CHAPTER I		
1.	Part of the occipital cortex from an adult human…….....	4
2.	The relationship between Brodmann's and Hassler's schemes of lamination	5
3.	Coronal sections of the grey squirrel processed for Nissl substance (left) and myelin (right)……..…….	7
4.	An evolutionary tree showing the phylogenetic relationship of major orders of mammals and the cortical organization of common cortical areas that have been identified ……...……	12
5.	A phylogenetic tree deduced from recent molecular data…….	16
CHAPTER II		
6.	Architectonic characteristics of visual areas 17 and 18…….	37
7.	Architectonic characteristics of visual and adjoining retrosplenial cortex…	38
8.	Adjacent coronal brain sections through occipital cortex stained for Nissl substance (A) or myelin (B)…….....	39
9.	Architectonic characteristics of the bordering region between area 17 and 18……..…….	41
10.	The laminar architecture of area 17 at higher magnification…….	43
11.	Architectonic characteristics of subdivisions of occipital and temporal cortex in squirrel 06-18……..	47
12.	Architectonic characteristics of subdivisions of temporal cortex in squirrel 06-34……...……	52
13.	Barrel field of the grey squirrel……..	55
14.	The laminar architecture of area Pa(S1) at higher magnification……..	58
15.	Architectonic characteristics of subdivisions of the somatosensory cortex in	

squirrel 05-19……..…… 59

16. Architectonic characteristics of subdivisions of the motor and somatosensory cortex in squirrel 05-19……..…… 60

17. Architectonic characteristics of subdivisions of parietal and primary auditory cortices in squirrel 06-34……..…… 61

18. Architectonic characteristics of subdivisions of the parietal and limbic cortices in squirrel 06-18……..……... 64

19. Architectonic characteristics of subdivisions of frontal and cingulate cortices in squirrel 06-34……...……. 66

20. Architectonic characteristics of subdivisions of frontal and cingulate cortices in squirrel 06-34…….…… 68

21. Architectonic characteristics of subdivisions of the frontal cortex in squirrel 06-18……... 70

22. Architectonic characteristics of subdivisions of frontal and cingulate cortices in squirrel 06-34…….…… 71

23. Architectonic characteristics of subdivisions of retrosplenial cortex in squirrel 06-60…….……. 75

24. Architectonic characteristics of subdivisions of temporal and insular cortices in squirrel 06-34…….……..... 79

25. Architectonic characteristics of subdivisions of rhinal cortex in squirrel 06-34…….…….. 80

CHAPTER III

26. Architectonic characteristics of visual areas 17, 18 and TD……... 135

27. Architectonic characteristics of visual areas and adjoining retrosplenial cortex …….. 136

28. The laminar characteristics of area 17 at higher magnification.……. 138

29. Patchy staining pattern of area 17……...…… 139

30. Architectonic characteristics of visual and temporal visual areas…….. 142

31. Architectonic characteristics of temporal and inferior temporal cortex in

flattened preparations…….. 143

32. Architectonic characteristics of occipital and temporal visual areas……. 145

33. Architectonic characteristics of the temporal dorsal area……... 146

34. Architectonic characteristics of the temporal posterior and inferior temporal areas……. 147

35. Architectonic characteristics of the inferior temporal areas…..…… 151

36. Architectonic characteristics of the termporal intermediate area and adjoining areas…… 152

37. Architectonic characteristics of the auditory areas……. 155

38. Architectonic characteristics of the auditory areas in PV and SMI-32 preparations……..…… 158

39. Architectonic characteristics of the primary somatosensory cortex……..…. 160

40. Architectonic characteristics of the secondary somatosensory cortex and insular cortex…….. 162

41. Architectonic characteristics of primary somatosensory and motor areas….. 163

42. Architectonic characteristics of somatosensory and motor areas..……. 165

43. Architectonic characteristics of the medial frontal and cingulate areas…….. 170

44. Architectonic characteristics of the medial frontal and cingulate ventral area…….. 173

45. Architectonic characteristics of the infraradiata areas...……. 177

46. Architectonic characteristics of the retrosplenial areas……... 178

CHAPTER IV

47. Architectonic characteristics galago cortex in flattened preparations stained for myelin (A) and for synaptic zinc (B) …… 223

48. Architectonic characteristics of visual areas 17, 18, 19d and DM..…… 225

49. Patchy staining pattern of area 17…….…. 228

50. The laminar characteristics of area 17 at higher magnification…….……. 229

51. Architectonic characteristics of visual and temporal visual areas…..…… 232

52. Architectonic characteristics of visual areas and adjoining retrosplenial cortex……...…….... 234

53. Architectonic characteristics of middle temporal cortex…… 235

54. Architectonic characteristics of middle temporal cortex…… 237

55. Architectonic characteristics of middle temporal cortex in flattened preparations stained for CO (A), VGluT2 (B) and PV (C)..……..... 241

56. The laminar characteristics of MT at higher magnification…… 243

57. Architectonic characteristics of inferior temporal cortex…… 244

58. Architectonic characteristics of inferior temporal cortex..…….. 247

59. Architectonic characteristics of auditory cortex in flattened preparations..… 249

60. Architectonic characteristics of auditory cortex …… 251

61. The laminar characteristics of primary auditory area at higher magnification…….. 253

62. Architectonic characteristics of somatosensory cortex...…… 257

63. The laminar characteristics of primary somatosensory area at higher magnification……..…… 258

64. Architectonic characteristics of somatosensory cortex in flattened preparations…….…… 259

65. Architectonic characteristics of somatosensory cortex...…… 260

66. Architectonic characteristics of somatosensory cortex...…… 263

67. Architectonic characteristics of posterior parietal cortex…...…… 266

68. Architectonic characteristics of frontal cortex…… 271

69. Architectonic characteristics of frontal cortex…… 273

70. Architectonic characteristics of frontal cortex…… 277

CHAPTER IV

71. An evolutionary tree showing the phylogenetic relationship of grey squirrels, tree shrews and galagos……... 342

CHAPTER I

INTRODUCTION

Architectonic studies are aimed at parcellating the neocortex through understanding and characterizing the morphology of various cortical areas. Since the discovery of the first anatomical feature that adheres to a discrete location in the neocortex, the white stripe that is now known as the Stria of Gennari (Finger, 1994), there have been many published maps of the human cortex (Zilles et al., 2002). One of the more influential cortical maps is the map by Brodmann (1909), which is still frequently referenced. Brodmann subdivided the human neocortex into areas based on variations in the cytoarchitecture of the cortical sheet. Each defined cortical area had a characteristic histological appearance and was thought to have a specific function (Matelli and Luppino, 2004). Brodmann (1909) viewed these cortical areas as the 'organs' of the neocortex (Creutzfeldt, 1995), working in harmony to ensure the proper functioning of the neocortex. Now, it is widely accepted that the neocortex can be subdivided into distinct functional and anatomical areas (Yamamori, 2006). However, other than the calcarine cortex, which is easily identified in an unstained tissue section due to the presence of the white bands of myelin that form the Stria of Gennari and inner band of Baillarger, most other cortical areas require staining processes before they can be visualized. As a result, progress in our understanding of cortical organization is determined by progress in staining methods, and other technological methods (Cavada, 2004). Currently, our understanding of cortical organization is still rather crude, fraught

with ambiguous borders drawn by different investigators (Kaas, 2005). It is essential to come up with improved processing methods that when added to our current repertoire of histological methods, will establish reliable cortical maps that can better guide functional studies.

A general anatomical and functional design, a *Bauplan*, of the cerebral cortex is common to all neocortical areas (Creutzfeldt, 1995). This principle was derived from classical research done by Brodmann and von Economo on an extensive range of mammalian species, showing that the entire neocortex has an almost identical structure during embryonic life (Brodmann, 1909; Creutzfeldt, 1995). However, embryonic neuroprogenitor cells are not equipotential and they possess some intrinsic information about their species-specific cortical organization (Rakic, 1988). As such, the basic pattern of cytoarchitectonic areas arises from a combination of intrinsic signals from the cortical neuroprogenitor neurons and extrinsic signals from inputs by subcortical structures (Rakic, 1988). Modifications to this *Bauplan* during the course of mammalian evolution have led to the diversity in the structure of the neocortex in mammalian species, which led to the variations in behavior and cognitive abilities observed in various species. Identifying and characterizing the various cortical areas in representative mammalian species from different orders would help shed light on the evolutionary processes that have taken place to give rise to the complex neocortex of humans.

Variability in the Neocortex

The diversity of neocortical areas arises from local transformations in the neocortical sheet. These changes occur within defined boundaries, allowing the

delimitation of anatomically distinct cortical areas. These local transformations may involve changes to the laminar structure of the neocortex through two principle processes.

The first process is the retraction or disappearance of layers, such as the disappearance of layer 4 that gives rise to the agranular cortex, such as the motor cortex. The motor cortex lacks the koniocellular appearance of a primary sensory cortex that developed because their primary input is from thalamic projections to layer 4. In contrast, thalamocortical projections to motor cortex are comparatively weaker and inputs are mainly from other sensory areas.

The second process is the sublamination of cortical layers. In humans, or species that are highly dependent on the visual system, the visual cortex is distinctively laminated and layer 4 is split into sublayers (Brodmann, 1909). Neurons performing the same function are grouped into a sublayer and specialized neurons may develop in a sublayer to carry out particular functions (Kaas 2002). This organization adds functional flexibility to the pertinent cortex. Conversely, for animals with poor vision, such as the rat, the layers in visual cortex are poorly differentiated and the neurons are not morphologically specialized as they need only retain general functions (Kaas, 2002). Due to the metabolic costs of increased cortical layers, there is a trade-off between the number of cortical layers or sub-layers and the extent of cortical specialization required to support the species specific behavior. The opposing processes generally operate in parallel. Some of the basic cortical layers may further differentiate into sublayers, while other basic cortical layers may regress and fuse with each other. The human visual cortex provides a good example of this phenomenon (Fig. 1) (Brodmann, 1909). Brodmann wrongly concluded

that the basic granular layer 4 splits into three sublayers; two dark cell-dense layers, layer 4A and 4C, and a light cell-poor stripe, layer 4B, also known as the stria of Gennari (1909). In addition, the basic layer 6 differentiates into two sublayers, 6A and 6B (Brodmann, 1909). A regression of lamination is observed in the supragranular layers, where layer 2 is almost fused with layer 3 (Brodmann, 1909). It should be noted that there is a different nomenclature for sublayers of V1 by Hassler (1966) (Fig. 2).

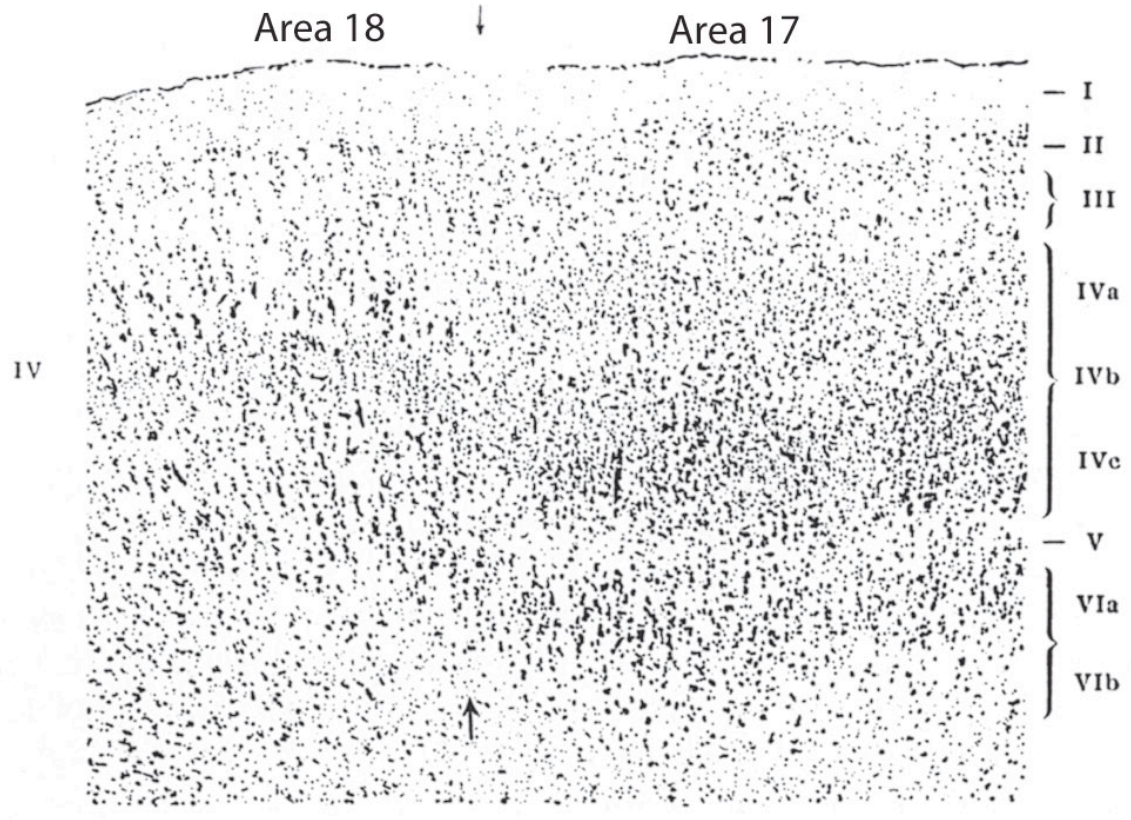

Figure 1. Part of the occipital cortex from an adult human. The border between area 17 and area 18 is shown by the decrease in thickness of layer 4 in area 18. The 6-layered scheme by Brodmann is shown on the left. Scale: 25:1, 10µm. Reproduced from Fig. 12, Brodmann, 1909.

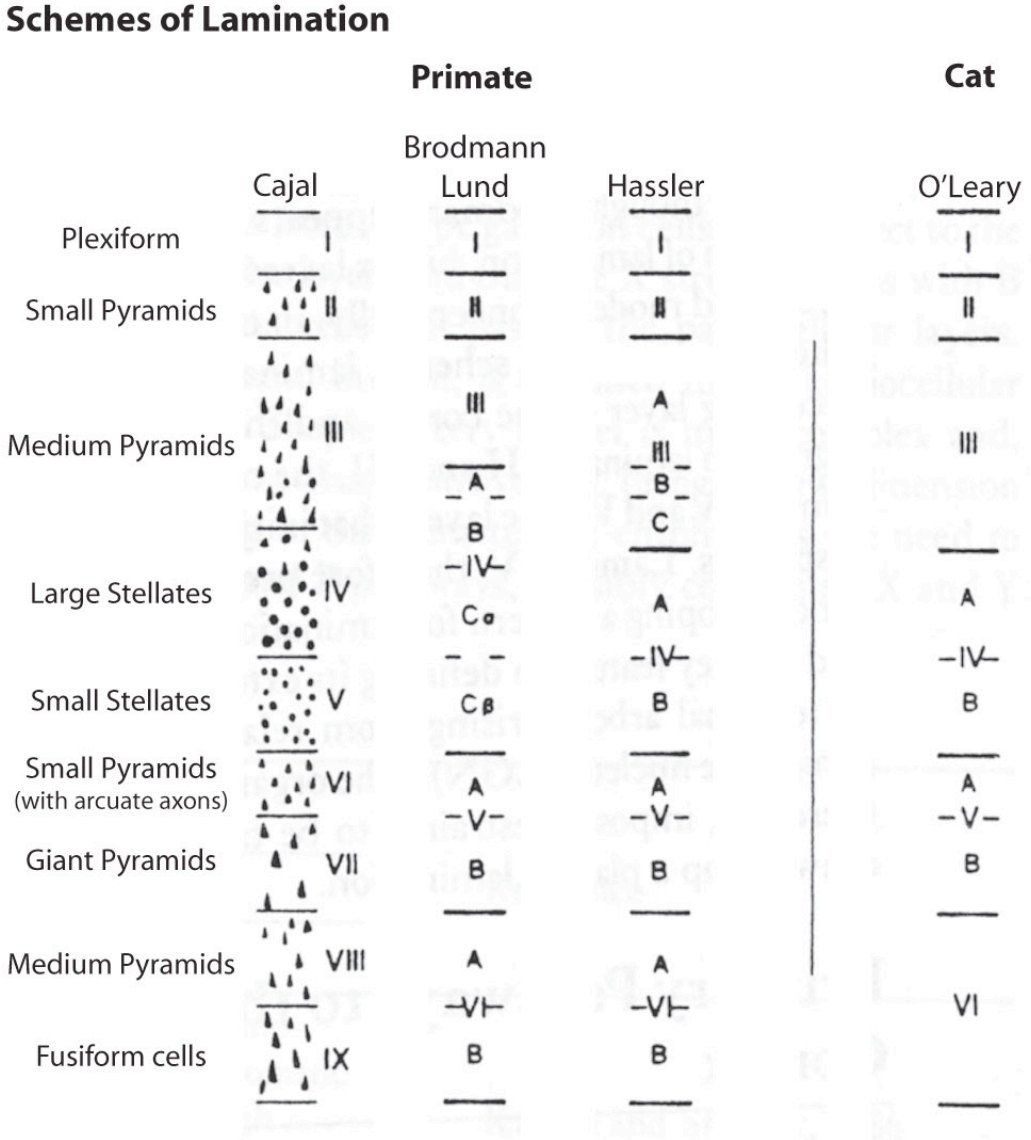

Figure 2. The relationship between Brodmann's and Hassler's schemes of lamination. Brodmann's scheme shows more similarity with Cajal's 9-layered cortex, while Hassler's scheme allows for comparison across species without having forming composite sub-layers in mammals such as cats. Reproduced from Fig. 9.1, Henry, 1991.

Hassler's scheme regarded Brodmann's layer 4A and 4B to be part of layer 3 and as a result changed layer 4Ca and 4Cb to layer 4A and 4B (Henry, 1991). There are three main pieces of evidence that support Hassler's nomenclature. First, comparing the

lamination patterns of V1 across primates, Hassler (1967, as cited in Casagrande and Kaas, 1994) showed that in most New World monkeys, layer 4A and 4B of Brodmann correspond to the less developed sublayers of layer 3, and in prosimians, such as galagos, Brodmann's layer 4A and 4B are nearly indistinguishable as sublayers of layer 3. Second, Hassler's scheme provides a simpler explanation for the connections of the layers, where layer 3C neurons in primates and layer 3 neurons in non-primates both project to extrastriate cortex. However, according to Brodmann's scheme, the source of projections to extrastriate cortex in primates would differ from prosimians. In primates, layer 4 cells are the source of projections to the extrastriate cortex, and in prosimians, layer 3 cells are the source of projections (Casagrande and Kaas, 1994). Thirdly, if one were to follow Brodmann's scheme, then layer 4B of monkeys would consist of large pyramidal cells (e.g. Lund et al., 1979), but large pyramidal cells are not a typical feature of layer 4 defined in other architectonic studies (Casagrande and Kaas, 1994). In addition, this pyramidal cell layer 4B of V1 is observed to merge with pyramidal cell layer 3C of area 18 (Colonnier and Sas, 1978, as cited in Casagrande and Kaas, 1994). With Hassler's scheme, the granular cells of sublayer 4A and 4B are similar across a range of species (Henry, 1991).

Variability within the cortex can develop even when the number of cortical layers remains the same. Changes can take the form of differences in the total thickness of the cortex or differences in the relative thickness of different cortical layers. Variation in total thickness of the cortex allows for parcellation of different cortical areas. For example, the posterior temporal area (Tp) of the grey squirrel is unusually thick compared to the surrounding cortical areas (Fig. 3).

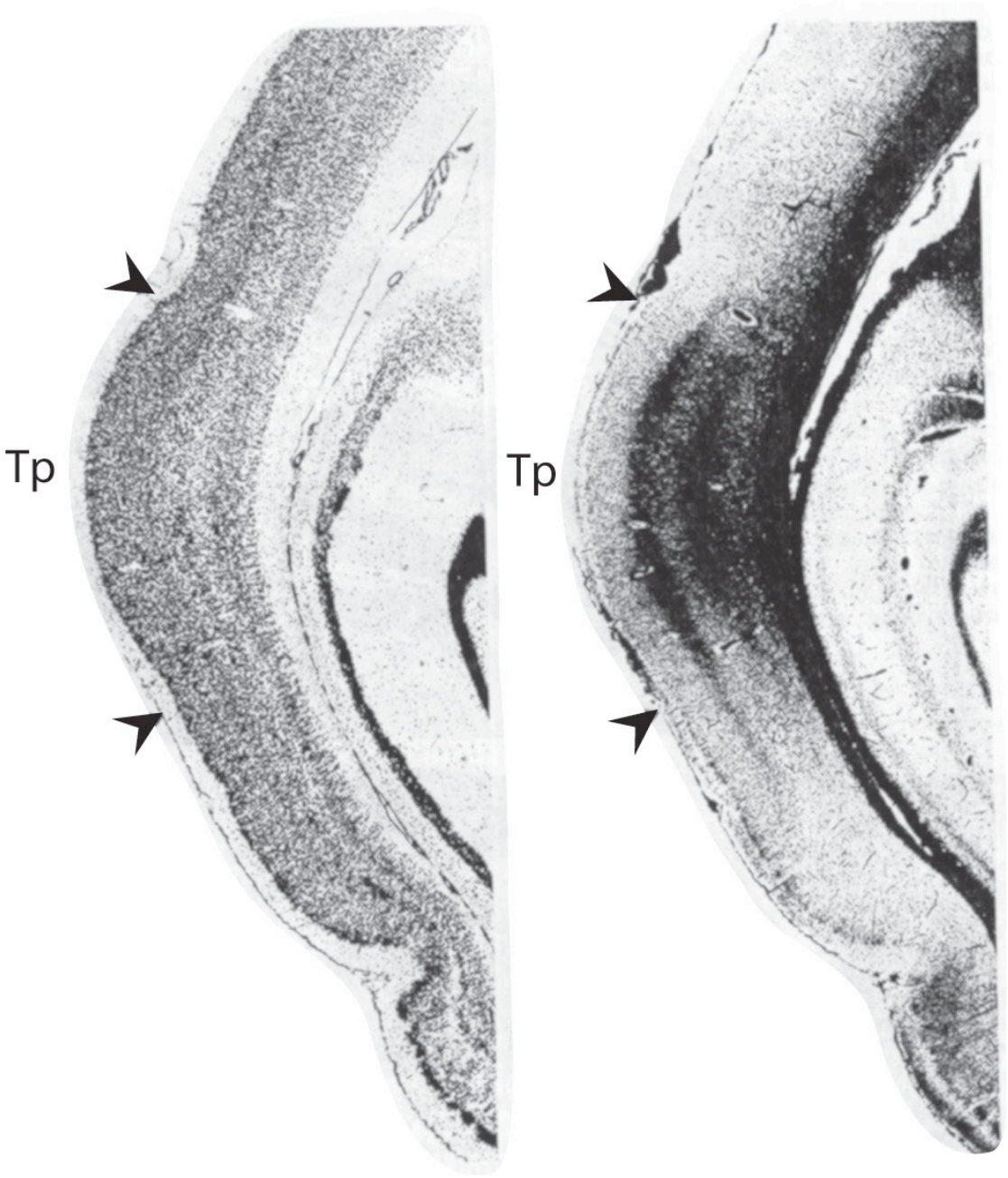

Figure 3. Coronal sections of the grey squirrel processed for Nissl substance (left) and myelin (right). Area temporal posterior (Tp) is shown here between the arrowheads. Tp is an example of unusually thick cortex compared to the adjacent area. The myelin section shows well-defined inner and outer bands of Baillarger. Reproduced from Fig. 6 of Kaas et al., 1972.

Cortical areas also vary in architectonic appearances due to differences in packing density and size of cellular elements. Areas may possess a thick layer 4 that is

predominantly densely packed with small stellate cells, giving them a koniocellular appearance, and a thinner layer 5 populated with small pyramidal cells (Creutzfeldt, 1995). Such areas are primarily involved with receiving inputs and include the primary visual, auditory and somatosensory areas (Creutzfeldt, 1995). In contrast, areas may possess a thinner layer 4 with low packing density, and a thicker layer 5 packed with large pyramidal cells, such as the Betz cells (Creutzfeldt, 1995). Such areas are primarily involved with output and include the motor cortex (Creutzfeldt, 1995).

A final contributor to the variability and specialization of the neocortex is modular organization. The modules are formed from groups of neurons that are carrying out similar functions and located in the same area (Kaas, 2002). These modules form the basis of parallel processing. Information spread through the layers is restricted to the confines of a module. This organization allows information sent to the neocortex to be processed simultaneously but separately (Kaas, 2002). Cortical modules reduce the length of connections between neurons and allow the different modules to specialize separately according to the needs of the species (Kaas, 1997). The concept of cortical modules was introduced by Vernon Mountcastle, a neurophysiologist who had recorded neural activity from somatosensory cortex and noticed that neurons with similar response properties were grouped into regions less than one mm in width across the thickness of cortex (Mountcastle et al., 1955). Similar observations in the primary visual cortex of cats and monkeys showed that inputs from each eye were separated into alternating bands in layer 4. These bands were termed as “ocular dominance” columns by Hubel and Wiesel in 1977. In 1970, Woolsey and Van der Loos observed modular organization in layer 4 of mouse primary somatosensory cortex. This modular organization, known as the “barrel

field" arose from the segregation of thalamic inputs from cortical inputs, with the thalamocortical afferents found mainly in the barrels (Agmon et al., 1993; Senft and Woolsey, 1991), and the corticocortical connections terminating around the barrels, forming the septa (Koralek et al., 1990; Miller et al., 2001). Each barrel in layer 4 represents an individual mysterical vibrissa on the contralateral face (Simons et al., 1984; Strominger and Woolsey, 1987). Similar modular organization has been described in other rodents such as rats and squirrels (Woolsey et al., 1975; Wong and Kaas, 2008).

In summary, the mammalian neocortex is organized in a vertical and a horizontal manner, and the layers and vertical modules of neocortex are essential for neural function. This dual organization increases the computational capacity of the neocortex (Grossberg, 1999), and forms the structural basis for the separation and integration of inputs and outputs, and serial and parallel processing. Due to different evolutionary demands, environments, genetic mutations and experience, diversification and variability of the neocortex arose across species. The size and thickness of neocortex, as well as the thickness of each layer, varies between species and cortical areas. Different cortical areas possess different cellular characteristics, such as packing density, size and type of neurons. The differences in cytoarchitecture between two given cortical areas may be due to different input-output connections, varying intrinsic connectivity, or both (Matelli and Luppino, 2004). Specializations of cortical areas take place within set boundaries, and transitions between areas may be sharp and distinct, such as the transition from area 17 to 18 (Fig. 3), or may be subtler and take place gradually, such as the transition dysgranular zone, area 3a, between primary somatosensory cortex to motor cortex (Brodmann, 1909).

These local differences between cortical areas set the criteria for studies involving the parcellation of the neocortex.

Comparative Architectonic Studies

Architectonic studies involve the parcellation of the neocortex into areas based on the cytoarchitectural variations present. Anatomical features of the different cortical areas are characterized through the use of histological and immunohistochemical methods to visualize the cell morphology and laminar patterns in the neocortex. Knowing the distinguishing features of different cortical areas will provide an anatomical framework for investigating the functional organization of the neocortex. Additionally, it will allow the identification of homologous regions of the neocortex across species based on the structural features of an area. Closely related species are expected to share more neocortical features than distantly related species. Comparing and contrasting the brain features of extant mammalian species across different branches of the phylogenetic tree, will provide insight about the neocortex organization of the common mammalian ancestor (Kaas and Preuss, 2003). In addition, by understanding the organization of the neocortex in extant mammals, we will be better able to understand how the large, complexly folded human neocortex evolved from the small, simple, and probably smooth brains of the common mammalian ancestor (Kaas and Preuss, 2003). As such, this comparative cytoarchitectonic approach lends itself to studying brain evolution.

Nearly a century after Brodmann's comprehensive architectonic studies, several common cortical areas have been identified in nearly all the mammals that have been examined (Krubitzer, 1995; Krubitzer and Kahn, 2003)(Fig. 4). These areas include the

primary visual area (Inouye, 1909, as cited in Leff, 2003; Sholl, 1995; Rosa and Krubitzer, 1999), the primary somatosensory area (Kaas, 1983; Johnson, 1990) and the primary auditory area (Evans et al., 1965; Ehret, 1997). In spite of evolutionary pressure and functional usage that influences the diversification of cortical phenotypes, these three cortical areas persist in all mammals, regardless of the morphological or behavioral specializations of the animal (Krubitzer, 1995; Catania, 2000; Henry et al., 2005). Even if a particular sensory system is not used, such as lack of vision in the blind mole rat, the sensory cortical area is not eliminated. In the case of the mole rat, a rudimentary primary visual area can still be architectonically defined (Heil et al., 1991; see Cooper et al., 1993; Bronchti et al., 2002 for more examples). Since these three cortical areas can be found in all living mammalian species, it is likely that they were present in the neocortex of the first mammals.

Figure 4. An evolutionary tree showing the phylogenetic relationship of major orders of mammals and the cortical organization of common cortical areas that have been identified. All the species shown here possess common cortical regions such as the primary somatosensory area (S1)(red), second somatosensory area (S2)(orange), primary auditory area (A1)(green), primary visual area (V1)(dark blue) and second visual area (V2)(light blue). Some areas such as the middle temporal area (MT)(pink) have only been observed in primates and may have evolved from an ancestor from the primate branch. Rostral is left, medial is up. Reproduced from Fig. 1, Krubitzer and Kahn, 2003.

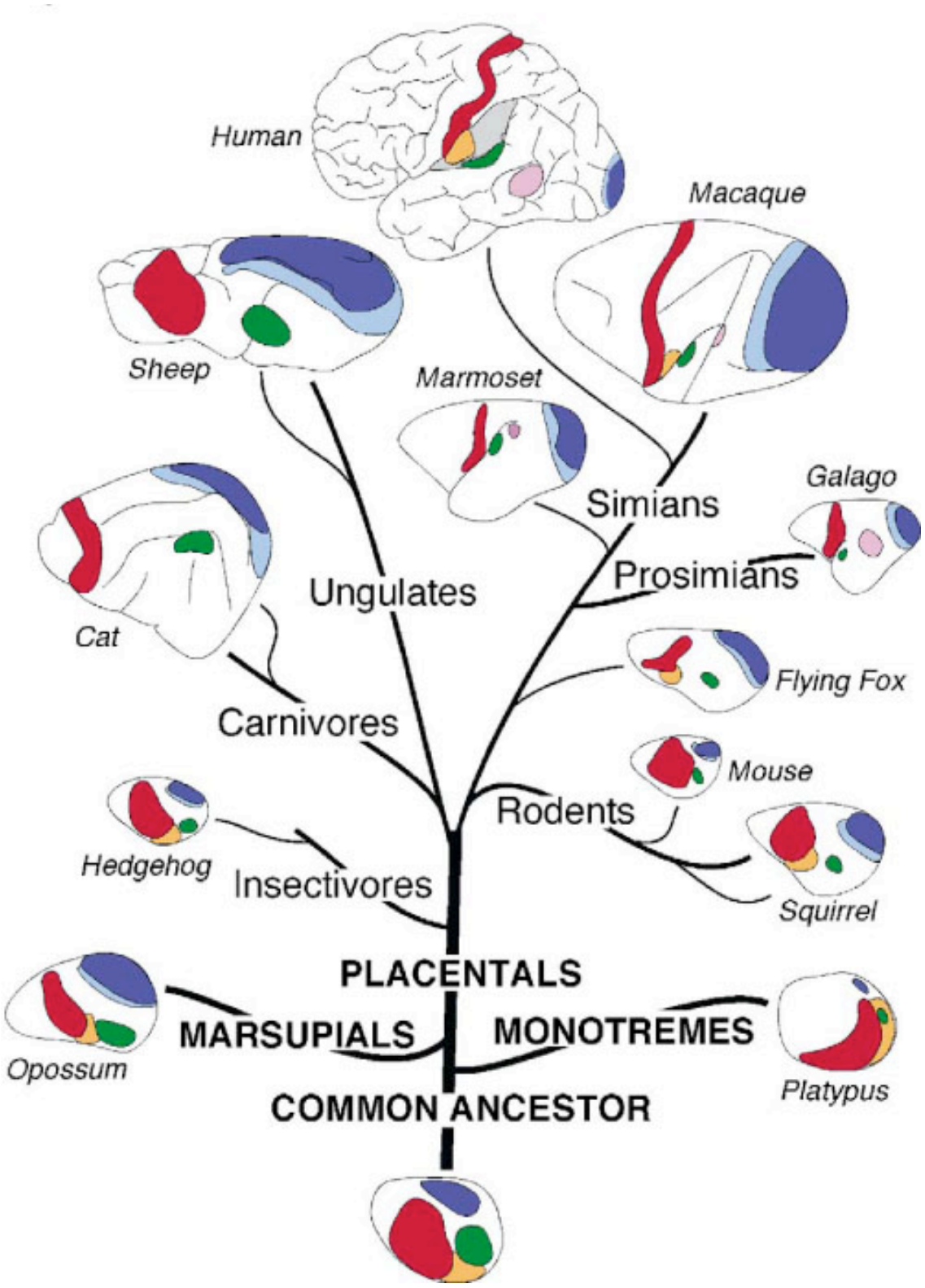
Human
Macaque
Sheep
Marmoset
Galago
Simians
Prosimians
Ungulates
Cat
Flying Fox
Carnivores
Mouse
Rodents
Hedgehog
Insectivores
Squirrel
PLACENTALS
MARSUPIALS
MONOTREMES
Opossum
Platypus
COMMON ANCESTOR

During the course of evolution, new cortical areas may come about as a result of morphological and behavioral specializations of different species. These areas may be involved in the integration of sensory information and higher-order processing. One such area is the middle temporal (MT) area that appears to have emerged in primates (Kaas, 2005). Neurons in this area are specialized for processing visual motion (Maunsell and Van Essen, 1983).

Architectonic studies are useful in studying brain organization. However, there have been criticisms of such studies. First, the borders drawn by investigators may be questionable due to the limited histological stains and lack of stringent parcellation criteria (Lashley and Clark, 1946). Due to a lack of staining methods available, most of the previous architectonic studies made use of only the Nissl and myelin stains. The reliability of the borders is dependent on the certainty and precision with which areas can be recognized. Borders that are identified based on a single criterion, especially if they are based on the presence of certain cell types, are likely to be highly unreliable. An example would be using the changes in density distribution of the giant pyramids in layer 5 as the basis for delimiting the border between area 4 and area 6 in primates. The density distribution of these cells does not change abruptly, but instead reduces progressively at the area 4/6 border. Identification of the area 4/6 border based on this single criterion would thus be a subjective one (Matelli and Luppino, 2004). These borders can be made more reliable by employing a battery of staining methods. Therefore, it is necessary to revisit the cortical maps that have been drawn, this time, using a battery of staining methods that are now available. Additional histological and immunohistochemical stains allow corroboration of cortical borders on separate but adjacent sections. Moveover, the

utility of multiple, and more sensitive stains may identify previously undocumented cortical borders.

Second, previous architectonic studies have a small sample sizes (Lashley and Clark, 1946). Including more cases will address the significant variability of neocortex across individuals of the same species (Lashley and Clark, 1946; Amunts et al., 1999). On the large scale, there are variations in the convolutions of the neocortex and the size of each cortical area (Von Economo and Koskinas, 1925, as cited in Lashley and Clark, 1946; Amunts et al., 2001; Van Essen, 2004). Microscopically, the same cortical area in different hemispheres can vary in cell density by as much as ten percent (Von Economo and Koskinas, 1925, as cited in Lashley and Clark, 1946).

By following the guidelines above, the main pitfalls of architectonic studies can be avoided. Consistent borders can be drawn and the cortical maps generated will be reliable enough to serve as guides in functional studies. Cortical organizations across different species can also be meaningfully compared and this will aid us in our understanding of brain evolution.

Research Rationale

The aim of this present study is to define the cortical areas and form reliable cortical maps of grey squirrels, tree shrews and galagos. These cortical maps can then serve as guides to electrophysiological and connectional studies in animals. The nomenclature of the cortical areas used in this study will closely follow the existing nomenclature where possible.

Species Rationale

In addition to the usefulness of the cortical maps as guides for functional brain studies, obtaining cortical maps of these species is part of a greater effort to understand the evolutionary processes that have taken place in order to give rise to the complex brain of humans. The mammalian species chosen for the present studies, the grey squirrels, tree shrews and galagos, are from different orders of the phylogenetic tree, Rodentia, Scandentia and Prosimian orders respectively, and are from the same branch of mammalian radiation, the Euarchontoglires. Therefore, they should share enough characteristics for a meaningful comparison, than with species from other branches of the mammalian radiation, such as the Laurasiatherian branch that includes the carnivores such as cats (Fig. 5).

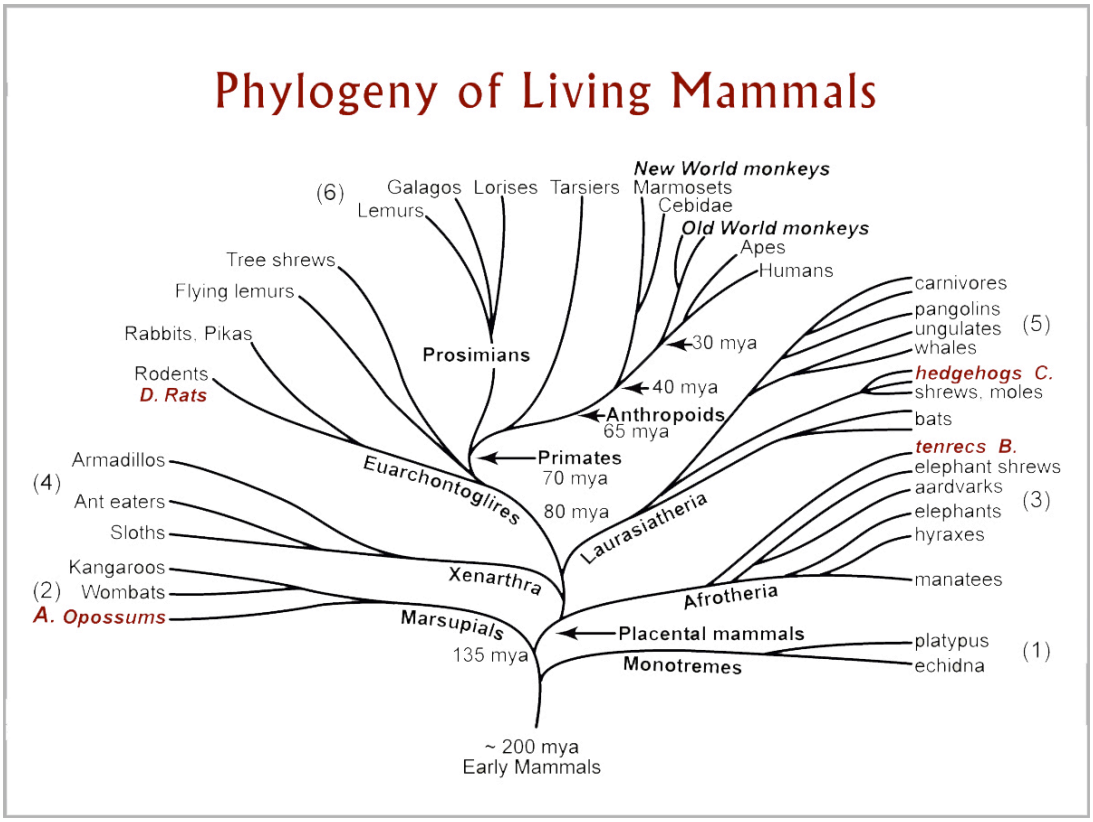

Figure 5. A phylogenetic tree deduced from recent molecular data. From Kaas, 2004.

Grey squirrels (*Sciurus carolinenesis*)

The grey squirrel is the rodent of choice here for several reasons. Firstly, squirrels have a well-developed visual system compared to other members of the rodent family, such as nocturnal mice and rats. Squirrels are diurnal and have a cone-dominated retina (West and Dowling, 1975; Long and Fisher, 1983; Szel and Rolich, 1992). They have several visual areas (Kaas et al., 1989; Sereno et al., 1991), including a large primary visual cortex with a fine-grain retinotopic map (Hall et al., 1971) and a well-defined second visual area. This makes them good candidates for comparisons to other mammals with well-developed visual systems, such as primates, cats and tree shrews. Secondly, there have been several functional studies on the somatosensory and auditory system of squirrels. It has been shown that squirrels have a well-developed sensorimotor system, with up to five somatosensory areas (Krubitzer et al., 1986; Slutsky et al., 2000), and an auditory cortex that contains several auditory areas (Luethke et al., 1988). These electrophysiological and anatomical studies have produced results that are congruent with cortical architectonic studies in squirrel neocortex (Kaas, 1982; 1989).

Tree shrews (*Tupaia belangeri*)

Tree shrews are diurnal, arboreal mammals that bear some semblance to squirrels, but are actually the closest living relatives of primates (Liu et al., 2001; Murphy et al., 2001 a,b; Springer et al., 2003). They are the only members of the order Scandentia that diversified from the Euarchontoglire clade about 85 million years ago (Murphy et al., 2001a: Huchon et al., 2002). Like primates, tree shrews have high visual acuity and reduced dependence on olfaction (Sorenson, 1970). They are visually oriented animals

with their retinas consisting of mostly cones (Kaas, 2002). The visual system of tree shrews is well developed with several distinct visual areas (Lyon et al., 1998; Kaas et al., 1972) and this makes them good animal models for studies of the visual system (e.g. Lund et al., 1985). Unlike primates, tree shrews have an exceptionally large superior colliculus (Kaas and Huerta, 1988) that is more distinctly laminated than that of primates (Abplanalp, 1970; Lane et al., 1971). This large and well-laminated superior colliculus is a feature that tree shrews and squirrels share (Abplanalp, 1970; Lane et al., 1971; Cusick and Kaas, 1982). Tree shrews also share cytoarchitectural features of visual cortex with both primates and non-primates. The pyramidal cells in the visual cortex of tree shrews have a similar branching pattern to those found in primates. However, they are more branched and spinous than those found in galagos and other primates (Elston et al., 2005). These cytoarchitectural features suggest that while tree shrews are close relatives of primates, there are certain traits that have evolved independently in tree shrews from the common ancestor with primates (Kaas, 2002).

Galagos (*Otolemur garnetti*)

Prosimians, such as galagos, represent one of the major branches of the primate evolution that diverged from anthropoids about 50 million years ago (Simons and Rasmussen, 1994; Martin, 2004). These prosimian primates have smaller brain weight to body weight ratio compared to the anthropoid primates (Jerison 1979; Stephan et al., 1981; Preuss and Goldman-Rakic 1991) and more limited behavioral repertoires (Fang et al., 2006). They have also retained many anatomical features of early primates, whereas these anatomical features have been modified during the course of anthropoid evolution

(Fleagle, 1999; Martin, 1990). From this, it can be assumed that features of neocortical organization in early primates will be conserved to a greater degree in prosimians than in anthropoids (Preuss and Goldman-Rakic 1991). This has been shown in electrophysiological experiments, where prosimians and anthropoids share many visual and somatosensory areas, anthropoids have additional features not found in prosimians (Allman et al., 1979; Kaas, 1983). Therefore, by studying the cortical organization of galagos and comparing it to anthropoid primates, such as macaque monkeys, we may be able to identify features that are found in early primates and features that are products of anthropoid evolution.

Specific Aims

1. Parcellate the hemispheric surface of grey squirrel, tree shrew and galago on the basis of architectonic variations, from which an updated cortical map for each of these three species will be obtained. This will be achieved by using a battery of histological and immunohistochemical stains in adjacent sections.

2. Establish the architectonic characteristics of the various cortical areas in the grey squirrel, tree shrew and galago. Similarities and differences in the architectonic characteristics of common cortical areas in the three mammals will be identified to better understand the evolutionary processes that have taken place in the Rodentia, Scandentia and Prosimian orders.

References

Abplanalp P. 1970. Some subcortical connections of the visual system in tree shrews and squirrels. Brain Behav Evol 3(1):155-168.

Agmon A, Yang LT, O'Dowd DK and Jones EG. 1993. Organized growth of thalamocortical axons from the deep tier of terminations into layer IV of developing mouse barrel cortex. J Neurosci 13(12):5365-382.

Allman JM, Campbell CB and McGuinness E. 1979. The dorsal third tier area in Galago senegalensis. Brain Res 179(2):355-361.

Amunts K and Zilles K. 2001. Advances in cytoarchitectonic mapping of the human cerebral cortex. Neuroimaging Clin N Am 11(2):151-69, vii.

Amunts K, Schleicher A, Burgel U, Mohlberg H, Uylings HB and Zilles K. 1999. Broca's region revisited: cytoarchitecture and intersubject variability. J Comp Neurol 412(2):319-341.

Brodmann K. 1909. Brodmann's 'Localisation in the Cerebral Cortex'. L.J. Garey, eds. London: Eldred Smith-Gordon.

Bronchti G, Heil P, Sadka R, Hess A, Scheich H and Wollberg Z. 2002. Auditory activation of "visual" cortical areas in the blind mole rat (Spalax ehrenbergi). Eur J Neurosci 16(2):311-329.

Casagrande VA, and Kaas JH. 1994. The afferent, intrinsic, and efferent connections of primary visual cortex in primates. In Cerebral Cortex: Primary Visual Cortex in Primates, K.S. Rockland, and A. Peters, eds. New York: Plenum. 201-259.

Catania KC. 2000. Cortical organization in insectivora: the parallel evolution of the sensory periphery and the brain. Brain Behav Evol 55:311-321.

Cavada C. 2004. Neuroanatomy in understanding primate brain function: status and challenges. Cortex 40(1):5-6.

Cooper HM, Herbin M and Nevo E. 1993. Visual system of a naturally microphthalmic mammal: the blind mole rat, Spalax ehrenbergi. J Comp Neurol 328(3):313-350.

Creutzfeldt OD. 1995. Cortec Cerebri: Performance, structural and functional

organization of the cortex. New York: Oxford Univ Pr.

Cusick CG and Kaas JH. 1982. Retinal projections in adult and newborn grey squirrels. Brain Res 256(3):275-284.

Ehret G. 1997. The auditory cortex. J Comp Physiol 181:547-557.

Elston GN, Elston A, Casagrande V and Kaas JH. 2005. Areal specialization of pyramidal cell structure in the visual cortex of the tree shrew: a new twist revealed in the evolution of cortical circuitry. Exp Brain Res 163(1):13-20.

Evans EF, Ross HF and Whitfield IC. 1965. The spatial distribution of unit characteristic frequency in the primary auditory cortex of the cat. J Physiol 179(2):238-247.

Fang PC, Stepniewska I and Kaas JH. 2006. The thalamic connections of motor, premotor, and prefrontal areas of cortex in a prosimian primate (Otolemur garnetti). Neuroscience 143(4):987-1020.

Finger S. 1994. Origins of Neuroscience: A History of Explorations into Brain Function. Cary, North Carolina, USA: Oxford Univ Pr.

Fleagle JG. 1999. *Primate adaptation and Evolution.* San Diego: Academic Press.

Grossberg S. 1999. How does the cerebral cortex work? Learning, attention, and grouping by the laminar circuits of visual cortex. Spat Vis 12(2):163-185.

Hall WC, Kaas JH, Killackey H and Diamond IT. 1971. Cortical visual areas in the grey squirrel (Sciurus carolinesis): a correlation between cortical evoked potential maps and architectonic subdivisions. J Neurophysiol 34(3):437-452.

Hassler R. 1966. Comparative anatomy of the central visual systems in day- and night-active primates.,R. Hassler, and H. Stephen, eds. Stuttgart: Thieme.

Heil P, Bronchti G, Wollberg Z and Scheich H. 1991. Invasion of visual cortex by the auditory system in the naturally blind mole rat. Neuroreport 2(12):735-38.

Henry EC, Marasco PD and Catania KC. 2005. Plasticity of the cortical dentition representation after tooth extraction in naked mole-rats. J Comp Neurol 485(1):64-74.

Henry GH. 1991. Afferent Inputs, Receptive Field Properties and Morphological Cell Types in Different Laminae of the Striate Cortex. A.G. Leventhal, eds. Macmillan Press.

Hubel DH, Wiesel TN and Stryker MP. 1977. Orientation columns in macaque monkey visual cortex demonstrated by the 2-deoxyglucose autoradiographic technique. Nature 269(5626):328-330.

Huchon D, Madsen O, Sibbald MJ, Ament K, Stanhope MJ, Catzeflis F, de Jong WW and Douzery EJ. 2002. Rodent phylogeny and a timescale for the evolution of Glires: evidence from an extensive taxon sampling using three nuclear genes. Mol Biol Evol 19(7):1053-065.

Jerison HJ. 1979. Brain, body and encephalization in early primates. J Hum Evol 8615-635.

Johnson JI. 1990. Comparative development of somatic sensory cortex.

Kaas JH and Catania KC. 2002. How do features of sensory representations develop? Bioessays 24(4):334-343.

Kaas JH and Heurta MF. 1988. Subcortical visual system of primates. Comparative Primate Biology; Neurosciences 4327-391.

Kaas JH. 2005. From mice to men: the evolution of the large, complex human brain. J Biosci 30(2):155-165.

Kaas JH. 2002. Neocortex. Elsevier Science.

Kaas JH. 1997. Topographic maps are fundamental to sensory processing. Brain Res Bull 44(2):107-112.

Kaas JH. 1983. What, if anything, is SI? Organization of first somatosensory area of cortex. Physiol Rev 63(1):206-231.

Kaas JH, and Preuss TM. 2003. Human brain evolution. In Fundamental neuroscience, L.R. Squire, F.E. Bloom, S.K. McConnell, J.L. Roberts, N.C. Spitzer, and M.J. Zigmond, eds. San Diego: Academic Press. 1147-1166.

Kaas JH, Hall WC, Killackey H and Diamond IT. 1972. Visual cortex of the tree shrew (Tupaia glis): architectonic subdivisions and representations of the visual field. Brain Res 42(2):491-96.

Kaas JH, Krubitzer LA and Johanson KL. 1989. Cortical connections of areas 17 (V-I) and 18 (V-II) of squirrels. J Comp Neurol 281(3):426-446.

Koralek KA, Olavarria J and Killackey HP. 1990. Areal and laminar organization of

corticocortical projections in the rat somatosensory cortex. J Comp Neurol 299(2):133-150.

Krubitzer LA and Kahn DM. 2003. Nature versus nurture revisited: an old idea with a new twist. Prog Neurobiol 70(1):33-52.

Krubitzer LA. 1995. The organization of neocortex in mammals: are species differences really so different? Trends Neurosci 18(9):408-417.

Krubitzer LA, Sesma MA and Kaas JH. 1986. Microelectrode maps, myeloarchitecture, and cortical connections of three somatotopically organized representations of the body surface in the parietal cortex of squirrels. J Comp Neurol 250(4):403-430.

Lane RH, Allman JM and Kaas JH. 1971. Representation of the visual field in the superior colliculus of the grey squirrel (Sciurus carolinensis) and the tree shrew (Tupaia glis). Brain Res 26(2):277-292.

Lashley KS and Clark G. 1946. The cytoarchitecture of the cerebral cortex of ateles: A critical examination of architectonic studies. J. Comp Neurol. 85:223-305.

Leff A. 2004. A historical review of the representation of the visual field in primary visual cortec with special reference to the neural mechanisms underlying macular sparing. Brain Lang 88:268-278.

Liu FG, Miyamoto MM, Freire NP, Ong PQ, Tennant MR, Young TS and Gugel KF. 2001. Molecular and morphological supertrees for eutherian (placental) mammals. Science 291(5509):1786-89.

Long KO and Fisher SK. 1983. The distributions of photoreceptors and ganglion cells in the California ground squirrel, Spermophilus beecheyi. J Comp Neurol 221(3):329-340.

Luethke LE, Krubitzer LA and Kaas JH. 1988. Cortical connections of electrophysiologically and architectonically defined subdivisions of auditory cortex in squirrels. J Comp Neurol 268(2):181-203.

Lund JS, Fitzpatrick D, and Humphrey AL. 1985. The striate visual cortex of the tree shrew. In Visual cortex, E.G. Jones, and A. Peters, eds. New York: Plenum Press. 157-205.

Lund JS, Henry GH, MacQueen CL and Harvey AR. 1979. Anatomical organization of the primary visual cortex (area 17) of the cat. A comparison with area 17 of the macaque monkey. J Comp Neurol 184(4):599-618.

Lyon DC, Jain N and Kaas JH. 1998. Cortical connections of striate and extrastriate visual areas in tree shrews. J Comp Neurol 401(1):109-128.

Martin RD. 2004. Palaeontology: Chinese lantern for early primates. Nature 427:22-23.

Matelli M and Luppino G. 2004. Architectonics of the primates cortex: usefulness and limits. Cortex 40(1):209-210.

Maunsell JH and van Essen DC. 1983. The connections of the middle temporal visual area (MT) and their relationship to a cortical hierarchy in the macaque monkey. J Neurosci 3(12):2563-586.

Miller B, Blake NM, Erinjeri JP, Reistad CE, Sexton T, Admire P and Woolsey TA. 2001. Postnatal growth of intrinsic connections in mouse barrel cortex. J Comp Neurol 436(1):17-31.

Mountcastle VB, Berman AL and Davies PW. 1955. Topographic organization and modality representation in first somatic area of cat's cerebral cortex by method of single unit analysis. Am J Physiol 183, 646.

Murphy WJ, Eizirik E, Johnson WE, Zhang YP, Ryder OA and O'Brien SJ. 2001a. Molecular phylogenetics and the origins of placental mammals. Nature 409(6820):614-18.

Murphy WJ, Eizirik E, O'Brien SJ, Madsen O, Scally M, Douady CJ, Teeling E, Ryder OA, Stanhope MJ, et al.. 2001b. Resolution of the early placental mammal radiation using Bayesian phylogenetics. Science 294(5550):2348-351.

Preuss TM and Goldman-Rakic PS. 1991. Architectonics of the parietal and temporal association cortex in the strepsirhine primate Galago compared to the anthropoid primate Macaca. J Comp Neurol 310(4):475-506.

Rakic P. 1988. Specification of cerebral cortical areas. Science 241(4862):170-76.

Rosa MG and Krubitzer LA. 1999. The evolution of visual cortex: where is V2? Trends Neurosci 22(6):242-48.

Senft SL and Woolsey TA. 1991. Growth of thalamic afferents into mouse barrel cortex. Cereb Cortex 1(4):308-335.

Sereno MI, Rodman HR and Karten HJ. 1991. Organization of visual cortex in the california ground squirrel. Society for Neuroscience Abstract 17.

Sholl DA. 1955. The organization of the visual cortex in the cat. J Anat 89(1):33-46.

Simons DJ, Durham D and Woolsey TA. 1984. Functional organization of mouse and rat SmI barrel cortex following vibrissal damage on different postnatal days. Somatosens Res 1(3):207-245.

Simons EL and Rasmussen T. 1994. A whole new world of ancestors: eocene anthropoids from Africa. Evol Anthropol 3:128-139.

Slutsky DA, Manger PR and Krubitzer L. 2000. Multiple somatosensory areas in the anterior parietal cortex of the California ground squirrel (Spermophilus beecheyii). J Comp Neurol 416(4):521-539.

Sorenson M. 1970. Behaviour of tree shrews. Primate Behaviour 1:141-193.

Strominger RN and Woolsey TA. 1987. Templates for locating the whisker area in fresh flattened mouse and rat cortex. J Neurosci Methods 22(2):113-18.

Szel A and Rohlich P. 1992. Two cone types of rat retina detected by anti-visual pigment antibodies. Exp Eye Res 55(1):47-52.

Van Essen DC. 2004. Towards a quantitative, probabilistic neuroanatomy of cerebral cortex. Cortex 40(1):211-12.

Von Economo C, and Koskinas GN. 1925. The Cytoarchitectonics of the Adult Human Cortex. H.L. Seldon, eds. Vienna: Julius Springer Verlag.

West RW and Dowling JE. 1975. Anatomical evidence for cone and rod-like receptors in the gray squirrel, ground squirrel, and prairie dog retinas. J Comp Neurol 159(4):439-460.

Wong P and Kaas JH. 2008. Architectonic subdivisions of neocortex in the gray squirrel (Sciurus carolinensis). Anat Rec (Hoboken) 291(10):1301-333.

Woolsey TA and Van der Loos H. 1970. The structural organization of layer IV in the somatosensory region (SI) of mouse cerebral cortex. The description of a cortical field composed of discrete cytoarchitectonic units. Brain Res 17(2):205-242.

Woolsey TA, Welker C and Schwartz RH. 1975. Comparative anatomical studies of the SmL face cortex with special reference to the occurrence of "barrels" in layer IV. J Comp Neurol 164(1):79-94.

Yamamori T and Rockland KS. 2006. Neocortical areas, layers, connections, and gene

expression. Neurosci Res 55(1):11-27.

Zilles K, Palomero-Gallagher N and Schleicher A. 2004. Transmitter receptors and functional anatomy of the cerebral cortex. J Anat 205(6):417-432.

CHAPTER II

ARCHITECTONIC SUBDIVISIONS OF NEOCORTEX IN THE GREY SQUIRREL (*SCIURUS CAROLINENSIS)*

Introduction

Over the last 55 million years of evolution, the rodent clade has had considerable success and diversification, radiating into some 28 families, 400 genera and over 2000 extant species (Huchon et al., 2002). Squirrels diverged from other rodents about 40 million years ago, diversified into 50 genera and 273 species (Mercer and Roth, 2003), and developed distinguishing characteristics that make them attractive for neurobiological studies. Most notably, grey squirrels and other squirrels have been used in a number of studies of the visual system because this system is especially well developed (Van Hooser and Nelson, 2006). As a result of such studies, the visual system in squirrels can be productively compared to other well-developed visual systems, such as those of primates, cats and tree shrews, for common features and alternative specializations. As examples of specializations of the visual system, diurnal squirrels have large eyes with a majority of cones over rods in their retina (West and Dowling, 1975; Long and Fisher, 1983; Szél and Röhlich, 1988), a distinctly laminated dorsal lateral geniculate nucleus (Kaas et al., 1972; Cusick and Kaas, 1982; Major et al., 2003), and a patently laminated superior colliculus (Abplanalp, 1970; Lane et al., 1971; Cusick and Kaas, 1982) that is approximately ten times larger than in rats matched for body size (Kaas and Collins, 2001). In the neocortex, primary visual cortex is large, with a fine-grain retinotopic map (Hall et al., 1971), the second visual area, V2, is well-defined, and

This chapter has been published: Wong P, Kaas JH. 2009. Architectonic subdivisions of neocortex in the grey squirrel (*Sciurus carolinensis)*. Anatomical Record 2192(10) 1301-1333.

additional visual areas have been proposed (Kaas et al., 1989; Sereno et al., 1991). Given that tree squirrels are also skilled in climbing and exploring the fine branches of their arboreal niche, and use their forepaws to manipulate food items, as do most primates, it is not surprising that their sensorimotor system and cortex are well-developed and proportionately large with as many as five somatosensory areas (Krubitzer et al., 1986; Slutsky et al., 2000). The auditory cortex has also been explored in squirrels and several auditory areas have been described (Luetheke et al., 1988). These studies on aspects of cortical organization and function in squirrels have produced results that can be compared with architectonic studies of how the cortex is subdivided into areas, as the borders of cortical areas are most reliably defined when architectonic evidence is congruent with evidence from neurophysiological and anatomical studies (Kaas, 1972; 1989).

Most studies of cortical architecture in rodents have focused on laboratory rats (e.g., Krieg, 1946; Schober, 1986; Wise and Donoghue, 1986; Zilles and Wree, 1995; Swanson, 1992; 2003; Uylings et al., 2003) and, to a lesser extent, on laboratory mice (e.g., Rose, 1912; Caviness 1975; Wallace, 1983; Lorente de Nó, 1992; Paxinos and Franklin, 2003). Compared to rats and mice, cortical organization and function in squirrels has been limited to a few investigations. This is surprising considering the characteristic functional adaptations of squirrels that cannot be gleaned from examining rat brains. In the present study, we reexamine the cortical architecture of the grey squirrel using a number of recently developed immunohistochemical stains with the goal of defining and describing the areas that form the functional subdivisions of the neocortex.

For the present study, an important additional procedure was to use a histochemical procedure to reveal unbound ionic zinc (Zn^{2+}) in cortical tissues (Danscher,

1981; 1982; Danscher and Stoltenberg, 2005). Detectable levels of synaptic zinc are contained in cortical neurons, especially in the synaptic vesicles of cortical neuron terminations and synaptic clefts. As thalamocortical neurons and their cortical terminations are not synaptic zinc positive, cortical areas with dense or sparse thalamocortical inputs can be distinguished by reactions for zinc (e.g., Valente et al., 2002). As a notable example, primary sensory areas can be distinguished by an almost total lack of zinc in layer 4. Some brain sections were processed for cytochrome oxidase, which is expressed at high levels in layer 4 of sensory areas (Wong-Riley, 1979). Other brain sections were immunostained with a monoclonal selective neurofilament marker, SMI-32, parvalbumin (PV), calbindin (CB), vesicle glutamate transporter 2 (VGluT2) and limbic-associated membrane protein (LAMP). SMI-32 is a monoclonal antibody that reacts with non-phosphorylated epitopes in neurofilaments M and H (Lee et al., 1988), and reveals a subset of pyramidal cells (Campbell and Morrison, 1989). PV is a calcium-binding protein and PV immunoreactive neurons include subsets of GABAergic, non-pyramidal cells, thought to be basket and double bouquet interneurons (Celio, 1986; Condé et al., 1996; DeFelipe, 1997; Hof et al., 1999). Perhaps, more importantly for the present study, PV also labels afferent cortical terminals from sensory thalamic nuclei (Van Brederode et al., 1990; DeFelipe and Jones, 1991; DeVencia et al., 1998; Hackett et al., 1998; Latawiec et al., 2000; Cruikshank et al., 2001). The large to medium PV positive thalamic neurons projecting to sensory cortex belong to the “leminiscal” subsystem of relay cells that project most densely to layer 4 (e.g., Jones and Hendry, 1989; Rausell and Jones, 1991; Diamond et al., 1993). Another calcium-binding protein, calbindin (CB) reveals a different subset of GABA immunoreactive interneurons

compared to PV (Van Brederode et al., 1990). VGluT2 immunostaining also reveals thalamocortical terminations in layer 4, but not those of cortical neurons (Fujiyama et al., 2001; Kaneko and Fujiyama, 2002; Nahami and Erisir, 2005). The limbic-associated membrane protein (LAMP) is a cell-surface glycoprotein expressed in limbic areas (Levitt, 1984; Horton and Levitt 1988; Côté et al., 1995).

By using this battery of additional procedures, together with traditional Nissl and myelin stains, we were able to more fully characterize the areal subdivisions of neocortex in grey squirrels. A brief abstract of the present findings has appeared (Wong and Kaas, 2006).

Materials and Methods

Animal subjects

Architectonic subdivisions of the neocortex were studied in nine grey squirrels (*Sciurus carolinensis*). All procedures were approved by the Vanderbilt Institutional Animal Care and Use Committee and followed NIH guidelines.

Tissue preparation

All animals were given a lethal dose of sodium pentobarbital (100mg/kg). To reveal synaptic zinc, the animals were given 200mg/kg body weight of sodium sulfide with 1ml of heparin in 0.1M phosphate buffer, (PB), pH 7.2, intravenously. The animals were perfused transcardially, in sequence, with 0.9% saline, 4% paraformaldehyde in 0.1M PB and subsequently with 4% paraformaldehyde and 10% sucrose. The brains were removed from the skull, bisected and post-fixed for about 3 hrs in 4% paraformaldehyde

and 10% sucrose in 0.1M PB. The hemispheres were immersed in 30% sucrose solution for cryoprotection until they sank to the bottom of the vial before being cut into 40μm–thick coronal, parasagittal or horizontal sections on a freezing microtome. Serial sections were divided into four or up to six series. For some cases, after an injection of sodium sulfide, the animals were perfused with 0.9% saline, 2% paraformaldehyde in 0.1M PB, followed by 2% paraformaldehyde with 10% sucrose. The brains were then removed, artificially flattened, and then cut tangentially, parallel to the pia.

Zinc Histochemistry

Our protocol followed that outlined by Ichinohe and Rockland (2004). Brain sections were washed thoroughly with 0.1M PB, pH 7.2, followed by 0.01M PB, pH 7.2. The IntenSE M Silver enhancement kit (Amersham International, Little Chalfont Bucks, UK) was used to visualize the Zn^{2+}-enriched terminals. A one-to-one cocktail of the IntenSE M kit solution and a 50% gum arabic solution was used as the developing reagent. When a dark brown/black signal was seen, which usually takes about 4 hours to appear, the development of reaction products was terminated, by rinsing the sections in 0.01M PB. Sections were then mounted and dehydrated in an ascending series of ethanols, (70% for 20 min, 95% for 10 min, 100% for 10 min), cleared in xylene and coverslipped using Permount (Fisher Scientific, Pittsburgh, PA).

Immunohistochemistry

In some cases, a series of one in four or five brain sections was immunostained for SMI-32 (mouse monoclonal anti-SMI-32 from Covance Inc. Princeton, NJ; 1:2000),

parvalbumin (PV) (mouse monoclonal anti-PV from Sigma-Aldrich, St. Louis, Mo; 1:2000), calbindin (CB) (mouse monoclonal anti-CB from Swant, Bellinzona, Switzerland; 1:5000), vesicle glutamate transporter 2 (VGluT2) (mouse monoclonal anti-VGluT2 from Chemicon now part of Millipore, Billerica, MA; 1:2000), or Limbic Associated Membrane protein (mouse monoclonal anti-LAMP) (kindly provided by Drs Aurea Pimenta and Pat Levitt; Horton and Levitt, 1998; Reinoso et al., 1996; 1:1000). Sections processed for PV, CB, VGluT2 and SMI-32 were reacted using the protocol described in Ichinohe et al. (2003). Briefly, sections were incubated in a blocker of 01.M PBS, pH 7.2, with 0.5% Triton X-100 and 5% normal horse serum for an hour at room temperature before incubation in their respective primary antibodies in the blocker for 40 to 48 hours at 4ºC. After rinsing, the sections were incubated in the blocker containing biotynylated horse anti-mouse IgG (Vector, Burlinggame, CA; 1:200) for 90 minutes at room temperature, followed by ABC incubation (one drop each of reagent A and B per 7ml of 0.1M PB, pH 7.2; ABC kits, Vector, Burlingame, CA) for 90 minutes, also at room temperature. Immunoreactivity was visualized by developing sections in diaminobenzidine histochemistry with 0.03% nickel ammonium sulfate. Processing procedures for LAMP have been described in Chesselet et al., (1991) and a brief description follows. Sections were incubated in 0.1M PBS, pH 7.2, containing 4% non-fat dry milk and the anti-LAMP antibody for 24h at 4ºC . Procedures for the secondary antibody and immunoreactivity visualization are as described above.

Histochemistry

Apart from the sections processed with the antibodies stated above, one section from each parasagittal or coronal series was processed for Nissl substance (with thionin). In cases cut in the horizontal plane, one series of sections was processed for Nissl substance (with thionin) and another series of sections was processed for myelin using the Gallyas (1979) silver procedure. In flattened brain sections, one in every three sections was processed for cytochrome oxidase (CO) (Wong-Riley, 1979).

Light microscopy

A number of histological procedures were used to delineate architectonic borders in brain sections, including those for Nissl substance, myelin, CO, zinc, PV, CB, VGluT2, SMI-32 and LAMP. Cortical borders were revealed by laminar and cell density changes in the processed sections. The locations of borders were established by viewing sections with a high-powered microscope. Nissl and zinc preparations were the most useful for defining primary sensory areas, while Nissl and SMI-32 preparations were useful for defining cortical areas in the sensorimotor cortex. Other histochemical procedures were used for corroborating otherwise ambiguous borders. Processed sections were viewed under a Nikon E800 microscope (Nikon Inc., Melville, NY) and digital photomicrographs of sections were acquired using a Nikon DXM1200 camera (Nikon Inc., Melville, NY) mounted on the microscope. Digitized images were adjusted for levels, brightness and contrast using Adobe Photoshop (Adobe Systems Inc., San Jose, CA), but they were not otherwise altered.

Anatomical reconstruction

The first brain section in every series was projected onto a white sheet of paper using a Bausch and Lomb Microprojector (Bausch & Lomb, Rochester, NY) and the outline of the section was drawn. Blood vessels and other landmarks were marked on the outline so that sections from adjacent series could be aligned. Areal borders of adjacent sections processed for different preparations in a series were independently assessed and marked on the outline. The locations of the independently identified borders in the different preparations were within 500µm, usually less, of each other. On rare occasions where the deviation in distances between the identified borders is greater than 500µm, it would usually be the result of histological artifacts, such as tears in the section. These sections were not included in the analysis. Borders are assigned only when changes in architectonic characteristics were observed in at least three preparations and the location of the changes were within 500µm of each other.

The outlines of the brain sections with the architectonic borders marked out were then digitized and imported into Adobe Illustrator (Adobe Systems Inc., San Jose, CA), where they are aligned into stacks using the contour of the outlined section and the landmarks stated above. For brains that were cut coronally, straight lines drawn parallel, perpendicular, and at a 45° angle to the midline on the image of each outline served as axes of reference to obtain the lateral, dorsal and dorsolateral view of the brain respectively. Brains cut in the sagittal and horizontal planes were used to reconstruct the dorsal and lateral view of the brain respectively by drawing an axis of reference parallel to the midline. The rostral and caudal poles of the section, and the position of the borders were marked along these axes, and subsequently charted on their respective views of the

brain. The points on the brain chart were then joined, thus obtaining the areal boundaries. In general, the different histological procedures revealed nearly identical boundaries between areas, suggesting that functionally relevant borders were being detected.

Summary diagrams of the arrangement of proposed cortical areas were constructed as guides to viewing the histological material by transposing the most reliably identified areal borders from reconstructed cases cut in the coronal, sagittal or horizontal planes. The coronal plane was most useful for charting borders that coursed predominantly in the rostrocaudal direction, sagittal sections were most useful for mediolateral coursing borders of the dorsal surface, and horizontal sections were most useful for mediolateral borders of the lateral and medial brain surfaces. Some areal borders have been included, even though architectonic distinctions have not been well documented here, either because these borders were well described in pervious publications, or because distinctions depend on previously published electrophysiological results. For example, the temporal anterior field, Ta, contains several auditory areas that have been defined electrophysiologically, but were not distinguished architectonically in the present study. In some of the diagrams of cortical areas in squirrels, these areas are depicted. Likewise, we did not find clear architectonic differences between part of the previously identified parietal lateral field, Pl, that contains the electrophysiologically identified second somatosensory area, S2 and remaining caudal region, but S2 is distinguished in some of the figures.

Results

The present results provide further evidence for the validity of several previously proposed subdivisions of cortex in squirrels (Kaas et al., 1972), while providing evidence for the modification of the boundaries of some areas, and evidence for other areas not previously described. The proposed areas are outlined on a dorsolateral view of a squirrel brain in Fig. 1f and in figures that follow. Descriptions of cortical areas, region by region, follow.

Occipital cortex

The occipital region of the grey squirrel comprises of three areas, 17, 18 and 19, following Brodmann's (1909) terminology (Fig. 6-10).

Primary visual area, Area 17. The striate area 17 is very distinct, and its borders are easily identified. The greater extent of area 17 in squirrels compared to other rodents can be appreciated in low magnification photomicrographs of coronal (Fig. 6) and sagittal brain sections (Fig. 7). Note that even at low magnification, the borders of area 17 are apparent in Nissl, zinc, PV, VGluT2 and SMI-32 preparations. Much of the border of area 17 is with the laterally adjoining area 18, or V2, where the distinctive laminar appearance of area 17 disappears (Fig. 6). Area 17 extends onto the medial wall and even well onto the ventral surface of the hemisphere where it is bordered by the agranular division of the retrosplenial cortex (Fig. 7). A rostral segment of area 17 is bordered medially by cortex presumed to be a subdivision of limbic cortex, termed area L after Kaas et al., 1972. A ventromedial portion of V1 is bordered by cortex widely described as

prostriata (PS) (e.g., Rosa, 1999). All borders of area 17 are sharp and easily identified in all the preparations used in the present study.

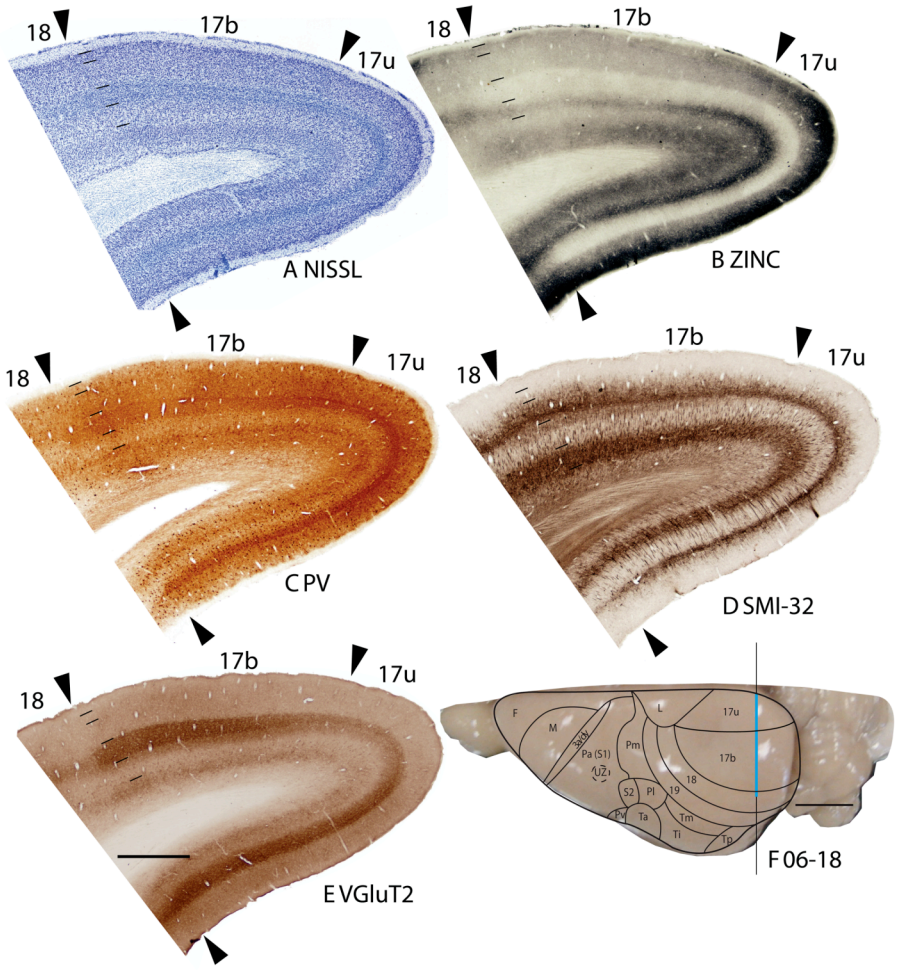

Figure 6. Architectonic characteristics of visual areas 17 and 18. Coronal sections from occipital cortex were processed for (A) Nissl substance, (B) synaptic zinc, (C) parvalbumin (PV), (D) neurofilaments with the SMI-32 antibody, or (E) the vesicle glutamate transporter 2 (VGluT2). The boundaries of proposed cortical areas are shown on a dorsal view of a squirrel brain in panel F. The vertical line through areas 17 and 18 indicates the locations where sections were taken for panels A-E. The blue line marks the regions shown in these sections. Occipital areas 17, 18 and 19 are adopted from Brodmann (1909). 17u refers to the monocular region, while 17b refers to the binocular region of area 17. Arrowheads mark architectonic boundaries. Short lines under 17/18 arrow heads separate cortical layers 1-6. See table 1 for abbreviations for other areas. The scale bar for brain sections (panel E) = 2mm. The scale bar on the brain (panel F) = 5mm. Sections were from squirrel 06-18.

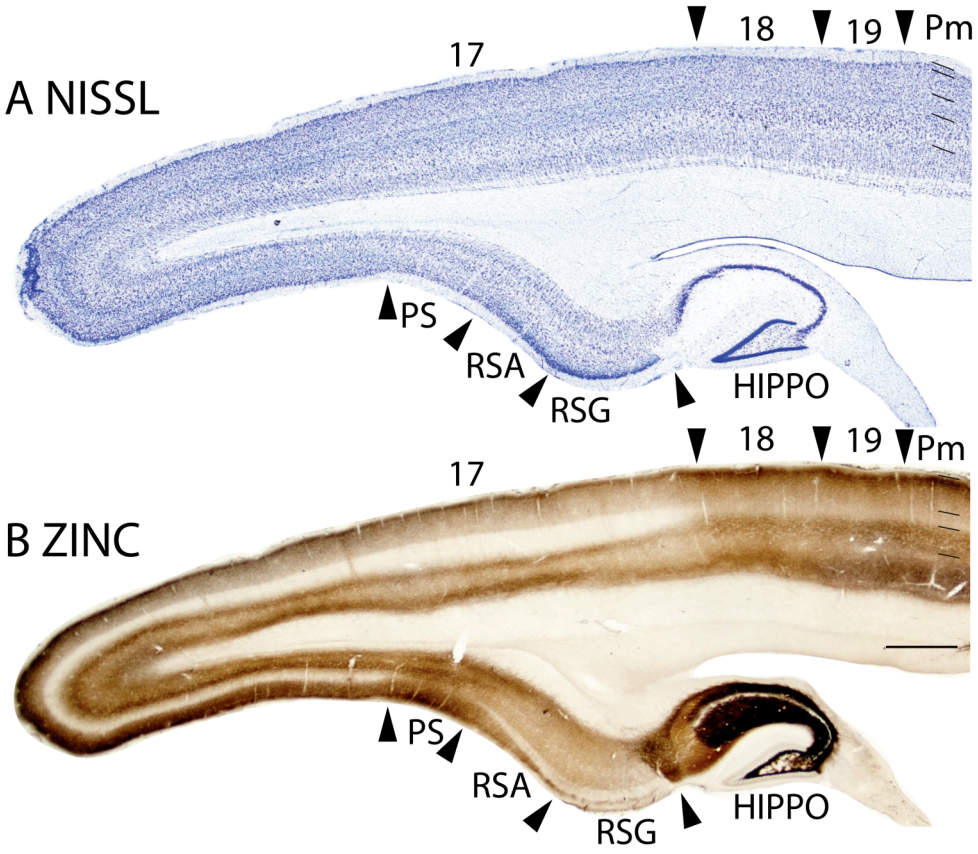

Figure 7. Architectonic characteristics of visual and adjoining retrosplenial cortex. Brain sections were cut in the parasagittal plane. The sections processed for Nissl substance (A) and zinc (B) were from near the medial wall of the caudal hemisphere. See table 1 for abbreviations. Scale bar = 2mm. Sections were from 05-19. 2. Architectonic characteristics of visual and adjoining retrosplenial cortex. Brain sections were cut in the parasagittal plane. The sections processed for Nissl substance (A) and zinc (B) were from near the medial wall of the caudal hemisphere. See table 1 for abbreviations. Scale bar = 2mm. Sections were from 05-19.

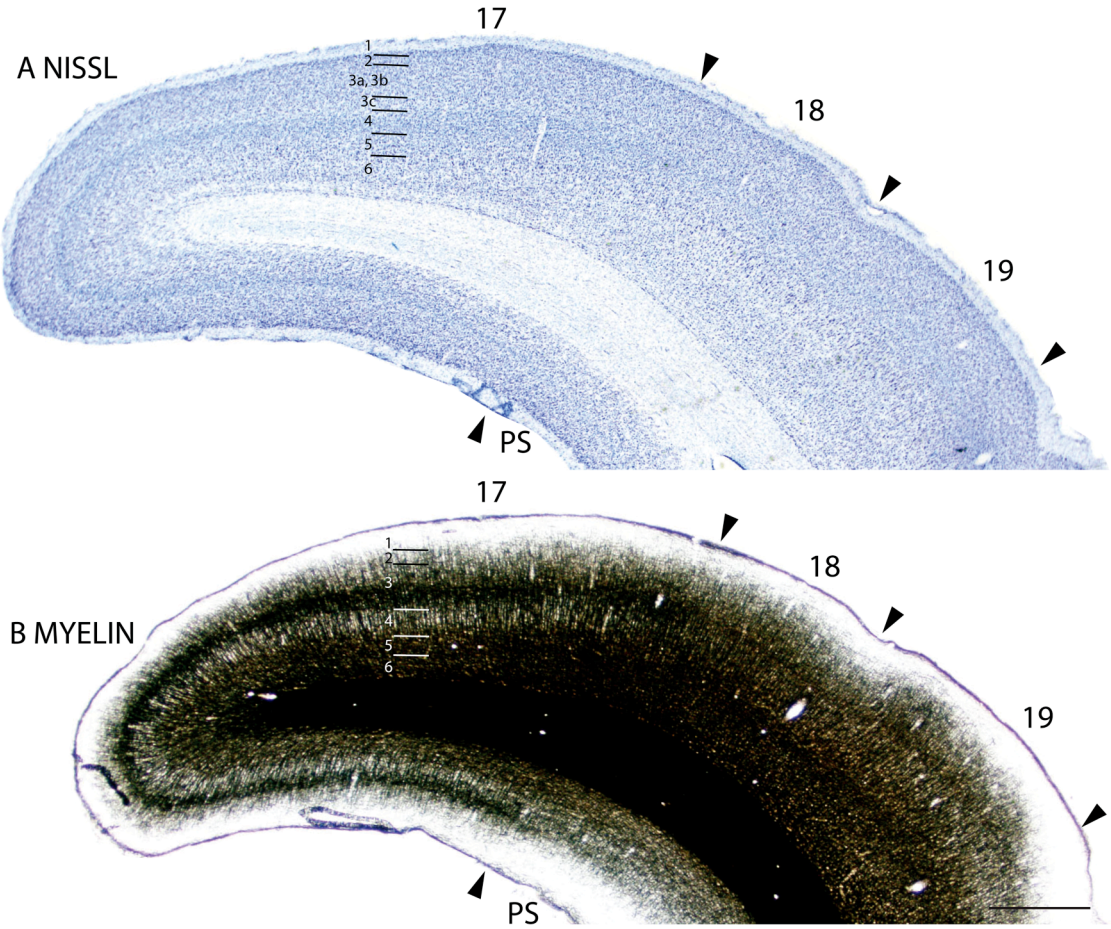

Figure 8. Adjacent coronal brain sections through occipital cortex stained for Nissl substance (A) or myelin (B). Scale bar = 2mm. Sections were from 06-60.

The myeloarchitecture of area 17 and other visual areas can be compared to the cytoarchitecture in figure 8. Note that the inner half of layer 3 of area 17 is occupied by a band of densely myelinated fibers, known as the outer band of Baillarger. This band corresponds to a light zone of more sparsely distributed cells in inner layer 3 in Nissl-stained sections (layer 3C). Layer 4 of area 17, in contrast, is lightly myelinated, with very few myelinated horizontal fibers. Layers 5 and 6 in area 17 are again densely myelinated. These two densely myelinated bands are characteristic of area 17 and other primary sensory areas in other mammals (e.g., Annese et al., 2004). While the outer band

of Baillarger, also known as the line of Gennari in area 17 is usually attributed to layer IVb of V1, comparative studies suggest that layer IVa and IVb of area 17 of anthropoid primates are actually sublayers of layer 3 (e.g., Hässler, 1966; see Casagrande and Kaas, 1994 for review). The outer band of Baillarger in area 17 of squirrels is external to layer 4 of densely packed granule cells and is thicker in the dorsal binocular portion than the ventral monocular portion of area 17.

The laminar pattern of staining in area 17 is more fully appreciated in brain sections shown at a higher magnification (Fig. 9). Nissl preparations (Fig. 9B) reveal a layer 4 that is densely populated with small cells that give it a dark appearance. In some regions, a lighter, more sparsely populated zone in the middle of layer 4 suggests that sublayers exist (Kaas et al., 1972). Medially, layer 4 thins (Fig. 6A) at the point where area 17 changes from being binocular to monocular (Hall et al., 1971). Laterally, layer 4 tapers somewhat near the border with area 18 (see Figs. 8, 9, 11), corresponding to a narrow transition zone that has callosal connections with the other cerebral hemisphere (Gould, 1984). Other layers in area 17 are also quite distinct in Nissl preparations. Layer 2 is densely populated with small cells. Layer 3 is broad and has a mixture of cell types, with an inner sublayer of less densely packed cells that has been identified as layer 3C in squirrels (Fig. 8A, 10A; Kaas et al., 1972). A similar sublayer has been identified in tree shrews (Jain et al., 1994) and monkeys (see Casagrande and Kaas, 1994 for review).

In Nissl preparations of areas 17 and 18 (Figs. 6, 9, and 11) and elsewhere, a narrow band of cells can be seen below layer 6. Reep (2000) has identified this deeper layer of cells in a range of mammalian species, including grey squirrels and other rodents, but not in cats and monkeys. This layer appears to consist of subplate cells that persist

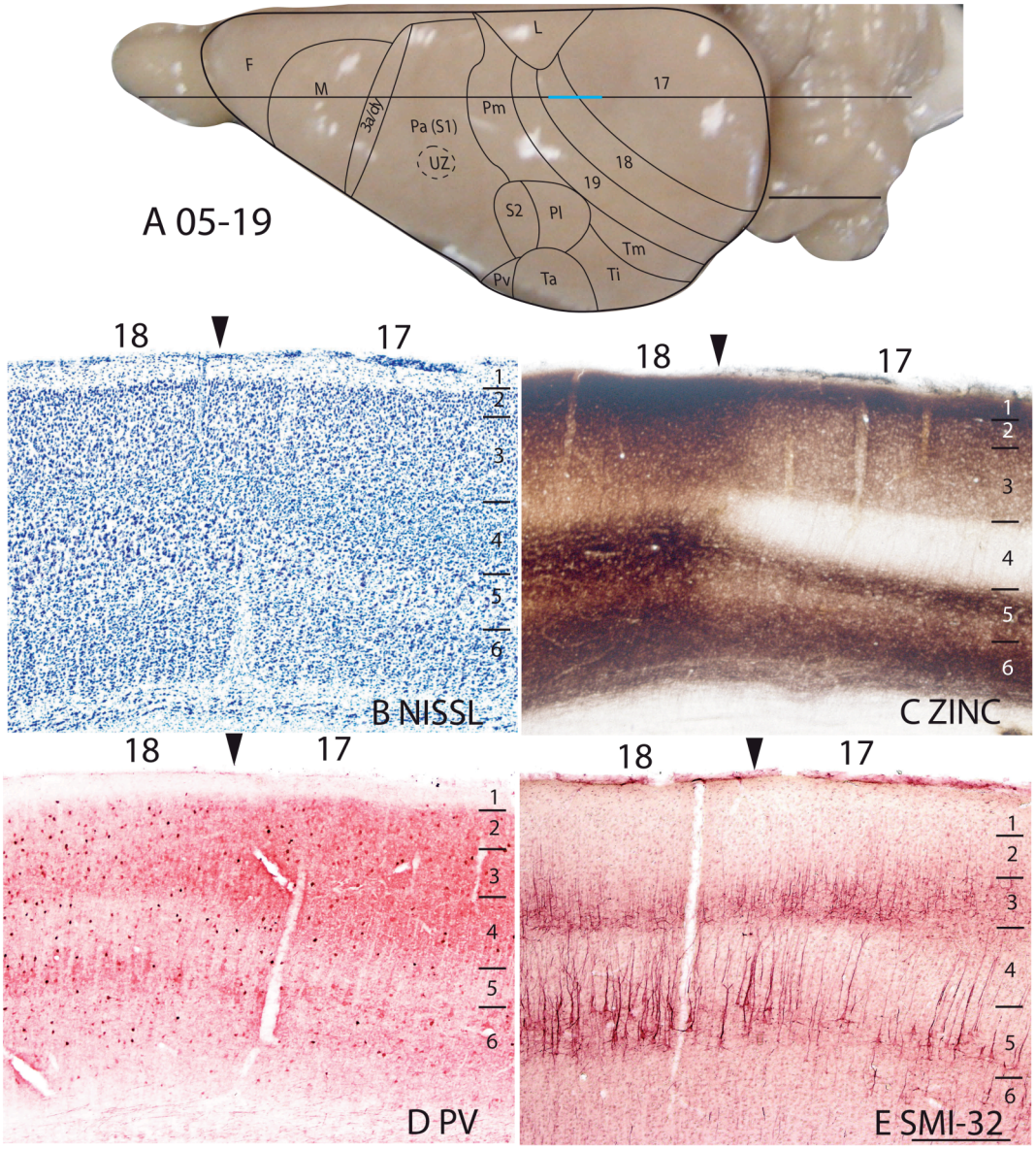

Figure 9. Architectonic characteristics of the bordering region between area 17 and 18. The horizontal line across the dorsal view of the brain in panel A indicates the location of the sagittal sections used in this figure, and the blue line marks the extent of the sections shown in panels B-E. The higher magnification of these panels than in previous figures allows some of the laminar features of area 17 and 18 to be seen more distinctly. The scale bar in panel A = 5mm, panel E = 0.5mm. Squirrel 05-19. The cortical areas depicted on the dorsal view of a squirrel brain in Panel A and similar views in subsequent figures are based on present and previous architectonic and physiological results (see Methods).

rather than undergoing apoptosis. In other preparations, area 17 is also distinct. In zinc preparations, layer 4 is nearly devoid of synaptic zinc, standing out as a white band (e.g., Figs. 7B, 9C). The adjoining area 18 and agranular retrosplenial area (RSA) have much more synaptic zinc in layer 4 (Fig. 7B). Layer 3, especially inner layer 3, and layer 6 of area 17 also express less synaptic zinc than the corresponding layers in adjoining cortex, but more synaptic zinc than layer 4 (Fig. 9C). The reduction of synaptic zinc in layers 3 and 6 suggests that a greater proportion of axon terminals in these layers represent thalamic inputs than in adjoining areas of cortex. The vesicle glutamate transporter, VGluT2, is densely expressed in layer 4, and to a lesser extent in layer 6 of area 17, so the extent of area 17 is very obvious in this preparation (Fig. 6E, 10C). Adjoining cortical areas express much less VGluT2 in these layers. The VGluT2 protein is expressed in the terminals of thalamocortical connections (Nahamani and Erisir, 2005). In a similar manner, PV is expressed at higher levels in layers 4 and 6 in area 17 compared to adjacent cortex (Figs. 6C, 9D, 10B), but the density contrast in these layers is less than that in VGluT2 preparations (Figs. 6E, 10C). PV preparations differed somewhat, with the section in Fig. 6C reflecting the staining of the thalamocortical terminals in layer 4, and to a lesser extent in layer 6, whereas the preparation in Fig. 9D more clearly stains the subset of GABAergic interneurons that express the calcium-binding protein, parvalbumin (Celio, 1986). The distribution of PV positive interneurons was similar in area 17 and 18 (Fig. 9D). SMI-32 labels dark bands of pyramidal neurons in layers 3 and 5, without labeling neurons in layer 4 (Figs. 6D, 9E). The stained pyramidal cells in layer 3 are largely within layer 3C, where they are much smaller than those in layer 5. Layers 4 and 6 express more cytochrome oxidase (CO) protein than other layers, and the layers

were more CO-dense in area 17 than in adjoining cortex (not shown). The distinctiveness of layer 4 in PV and VGluT2 preparations is shown at higher magnification photomicrograph in Fig. 5. Also note the greater expression of these proteins in layer 5b. In contrast, layer 5a expresses more calbindin (Fig. 10D).

In summary, area 17 is easily distinguished in most preparations in squirrels. Layer 4 is densely packed with granule cells, is lightly myelinated, expresses little synaptic zinc, is densely populated with PV- and VGluT2- immunoreactive thalamocortical terminations and lacks SMI-32 stained pyramidal cells. Layer 4 is thinner in the monocular than the binocular portion of area 17.

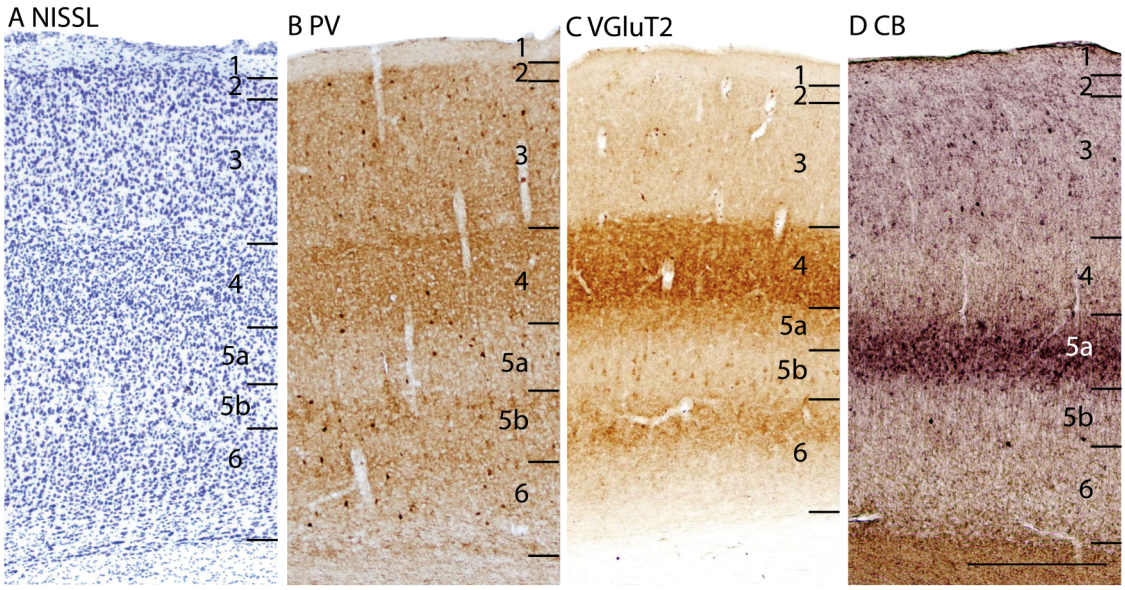

Figure 10. The laminar architecture of area 17 at higher magnification. Note how the PV, VGluT2 and CB preparations reveal sublayers. Scare bar = 0.5mm. Sections are in the sagittal plane, from case 05-19.

Area 18. The lateral border of area 17 in squirrels is bound by area 18, which corresponds to the second visual area, V2 (Hall et al., 1971). The representation of the contralateral visual hemifield in V2 approximates a mirror reversal of that in V1, and the

common border of V1 and V2 represents the zero vertical meridian through the center of gaze. Thus, area 18 (V2) borders area 17 along the complete representation of the vertical meridian (Hall et al., 1971), which extends from the rostral border of area 17 with area L, and continues caudally over the occipital pole and even somewhat onto the ventral surface of the hemisphere. As area 18 is only about 2mm wide, it forms a long band, with area 19 on its lateral border.

In Nissl preparations, the layers of area 18 are less distinct than those of either of the bordering areas, 17 and 19 (Figs. 6A, 7A, 8A, 9B). Layers 4 and 6 are less densely packed with cells, and these cells are less darkly stained then in area 17 and 19 (Fig. 7A, 9B) such that the density contrast between layers is lower. While layer 4 and, to a lesser extent, layer 6 in area 17 are relatively free of synaptic zinc, and therefore unstained in zinc preparations, there is only a moderate reduction of synaptic zinc in layers 4 and 6 of area 18. Hence, these layers are darker in area 18 than in area 17 (Figs. 7B, 9C). This indicates that there are fewer inputs to area 18 from the thalamus, especially the pulvinar (Robson and Hall, 1977), and more are from other areas of cortex, including dense layer 4 inputs from area 17 (Kaas et al., 1989). Area 19 resembles area 18 in zinc preparations, although slightly more synaptic zinc is expressed in layers 4 and 6. Layers 4 and 6 also express less PV and VGluT2 in area 18 than in area 17, and slightly less than in area 19 (Figs. 6C, 6E, 9D, 11C, 11E). Areas 17, 18 and 19 all have high levels of neuropil and pyramidal cell labeling in layers 3 and 5 in SMI-32 preparations, but the labeled zone in layer 3 is broader in binocular area 17 than in area 18 (Fig. 11D), whereas layer 5 of area 18 has somewhat larger pyramidal cells than area 17 (Fig. 9E). Area 18 is not densely myelinated as area 17 and has distinct bands of Baillarger than both areas 17 and 19 (Fig.

8B), and does not express high levels of CO in layers 4 and 6 (not shown). Overall, area 18 is one of the more clearly defined areas of the neocortex in squirrels. In the present preparations, area 18 was relatively uniform in appearance, without obvious architectonic subdivisions. However, in sections cut parallel to the cortical surface and stained for myelin, area 18 has a series of myelin-light patches along its length (Kaas et al., 1989). The patches receive most of the inputs from area 17, while the myelin-dense surround receive dense callosal inputs (Gould, 1984).

In summary, area 18 has a less densely packed layer 4 than area 17, and is less densely myelinated as well. Area 18 expresses less PV and VGluT2 in layers 4 and 6 compared to area 17.

Area 19. As noted above, area 19 has slightly more distinct lamination than area 18 in Nissl preparations as indicated by somewhat more darkly stained neurons in layers 4 and 6 (Figs. 7A, 8A; see Kaas et al., 1972 for more documentation). As several areas border area 19 laterally, the distinction between area 19 and these adjoining areas in Nissl preparations varies, but typically, layers 4 and 6 are more darkly stained in area 19 (Fig. 11A). In zinc preparations (Figs. 7B, 11B), middle layers express less synaptic zinc in area 19 than adjoining temporal mediodorsal area, Tm, and other layers have less synaptic zinc as well (Fig. 11B). Area 19 has higher PV and VGluT2 levels than more lateral cortex (e.g., Figs. 11C, 11E), and increased SMI-32staining in layers 3 and 5 (Fig. 11D). Overall, area 19 is not as well defined as area 18. The architectonic evidence, although not completely compelling, suggests that area 19 is a single subdivision of occipital cortex.

In summary, area 19 is more myelinated than area 18, and the neurons in layers 4 and 6 are more darkly stained in area 19 than area 18, giving area 19 a more distinct lamination pattern. In addition, area 19 stained more darkly for PV, VGluT2 and SMI-32 compared to the adjacent temporal areas.

Temporal Cortex

Temporal cortex in squirrels is a large region that contains areas devoted to visual and auditory functions. Kaas et al. (1972) divided the region into three large fields, an anterior temporal field, Ta, with auditory functions, an intermediate temporal field, Ti, possibly with auditory functions, and a posterior temporal field, Tp, with visual functions (Fig. 12). Ta includes the primary auditory field, A1, first identified by Merzenich et al., (1976), a rostral auditory field, R (Leutheke et al., 1988), as well as an intermediate (Ta_i) and a ventral (Ta_v) subdivisions. A redefined temporal mediodorsal region, Tm, was formerly considered to be a peripheral extension of area 19, 19p (Kaas et al., 1972), but pulvinar connections (see Fig. 1D of Robson and Hall, 1977) and architecture align this region more with Tp.

The temporal posterior region, Tp. Previously, Tp was characterized as a field with densely myelinated inner and outer bands of Baillarger (Kaas et al., 1972). In Nissl-stained sections, layer 4 is well developed. Although layer 4 is not developed to the extent seen in primary sensory areas, it is more prominent than in adjoining cortices (Figs. 11A, 12B). Tp stands out as a densely myelinated field (Fig. 12D), bordered rostrally and caudally by less myelinated fields, areas Ti and perirhinal cortex,

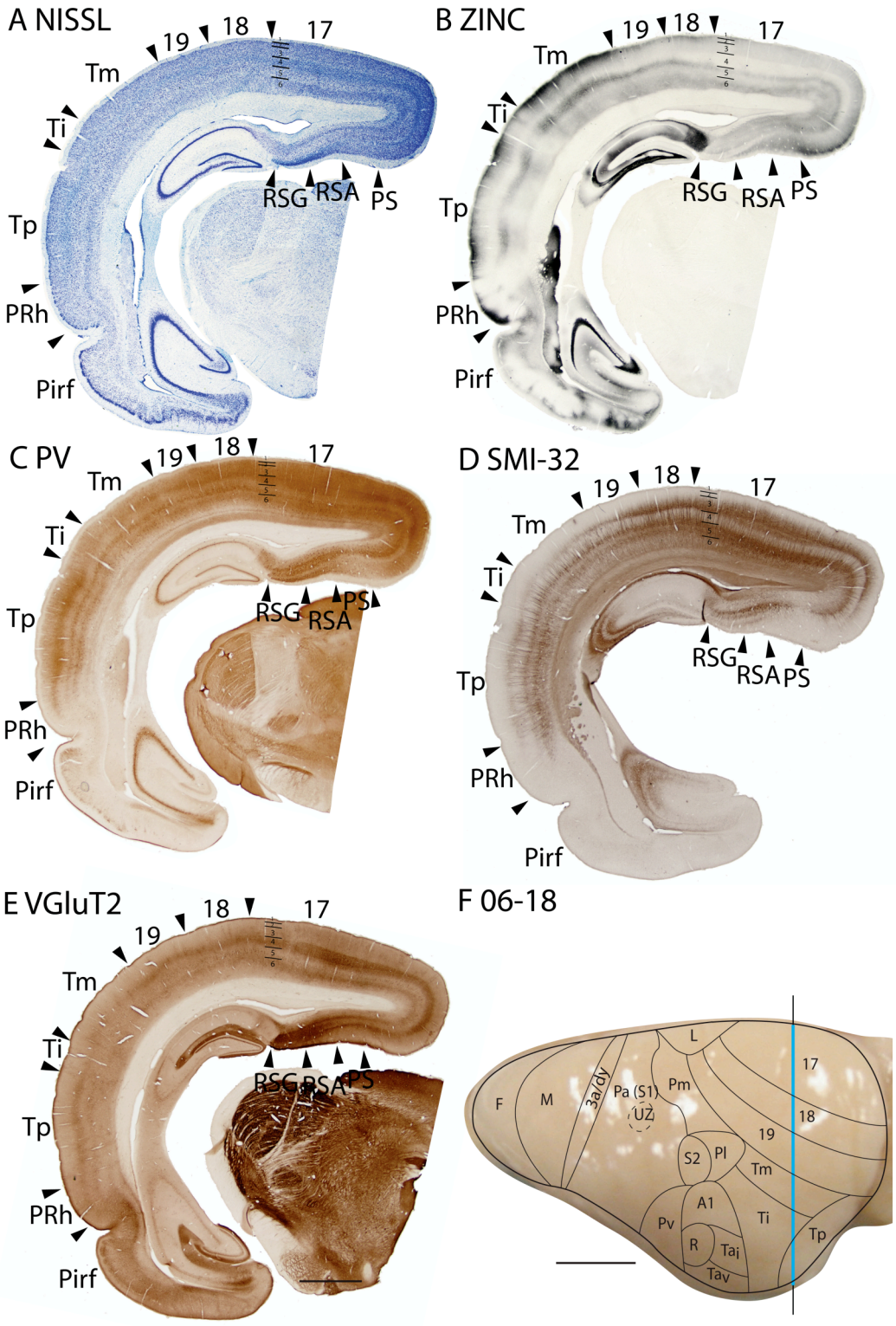

Figure 11. Architectonic characteristics of subdivisions of occipital and temporal cortex in squirrel 06-18. Borders of cortical layers are marked at the 17/18 boundary. The blue portion of the vertical line across the cortex indicates the location where the coronal brain sections in panels A-E were obtained. Scale bar in panel E = 2mm, panel F = 5mm.

respectively. In zinc preparations, Tp resembles primary sensory cortex in that layer 4 expresses little synaptic zinc and only moderate levels of synaptic zinc are present in outer layer 3, layer 2 and layer 5 (Figs. 11B, 12C). Tp also has features of sensory cortex in PV preparations, as layer 4 is much more darkly stained with PV-positive thalamocortical terminals than layer 4 in adjoining regions of cortex. There are also two thin PV-dense bands are present in layer 6 (Fig. 11C). In addition, Tp expresses high levels of VGluT2 in the thalamocortical terminations in layer 4 (Figs. 11E, 12E). Finally, SMI-32 processing reveals three distinct bands of labeled pyramidal cells in Tp, one in deep layer 3, one in layer 5, and another in deep layer 6 (Figs. 11D, 12F). Thus, Tp has architectonic features that are much like those of sensory cortex. Although Tp is not a primary sensory area, Tp does receive dense inputs from a caudal division of the visual pulvinar, which relays visual information from the superior colliculus (Robson and Hall, 1977).

The temporal mediodorsal region, Tm. Area Tm was previously defined as a distinct part of area 19, area 19p. We now include Tm as a separate field that has less distinct bands in layer 4 and 6 in VGluT2 preparations than adjoining area 19 and Tp, but more than in Ti (Fig. 11E). The darker appearance of Tm in zinc preparations suggests that Tm receives less dense thalamic inputs than area 19 or Tp (Fig. 11B). The SMI-32 band of smaller pyramidal cells is less densely stained in Tm than area 19 (Fig. 11D).

The temporal intermediate area, Ti. The large Ti region was originally characterized as a field of sparse myelination (Kaas et al., 1972). This feature is especially apparent in figure 12D, where a brain section in the horizontal plane was stained for myelin, allowing the adjoining myelin-dense Ta and Tp fields to be distinctly

contrasted with myelin-poor Ti. In Nissl preparations, layer 4 of Ti is less dense in appearance than in Ta and Tp, as neurons are less darkly stained and packed (Fig. 12B). Thus, Ti is easily distinguished from Ta and Tp in traditional Nissl and myelin preparations.

In our sections processed for zinc, Ti expresses more synaptic zinc, especially in layers 2, 3 and 5, than Ta and Tp (Fig. 12C). As there is a moderate level of synaptic zinc present even in layer 4, much of the input to Ti must come from other cortical areas, rather than the thalamus. Ti expresses only low levels of PV (not shown) and VGluT2 (Fig. 12E). The SMI-32 preparations reveal few darkly stained pyramidal cells (Fig. 12F). Overall, Ti can be reliably distinguished from Ta and Tp. The lack of architectonic characteristics of sensory fields suggests that Ti receives relatively few inputs from the thalamus and likely functions as a higher-order processing area.

Region Ta and its subdivisions. In Nissl and myelin preparations, Ta was described as a region where a broad layer 4 was densely packed with small, darkly stained neurons, whereas prominent outer and inner myelinated bands of Baillarger occupied inner layer 3, and layers 5 and 6 respectively (Kaas et al., 1972). However, these features were not uniform in Ta, as they were more pronounced in dorsal than in ventral Ta. Subsequently, Luethke et al., (1988) demonstrated that dorsal Ta corresponds to two primary auditory areas, the rostral area, R, and the caudal area, A1. In addition, intermediate (Ta_i) and ventral (Ta_v) divisions of Ta were identified by connections as secondary auditory areas. Our observations from Nissl and myelin preparations (Figs. 12B, 12D) agree that layer 4 is more developed in the A1 and R regions of Ta (R is actually more ventral than rostral to A1), and that A1 and R are more myelinated than

other parts of Ta. Areas A1 and R are very similar in Nissl and myelin preparations. Thus, the outlines of these areas (Fig. 12A) are estimates based on the microelectrode mapping results of Luetheke et al. (1988).

In zinc preparations, A1 and R express little synaptic zinc, and layers 4, 6 and inner layer 3 are almost devoid of staining (Fig. 12C). This is expected for primary sensory cortex with dense thalamic projections from the medial geniculate complex. More ventral portions of Ta also have little synaptic zinc, although more than in A1 and R. A1 and R also show higher expression of PV than adjoining areas Ti and Pv (not shown). As layer 4 is densely stained, and layers 6 and inner 5 are moderately stained, this part of Ta stands out as a field with these PV-dense bands. Layer 3 is also moderately stained. Layer 4 of dorsal Ta also expresses more VGluT2 than adjoining areas (Fig. 12E). In SMI-32 preparations, stained pyramidal cells and their apical dendrites are densely stained in inner layer 3, outer layer 5 and inner layer 6, such that three dense bands of labeled cells are apparent (Fig. 12F).

Overall, region Ta is very distinct from surrounding cortex in a number of preparations, including those for myelin, zinc, PV and SMI-32. The dorsal part of Ta is more sharply and distinctly defined than the ventral part, but no obvious difference is detected between the territories of A1 and R in dorsal Ta.

Parietal Cortex

Parietal cortex includes areas that can be considered to be primarily somatosensory in function (Figs. 13, 15). These include the parietal anterior area, Pa(S1), which corresponds to the primary somatosensory area, S1 (Sur et al., 1978). A strip of

dysgranular cortex, 3a/dy, borders Pa(S1) rostrally, separating Pa(S1) from motor cortex. The parietal medial area, Pm, forms the medial half of the caudal border of Pa(S1). The parietal lateral area, Pl, of Kaas et al. (1972) is retained here, but subdivided into a rostral half that is coextensive with second somatosensory area, S2 (Nelson et al., 1979), and a caudal half that has uncertain functions. The parietal ventral area, Pv, just ventral to S2, is a secondary somatosensory area first identified in squirrels (Krubitzer et al., 1986).

Anterior parietal cortex, Pa or S1. Pa(S1) is the largest division of the parietal cortex. The area has all the characteristic features of a primary sensory cortex, but the area is also not homogenous in structure. Instead, Pa(S1) is disrupted by zones of dysgranular cortex that relate to the way the contralateral body surface is represented in S1 (Sur et al., 1978; Krubitzer et al., 1986; Gould et al., 1989). In brief, a large, circular dysgranular zone with narrow rostral extensions separates the representation of the forepaw from that of the face (Figs. 13A, B, and C). A second narrow ventral extension separates the representation of the upper lip from that of the lower lip. The large circular part of the dysgranular zone was termed the unresponsive zone (UZ) in microelectrode recording experiments (Sur et al., 1978), as neurons in this zone failed to respond to light tactile stimulation in anesthetized squirrels. The location of the UZ is indicated on the illustrations of the cortical areas on the squirrel brain in Fig. 11F and other subsequent figures. In all preparations, the UZ and its narrow extensions have the histological features of dysgranular cortex rather than primary sensory cortex. As such, it is possible to consider this dysgranular cortex as outside of S1, and part of area 3a/dy. However, both S1 proper and the embedded dysgranular zone are included here as parts of Pa(S1).

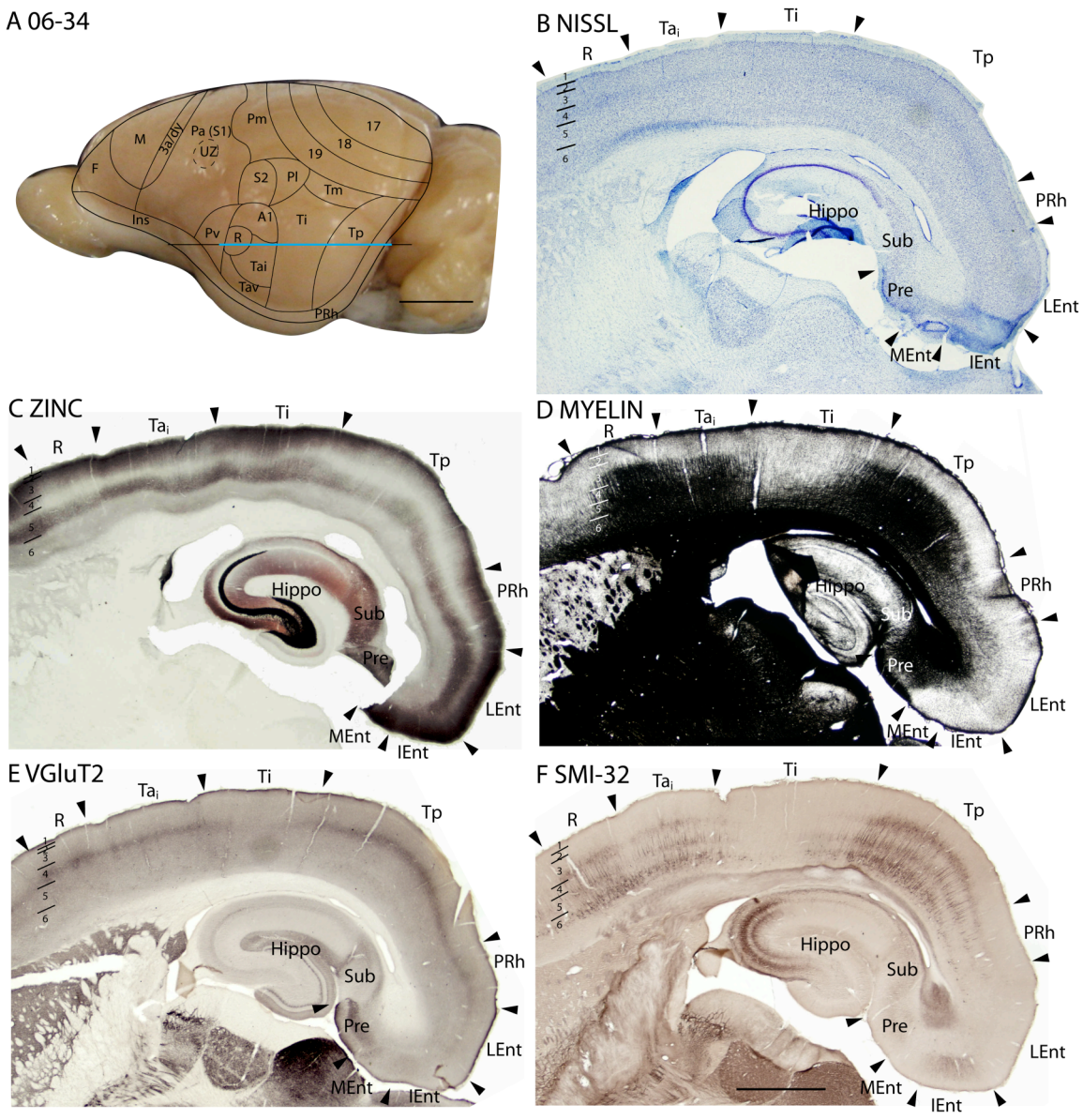

Figure 12. Architectonic characteristics of subdivisions of temporal cortex in squirrel 06-34. Cortical areas are shown on a lateral view of the left caudal hemisphere in panel A. The blue part of the horizontal line across the brain indicates the location of the horizontal brain sections illustrated in panels B-F. Scale bar in panel A = 5mm, panel F = 2mm.

In addition to the UZ, and its rostral and ventral extensions, brain sections cut parallel to the surface of flattened cortex reveal a modular organization that is similar to that described in rats (Dawson and Killackey, 1987; Remple et al., 2003), but not as

clearly expressed (also see Woolsey et al., 1975). These modules constitute small zones where CO (Fig. 13D), or PV (Figs. 13C, E) is densely expressed. These zones are separated by narrow septa, where little CO or PV is expressed, as in the UZ and its extensions. In rats, such modules correspond to semi-isolated groups of body surface mechanoreceptors related to individual whiskers and other body hairs, as well as segregated parts of the body, such as pads on the palm and segments of digits. In squirrels, a correspondence of specific CO or PV modules in Pa(S1) with receptor groups in the skin has not yet been established, but they exist in the regions representing mystacial vibrissae and the hairs of the buccal pad (upper lip) and lower lip. In rats, and other rodents, the modules representing individual mystacial vibrissae are called barrels (Woolsey and Van der Loos, 1970).

Previously, Pa(S1) has been described from Nissl-stained sections as having a distinctive layer 4 that is densely packed with darkly stained cells, and darkly stained outer and inner bands of Baillarger in sections stained for myelin (Kaas et al., 1972). In agreement with these earlier findings, Pa(S1) proper has a thick layer 4 that is densely packed with small cells (Fig. 14A). This feature is more pronounced in Pa(S1) than in adjoining cortical areas. Thus, a border between Pa(S1) and Pm is obvious in Nissl-stained sections (Fig. 15B, 18A). A similar distinction is apparent between Pa(S1) and the dysgranular cortex along the rostral border of Pa(S1) (Fig 16B). The transition from Pa(S1) to Pv is somewhat different, in that layer 4 is somewhat thinner, but also denser in Pv (Fig. 17B). In sections stained for myelin, the inner and outer bands of Baillarger are darker in Pa(S1) than in adjoining cortex (Fig. 17C). Pa(S1) can also be seen as more densely myelinated than surrounding cortex in favorable sections cut parallel to the

surface of flattened cortex, whereas the UZ and its ventrolateral extensions are less myelinated and resemble 3a/dy (Figs. 13A, B).

In brain sections processed for synaptic zinc, Pa(S1) clearly stands out as a primary sensory area. A broad middle zone, corresponding to layer 4 and the deepest part of layer 3, expressed little synaptic zinc, indicating that many of the synaptic terminals in these layers belong to zinc free inputs from the thalamus (Figs. 15C, 16C, 17D, 18B). Pa(S1) is known to receive dense inputs from the ventroposterior nucleus (Krubitzer and Kaas, 1987). A narrower layer 4 stains darker in adjoining cortex, indicating more synaptic zinc and fewer thalamic inputs. A comparative reduction of synaptic zinc was also apparent in layer 6 of Pa(S1), indicating the presence of more thalamic inputs to this layer in Pa(S1) than in adjoining areas.

Pa(S1) is apparent as an area with a denser expression of PV in layer 4 than neighboring areas. This feature of Pa(S1) is best seen in the low magnification photomicrograph in Fig. 14E (also see Figs. 16D, 18C), where labeled thalamic afferents form a band in layer 4 and to a lesser extent in inner layer 3, as well as bands in layers 5 and 6. Distribution of PV-positive GABAergic neurons and their neuropil does not differ much between Pa(S1) and other areas. Pa(S1) expresses more VGluT2 in layer 4 than in adjoining cortex (Figs. 14D, 17F, 18E), but a clear difference between Pa(S1) and adjoining sensory areas (S2 and Pv) is not always apparent. In Pa(S1), the SMI-32 antibody labels pyramidal neurons and their apical dendrites in inner layers 3 and layer 5, so that two distinct bands are apparent (Fig. 16E, 17E, 18D). A deeper staining of neurons in layer 6 may be apparent in some preparations (Fig. 17E). Overall, Pa(S1) does not stand out from adjoining parietal areas in SMI-32 preparations.

Figure 13. Barrel field of the grey squirrel. A. A myelin stained section cut parallel to the surface of an artificially flattened cerebral hemisphere. Dashed lines show approximate cortical boundaries comparable to the reconstructed dorsal view of the brain in Fig. 1. The boxed region in A is shown in B and C at higher magnification in myelin and PV preparations respectively. D and E are from a separate case and show the barrel field in cytochrome oxidase (CO) and PV preparations respectively. See table 1 for abbreviations. Scale bar for flattened section = 2.0mm, for B and C = 1.0mm, for D and E = 2.0mm.

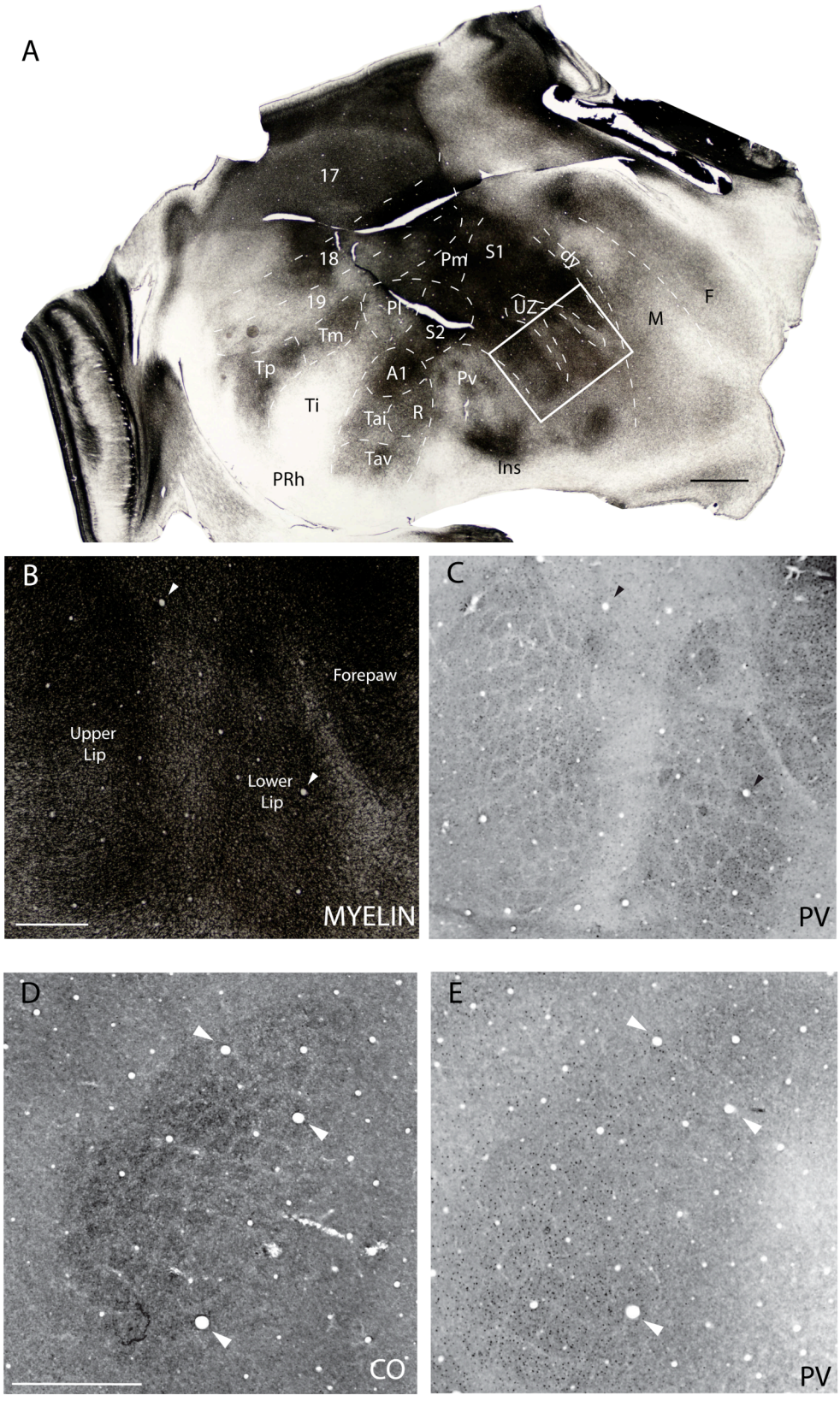
A
17
18
19
Pm
S1
Pl
UZ
S2
Tm
Tp
A1
Pv
Ti
Tai
R
Tav
PRh
Ins
M
F
B
Forepaw
Upper
Lip
Lower
Lip
MYELIN
C
PV
D
CO
E
PV

When viewed at higher magnification, the various preparations used in the present study reveal several obvious sublayers in Pa(S1) (Fig. 14). The Nissl-stained section shows that layer 4 is densely packed with small granule cells, whereas the adjoining sublayer 3c is less densely packed with cells than either layer 4 or the outer layer 3. This situation is similar to that observed in area 17 (Fig. 10A). Likewise, the dense myelination of the outer band of Baillarger is clearly co-extensive with sublayer 3c as defined in Nissl preparations, which is again similar to that of area 17 (Fig. 8B). As with other sensory areas, CO expression is most dense in layer 4 of Pa(S1), but layer 6a is also dense. PV-positive neuropil is nicely concentrated in layer 4, reflecting the terminations of PV-positive relay cells in the ventroposterior nucleus, whereas less dense neuropil staining is observed in layers 5b and 6b. VGluT2 neuropil densely populates layer 4, while extending somewhat into inner sublayers of layer 3, suggesting the presence of thalamic inputs, in addition to those from the ventroposterior nucleus. Pa(S1) also receives inputs from the posteriomedial nucleus (Krubitzer and Kaas, 1987), which possibly contributes to the VGluT2-positive staining in layer 3. The synaptic zinc-poor regions of Pa(S1) also suggest a distribution of thalamocortical terminations that is broader than layer 4, as the deeper sublayers of layers 3 and 6 are zinc-poor, whereas layers 2, outer 3 and 5B are synaptic zinc-rich. Layer 4 is CB-poor (Fig. 14F).

In summary, Pa(S1) is characterized by histological features that are typical of primary sensory cortex, including a thick layer 4 that is densely packed with small cells, and prominent inner and outer bands of Baillarger in myelin stains. The zinc stain reveals a layer 4 with little synaptic zinc and zinc poor bands in layer 6. The PV-positive thalamocortical afferents terminate in a similar laminar pattern. Pa(S1) also demonstrates

specializations not found in other primary sensory areas, including a large dysgranular zone (UZ), with radiating dysgranular septa that separate the representations of body

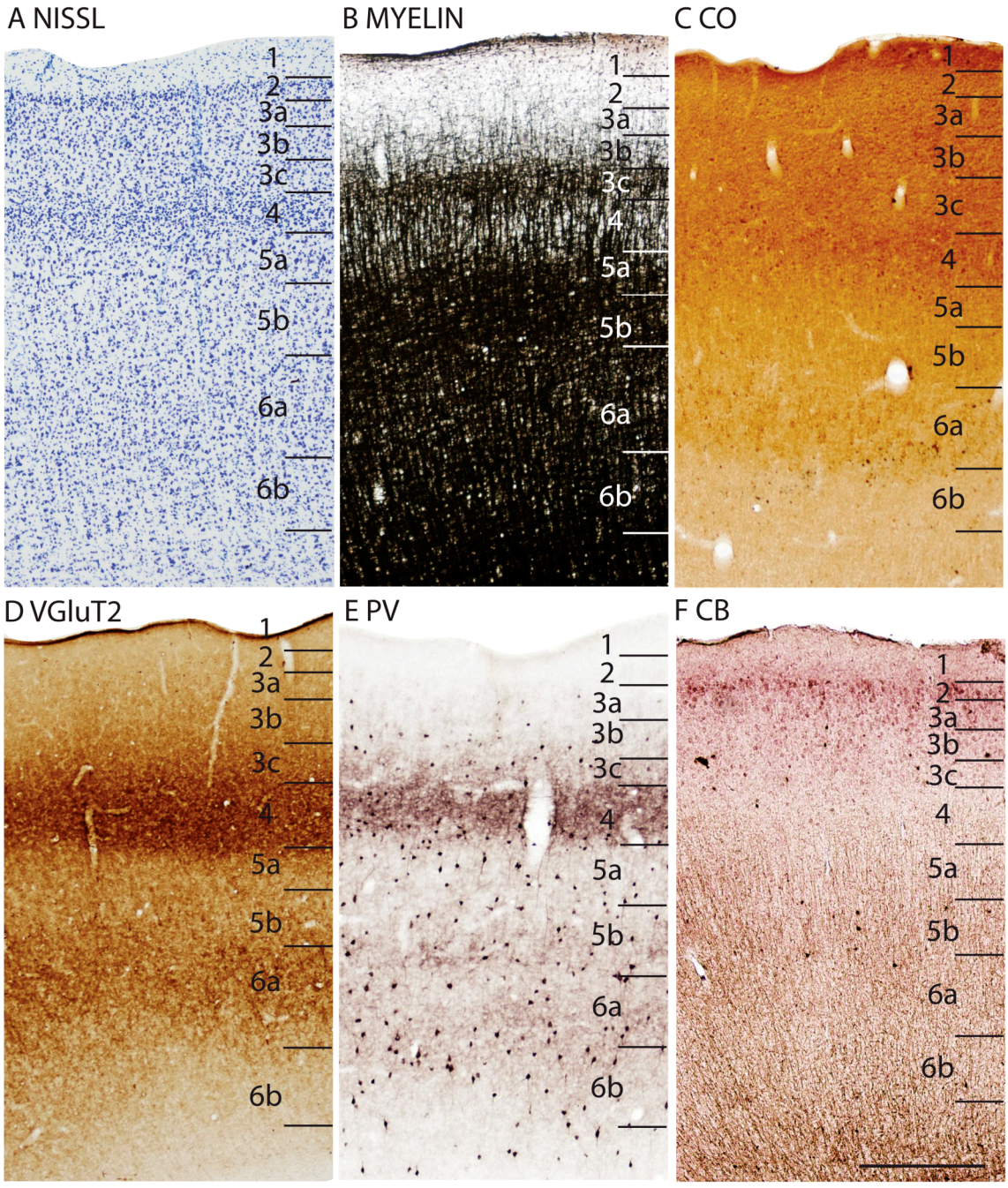

Figure 14. The laminar architecture of area Pa(S1) at higher magnification. Scale bar = 0.5mm.

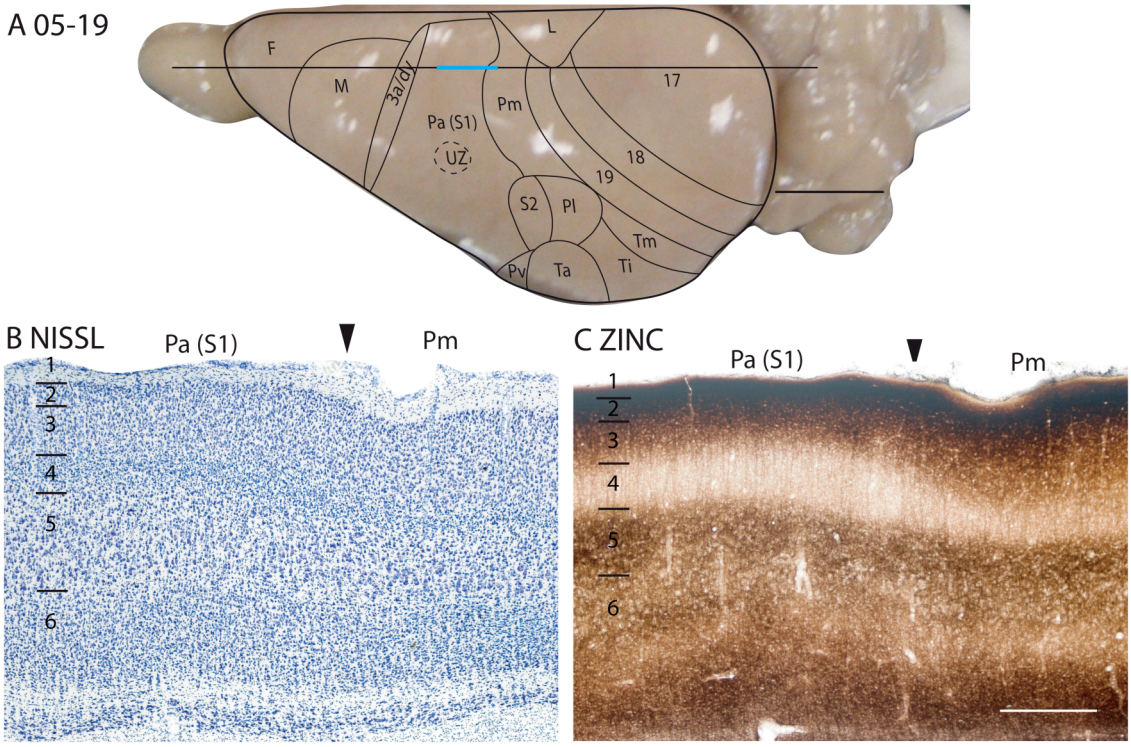

Figure 15. Architectonic characteristics of subdivisions of the somatosensory cortex in squirrel 05-19. The horizontal line across the dorsal view of the brain in panel A indicates the location of the sagittal sections used in this figure, and the blue line marks the extent of the sections shown in panels B and C. The extent of each cortical layers 1 to 6 is indicated by the short horizontal lines on panels B-E. The scale bar on the brain (panel A) = 5mm. The scale bar for brain sections (panel E) = 0.5mm.

parts that are adjacent in S1, but separated on the receptor sheet (skin). Similar separating septa have been described in S1 of various mammals (see Qi and Kaas, 2004, for review). In addition, a modular organization in parts of S1, best seen in brain sections cut parallel to the surface, corresponds to those seen in the barrel field and other parts of S1 in rats and other rodents.

Area Pm. The parietal medial area, Pm is a subdivision of cortex between Pl rostrally, area 19 caudally, limbic L medially, and S2/Pl, laterally. In general, Pm lacks distinctive characteristics, as with other secondary or higher-order sensory fields. Due to

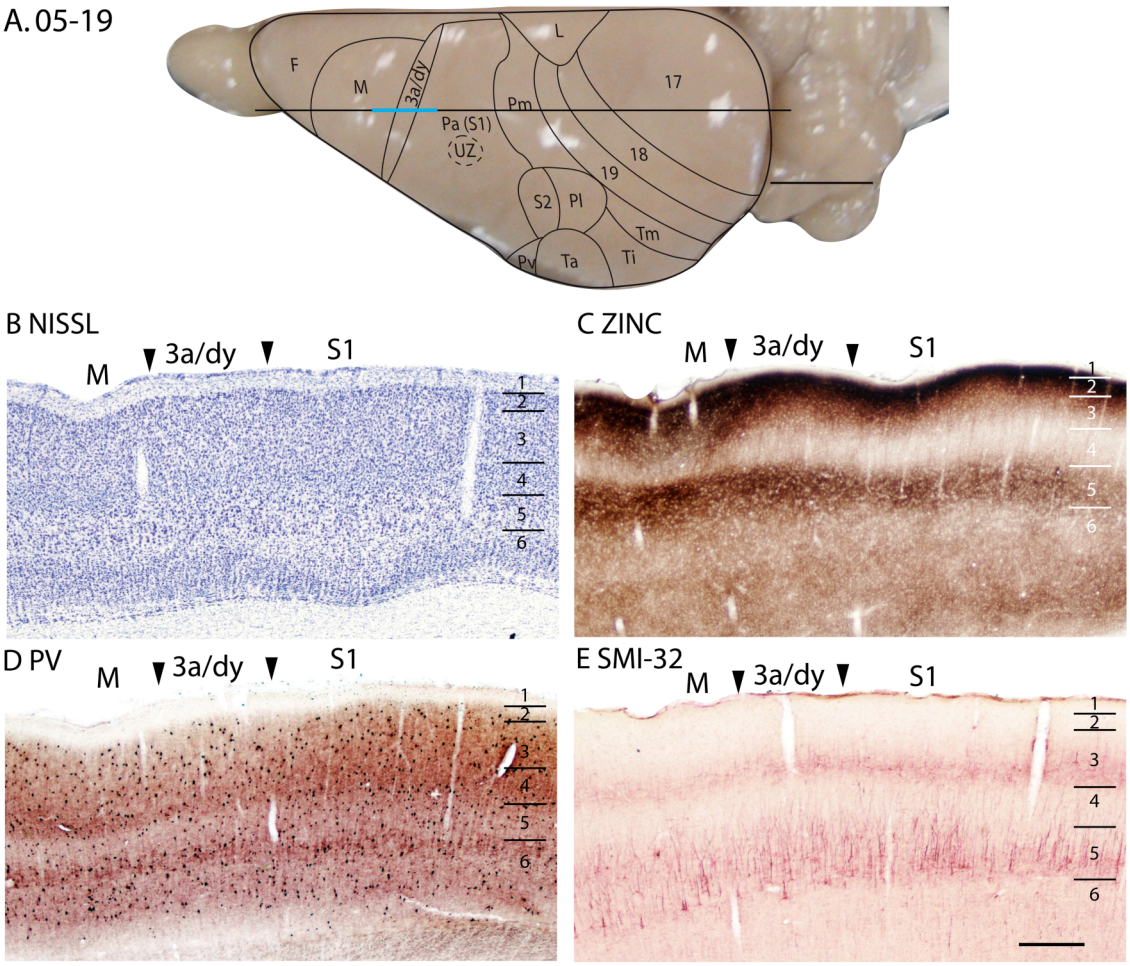

Figure 16. Architectonic characteristics of subdivisions of the motor and somatosensory cortex in squirrel 05-19. The horizontal line across the dorsal view of the brain in panel A indicates the location of the sagittal sections used in this figure, and the blue line marks the extent of the sections shown in panels B-E. The extent of each cortical layers 1 to 6 is indicated by the short horizontal lines on panels B-E. Scale bar on the brain (panel A) = 5mm. Scale bar for brain sections (panel E) = 0.5mm.

the lack of marked identifying features, Pm possibly contains more than one functional division. In Nissl preparations, layer 4 is thinner and less pronounced than in Pa(S1) (Figs. 15B, 18A). The Pm and limbic (L) border is marked by the lack of a distinctive laminar pattern in L in the Nissl stain, whereas the lateral border with the parietal lateral area (Pl/S2) shows an increase in the thickness of layer 4 in Pl/S2. Pm expresses more

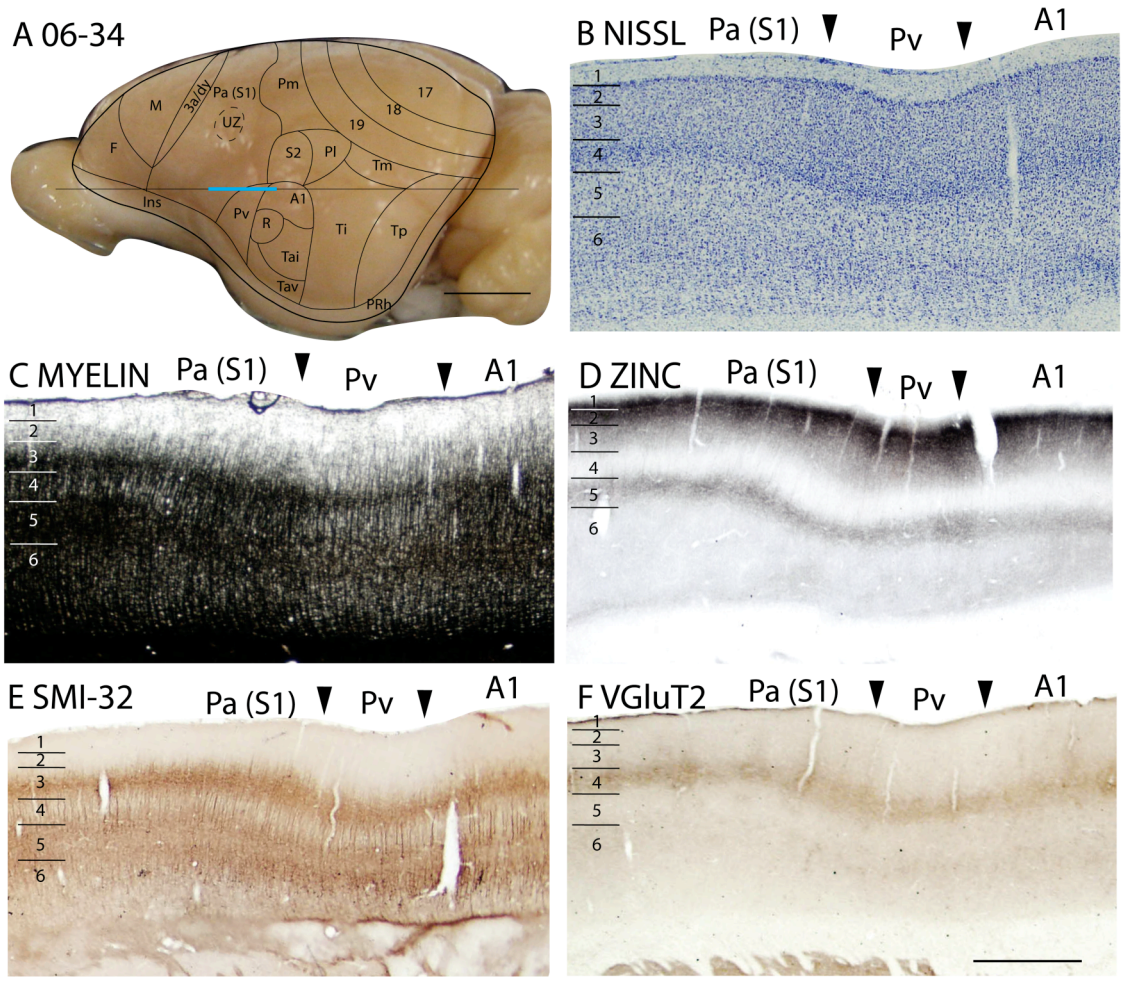

Figure 17. Architectonic characteristics of subdivisions of parietal and primary auditory cortices in squirrel 06-34. Cortical areas are shown on a lateral view of the left hemisphere in panel A. The blue horizontal line across the brain indicates the location of the brain sections illustrated in panels B-F. Short horizontal lines on panels B-F indicate the extent of the 6 cortical layers. Scale bar on the brain (panel A) = 5mm. Scale bar for brain sections (panel F) = 1mm.

synaptic zinc than Pa(S1) (Figs. 15C, 18B), especially in layer 4, but also in layers 3 and 6. However, Pm has similar levels of synaptic zinc with area 19, except in layer 6 where Pm has a slightly increased synaptic zinc expression. In VGluT2 preparations, Pm is distinct from area L, as layers 4 and 6 of area L express much less of the vesicle glutamate transporter protein (Fig. 18F). Layer 3 stains less darkly for PV in Pm than in either Pa(S1) or L, and outer layer 6 is more darkly stained in L than Pm (Fig. 18C).

Pl/S2 has a darker, more prominent inner layer 3 in PV stain than Pm. In most preparations, Pm has obvious borders with L and Pa(S1), a reasonably clear border with Pl/S2, and a somewhat uncertain border with area 19.

Pl(S2) and Pv. The second somatosensory area, S2, occupies much of Pl, whereas the more ventrally located Pv constitutes an additional somatotopic representation of the contralateral cutaneous mechanoreceptors (Krubitzer et al., 1986). In Nissl preparations, Pl/S2 has a thinner layer 4 than Pa(S1) and with a lower packing density of cells in both layer 4 and layer 6 (Fig. 18A). In myelin preparations, Pl/S2 has a more distinctive outer band of Baillarger than area 19, but is less myelinated overall than Pa(S1) (not shown). The lateral border between Pl/S2 and Ti stands out clearly with a decrease in myelination in Ti and an increase in myelination in A1 (not shown). In the zinc stain, Pl/S2 has more synaptic zinc expression in all layers than Pa(S1) (Fig. 18B), suggesting a greater proportion of cortical inputs. However the zinc staining is not homogenous, as the caudal part of Pl/S2 shows an increase in zinc staining across the layers. The border between Pl/S2 and area 19 is marked by the increase in zinc staining especially in the supragranular layers in Pl/S2. In the VGluT2 preparations, Pl/S2 show staining in layers 4 and 6 that is as pronounced as that in Pa(S1) (Fig. 18E). The pyramidal cells in inner layer 3 of Pl/S2 are less darkly stained in SMI-32 preparations than in Pa(S1) (Fig. 18D). In PV preparations, layer 4 of Pl/S2 is thinner and more lightly stained, whereas the outer layer 6 is more lightly stained than in Pa(S1) (Fig. 18C). A reduction in myelin stain marks the border of Pl/S2 with Ti (see Fig. 12F for the sparse myelination of Ti). With the staining preparations used here, the border between Pl/S2 and area 19 is not dependably determined. In general, most stains define Pl/S2 as an area that lacks the

characteristics of a primary sensory area, allowing it to be reliably distinguished from Pa(S1) and A1.

Area Pv has a thinner layer 4 in the Nissl-stained sections (Fig. 17B) and less myelinated inner and outer bands of Baillarger in myelin-stained sections (Fig. 17C) than adjoining areas, Pa(S1) and Ta. The moderate zinc staining across the layers in Pv (Fig. 17D) suggests that Pv receives more cortical inputs, although thalamic inputs to layer 4 do exist (Krubitzer et al., 1986). Layer 4, and inner and outer layer 6 stain less darkly for PV in area Pv compared to areas Pa(S1) and Ta (Fig. 18C). Area Pv has less VGluT2 expression as well (Fig. 17F, 18E). In SMI-32 preparations, Pv is not distinct from adjoining cortical areas (Figs. 17E, 18D). The architectonic characteristics of Pv, as shown by the stains used here, are consistent with the view that the parietal ventral area (Pv) is a secondary rather than a primary sensory area.

The dysgranular strip (3a/dy). A dysgranular strip of transition cortex, lies between the areas M and Pa(S1). As this dysgranular strip resembles area 3a of cats (Dykes et al., 1980; Felleman et al., 1983; Dykes et al., 1986; Avendaño and Verdu, 1992) and primates (Jones and Porter, 1980; Huffman and Krubitzer, 2001; Krubitzer et al., 2004) in location, shape and architectonic characteristics, we label the region 3a/dy. In Nissl preparations, 3a/dy combines, in a muted form, some of the laminar characteristics of M and Pa(S1). A layer 4 of granular cells is present in 3a/dy, but it is less pronounced than in Pa(S1). Layer 5 pyramidal cells are larger in 3a/dy than in Pa(S1), but not as large as in M. Layer 5 of 3a/dy is also much thinner than that of M (Fig. 16B). Layer 3 of 3a/dy is less myelinated than Pa(S1) (Fig. 19D). In the zinc stain,

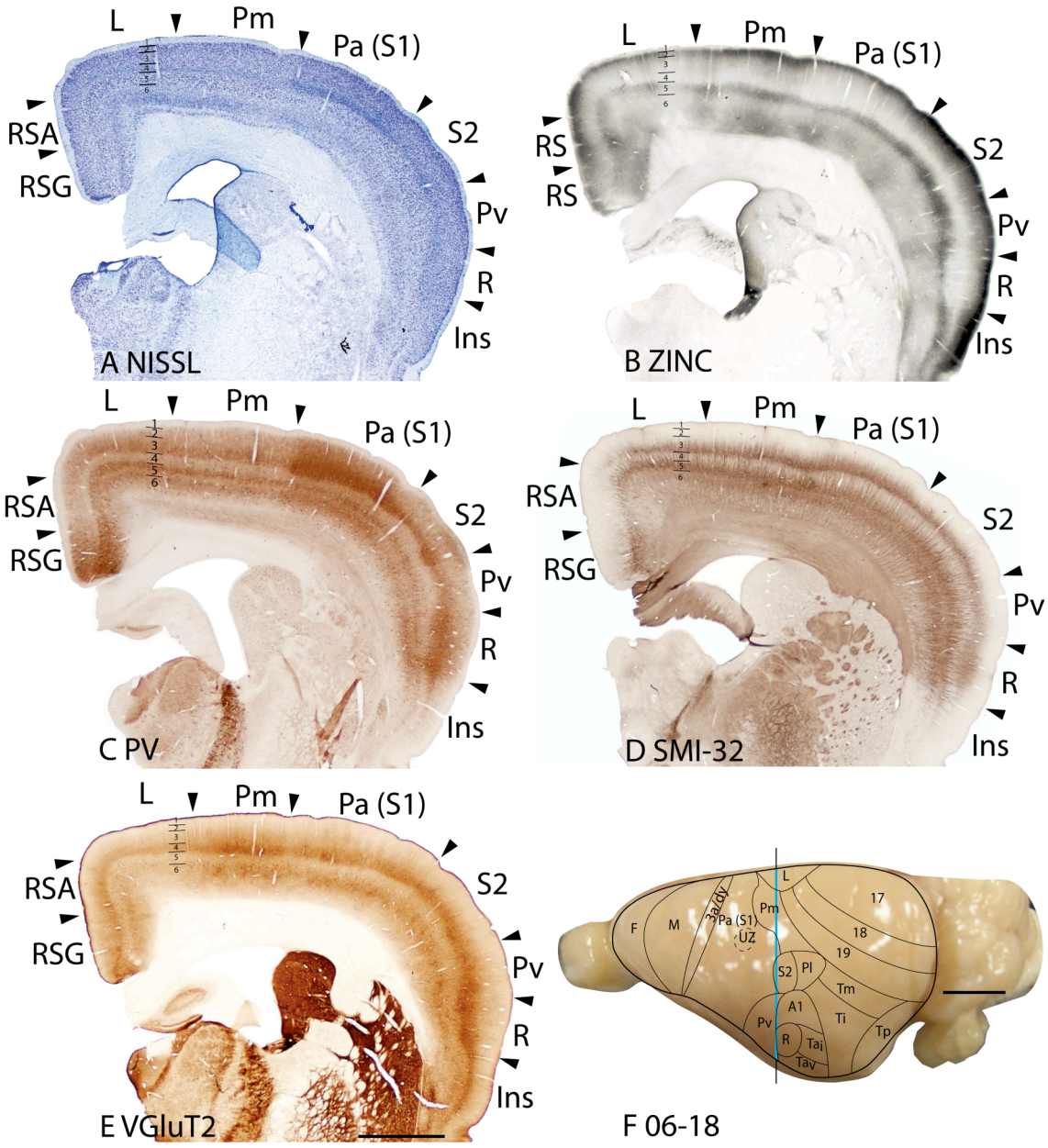

Figure 18. Architectonic characteristics of subdivisions of the parietal and limbic cortices in squirrel 06-18. Borders of cortical layers are marked at the limbic (L) area. The blue vertical line across the cortex (panel F) indicates the location where the brain sections in panels A-E were obtained. Short horizontal lines on panels A-E indicate the extent of the 6 cortical layers. Scale bar in panel E = 2mm, panel F = 5mm.

3a/dy has more staining than Pa(S1) in layers 4 and 5, although the intensity of staining in those layers is lower than that of M (Figs.16C; 19C; 20C). Area 3a/dy also has less dense staining of layers 4 and 6 in sections prepared for PV (Figs. 16D; 20D) and

VGluT2 (Fig. 19E) than Pa(S1). However, in the more lateral sections, dy showed concentrations of PV stain in layer 4 and inner 3, and inner and outer layer 6, similar to, but to a lesser extent, the tri-banded appearance of Pa(S1) in PV preparations. This results in a more distinct border between dy and M, as dy shows higher PV expression in those layers than M (Fig. 20D). In layer 5 of dy, pyramidal cells immunoreactive for the SMI-32 antibody had larger cell bodies and shorter apical dendrites than those in Pa(S1) (Figs. 16E, 19F).

Frontal Cortex

The frontal cortex in squirrels (F) was not subdivided by Kaas et al. (1972). Here we divide frontal cortex into an "agranular" primary motor field (M) and the remaining frontal cortex (F). In rats, a complete motor map (Hall and Lindholm, 1974; Neafsey et al., 1986; Brecht et al., 2004) has been cytoarchitectonically matched to lateral agranular cortex (AGl), which is characterized by the absence of a granular layer 4 (Donoghue and Wise, 1982; Wise and Donoghue, 1986; Li et al., 1990; Neafsey, 1990). In squirrels,electrical stimulation of neurons in the caudal part of the frontal cortex with microelectrodes produced movements of different body parts, but these results were not illustrated (Sur et al., 1978). However, accesses to these and more recent microstimulation results from motor cortex of squirrels in our laboratory indicate that M as defined here corresponds closely to the extent of primary motor cortex, M1. Rats also have a second motor area on the rostromedial border of M1 (Neafsey et al., 1986), as well as ventrolateral (orbital) and medial prefrontal regions (Öngür and Price, 2000). These regions are only briefly described in squirrels here.

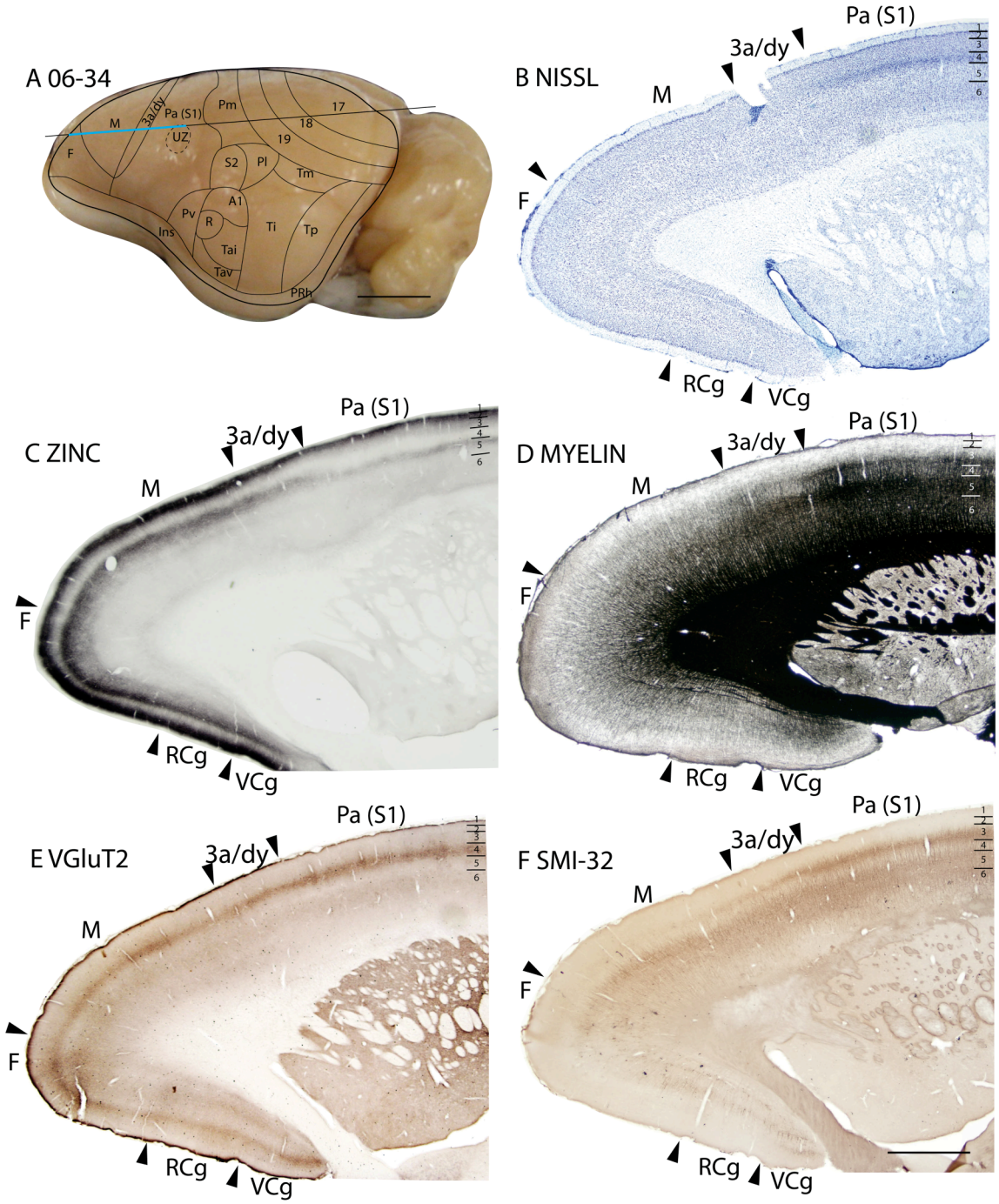

Figure 19. Architectonic characteristics of subdivisions of frontal and cingulate cortices in squirrel 06-34. Cortical areas are shown on a lateral view of the left rostral hemisphere in panel A. The blue horizontal line across the brain indicates the location of the brain sections illustrated in panels B-F. Short horizontal lines on panels B-Fshow the extent of the cortical layers. Scale bar on the brain (panel A) = 5mm. Scale bar for brain sections (panel F) = 2mm.

Area M. In Nissl preparations, area M is characterized by the lack of a distinct layer 4 (although a thin layer 4 seems to be present), a much thicker layer 5 than the surrounding cortex, and large cell bodies in layer 5 (Fig. 16B). In myelin preparations, area M is less densely myelinated than caudally located 3a/dy and Pa(S1), and the bands of Baillarger are less distinct (Fig. 19D). Area M expresses high concentrations of synaptic zinc in layers 3, 5 and 6. Layers 3 and 4 of area M have more zinc staining than the adjoining 3a/dy and Pa(S1) cortex (Figs. 16C, 19C). The presence of zinc staining in the middle layers of area M in squirrels, is not surprising. In addition to receiving synaptic zinc-free inputs from the ventrolateral (VL) complex of the thalamus, the motor cortex in squirrels receives zinc-positive cortical inputs from areas such as S1, 3a/dy, and Pv (Krubitzer et al., 1986). Area M has reduced PV-immunopositive terminations in middle layers compared to the cingulate cortex located medially, but less PV staining than in Pa(S1) (Fig. 20D). Middle layers of area M stain lighter in sections prepared for VGluT2 than in area 3a/dy and area Pa(S1), as expected of the poorly developed granular layer 4 of area M. Layer 5 and inner layer 6 of area M show SMI-32 stained pyramidal cells with large cell bodies, a characteristic of motor areas (Fig. 16E).

In summary, area M can be distinguished from 3a/dy and Pa(S1) by the lower levels of myelin present in area M, a thin and indistinct layer 4, and a thick layer 5 with large pyramidal cell bodies. As expected from a poorly developed layer 4, there is less expression of PV and VGluT2 in the neuropil of middle cortical layers than in sensory areas. Unlike sensory cortices, area M had some zinc staining in layer 4, likely due to the presence of cortical inputs from other areas, such as S1.

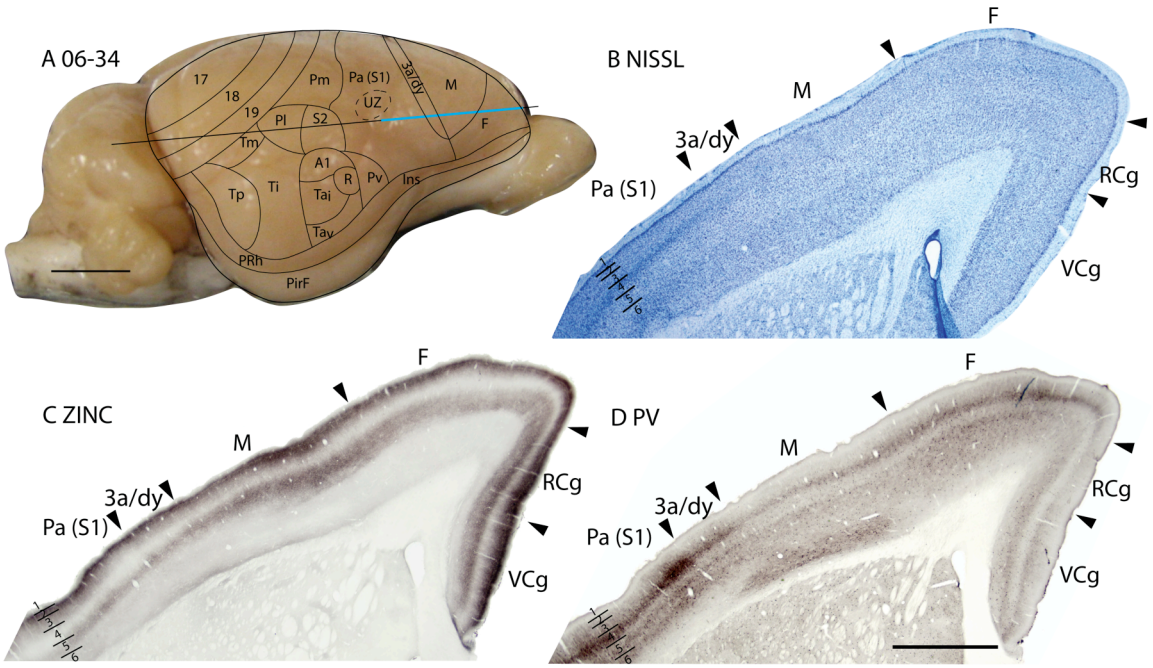

Figure 20. Architectonic characteristics of subdivisions of frontal and cingulate cortices in squirrel 06-34. Cortical areas are shown on a lateral view of the right rostral hemisphere in panel A. The blue horizontal line across the brain indicates the location of the brain sections illustrated in panels B-D. Short horizontal lines on panels B-D show the extent of the cortical layers. Scale bar on the brain (panel A) = 5mm. Scale bar for brain sections (panel D) = 2mm.

The remaining frontal areas. We have simply defined a large frontal (F) region rostral and medial to area M that is not sharply distinguished from area M. The frontal region extends to the border of anterior cingulate cortex (Fig. 22A). Frontal cortex likely includes a granular rostral motor area (Neafsey et al., 1986), as well as medial and orbital prefrontal areas of rats (Öngür and Price, 2000). The borders between these proposed divisions were difficult to identify in our preparations and thus were left unmarked. There are, however, some cytoarchitectonic differences between the frontal and motor cortices. In Nissl preparations, the rostromedial border of area M with the frontal cortex is marked by the emergence of a well-developed layer 4, packed with granular cells, and a thinner layer 5 then in area M (Figs. 19B, 20B, 21A). Area F also has better defined cortical

layers in Nissl preparations than the adjoining cingulate areas (Figs. 19B, 20B). In the myelin stain, there is no distinct difference between area F and M, whereas there is slightly increased myelination in area F than in the adjacent cingulate areas (Figs. 19D, 22D). The zinc stain in area F is less intense across the cortical layers than in area M and the cingulate areas, with the decrement being especially marked in layer 4 (Figs. 20C, 21B, 22E). Area F shows increased VGluT2 staining, in layer 4 compared to area M (Figs. 19E, 21D, 22C), whereas in PV preparations, area F showed denser staining in layer 4 and inner layer 3, and outer layer 6 (Figs. 20D, 21C). Area F can be distinguished from the cingulate areas by the sharp decrease in PV staining of layer 4 in the cingulate regions (Fig. 20D). The large pyramidal cells in layer 5 that were revealed by SMI-32 immunostaining in area M are not observed in area F and the expression of SMI-32 immunopositive cells in layer 3 of area F is reduced compared to area M and the rostral cingulate area (Figs. 21E, 22F).

In summary, most of the staining methods applied show differences between the frontal cortex, F, and the adjacent motor and cingulate cortex. However, the myelin stain was less useful in delimiting the borders of area F.

Cingulate and Retrosplenial Cortex

Cingulate and retrosplenial cortex are parts of the classical limbic system that are found in all mammals. Cingulate cortex is located along much of the medial wall of the cerebral hemisphere, and is generally divided into anterior motor-related, and posterior sensory-related divisions (Vogt et al., 1992). Retrosplenial cortex forms the most caudal part of the medial limbic cortex. The cingulate and retrosplenial cortical areas receive

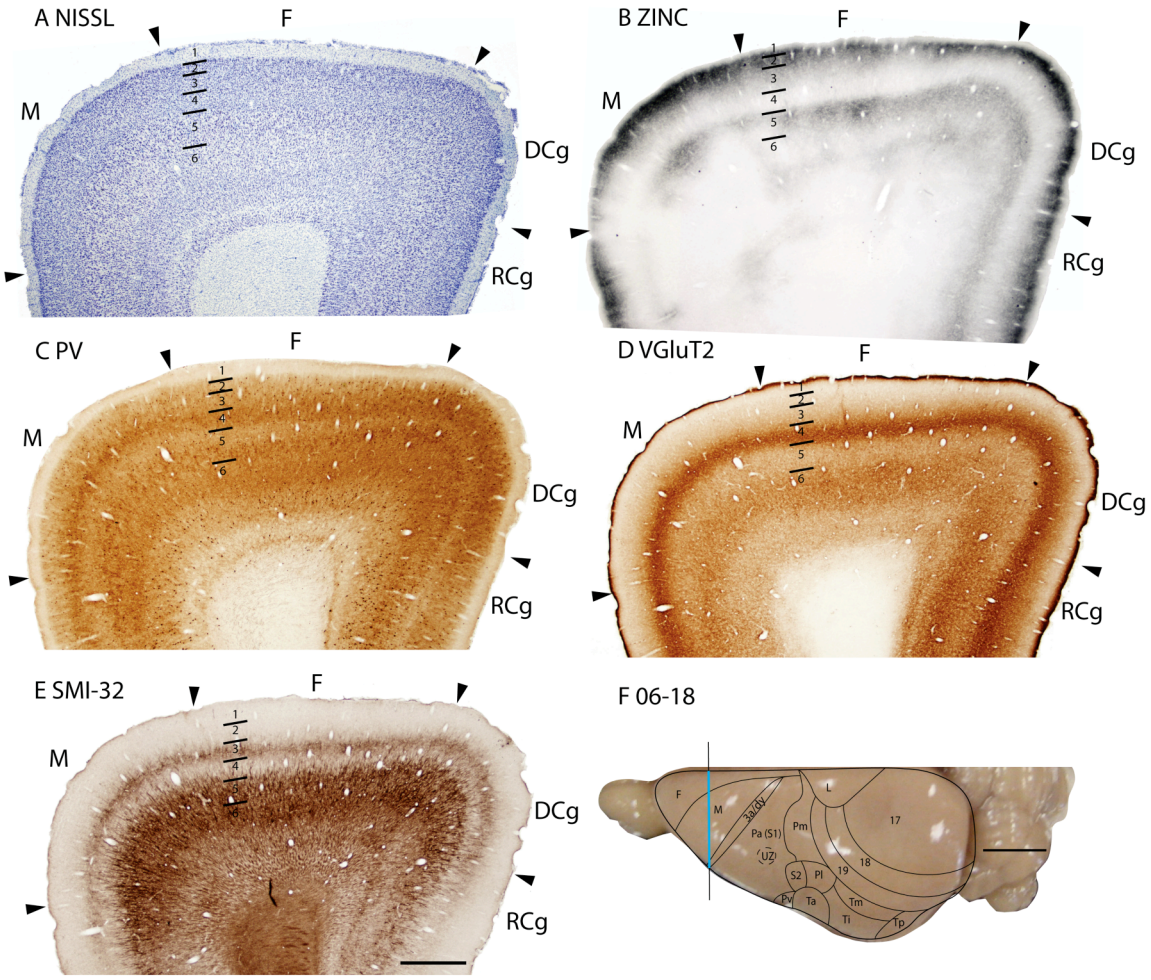

Figure 21. Architectonic characteristics of subdivisions of the frontal cortex in squirrel 06-18. Borders of cortical layers are marked at the frontal (F) area. The blue vertical line across the cortex (panel F) indicates the location where the brain sections in panels A-E were obtained. Scale bar in panel E = 2mm, panel F = 5mm.

inputs from the anterior and lateral dorsal nuclei of the thalamus (Jones, 2007). A comparison of the different nomenclature used for areas of cingulate and retrosplenial cortex can be found in Jones et al. (2005).

Cingulate cortex. Early investigators divided cingulate cortex into areas somewhat differently and used different nomenclatures in mice (Rose, 1929) and rabbits or ground squirrels (Brodmann, 1909). Those of Rose were retained by Domensick (1969) in studies using rats, whereas Vogt and Peters (1981) favored Brodmann's

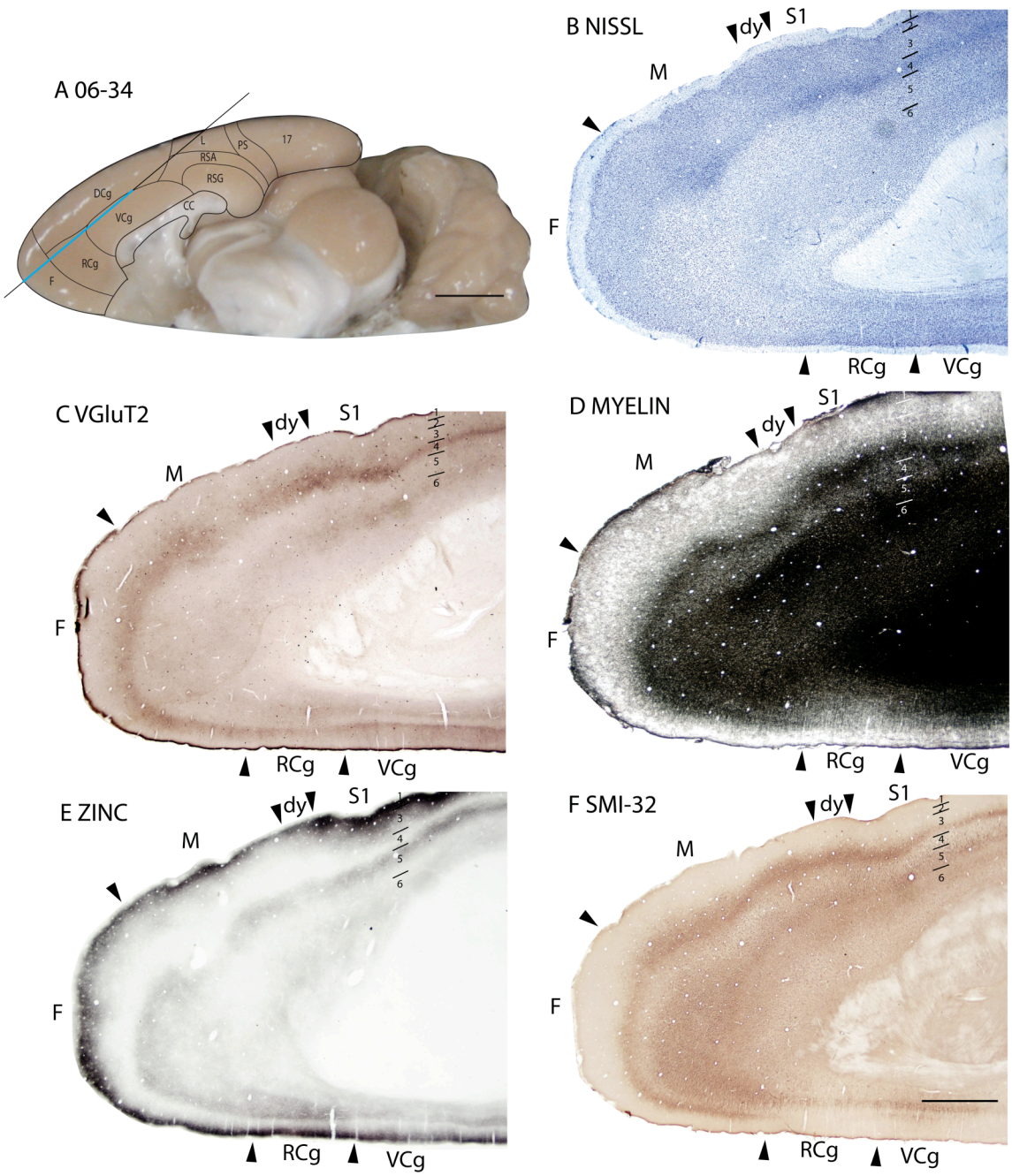

Figure 22. Architectonic characteristics of subdivisions of frontal and cingulate cortices in squirrel 06-34. Cortical areas are shown on a medial view of the left hemisphere in panel A. The blue horizontal line across the brain indicates the location of the brain sections illustrated in panels B-F. Short horizontal lines on panels B-F show the extent of the cortical layers. Scale bar on the brain (panel A) = 5mm. Scale bar for brain sections (panel F) = 2mm.

terminology. The three divisions identified in rats by Zilles and Wree (1995), cingulate areas 1, 2, and 3, are respectively identified here as dorsal (DCg), ventral (VCg) and rostral (RCg) subdivisions of the cingulate cortex in squirrels. DCg roughly corresponds to area 24b of Vogt and Peters (1981), VCg to much of area 24a, and RCg to the rostral part of 24a and adjoining area 32. The cingulate cortex of squirrels encompasses the rostral half of the cortex along the medial wall of cerebral hemisphere (Fig. 22A).

Dorsal cingulate area (DCg). In Nissl preparations, DCg has a layer 2 that is densely packed, an indistinct layer 4, and a population of relatively large cell bodies in layer 5 (Fig. 21A). In myelin-stained sections, DCg is lightly myelinated with a faint outer band of Baillarger (not shown). Layer 2 of DCg is darkly stained for synaptic zinc ions compared to the adjoining frontal cortex (Fig. 21B) in zinc preparations. Layer 4 and inner layer 3 of DCg have increased staining in VGluT2 prepared sections compared to the frontal cortex and the ventrally adjacent cingulate region (Fig. 21D). In SMI-32 immunostained sections, DCg shows darkly stained pyramidal cell bodies in layer 5 that are larger than those in the frontal cortex (Fig. 21E) and a band of SMI-32 stained pyramidal cell neuropil in layer 3 that terminates at the DCg/RCg border (Fig. 21E).

Ventral cingulate area (VCg). VCg is bordered dorsally by DCg, rostrally by RCg, and caudally by the retrosplenial cortex. In Nissl-stained sections, layer 2 of VCg has a higher packing density of cells and a thinner layer 5 than in DCg and inner layer 4 is very cell sparse (Figs. 19B, 20B, 22B). VCg shows higher myelination than RCg and can be delimited as such (Figs. 19D, 22D). VCg shows very dark zinc staining of layer 2 and slightly lighter zinc staining in outer layer 5 (Figs. 19C, 20C, 22E). Layers 4 and inner 3 of VCg have moderate levels of synaptic zinc (Figs. 19C, 20C, 22E), suggesting

the presence of cortical afferents. The level of zinc staining in VCg is higher than in DCg, but lower than in RCg (Figs. 19C, 20C, 22E). VCg shows a double banded staining pattern in sections prepared for PV, the outer band in layers 3 and 4, and the inner band in outer layer 6 (Fig. 20D). In VGluT2 immunostained sections, VCg shows light staining in layer 4 and 6 (Figs. 19E, 22C), whereas in SMI-32 immunostained sections, there are almost no stained pyramidal cells bodies in layer 3 and a very sparse population of SMI-32 immunopositive pyramidal cell bodies in layer 5 (Figs. 19F, 22F).

Rostral cingulate area (RCg). In Nissl-stained sections, RCg does not have a well-developed laminar pattern and the large pyramidal cell bodies present in layer 5 of DCg and to a lesser extent, in VCg, are almost absent in RCg (Figs. 19B, 20B, 21A, 22B). RCg is the least myelinated out of the three cingulate areas (Figs. 19D, 22D). In zinc preparations, RCg shows some staining in layer 4 (Figs. 19C, 20C, 21B, 22E) and darker staining of layer 5 than VCg (Figs. 19C, 22E). The PV immunopositive band in layer 4 of VCg is almost absent in RCg, providing a distinct border between VCg and RCg (Fig. 20D) and layer 6 of RCg stains lighter in PV preparations than that in DCg (Fig. 21C). In VGluT2 immunostained sections, RCg has a moderately dark staining of layer 4, although no clear borders of RCg can be detected in these preparations (Figs. 19E, 21D, 22C). There are almost no SMI-32 immunopositive pyramidal cells in layer 3 of RCg and very few immunostained small pyramidal cells in layer 5 (Figs. 19F, 21E, 22F).

Retrosplenial cortex. Brodmann (1909) distinguished three subdivisions of retrosplenial cortex in ground squirrels, areas 29a, 29b and 29c. More recently, Vogt and Peters (1981) described four divisions (29a, b, c and d), and Domensick (1969) described

only agranular and granular divisions in rats. Here, we follow Zilles and Wree (1985) and Domensick (1969) by distinguishing two main divisions of retrosplenial cortex, a granular area, RSG and an agranular area, RSA.

Retrosplenial granular area (RSG). In Nissl sections, RSG is characterized by a conspicuous band in layer 2 that is densely packed with deeply stained cells (Fig. 7A). The underlying granular layer appears to be part of layer 3, just over a sparse granular layer 4 (Vogt and Peters, 1981). RSG is poorly myelinated, without marked inner and outer bands of Baillarger (Fig. 23B). RSG is poorly stained in sections processed for zinc, especially in layers 3 and outer 4, which are almost free of synaptic zinc (Fig. 7B). This suggests that most of the afferents to RSG in squirrels originate from the thalamus or other subcortical structures. With the PV stain, layer 4 of RSG is light, whereas layers 2 and 3 are very dark. Layer 6 has moderate staining, giving rise to a banded appearance (Fig. 11C). RSG shows a dark staining of layer 3, outer layer 4 and inner layer 6 in the VGluT2 stain (Fig. 11E). In SMI-32 prepared sections, RSG shows light staining of pyramidal cells in outer layer 3, some staining of pyramidal cells in inner layer 5, somewhat more stained pyramidal cells in outer layer 6, forming a tri-banded staining pattern as well (Fig. 11D). Layer 4 of RSG is immunopositive for the LAMP antibody, as well as layer 6, though to a lesser extent. The expression of LAMP in RSG is less compared to the ventrally adjacent subicular areas, but the LAMP-positive band in layer 4 of RSG is thicker than that in RSA (Fig. 23C).

Retrosplenial agranular area (RSA). The retrosplenial agranular area neither shows well-defined laminar differentiation nor a developed granular layer 4 in the Nissl

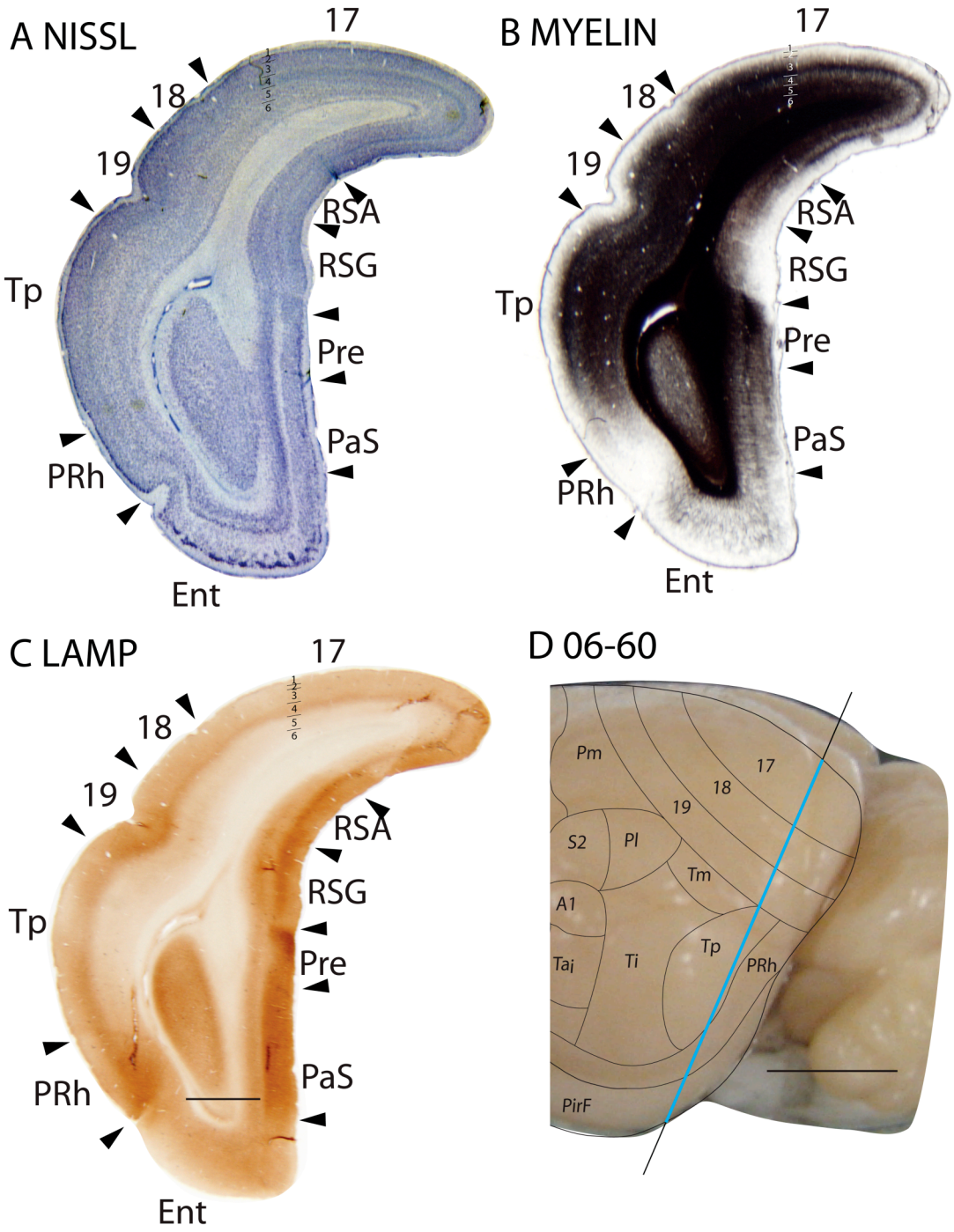

Figure 23. Architectonic characteristics of subdivisions of retrosplenial cortex in squirrel 06-60. Cortical areas are shown on a lateral view of the left caudal hemisphere in panel D. The blue horizontal line across the brain indicates the location of the brain sections illustrated in panels A-C. Short horizontal lines on panels A-C show the extent of the cortical layers. The limbic areas show darker staining in the Limbic Associated Membrane protein (LAMP) compared to other cortical areas, such as area 17 and 18. Scale bar on the brain (panel D) = 5mm. Scale bar for brain sections (panel C) = 2mm

stain (Figs. 7A, 11A). RSA is poorly myelinated and has no obvious bands of Baillarger detected (Fig. 23B). In sections prepared for zinc, RSA shows higher intensity of staining, especially of layer 3, than RSG (Figs. 7B, 11B), suggesting that RSA receives more cortical afferents than RSG. There is very little PV staining in RSA, except in outer layer 6 (Fig. 11C). In the VGluT2 stain, two thin, well-stained bands are seen in layer 4 and 6 (Fig. 11E). RSA shows almost no staining of pyramidal cells in SMI-32 prepared sections (Fig. 11D). RSA expressed more staining for LAMP than the adjoining prostriata area, but less than the granular region of the retrosplenial cortex (Fig. 23C).

Area prostriata (PS)

Cortex along the medial border of area 17, the portion representing peripheral vision of the contralateral visual hemifield, has been distinguished in primates as area prostriata by Sanides (1972). In cats and in several other non-primates, the prostriata region has been called the splenial visual area (see Rosa, 1999 for review). In rats and mice, the comparable region has been called the posteromedial visual area (Wang and Burkhalter, 2007), medial area 18b (Krieg, 1946; Caviness, 1975), Oc2MM (Zilles and Wrree, 1995), or part of the agranular retrosplenial cortex (Krettek and Price, 1977). We have used the term prostriata here for this area, with visual connections and visually responsive neurons, in an effort to standardize the nomenclature, and promote comparisons with primates. Area prostriata is considered part of the limbic, rather than occipital cortex. It is described here as an area bordering area 17 that is visual in function. As with primates (see Allman and Kaas, 1971), prostriata in squirrels has an indistinct layer 4 and is poorly myelinated (Figs. 3, 6). Thus, there is little evidence of layer 4 in PV

or VGluT2 preparations. Layer 2 shows dense zinc staining and SMI-32 staining disappears in layer 3.

Perirhinal Areas

Cortex along the dorsal bank of the rhinal fissure has been called transitional cortex, as the six distinct layers of most of neocortex are not always apparent (Zilles and Wree, 1995). Here, we define an insular region (Ins) of cortex, just ventral and rostral to primary somatosensory cortex Pa(S1), a more caudal perirhinal (PRh) region, and a caudal entorhinal (Ent) cortex. Ins likely has functional subdivisions related to gustatory, general visceral, somatosensory, and multisensory functions (Guldin and Markowitsch, 1983; Kosar et al., 1986; Cechetto and Saper, 1987). Perirhinal and entorhinal areas relate to hippocampal memory functions (Burwell and Amaral, 1998).

The insular cortex defined here in squirrels corresponds to the agranular insular cortex of previous descriptions in rats (e.g., Kosar et al., 1986; Cechetto and Saper, 1987). The granular and dysgranular insular regions are included in the parietal region of secondary somatosensory cortex. In Nissl preparations, Ins has a darkly stained layer 2 that is densely packed with cell bodies that does not form a continuous layer. Instead, the cells form groups, or islands giving the layer a ‘scallop-like’ pattern. There is a lack of a well-developed granular layer 4 (Fig. 24B). In myelin-stained sections, the Ins area stands out as an area with almost no myelination (Fig. 24D). Ins is darkly stained in zinc preparations, especially in layers 2 and 3 (Fig. 24C), indicating that most of the input is from other cortical areas. The laminar staining pattern in the Ins region is uniform in PV (not shown), VGluT2 (Fig. 24E) and SMI-32 (Fig. 24F) immunostained sections.

In Nissl preparations, the perirhinal (PRh) cortex does not have a distinct laminar pattern. However, layer 2 stands out due to the densely packed, Nissl-stained cell bodies that form a continuous layer (Figs. 18B, 19B, 20B). This feature allows the differentiation of PRh from the Ins cortex (Fig. 24B). Like the Ins area, PRh is very poorly myelinated (Figs. 18B, 19D) and does not have distinct laminar patterns in the PV (Fig. 25D), VGluT2 (Fig. 24E) and SMI-32 (Fig. 24F) immunostained sections. Area PRh, being part of the limbic cortex, expresses a higher amount of the LAMP antibody compared to surrounding cortical areas (Fig. 23C).

Entorhinal cortex in rats is generally divided into lateral and medial areas (Blackstad, 1956; Hevner and Wong-Riley, 1992). In the entorhinal cortex of squirrels, we distinguish the lateral (LEnt), intermediate (IEnt) and medial (MEnt) entorhinal areas. In Nissl-stained sections, all three areas have almost no cell bodies in layer 4 (Figs. 19B, 25B). Layer 2 of LEnt shows higher packing density of cell bodies than IEnt, whereas in MEnt, the cells in layer 2 are grouped into 'islands' in Nissl preparations (see Figs. 19B, 25B). The entorhinal cortex has very low levels of myelination, with MEnt having the lowest level of myelination (not shown). Layer 2 of the MEnt region stains darkly for synaptic zinc, IEnt has much lighter staining and LEnt has the lowest levels of staining (Fig. 24C). In PV immunostained sections, layer 2 of LEnt has the darkest staining, followed by MEnt and IEnt as the most lightly stained region (Fig. 25D). MEnt has lighter staining through the layers than IEnt and LEnt in VGlut2 immunostained sections (Fig. 24E). SMI-32 immunopositive pyramidal cells are present in the upper cortical layer of LEnt and IEnt, and in the lower cortical layer of MEnt (Fig. 24F).

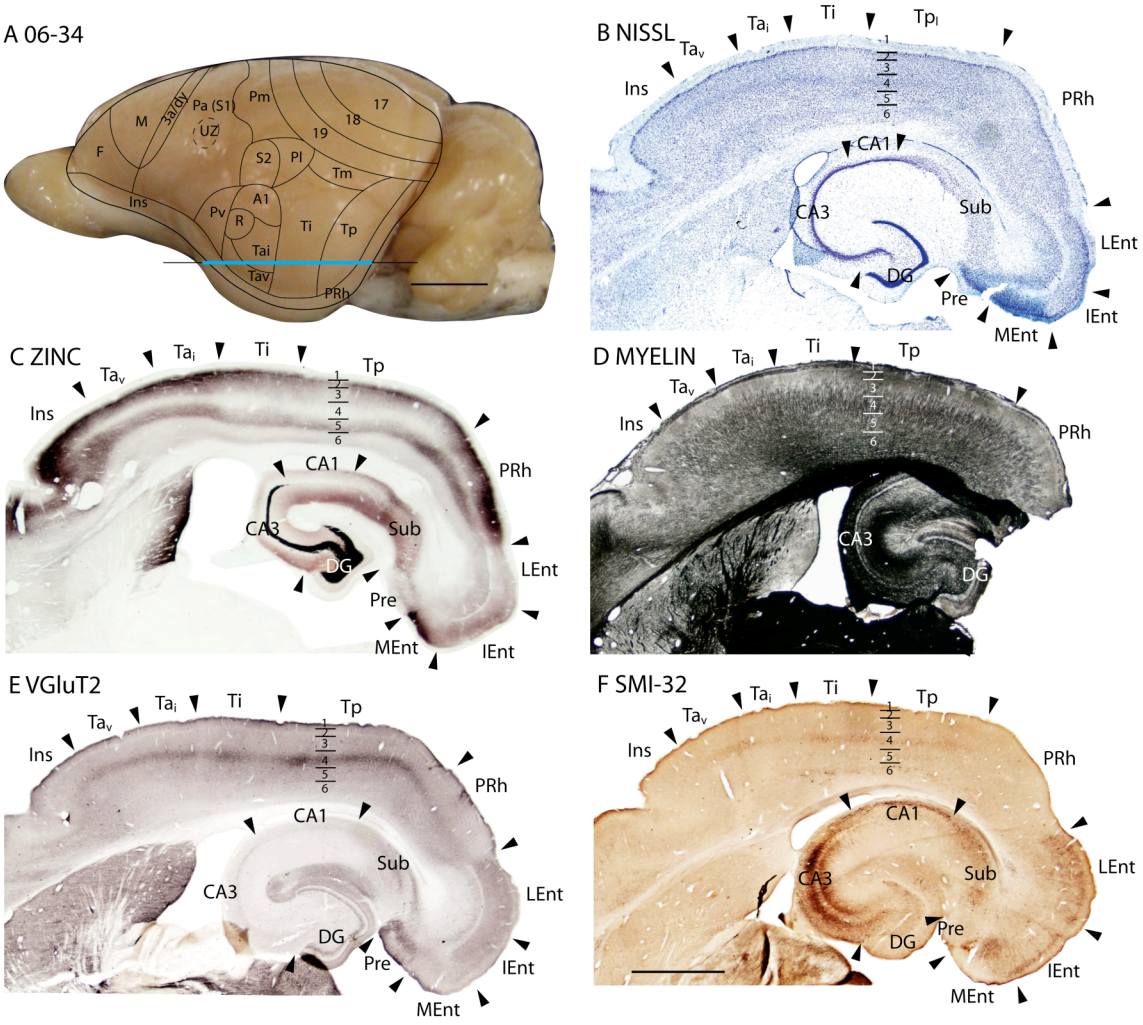

Figure 24. Architectonic characteristics of subdivisions of temporal and insular cortices in squirrel 06-34. Cortical areas are shown on a medial view of the left hemisphere in panel A. The blue horizontal line across the brain indicates the location of the brain sections illustrated in panels B-F. Short horizontal lines on panels B-F show the extent of the cortical layers. Scale bar on the brain (panel A) = 5mm. Scale bar for brain sections (panel F) = 2mm.

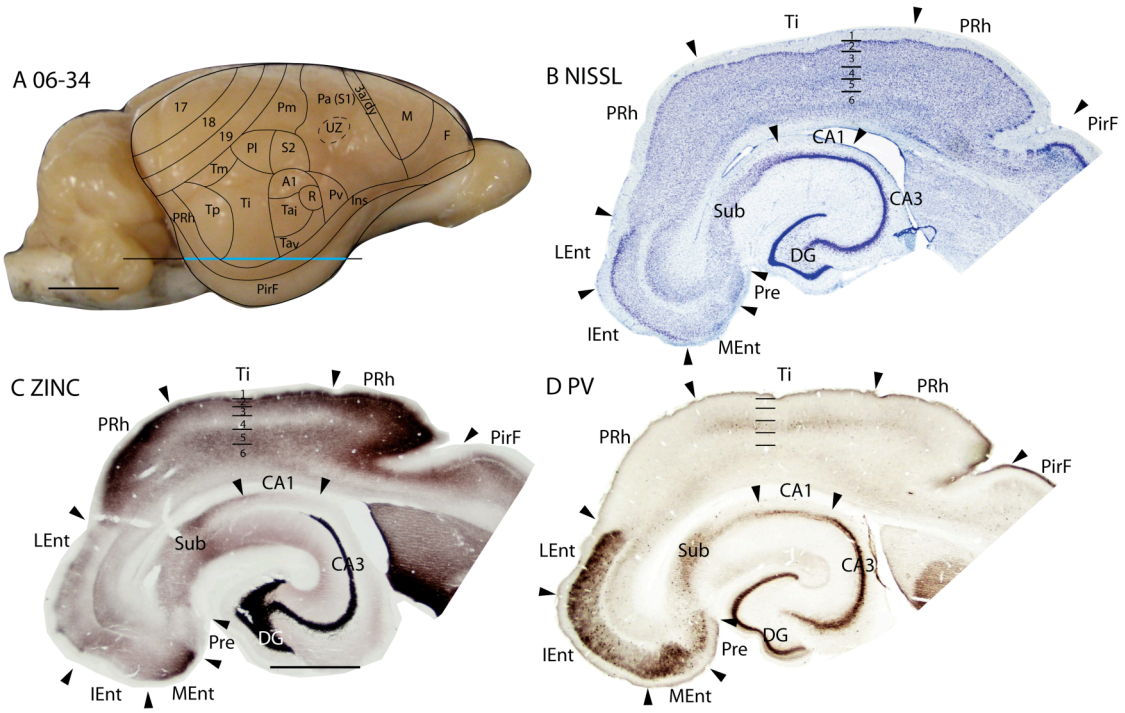

Figure 25. Architectonic characteristics of subdivisions of rhinal cortex in squirrel 06-34. Cortical areas are shown on a lateral view of the right hemisphere in panel A. The blue horizontal line across the brain indicates the location of the brain sections illustrated in panels B-D. Short horizontal lines on panels B-D show the extent of the cortical layers. Scale bar on the brain (panel A) = 5mm. Scale bar for brain sections (panel D) = 2mm.

Discussion

The focus of the present research effort was to provide an improved overview of how the neocortex in squirrels is subdivided into areas, the 'organs' of cortex (Brodmann, 1909). Just as how the early taxonomic system of Linnaeus was fundamental to the subsequent advances in the field of biology, the efforts of Brodmann (1909) and other early neuroanatomists in dividing cortex into a patchwork of areas with supposed functional significance usefully guided following generations of neuroscientists. The classification scheme of Linnaeus (c.f. Benton, 2005) was corrected and extended by subsequent research. Likewise, the early architectonic cortical maps of many studied

mammals have been revisited and altered as a result of further study. Here we present a revised interpretation of how the neocortex is organized in the common grey squirrel, based on our study of an extensive battery of histological preparations. The results are expected to provide a more detailed and accurate portrayal of how the neocortex of squirrels is subdivided into areas, as squirrels, with their well-developed visual system, have become useful in neuroscience research (Van Hooser and Nelson, 2006; Kaas, 2002). In addition, these results on the well-differentiated areas of the squirrel cortex reflect on theories of how the cortex of other rodents, in particular the extensively studied rats and mice, is subdivided, as the brains of various rodents likely resemble each other in how they are organized. Thus, our broader goal is to understand what features of cortical organization are shared by the various species of rodents, and how the differences that do exist evolved. The present results are discussed in relation to previous architecture studies, especially on rodents, and other portrayals of the areal organization of cortex.

Most architectonic studies in rodents, such as rats and mice, employed the use of Nissl, myelin, and occasionally the acetylcholinesterase stains to subdivide the neocortex (e.g., Krieg, 1946; Caviness, 1975; Swanson, 1992; 2003; Zilles and Wree 1985, 1995; Paxinos and Franklin, 2003; see Kaas et al., 1972 for squirrels). However, the potential use of other histochemical procedures now provides a richness that can greatly enhance architectonic studies. Thus, the immunoreactivity and staining patterns produced by antibodies, such as VGluT2 (Nahami and Erisir, 2005), PV (Condé et al., 1996; Budinger et al., 2000; Cruikshank et al., 2001), and SMI-32 (Voelker et al., 2004; Boire et al., 2005) have been analyzed in the cortex of rodents, and there is a chemoarchitectonic atlas for rats (Paxinos et al., 1999). Yet, variations in staining patterns produced with these

antibodies have not often been used as criteria for parcellating the neocortex. Similarly, the distribution of zinc-enriched terminals has been described in the neocortex of rodents, such as mice (Garrett et al., 1991; Brown and Dyck, 2004; Czupryn and Skangiel-Kramska, 1997), rats (Ichinohe et al., 2003; Miro-Bernie et al., 2006), and in the visual cortex of parma wallabies (Garrett et al., 1994). These zinc-enriched terminals originate from a subset of glutamatergic neurons in the neocortex, as well as neurons in the claustrum and amygdala, and they are not found in terminals of neurons that originate in the thalamus (Danscher, 1982; Frederickson and Moncrieff, 1994; Frederickson et al., 2000, Ichinohe et al., 2003; Ichinohe and Rockland, 2004). Of course, all cortical areas get thalamic inputs, and layer 4 of all areas has intrinsic connections that presumably use zinc ions. Nevertheless, cortical areas, and especially layer 4, vary greatly in zinc expression, and a high density of zinc-stained terminals in layer 4 of any cortical area likely reflects a dominance of corticocortical inputs, whereas a low density suggests a dominance of thalamocortical inputs. As such, the zinc stain that reveals these zinc-enriched terminals can act as a marker that allows a parcellation of cortical areas based on differences in the proportions of cortical and thalamic inputs to layer 4. Thus, we have used VGluT2, PV, and synaptic zinc, as well as Nissl, myelin, SMI-32, LAMP, CB and CO preparations in our study of cortical architecture in squirrels.

Visual areas of occipital cortex

Area 17. The occipital cortex of squirrels contains three large areas, areas 17, 18 and 19 after Brodman (1909). These designations and the boundaries of these areas have been retained from Kaas et al., (1972). Area 17 is an area common to most, if not all

mammals, and it is especially well developed in squirrels. The area is large, extending from the dorsomedial surface of the hemisphere, along the cortex of the medial wall and onto the cortex of the ventral surface. As with other mammals, area 17 of squirrels contains a systematic representation of the contralateral visual hemifield (Hall et al., 1971) and projects to the other occipital fields, areas 18 and 19 (Kaas et al., 1989). Area 17 is thicker and more developed in its lateral, binocular portion (Hall et al., 1971). Area 17 is bordered on the ventral surface by a subdivision of the cortex that may correspond to the visual limbic area, or prostriata, of primates and other mammals (Sanides, 1970; Rosa et al., 1997; Morecraft et al., 2000). The longer border of area 17, on the dorsolateral surface and extending onto the medial wall and the posterior pole of the hemisphere, is with area 18 (V2). Area 17 has a sharply defined layer 4 of densely packed granule and stellate cells, with suggestions of sublayers, as described previously (Kaas et al., 1972). The area is also very distinct in most preparations. Here we described the characteristics of area 17 of squirrels for the first time in sections processed for parvalbumin, SMI-32, VGluT2 and synaptic zinc. Layer 4 stands out in these preparations as a layer conspicuously poor in zinc, and densely expressing PV and VGluT2.

The low level of synaptic zinc in layer 4 of area 17 is consistent with the evidence that thalamocortical terminations do not have synaptic zinc, and that layer 4 of area 17, as a primary sensory area, receives dense thalamic inputs from the lateral geniculate nucleus of the dorsal thalamus, and few other inputs (e.g., Casagrande and Kaas, 1994; see Robson and Hall, 1975; Weber et al., 1977 for lateral geniculate projections to area 17 in squirrels). In addition to the low level of synaptic zinc expression in layer 4, layer 3 and

outer layer 5 have considerably less synaptic zinc than the corresponding layers in extrastriate cortex (Fig. 9C). This implies that these layers also receive a high proportion of inputs from the thalamus. In squirrels, the lateral geniculate nucleus projects densely to layer 4, and much less densely to the outer half of layer 6 (Robson and Hall, 1975). These less dense terminations in layer 6 may account for most or all of the thalamic input to this layer that results in the reduction of the presence of synaptic zinc. In these earlier studies in squirrels, there was no evidence for notable lateral geniculate projections to layer 3, although such projections may exist as they do in primates (Casagrande and Kaas, 1994). Another source of thalamic projections to superficial layers of area 17 in mammals is from nuclei of the pulvinar complex (Kaas and Lyon, 2007). Although the cortical projections of pulvinar nuclei in squirrels have been studied in the past (Robson and Hall, 1977), and projections to area 17 have not been directly demonstrated, they likely exist. Lesions of visual cortex that are confined to area 17 (Kaas et al., 1972) do not cause retrograde degeneration of nuclei in the pulvinar complex of squirrels, indicating that any projections to area 17 would have sustaining collaterals to other visual areas. If areas 18 and 19 are included in the cortical lesions, the anterior half of the pulvinar becomes massively degenerated. Possibly the anterior pulvinar in squirrels also projects to area 17, thereby accounting for the reduction of synaptic zinc in layer 3.

Area 17 of squirrels resembles area 17 of other rodents in its general location, architectonic features, and retinotopic organization, but area 17 of other less visual rodents is smaller and less distinctly differentiated. Area 17 and other areas have been repeatedly described in rats (Krieg, 1946; Swanson, 1992; 2003; Zilles et al., 1980; 1984; Reid and Juraska, 1991), and mice (Rose, 1930; Caviness, 1975; Paxinos and Franklin,

2003; Van der Gucht et al., 2007), and less frequently in other rodents, such as guinea pigs (Rose, 1912), hamsters (Lent, 1982; Dursteler et al., 1979) and agoutis (Picanço-Diniz et al., 1989). In a surface view, brain sections cut parallel to the cortical surface, and processed for cytochrome oxidase activity, or most other markers, area 17 is one of the most easily recognized and delimited areas of the mammalian brain. Here, we defined area 17, distinguished binocular and monocular sections of area 17, and described layers and significant sublayers of area 17.

Area 18. The concept of a medial area 18 (18b) and a lateral area 18 (18a) in rodents comes from Krieg (1946) in answer to a dilemma. In squirrels and rabbits, Brodmann (1909) described an area 18 along the medial border of area 17, but other areas, rather than area 18, were placed along the lateral border of area 17. At least in the squirrel, it seems likely by location that Brodmann was identifying the thinner, less-developed, monocular portion of area 17 as area 18. Rose (1912) soon followed with descriptions of an area 17 bordered medially, but not laterally, by an area 18 in guinea pigs and mice. The position of this medial area 18 was subsequently recognized as incompatible with the location of Brodmann's area 18 in carnivores and primates, and thus Krieg (1946) added a lateral area 18 to the cortex of rats. In modern studies of rodents, the medial "area 18" usually corresponds to the limbic visual area, prostriata (Sanides, 1970), also identified as the splenial visual area (Kalia and Whitteridge, 1973), rather than a part of area 18 (See Rosa, 1999 for review). Somewhat differently, cortex along the medial margin of area 17 has been divided into several proposed visual areas in mice and rats (e.g., Van der Gucht et al., 2007; Wang and Burkhalter, 2007). In either case, the medial region is not area 18 of other mammals, and the misidentification of this

cortex as area 18 should be discouraged. As Krieg (1946) recognized, the proposed medial area 18 (18b) and the lateral area 18 (18a) do not resemble each other histologically.

In the present study, we used our battery of histological stains to characterize a highly distinct band of cortex along the lateral border of area 17. The location of this band, along the complete representation of the zero vertical meridian of area 17, corresponds to the second visual area, V2 (Hall et al., 1971), as it does in a wide range of mammals, including carnivores, primates, and fruit bats (see Rosa and Krubitzer, 1999, for review). Area 18 in squirrels was defined earlier in Nissl and myelin preparations (Kaas et al., 1972). In Nissl preparations, layer 4 and 6 are less densely stained than in adjacent areas, giving the appearance of less distinct lamination. The increase in zinc staining in layer 4 and other layers of area 18 is marked (Fig. 9C), consistent with the evidence that layer 4 of area 18 gets a massive input from area 17 (Kaas et al., 1989). However, the lateral geniculate nucleus does provide some thalamic input to layer 4 of area 18 in squirrels (Weber et al., 1977), and inputs to the supragranular layers are likely to originate from the pulvinar complex. The adjoining area 19 has somewhat more synaptic zinc, suggesting less thalamic input. There is no evidence for significant geniculate projections to area 19. Area 18 also has a more pronounced laminar pattern of neurofilament protein staining than area 19, as does the cortex laterally adjoining area 17 in mice (Van der Gucht et al., 2007). Sections processed for VGluT2 or PV also reveal laminar differences in density of staining between areas 18 and 19. Finally, in surface-view of brain sections cut parallel to the brain surface and stained for myelin, area 18 is quite distinct as a slightly less densely myelinated strip along the outer border of area 17.

However, the myelin pattern is not homogenous within area 18 (Kaas et al., 1989). Rather, the strip contains a series of six to eight 500μm wide patches along its length, indicating that area 18, as with primates (Casagrande and Kaas, 1994), has a modular organization in squirrels. This supposition is supported by the results of a study of the corpus callosum connections in squirrels (Gould, 1984), as interhemispheric projections terminate broadly in area 18, while avoiding a series of patch-like regions that resemble the myelin-poor patches in size and number. It seems likely that the callosal-poor zones are those where area 17 projections are concentrated, just as with rats (Olavarria and Montero, 1984; Malach, 1989) and other rodents (Olavarria and Montero, 1989; Bravo et al., 1990).

As further support for the concept of an area 18 or V2 in rodents, an area 18 along the lateral border of area 17 has been defined architectonically in the large South American hystricomorph (related to guinea pigs) rodent, the agouti (*Dasyprocta aguti*). The area 18 is distinct in cytochrome oxidase preparations as a band of less dense staining, and characteristics in Nissl and myelin preparations are similar to those in squirrels (Picanço-Diniz, 1987; Picanço-Diniz et al., 1989). Microelectrode recordings from this area 18 revealed a simple representation of the contralateral visual hemifield, which was termed V2.

We conclude from this review of the histological evidence that area 18 is a valid subdivision of visual cortex, with a regular pattern of modular subdivisions relating to callosal and area 17 inputs. Other types of evidence support this conclusion. Most importantly, microelectrode recordings across the width of area 18 in a series of penetrations from rostral to caudal reveal a systematic representation of the contralateral

visual hemifield in area 18 (Hall et al., 1971), one that conforms to the retinotopic organization of V2 of other mammals, such as cats and monkeys. Thus, there is a reversal of retinotopic order at the area 17/18 border of squirrels so that forward vision is represented along the border and successively more temporal vision is represented away from the border in both V1 and V2. Lower vision is represented ventrally and upper vision is represented caudally in both areas. Highly similar results appear to have been obtained in microelectrode mapping studies in ground squirrels (Sereno et al., 1991). A summary of the Sereno et al. (1991) study has been published in a review by Van Hooser and Nelson (2006). It shows a V2 along the lateral border of V1 with the vertical meridian represented at the V1-V2 border, peripheral vision along the outer border of V2, and the lower quadrant is rostral to the upper quadrant. This proposed organization of area 18 in cortex lateral to V1 in grey squirrels and ground squirrels is highly consistent with the connection patterns between area 17 and area 18. Injections of tracers in area 17 labeled several patches of cells in area 18, but rostral injections labeled more rostral patches than caudal injections (Kaas et al., 1989). Thus, the connection pattern was less precise than the physiologically determined V1 and V2 representations would suggest, but the anatomical and physiological patterns of organization in V2 were globally consistent.

The reason for this lengthy discussion of what seems to be an uncontroversial point is that squirrels are rodents, and a different type of organization has been proposed for cortex lateral to area 17 of rodents with a less developed visual system, such as rats and mice (e.g., Olavarria and Van Sluyters, 1982; Olavarria and Montero, 1984; 1990; Montero, 1993; Wang and Burkhalter, 2007). Thus, a series of six visual areas have been

proposed along the lateral border of area 17, where V2 (area 18) is in squirrels and other studied mammals. This proposal, based on a combination of anatomical and physiological results, is partly compatible with the classic cytoarchitecture map of mouse cortex by Rose (1930), which showed several architectonic fields along the lateral border of area 17. However, it is informative to note that Brodmann (1909) had previously failed to identify an area 18 along the lateral border of area 17 of squirrels, and instead portrayed a string of areas along this border (areas 7, 22, 21, 20 and 36). As the existence of a lateral area 18, or V2, in squirrels now seems clear, we conclude that at least the squirrel branch of the rodent radiation retained a visual area, V2 or area 18, an area that is basic to nearly all other mammals (See Rosa and Krubitzer, 1999 for review). We question whether other less visual branches of the rodent radiation abandoned this broadly conserved feature.

Not all investigators have placed a series of visual areas exist on the lateral border of area 17 in rodents. In the first extensive cytoarchitectonic and myeloarchitectonic study of cortical areas in rats, Krieg (1946) illustrated an area 18a along the complete lateral border of area 17. Subsequently, Caviness (1975) retained an area 18a lateral to area 17 in mice, as did Zilles and collaborators in several studies of rodent neocortex, with the modifications that the region of area 18a was termed occipital area 2 lateral (Oc2L) and it was extended rostrally, to include parts of Krieg's area 17 (e.g., Zilles et al., 1980; Zilles and Wree, 1995). A more recent architectonic study (Van der Gucht et al., 2007) of visual cortex in mice, based on patterns of immunoreactivity for the neurofilament protein, SMI-32, distinguished a narrow area V2L (with anterior and posterior halves) along the lateral border of V1 (area 17) that corresponds closely to the

territory of V2 (area 18) expected from microelectrode mapping data (see Wagor et al., 1980; also see Tiao and Blakemore, 1976). Interestingly, Olavarria and Mendez (1979) in their microelectrode mapping study of the diurnal rodent, *Octodon degus*, illustrated a much longer lateromedial area (LM) than usual for this proposed area. This LM, though incompletely mapped, had the shape and retinotopy expected in V2. While connection patterns, and some of the microelectrode mapping results, can be viewed as supporting the proposal of six or so areas along the lateral border of area 17 (e.g., Olavarria and Montero, 1984; Montero, 1993; Olavarria et al., 1982; Olavarria and Montero, 1990; Wang and Burkhalter, 2007), sometimes in a rather convincing manner (e.g., Wang and Burkhalter, 2007), Malach (1989) concluded, in a study of area 17 connections in rats, that the cortex adjoining lateral striate cortex contains a single, global map, V2. In a similar manner, Kaas et al., (1989) suggested that the acallosal modules of area 18 in squirrels and other rodents overlap slightly in visuotopic organization, so that injections in any region of area 17 could label several, but not all modules. Thus, rostral modules in area 18 would be labeled by rostral injections and caudal modules by caudal injections. After a review of the distribution of V2 across mammalian taxa, Rosa and Krubitzer (1999) concluded that rodents have a V2, and that an elongated LM in rats and other rodents corresponds to V2.

Area 19. The third division of occipital cortex that we have defined in squirrels is area 19. This area was also retained from the earlier study of Kaas et al. (1972). Overall, area 19 is less well-defined, and therefore more questionable as a valid visual area than areas 17 and 18. However, area 19 constitutes a band of cortex that is distinctly different in architectonic appearance from area 18 and the adjoining temporal areas. Yet, presently

defined area 19 may contain rostral and caudal subdivisions, as suggested by connection patterns (Kaas et al., 1989). On the other hand, area 19 is a subdivision of the cortex that has long been associated with the concept of a third representation of the contralateral visual hemifield. This seems to be the case in cats, and perhaps other carnivores, where cortex defined architectonically as area 19 corresponds to a third visual representation, one along the outer border of area 18 (V2), and forming a mirror reversal of representation in V2 (Hubel and Wiesel, 1965; Tusa et al., 1979; Albus and Beckmann, 1980). Presently, there is good evidence for such a V3 along the outer border of area 18 (V2) in primates (Kaas and Lyon, 2001), although it should be recognized that area 18 has been redefined in some primates and it does not correspond to the area 18 of Brodmann (1909). Except for the description of visual cortex in agoutis (Picanço-Diniz et al., 1989), other architectonic descriptions of the organization of occipital cortex in rodents do not include an area 19. Yet, the existence of a narrow V3, about half the width of V2, has been described in the visual cortex of ground squirrels (Sereno et al., 1991). Given the long history of uncertainties about the existence of V3 in monkeys and the difficulties in obtaining conclusive evidence (see Kaas and Lyon, 2001), it seems possible that squirrels have a V3. However, the V3 proposed by Sereno et al. (1991) would occupy only the medial half of the area 19 depicted here. For now, we know that area 19 of squirrels receives visual inputs from areas 17 and 18 (Kaas et al., 1989), and that the pattern of connections appears to be more complicated that would be expected from the retinotopy proposed for V3.

Areas of the temporal cortex

Three major divisions of temporal cortex, areas Ta, Ti and Tp, are easily distinguished in squirrels. Ta and Tp have histological characteristics of sensory cortex, whereas Ti has the features of a secondary field. Thus, Ta and Tp have a conspicuous layer 4 of granule cells, dense myelination, express little synaptic zinc, have three obvious bands of stained pyramidal cells in SMI-32 preparations, and a darkly stained layer 4 in VGluT2 and CO preparations. In marked contrast, Ti lacks these distinguishing features. Ta, Ti and Tp were previously recognized by Kaas et al. (1972) in squirrels, and these three subdivisions of temporal cortex are retained here. We have also added a fourth subdivision, Tm.

Area Ta. The sensory nature of Ta is known, as it contains two primary auditory fields, A1 and R, as wells as several secondary auditory fields (Luetheke et al., 1988; Merzenich et al., 1976). In our unpublished studies of temporal cortex connections in squirrels, injections in Ta labeled neurons in the medial geniculate complex of the dorsal thalamus. Although Ta is not uniform in appearance, we were unable to reliably distinguish differences in architecture between the auditory fields contained within Ta. However, in brain sections cut parallel to the flattened cortex, the core areas, A1 and R, do appear to be slightly more myelinated than the rest of Ta (Krubitzer et al., 1986). In such myelin-stained, flat-mounted sections from the brains of ground squirrels, Ta has been identified as such (Slutsky et al., 2000), or simply referred to as auditory cortex (Paolini and Sereno, 1998).

There is no complete agreement on how auditory cortex is divided into areas across rodent taxa, but all rodents appear to have at least two core or primary-like areas,

as well as a number of associated secondary fields (e.g., Wallace et al., 2000; Thomas et al., 1993; Rutkowski et al., 2003; Polley et al., 2007). The core areas generally include an area identified as A1, and a more rostral area, the anterior auditory field. These areas receive inputs from the ventral nucleus of the medial geniculate complex, as well as other subdivisions (Ryugo and Killackey, 1974). These areas, and possibly adjoining auditory areas, have been included in an architectonic zone that has the sensory characteristics of Ta in squirrels. The region was termed *area auditoria* or area 41 in rats by Krieg (1946). Caviness (1975) described a similar area 41 in mice. Zilles and colleagues called the same region Te1 (temporal area 1) in rats (Zilles et al., 1980; Zilles and Wree, 1995). Given the distinctiveness of the auditory region, it is surprising that the region was not recognized in rodents by Brodmann (1909) or Rose (1930). Although Ta, area 41, or Te1 correspond to auditory cortex, the field includes at least two core areas and likely several secondary areas.

Area Tp. Area Tp is the other subdivision of temporal cortex in squirrels with architectonic characteristics suggestive of a core sensory field. This is a very distinct area in squirrels and has been delimited in a number of previous studies (Kaas et al., 1973; Krubitzer et al., 1986; Paolini and Sereno, 1998; Kaas et al., 1989; Slutsky et al., 2000). A comparable area Tp has been described in the agouti, identified by its dense myelination and ventroposterior position (Picanço-Diniz, 1987; Picanço-Diniz et al., 1989). Microelectrode recordings from Tp of agoutis indicate that the area responds to visual stimuli and possibly has a retinotopic organization. The source of the activating visual input to Tp of squirrels is uncertain. It appears to get no input from area 17 and, at best, sparse inputs from area 18. However, Robson and Hall (1977) demonstrated a dense

projection from the caudal part of the pulvinar complex to Tp in squirrels, and this subdivision of the pulvinar that receives inputs from the retinal-recipient layer of the superior colliculus. Thus, a relay from the retina to the superior colliculus, followed by the pulvinar, and finally to Tp, likely provides activating input to Tp. The superior colliculus of squirrels is about ten times larger than expected for a rat of similar size (Kaas and Collins, 2001), and it provides a massive input to the caudal pulvinar. As removal of all of area 17 in squirrels fails to completely abolish the components for visual discrimination (Levey et al., 1973; Kicliter et al., 1977; Wagor, 1978), a pathway from the superior colliculus to the cortex via the pulvinar may be the source for most of the preserved visual abilities. While considerable vision remains after a loss of primary visual cortex in such a diverse array of mammalian species such as cats, monkeys, tree shrews, and humans (see Payne et al., 1996 for review), the role of a pathway from the superior colliculus to cortex in preserving visual abilities remains uncertain (Fendrich et al., 2001).

No visual area comparable to Tp has been described in rats and mice. Krieg (1946) considered temporal cortex caudal to auditory cortex in rats to be poorly developed and of uncertain identity. The caudal division of temporal cortex of Zilles and Wree (1985), Te2, would seem to occupy the position of both Ti and Tp of squirrels, but the low level of myelination of Te2 and evidence of auditory functions suggest that this region more closely corresponds to Ti than Tp. Quite possibly, rats and mice, with less developed visual systems, have little cortex that corresponds to Tp.

Area Ti. Area Ti is the region between Ta and Tp. Ti has none of the pronounced architectonic features of a core sensory area of Ta and Tp, but rather has the appearance

of a higher-order or association area. The functions of Ti are not known, but its position between visual and auditory fields suggest that is might be responsive to both modalities. As suggested above, much of Ti may correspond to area Te2 of Zilles and Wree (1985) in rats.

Area Tm. The fourth subdivision of temporal cortex in squirrels is the most dorsal or medial portion, Tm. As the architecture of Tm resembles that of Tp, some of Tm was included in Tp by Kaas et al., (1972). However, part of the Tm region was distinguished as area 19p, as it differed from area 19 proper by having a somewhat denser layer 4 of granule cells and a somewhat greater expression of myelin. Together with Tp, Tm or parts of it may receive inputs from the caudal division of the inferior pulvinar (Robson and Hall, 1977). The Tm region appears to have connections with area 18 of grey squirrels (Kaas et al., 1989), and it is within the territory of temporal cortex that is responsive to visual stimuli in ground squirrels. Tm possibly overlaps with the proposed middle lateral (ML) visual field, where neurons were found to be directionally selective (Paolini and Sereno, 1998). Anatomical studies are needed to determine if the connections of Tm are distinct from those of Tp.

Areas of the parietal cortex

Areas Pa(S1), Pm, Pl, PV and dy are subdivisions of somatosensory cortex in squirrels. Areas Pa(S1), Pm and Pl have been retained from Kaas et al. (1972). Here we add the 3a/dy area and the parietal ventral area.

Area Pa(S1). The largest subdivision of somatosensory cortex is area Pa(S1). As somatosensory koniocortex (area 3b), Pa(S1) is characterized by a layer 4 that is densely

packed with granule cells. Amongst other architectonic features of primary sensory cortex, layer 4 is expresses very little synaptic zinc, and has a neuropil that is VGluT2 rich. This lack of synaptic zinc suggests that layer 4 receives inputs almost exclusively from the thalamus, rather than from other areas of cortex. As with primary somatosensory cortex (area 3b) of other mammals, Pa(S1) in squirrels receives dense inputs from the ventroposterior nucleus (Krubitzer and Kaas, 1987), and these inputs are expected to terminate largely within layer 4. Area Pa(S1) represents the contralateral body surface (Sur et al., 1978; Krubitzer et al., 1986; Slutsky et al., 2000) in a topographic pattern that conforms to the expected organization of the first somatosensory area, S1 (see Kaas, 1983 for review). Thus, the hindlimb and tail are represented medially, and the face is represented laterally in Pa(S1). As has been most clearly demonstrated in rats (e.g., Chapin and Lin, 1984; Dawson and Killackey, 1987; Remple et al., 2003), but also in other mammals including monkeys (see Qi and Kaas, 2004 for review), aspects of the somatotopy are reflected in the configuration of Pa(S1). Thus, protrusions of the rostral dysgranular area, dy, extend into Pa(S1), separating upper lip, lower lip and forepaw representations (Figure 8B; also see Figure 1 of Krubitzer et al., 1986). The two separate septa of dysgranular cortex merge in central Pa(S1), forming an oval of dysgranular cortex nearly 1mm wide where neurons fail to respond to light, tactile stimuli. This dysgranular oval was called “the unresponsive zone” (Sur et al., 1978), and it is known to have thalamic connections that implicate this and other parts of this dysgranular cortex in the processing of information from muscle spindle receptors (Gould, 1989). Functionally, the large dysgranular zones within Pa(S1) appear to be an extension of the rostral dysgranular cortex rather than part of Pa(S1).

The large forepaw region of Pa(S1) (Figure 8a; Sur et al., 1978) reflects the high density of cutaneous mechanoreceptors in the glaborous forepaw skin of tree squirrels (Brenowitz, 1980). Additional important sensory information in squirrels, as with other rodents, is relayed from the sinus hairs of the face, the mystiacal hairs and the smaller hairs on the skin adjoining the upper and lower lips. These regions of S1 of many rodents, and some other mammals, are subdivided histologically into a number of modules or barrel-like structures, first recognized by Woolsey and colleagues (1975). These modular subdivisions (called barrels), one for each whisker, can be seen in a number of histological preparations, including Nissl-stained sections cut parallel to the cortical surface. Such "barrels" have been described before in S1 of squirrels (Woolsey et al., 1975), and they are demonstrated here in brain sections processed for CO or PV (Fig. 13).

The primary somatosensory representation, S1, has been identified by microelectrode recordings in a number of rodent species and other mammals (see Johnson, 1985 for review). This primary representation has been consistently shown to be coextensive with an architectonically distinct zone of cortex that varies in histological differentiation, but always expresses more sensory characteristics than other areas of cortex, excluding primary auditory and primary visual cortex. As argued elsewhere, only the area 3b somatosensory representation of primates is homologous with S1 of other mammals (Kaas, 1983). Thus, the sensory cortex that is co-extensive with S1 can be termed as area 3b in all mammals, regardless of its degree of differentiation, as is now commonly done for area 17 as primary visual cortex. However, there has been a history of misidentification in architectonic studies. Brodmann (1909) identified much of the S1 region of squirrels as area 1. In rats, Krieg (1946) laterally divided the S1 region into a

puzzling patchwork of areas 1, 2 and 3. Caviness (1975) divided the S1 region of mice into areas 3 and 1, placing most of area 2 caudal to area 3. More recently, the full extent of S1 in rats has been recognized, and Zilles and Wree (1985) have accurately outlined S1 in Nissl-stained sections cut parallel to the flattened cortex as parietal area 1 (Par1), which includes both granular and dysgranular cortex of rats.

Although an overlap zone of S1 with motor cortex is commonly proposed in some rodents, especially rats (e.g., Donoghue et al., 1979; Donoghue and Wise, 1982; Hall and Lindholm 1974), the co-extensiveness of S1 with granular parietal cortex of rodents argues against this interpretation. Nevertheless, as Sanderson et al, (1984) noted, low-threshold movements can be elicited with electrical stimulation with microelectrodes from agranular, dysgranular, and even rostral granular parietal cortex in rats. This finding is similar to that obtained with microstimulation in primates, where low levels of current evoke movements from primary motor cortex (M1), dysgranular cortex (area 3a) between M1 and S1, and parts of S1 (area 3b) (see Wu et al., 2000; Burish et al., 2007). Yet, M1 (Area 4), area 3a, and S1(3b) areas are well established as separate areas without overlap. While some portions of S1(3b) in rodents may be more specialized for motor functions than others, these portions need not represent a more primitive overlap of functional areas, as often stated.

A second subdivision of parietal cortex, the dysgranular area, 3a/dy, lies along the rostral border of Pa(S1), while including the dysgranular zones that extend into Pa(S1). This arrangement is very much like the arrangement of dysgranular cortex relative to the granular cortex in rats (Chapin and Lin, 1984). Although a 3a/dy zone was not included in the earlier study of cortical architecture in squirrels of Kaas et al (1972), where brain

sections were cut in the coronal plane, the 3a/dy area is obvious in sections cut in the more favorable horizontal and sagittal planes. The 3a/dy area is identified by a marked reduction in the density of cells packed in layer 4 compared to Pa(S1), but a more obvious layer 4 than in motor cortex. By relative position and architectonic appearance, 3a/dy is homologous to area 3a of primates, an area that also appears to exist in other mammals as the cortical target of a thalamic projection of proprioceptive information, largely from muscle spindle receptors (see Krubitzer et al., 2004 for review). The area along the rostral border of S1 in cats has long been considered to be area 3a (e.g., Dykes et al., 1980). The 3a/dy area in squirrels has also been called the rostral area (Slutsky et al., 2000). As for area 3a of primates and cats, R or dys contains a representation of largely "deep" receptors (non-cutaneous) in a somatotopic pattern that parallels that of S1. These inputs come from a proprioceptive nucleus of the thalamus (Gould et al., 1989), and cortical inputs come from S1 (Krubitzer et al., 1986).

Area Pm. The medial half of the parietal cortex along the caudal border of Pa(S1) was termed Pm (Kaas et al., 1972). This band of cortex has less pronounced sensory features than Pa(S1), but Pm differs only slightly from adjoining areas 19 and Pl, which have somewhat more pronounced sensory features. Much of Pm has connections with Pa(S1), S2 and PV (Krubitzer et al., 1986), and in ground squirrels, neurons in Pm have been shown to respond to strong somatosensory stimulation (Slutsky et al., 2000). As such, Pm can be regarded as a somatosensory area, or possibly a multisensory area. An area Pm has also been defined along the caudal border of S1 in rats (Li et al., 1990; Fabri and Burton, 1991). Similar to Pm in squirrels, Pm in rats receives projections from S1 in a topographic pattern that indicates that a somatosensory representation in Pm parallels

the organization of S1. Pm in squirrels likely projects to motor cortex, as Pm does in rats (Donoghue and Parham, 1983; Reep et al., 1990; Reep et al., 1994; Wang and Kurata, 1998), and as cortex along the caudal border of S1 does in many mammals (see Remple et al., 2007 for review). The position of Pm, of course, is in the relative position of area 1 in primates, which contain a representation of cutaneous receptors in parallel to the S1 representation (see Kaas, 2004 for review). In rats, Pm has visual and perhaps auditory inputs, and functions as a multisensory area (Reep et al., 1994; Di et al., 1994; Wallace et al., 2004). In tree shrews, Pm consists of a rostral strip that is dominated by somatosensory inputs and a caudal strip that is multisensory (Remple et al., 2006). This possibility has not been investigated in squirrels.

As Pm in squirrels is not architectonically very distinct from adjoining occipital and lateral parietal areas, it is not surprising that a Pm region has not been distinguished in the major architectonic studies of neocortex in rats and mice. However, Rose (1912) distinguished a larger area 7 in mice that covered much of the region, whereas regions designated as areas 1 and 2, and perhaps 18a covered the Pm region in the depiction of Caviness (1975). In rats, Krieg (1946) included the Pm region in a larger area 7, whereas Zilles and coworkers included Pm in a large occipital region, Oc2L (Zilles 1990; Zilles and Wree, 1995).

Areas Pl and Pv. The lateral parietal region, Pl, has been retained from Kaas et al (1972), and the parietal ventral area, Pv, is newly distinguished as an architectonic field between Ta and Pa(S1). The second somatosensory area, S2 occupies a little more than the rostral half of Pl (Krubitzer et al., 1986). However, the only distinctive differences in the architecture of the two parts of Pl, is that caudal Pl has less zinc staining. Pl has less

dominant sensory characteristics than adjoining areas Pa(S1) and Ta, but more than Pm, Ti, and even area 19. S2 is known to receive direct thalamic connections from the ventroposterior nucleus in most mammals, as it does in squirrels (Krubitzer and Kaas, 1987). Other thalamic inputs are from the posterior medial nucleus. These thalamic inputs would reduce the expression of zinc in layer 4 and in supragranular layers of S2. However, S1 provides dense cortical inputs to S2, and Pv provides additional inputs (Krubitzer et al., 1987), increasing the expression of zinc. The significance of the more caudal part of Pl is unknown, but multisensory functions seem likely, given the adjacent somatosensory, auditory and visual regions.

Pv is a subdivision of somatosensory cortex that was first defined in squirrels, but has subsequently been identified in a range of mammalian species (see Slutsky et al., 2000, for review). As with S2, Pv contains a representation of the contralateral body surface. Typically, responses to auditory stimuli can be recorded in Pv as well. In squirrels, the sensory characteristics of Pv are less pronounced than in the adjoining areas Pa(S1) and Ta, as the cortical architecture resembles that of S2. Pv receives cortical inputs form S1 and S2 (Krubitzer et al., 1986) and thalamic inputs from the ventroposterior nucleus and parts of the medial geniculate complex (Krubitzer and Kaas, 1987). This mixture of thalamic and cortical inputs accounts for the increased expression of zinc in layer 4 and supragranular layers, compared to Pa(S1), but the increase is not as extensive as in area Ti, which appears to get fewer thalamic inputs.

Until recently, S2 and Pv were not distinguished from each other in other rodents, such as rats. However, the existence of both areas has now been well documented in rats (Fabri and Burton, 1991; Li et al., 1990; Remple et al., 2003). In surface-view sections,

Pv of rats expresses less cytochrome oxidase than either of the adjoining S1 of primary auditory areas, but the expression is uneven, suggesting a relationship to the body surface repesentation (Remple et al., 2003). In rats, both S2 and Pv would be contained in the cortex identified by Zilles and Wree (1985) as parietal area 2.

Frontal cortex

In frontal cortex of squirrels, we have distinguished an agranular motor area that might be more properly called dysgranular because a trace of layer 4 is present. Here we described other architectonic characteristics of this field, including the presence of a thin synaptic zinc-poor layer 4. Unpublished microstimulation results from our laboratory indicate that this agranular field, M, corresponds to primary motor cortex, M1. This M1 is in the relative position of M1 in other mammals, and it corresponds to the map of contralateral body movements that has been described in lateral agranular cortex of rats (Donoghue and Wise, 1982; Neafsey et al., 1986; Brecht et al., 2004). In rats, M1 appears to largely correspond to frontal area 1 (Fr1) of Zilles and Wree (1985), although not completely. Krieg (1946) defined an area 4 that overlaps with medial S1, and does not conform well to the extent of M1 in rats. In ground squirrels, Brodmann (1909) described a frontal region, with cytoarchitectonic features of both areas 4 and 6, that overlaps the present area M, whilst extending further rostrally.

The cortex rostromedial to area M is in the relative position of the second motor area of rats (Neafsey et al., 1986). In squirrels and rats, this rostromedial cortex has a more obvious layer 4, but this region is not fully characterized in the present report. The

second motor area of rats, whether a premotor area or the supplementary motor area, corresponds to the Fr2 region of Zilles and Wree (1995).

Other frontal areas in squirrels include the lateral orbital frontal cortex and the medial frontal cortex of the frontal pole. These regions were not well distinguished in the present preparations. In rats and rabbits, lateral and medial frontal regions have different connections and behavioral functions (Uylings et al., 2003; Gabbott et al., 2005; Leal-Campanario et al., 2007). Although the prefrontal cortex of rats is considered to be agranular (Öngür and Price, 2000), and thereby lacking the highly granular prefrontal cortex of primates (Preuss, 1995), frontal polar regions of squirrel cortex, have a clear layer 4. The frontal pole has been variously divided in rats, with Ray and Price (1992) defining medial and lateral frontal polar areas.

Cingulate and retrosplenial cortex

Cingulate cortex. In squirrels, we distinguish these subdivisions of cingulate cortex as areas DCg, VCg, and RCg. DCg corresponds to the dorsal cingulate area, VCg to the ventral cingulate area, and RCg to the prelimbic area of Ray and Price (1992). DCg approximately corresponds to area 24b and b', VCg to 24a' and RCg to 24a of Vogt et al. (2004). The cingulate cortex in squirrels, like in other mammals such as monkeys (Vogt et al., 1992) and rats (Zilles, 1990), surrounds much of the anterior portion of the corpus callosum (Fig. 21A). The cingulate cortex, part of the limbic system and the Papez circuit (Vogt et al., 1992), has cytoarchitectonic features of both isocortex and allocortex (Zilles, 1990). The lack of well-defined cortical layers and an indistinct layer 4, characteristics of the cingulate cortex in rats (Zilles, 1990; Vogt et al., 2004), are observed in grey squirrels

as well. SMI-32 preparations in grey squirrels showed that the dorsal part of the cingulate cortex, DCg, contains slightly more pyramidal neurons than the ventral areas, VCg and RCg (Fig. 21F). This is similar to the observation made by Jones and colleagues (2005) in Nissl preparation of rat brain sections, where this dorsal anterior cingulate (ACd) area (DCg here), contains slightly more pyramidal neurons than their ventral anterior cingulate (ACv) area (VCg and RCg). The cingulate cortex in rats receives diffuse projections from the mediodorsal, ventromedial and anteromedial portion of the thalamus (Domesick, 1969) and has been implicated in higher-order brain functions, such as attention, pain processing and motivational aspects of learning (Gabriel et al., 1980; Vogt et al., 1990; Jones et al., 2005).

Retrosplenial cortex. The retrosplenial cortex has a role in the processes of learning and memory (van Groen and Wyss, 1990). In grey squirrels, we have retained the retrosplenial granular (RSG), and retrosplenial agranular (RSA) nomenclature of Rose (1929) and these retrosplenial areas seem to correspond to areas 29a to c and 29d respectively, of Vogt (1993). The granular retrosplenial cortical area (RSG) in grey squirrels, as in rats (Vogt and Peters, 1981), is more dysgranular than agranular as there is some layer 4 stellate cells. Just as in rats, RSG in squirrels has a compressed layer 2 plus 3 that is densely packed with cells. This band of cells is less distinct in the poorly laminated RSA (Fig. 7A)(Palomero-Gallagher and Zilles, 2004). Both RSG and RSA show characteristics of periallocortex, with poor laminar differentiation, making them easily distinguishable from adjacent cortical areas. The middle layers of RSG are poorly stained in sections processed for zinc, suggesting the presence of thalamic inputs. RSA has more zinc staining, especially in layer 3. In rats, RSG receives afferents from the

anterodorsal (AD) and anteroventral (AV), and lateral dorsal (LD) thalamic nuclei (Domesick, 1969; 1972; van Groen and Wyss, 1990), as well as afferents from parts of the cingulate cortex, some visual areas (Vogt and Miller, 1983) and callosal fibers from the contralateral retrosplenial areas (Vogt et al., 1981). RSA has connections with the anteroventral (AV), anteromedial (AM) and the lateral dorsal (LD) nuclei of the thalamus (Sripanidkulchai and Wyss, 1986).

Perirhinal cortex

Perirhinal cortex forms a narrow belt along the dorsal bank of the rhinal fissure and the caudally adjoining cortex at the end of the rhinal sulcus. Traditionally, perirhinal cortex has been divided somewhat arbitrarily into a portion ventral and rostral to somatosensory cortex, the insular cortex, and a more caudal portion, the perirhinal cortex, of similar appearance. Even more caudoventrally, the entorhinal cortex has a distinct appearance that allows it to be identified as such in a wide range of mammalian species.

Insular cortex. The insular cortex (Ins) defined here is poorly laminated with an indistinct layer 4 (Fig. 24). In rats, this region corresponds to the "agranular" insular cortex (AI) of Zilles (1990) that lacks a distinct granular layer 4 and is poorly myelinated. Our insular cortex in squirrels does not include the granular insular cortex of other descriptions in rats and other rodents, as this cortex is included in our Pv region (Fig. 8A). As with rats (Zilles, 1990), the insular cortex in grey squirrels occupies the anterior half of the rhinal sulcus, with the claustrum marking the caudal border of the insular with the adjoining perirhinal cortex. The insular cortex has connections with several regions, including the cingulate, piriform, perirhinal and entorhinal cortices, and the mediodorsal

and lateroposterior nuclei of the thalamus (Groenewegen, 1988; Zilles, 1990; Ray and Price, 1992). Proposed to be part of the gustatory cortex, the agranular region of the insular in rats may be involved in taste (Kosar et al., 1986; Sewards and Sewards, 2001), as well as to having introceptive functions (Cechetto and Saper, 1987; Contreras et al., 2007).

Perirhinal cortex. The perirhinal cortex, PRh, in squirrels is bordered by temporal, insular and entorhinal cortices. PRh is retained from Zilles and Wree (1985), and corresponds to the posterior region of area 35 of Krieg (1946) and the ectorhinal and perirhinal areas of Swanson (1992). PRh is poorly myelinated in both grey squirrels (Fig. 24B) and rats (Burwell, 2001; Palomero-Gallagher and Zilles, 2004). In grey squirrels, PRh receives large amounts of cortiocortical inputs, especially in the superficial layers, as shown by the zinc stain (Fig. 24C). In rats, PRh has connections with the piriform, frontal, temporal and insular cortices (Furtak, 2007) and the anterior thalamic nuclei (Palomero-Gallagher and Zilles, 2004). Connections of PRh with the hippocampal formation suggest that PRh has a role in memory processes (Burwell and Amaral, 1998; Palomero-Gallagher and Zilles, 2004; Furtak, 2007**).**

Entorhinal cortex. The entorhinal cortex, area 28 of Brodmann's (1909) is part of the retrohippocampal field and is an important association pathway within the hippocampal region (Köhler, 1986). We have retained the term Ent of rats from Paxinos et al. (1999) and Zilles (Palomero-Gallagher and Zilles, 2004), which corresponds to the entorhinal cortex (EC) of Blackstad (1956) and Köhler (1986). EC cortex has been divided into medial (MEA) and lateral areas (LEA) (Köhler, 1986), or areas 28a and 28b respectively (Blackstad, 1956). On the basis of cytoarchitecture, we have further

subdivided LEA into intermediate (IEnt) and lateral (LEnt) portions. MEA corresponds to our MEnt.

Summary

Squirrels are rodents that have become useful and interesting in studies of neocortical areas and functions, in part because of their well-developed visual system, but also because of a brain that is larger than those in rats and mice. Here, we show that a number of cortical areas are more distinct architectonically than in more commonly studied laboratory rodents. In particular, primary and secondary visual areas as well as three main divisions of the temporal lobe are obvious. The distinctiveness of these fields invites further study, as well as comparisons with other rodents where homologous regions are expected, but not as easily defined. Such comparisons could lead to a better understanding of cortical organization and function in the widely used rats and mice. Other comparisons might be made with other members of the Euarchontoglire clade of mammals, including the closely related lagomorphs and the more distantly related tree shrews and primates. We would expect more overall similarities in cortical organization across members of this clade, than between members of this clade and those of the other five major clades of mammals. In this regard, it is interesting that evidence for a third visual area, V3, exists for some ground squirrels, but not for rats and mice, where even the existence of V2 has been questioned. V3 has been described in primates of the Euarchontoglire clade, but also in cats of the Laurasiatherian clade. While it is possible that a V3-like area evolved independently in squirrels, primates and cats, the other possibility is that present comparative understandings of cortical organizations within and

across clades are so incomplete and inaccurate that questions about the evolution of V3, and perhaps many cortical areas, cannot be fruitfully addressed without a host of further comparative studies. As such studies can be costly and labor-intensive, studies of brain organization and function have necessarily concentrated on a few species for practical or conceptual reasons. Further studies of brain organization in squirrels might promote a better understanding of cortical organization and evolution in members of the Euarchontoglire clade.

Table 1: Abbreviations

3a/dy	Dysgranular region
A1	Primary auditory cortex
CA1	*Cornu Ammonis 1*
CA3	*Cornu Ammonis 3*
CB	Calbindin
CO	Cytochrome oxidase
DCg	Dorsal cingulate area
DG	Dentate gyrus
Ent	Entorhinal area
F	Frontal area
Hippo	Hippocampus
IEnt	Intermediate entorhinal area
Ins	Insular area
L	Limbic area
LAMP	Limbic associated membrane protein
LEnt	Lateral entorhinal area
M1	Primary motor cortex
MEnt	Medial entorhinal area
Pa(S1)	Parietal anterior area
PaS	Parasubiculum
PB	Phosphate buffer
Pirf	Piriform cortex
Pl	Parietal lateral area
Pm	Parietal medial area
Pre	Presubiculum
PRh	Perirhinal area
PS	Prostriata
Pv	Parietal ventral area
PV	Parvalbumin
R	Rostral auditory area
RCg	Rostral cingulate area
RSA	Retrosplenial agranular area
RSG	Retrosplenial granular area
S1	Primary somatosensory cortex
S2	Secondary somatosensory cortex
Sub	Subiculum
Ta	Temporal anterior area
Ta_i	Temporal anterior intermediate area
Tav	Temporal anterior ventral area
Ti	Temporal intermediate area
Tm	Temporal mediodorsal area
Tp	Temporal posterior area
UZ	Unresponsive zone

V1	Primary visual area
V2	Secondary visual area
VCg	Ventral cingulate area
VGluT2	Vesicle glutamate transporter 2
Zn^{2+}	Zinc ions

References

Abplanalp P. 1970. Some subcortical connections of the visual system in tree shrews and squirrels. Brain Behav Evol 3(1):155-168.

Albus K, Beckmann R. 1980. Second and third visual area of the cat: interindividual variability in retinotopic arrangement and cortical location. J Physiol 299:276-297.

Allman JM, Kaas JH. 1971. Representation of the visual field in striate and adjoining cortex of the owl monkey (Aotus trivirgatus). Brain Res. 35(1):89-106.

Avendaño C, Verdu A. 1992. Area 3a in the cat. I. A reevaluation of its location and architecture on the basis of Nissl, myelin, acetylcholinesterase, and cytochrome oxidase staining. J Comp Neurol. 321(3):357-72.

Benton MJ. 2005. Vertebrate Palaeontology. Oxford: Blackwell.

Blackstad TW. 1956. Commissural connections of the hippocampal region in the rat, with special reference to their mode of termination. J Comp Neurol 105(3):417-537.

Boire D, Desgent S, Matteau I, Ptito M. 2005. Regional analysis of neurofilament protein immunoreactivity in the hamster's cortex. J Chem Neuroanat 29(3):193-208.

Bravo H, Olavarria J, Torrealba F. 1990. Comparative study of visual inter and intrahemispheric cortico-cortical cnnections in five native Chilean rodents. Anat Embryol 191:67-73.

Brecht M, Krauss A, Muhammad S, Sinai-Esfahani L, Bellanca S, Margrie TW. 2004. Organization of rat vibrissa motor cortex and adjacent areas according to cytoarchitectonics, microstimulation, and intracellular stimulation of identified cells. J Comp Neurol 479(4):360-373.

Brenowitz GL. 1980. Cutaneous mechanoreceptor distribution and its relationship to behavioral specializations in squirrels. Brain Behav Evol 17(6):432-453.

Brodmann K. 1909. Brodmann's 'Localisation in the Cerebral Cortex'. Garey LJ, translator. London: Eldred Smith-Gordon.

Brown CE, Dyck RH. 2004. Distribution of zincergic neurons in the mouse forebrain. J Comp Neurol 479(2):156-167.

Burish M, Stepniewska I, Kaas JH. 2007. Microstimulation and architectonics of frontoparietal cortex in common marmosets (Callithrix jacchus). J Comp Neurol 507(2):285-296.

Burwell RD. 2001. Borders and cytoarchitecture of the perirhinal and postrhinal cortices in the rat. J Comp Neurol 437(1):17-41.

Burwell RD, Amaral DG. 1998. Cortical afferents of the perirhinal, postrhinal, and entorhinal cortices of the rat. J Comp Neurol 398(2):179-205.

Campbell MJ, Morrison JH. 1989. Monoclonal antibody to neurofilament protein (SMI-32) labels a subpopulation of pyramidal neurons in the human and monkey neocortex, J Comp Neurol. 282(2):191–205.

Casagrande VA, and Kaas JH. 1994. The afferent, intrinsic, and efferent connections of primary visual cortex in primates. In Cerebral Cortex: Primary Visual Cortex in Primates, K.S. Rockland, and A. Peters, eds. New York: Plenum. 201-259.

Caviness VS, Jr. 1975. Architectonic map of neocortex of the normal mouse. J Comp Neurol 164(2):247-263.

Cechetto DF, Saper CB. 1987. Evidence for a viscerotopic sensory representation in the cortex and thalamus in the rat. J Comp Neurol 262(1):27-45.

Celio MR. 1986. Parvalbumin in most gamma-aminobutyric acid-containing neurons of the rat cerebral cortex. Science 231(4741):995-997.

Chapin JK, Lin CS. 1984. Mapping the body representation in the SI cortex of anesthetized and awake rats. J Comp Neurol 229(2):199-213.

Chesselet M-F, Gonzales C, Levitt P. 1991. Heterogeneous distribution of the limbic system-associated membrane protein in the caudate nucleus and substantia nigra of the cat. Neuroscience 40: 725-733.

Conde F, Lund JS, Lewis DA. 1996. The hierarchical development of monkey visual cortical regions as revealed by the maturation of parvalbumin-immunoreactive neurons. Brain Res Dev Brain Res 96(1-2):261-276.

Contreras M, Ceric F, Torrealba F. 2007. Inactivation of the interoceptive insula disrupts drug draving and malaise induced by lithium. Science 318:655-657.

Coté P-Y, Levitt P, Parent A. 1995. Distribution of limbic system-associated membrane protein (LAMP) immunoreactivity in primate basal ganglia. Neuroscience 69: 71-81.

Cusick CG, Kaas JH. 1982. Retinal projections in adult and newborn grey squirrels. Brain Res 256(3):275-284.

Czupryn A, Skangiel-Kramska J. 1997. Distribution of synaptic zinc in the developing mouse somatosensory barrel cortex. J Comp Neurol 386(4):652-660.

Danscher G. 1981. Histochemical demonstration of heavy metals. A revised version of the sulphide silver method suitable for both light and electronmicroscopy. Histochemistry 71(1):1-16.

Danscher G. 1982. Exogenous selenium in the brain. A histochemical technique for light and electron microscopical localization of catalytic selenium bonds. Histochemistry 76(3):281-293.

Danscher G, Stoltenberg M. 2005. Zinc-specific autometallographic in vivo selenium methods: tracing of zinc-enriched (ZEN) terminals, ZEN pathways, and pools of zinc ions in a multitude of other ZEN cells. J Histochem Cytochem 53(2):141-153.

Dawson DR, Killackey HP. 1987. The organization and mutability of the forepaw and hindpaw representations in the somatosensory cortex of the neonatal rat. J Comp Neurol 256(2):246-256.

de Nó R, Lorente. 1992. The cerebral cortex of the mouse (a first contribution--the "acoustic" cortex). Somatosens Mot Res 9(1):3-36.

DeFelipe J, Jones EG. 1991. Parvalbumin immunoreactivity reveals layer IV of monkey cerebral cortex as a mosaic of microzones of thalamic afferent terminations. Brain Res 562(1):39-47.

DeFelipe J, 1997. Types of neurons, synaptic connections and chemical characteristics of cells immunoreactive for calbindin-D28K, parvalbumin and calretinin in the neocortex. J Chem Neuroanat. 14:1–19.

Di S, Brett B, Barth DS. 1994. Polysensory evoked potentials in rat parietotemporal cortex: combined auditory and somatosensory responses. Brain Res 642(1-2):267-280.

Domesick VB. 1969. Projections from the cingulate cortex in the rat. Brain Res 12(2):296-320.

Domesick VB. 1972. Thalamic relationships of the medial cortex in the rat. Brain Behav Evol 6(1):457-483.

Donoghue JP, Kerman KL, Ebner FF. 1979. Evidence for two organizational plans within the somatic sensory-motor cortex of the rat. J Comp Neurol 183(3):647-663.

Donoghue JP, Wise SP. 1982. The motor cortex of the rat: cytoarchitecture and microstimulation mapping. J Comp Neurol 212(1):76-88.

Donoghue JP, Parham C. 1983. Afferent connections of the lateral agranular field of the rat motor cortex. J Comp Neurol 217(4):390-404.

Douzery EJ. 2002. Rodent phylogeny and a timescale for the evolution of Glires: evidence from an extensive taxon sampling using three nuclear genes. Mol Biol Evol 19(7):1053-1065.

Dursteler MR, Blakemore C, Garey LJ. 1979. Projections to the visual cortex in the golden hamster. J Comp Neurol 183(1):185-204.

Dykes R, Rasmussen D, Hoeltzell P. 1980. Ventroposterior thalamic regions projecting to cytoarchitectonic areas 3a and 3b in the cat. J Neurophysiol 56:1527-1546.

Dykes RW, Herron P, Lin CS. 1986. Ventroposterior thalamic regions projecting to cytoarchitectonic areas 3a and 3b in the cat. J Neurophysiol. 6(6):1521-41.

Fabri M, Burton H. 1991. Topography of connections between primary somatosensory cortex and posterior complex in rat: a multiple fluorescent tracer study. Brain Res 538(2):351-357.

Felleman DJ, Wall JT, Cusick CG, Kaas JH. 1983. The representation of the body surface in S-I of cats. J Neurosci. 3(8):1648-69.

Fendrich R, Wessinger CM, Gazzaniga MS. 2001. Speculations on the neural basis of islands of blindsight. Prog Brain Res 134:353-366.

Frederickson CJ, Moncrieff DW. 1994. Zinc-containing neurons. Biol Signals 3(3):127-139.

Frederickson CJ, Suh SW, Silva D, Frederickson CJ, Thompson RB. 2000. Importance of zinc in the central nervous system: the zinc-containing neuron. J Nutr 130(5S Suppl):1471S-1483S.

Fujiyama F, Furuta T, Kaneko T. 2001. Immunocytochemical localization of candidates for vesicular glutamate transporters in the rat cerebral cortex. J Comp Neurol 435(3):379-387.

Furtak SC, Wei SM, Agster KL, Burwell RD. 2007. Functional neuroanatomy of the parahippocampal region in the rat: the perirhinal and postrhinal cortices. Hippocampus. 17(9):709-22.

Gabbott PL, Warner TA, Jays PR, Salway P, Busby SJ. 2005. Prefrontal cortex in the rat: projections to subcortical autonomic, motor, and limbic centers. J Comp Neurol 492(2):145-177.

Gabriel M, Orona E, Foster K, Lambert RW. 1980. Cingulate cortical and anterior thalamic neuronal correlates of reversal learning in rabbits. J Comp Physiol Psychol 94(6):1087-1100.

Gallyas F. 1979. Silver staining of myelin by means of physical development. Neurol Res 1(2):203-209.

Garrett B, Geneser FA, Slomianka L. 1991. Distribution of acetylcholinesterase and zinc in the visual cortex of the mouse. Anat Embryol (Berl) 184(5):461-468.

Garrett B, Osterballe R, Slomianka L, Geneser FA. 1994. Cytoarchitecture and staining for acetylcholinesterase and zinc in the visual cortex of the Parma wallaby (Macropus parma). Brain Behav Evol 43(3):162-172.

Gould HJ, 3rd. 1984. Interhemispheric connections of the visual cortex in the grey squirrel (Sciurus carolinensis). J Comp Neurol 223(2):259-301.

Gould HJ, 3rd, Whitworth RH, Jr., LeDoux MS. 1989. Thalamic and extrathalamic connections of the dysgranular unresponsive zone in the grey squirrel (Sciurus carolinensis). J Comp Neurol 287(1):38-63.

Groenewegen HJ. 1988. Organization of the afferent connections of the mediodorsal thalamic nucleus in the rat, related to the mediodorsal-prefrontal topography. Neuroscience. 24(2):379-431.

Guldin WO, Markowitsch HJ. 1983. Cortical and thalamic afferent connections of the insular and adjacent cortex of the rat. J Comp Neurol 215(2):135-153.

Hall R, Lindholm E. 1974. Organzation of motor and somatosensory neocortex in the albino rat. Brain Res 66:23-38.

Hall WC, Kaas JH, Killackey H, Diamond IT. 1971. Cortical visual areas in the grey squirrel (Sciurus carolinesis): a correlation between cortical evoked potential maps and architectonic subdivisions. J Neurophysiol 34(3):437-452.

Herculano-Houzel S, Mota B, Lent R. 2006. Cellular scaling rules for rodent brains. Proc Natl Acad Sci U S A 103(32):12138-12143.

Hevner RF, Wong-Riley MT. 1992. Entorhinal cortex of the human, monkey, and rat: metabolic map as revealed by cytochrome oxidase. J Comp Neurol 326(3):451-469.

Hof PR, Glezer, II, Conde F, Flagg RA, Rubin MB, Nimchinsky EA, Vogt Weisenhorn DM. 1999. Cellular distribution of the calcium-binding proteins parvalbumin, calbindin, and calretinin in the neocortex of mammals: phylogenetic and developmental patterns. J Chem Neuroanat 16(2):77-116.

Horton HL, Levitt P. 1988. A unique membrane protein is expressed on early developing limbic system axons and cortical targets. J Neurosci 8:4653-4661.

Hubel DH, Wiesel TN. 1965. Receptive Fields and Functional Architecture in Two Nonstriate Visual Areas (18 and 19) of the Cat. J Neurophysiol 28:229-289.

Huchon D, Madsen O, Sibbald M, Ament K, Stanhope M, Catzeflis F, de Jong W, Douzery E. 2002. Rodent phylogeny and a timescale for the evolution of Glires: evidence from an extensive taxon sampling using three nuclear genes. Mol Biol Evol 19(7):1053-1065.

Huffman KJ, Krubitzer L. 2001. Area 3a: topographic organization and cortical connections in marmoset monkeys. Cereb Cortex 11(9):849-867.

Ichinohe N, Fujiyama F, Kaneko T, Rockland KS. 2003. Honeycomb-like mosaic at the border of layers 1 and 2 in the cerebral cortex. J Neurosci. 23(4):1372-82.

Ichinohe N, Rockland KS. 2004. Region specific micromodularity in the uppermost layers in primate cerebral cortex. Cereb Cortex 14(11):1173-1184.

Jain N, Preuss TM, Kaas JH. 1994. Subdivisions of the visual system labeled with the Cat-301 antibody in tree shrews. Vis Neurosci 11(4):731-741.

Johnson JI. 1985. Comparative development of somatic sensory cortex. Jones EG, Peters A, editors. New York: Plenum Press.

Jones BF, Groenewegen HJ, Witter MP. 2005. Intrinsic connections of the cingulate cortex in the rat suggest the existence of multiple functionally segregated networks. Neuroscience 133(1):193-207.

Jones EG, Porter R. 1980. What is area 3a? Brain Res. 203(1):1-43. Review.

Jones, EG. (2007) The Thalamus (Cambridge Univ Press, Cambridge, UK,) 2nd Ed.

Kaas JH. 1983. What, if anything, is SI? Organization of first somatosensory area of cortex. Physiol Rev 63(1):206-231.

Kaas JH, Collins CE. 2001. Evolving ideas of brain evolution. Nature 411(6834):141-142.

Kaas JH, Guillery RW, Allman JM. 1973. Discontinuities in the dorsal lateral geniculate nucleus corresponding to the optic disc: a comparative study. J Comp Neurol 147(2):163-179.

Kaas JH, Hall WC, Diamond IT. 1972. Visual cortex of the grey squirrel (Sciurus carolinensis): architectonic subdivisions and connections from the visual thalamus. J Comp Neurol 145(3):273-305.

Kaas JH, Krubitzer LA, Johanson KL. 1989. Cortical connections of areas 17 (V-I) and 18 (V-II) of squirrels. J Comp Neurol 281(3):426-446.

Kaas JH, Lyon DC. 2001. Visual cortex organization in primates: theories of V3 and adjoining visual areas. Prog Brain Res 134:285-295.

Kaas JH, Lyon DC. 2007. Pulvinar contributions to the dorsal and ventral streams of visual processing in primates. Brain Res Rev.

Kalia M, Whitteridge D. 1973. The visual areas in the splenial sulcus of the cat. J Physiol 232(2):275-283.

Kaneko T, Fujiyama F. 2002. Complementary distribution of vesicular glutamate transporters in the central nervous system. Neurosci Res 42(4):243-250.

Kicliter E, Loop MS, Jane JA. 1977. Effects of posterior neocortical lesions on wavelength, light/dark and stripe orientation discrimination in ground squirrels. Brain Res 122(1):15-31.

Kohler C. 1986. Cytochemical architecture of the entorhinal area. Adv Exp Med Biol 203:83-98.

Kosar E, Grill HJ, Norgren R. 1986. Gustatory cortex in the rat. I. Physiological properties and cytoarchitecture. Brain Res. 379(2):329-41.

Krieg W. 1946. Connections of the cerebral cortex. I. The albino rat. A. Topography of the cortical areas. J Comp Neurol 84:221-275.

Krubitzer L, Huffman KJ, Disbrow E, Recanzone G. 2004. Organization of area 3a in macaque monkeys: contributions to the cortical phenotype. J Comp Neurol 471(1):97-111.

Krubitzer LA, Kaas JH. 1987. Thalamic connections of three representations of the body surface in somatosensory cortex of gray squirrels. J Comp Neurol 265(4):549-580.

Krubitzer LA, Sesma MA, Kaas JH. 1986. Microelectrode maps, myeloarchitecture, and cortical connections of three somatotopically organized representations of the body surface in the parietal cortex of squirrels. J Comp Neurol 250(4):403-430.

Lane RH, Allman JM, Kaas JH. 1971. Representation of the visual field in the superior colliculus of the grey squirrel (Sciurus carolinensis) and the tree shrew (Tupaia glis). Brain Res 26(2):277-292.

Latawiec D, Martin KA, Meskenaite V. 2000. Termination of the geniculocortical projection in the striate cortex of macaque monkey: a quantitative immunoelectron microscopic study. J Comp Neurol 419(3):306-319.

Leal-Campanario R, Fairen A, Delgado-Garcia JM, Gruart A. 2007. Electrical stimulation of the rostral medial prefrontal cortex in rabbits inhibits the expression of conditioned eyelid responses but not their acquisition. Proc Natl Acad Sci U S A 104(27):11459-11464.

Lee VM, Carden MJ, Schlaepfer WW, Trojanowski JQ. 1987. Monoclonal antibodies distinguish several differentially phosphorylated states of the two largest rat neurofilament subunits (NF-H and NF-M) and demonstrate their existence in the normal nervous system of adult rats. J Neurosci 7(11):3474-3488.

Lent R. 1982. The organization of subcortical projections of the hamster's visual cortex. J Comp Neurol 206(3):227-242.

Levey NH, Harris J, Jane JA. 1973. Effects of visual cortical ablation on pattern discrimination in the ground squirrel (Citellus tridecemlineatus). Exp Neurol 39(2):270-276.

Levitt P. 1984. A monoclonal antibody to limbic system neurons. Science 223: 299-301.

Li XG, Florence SL, Kaas JH. 1990. Areal distributions of cortical neurons projecting to different levels of the caudal brain stem and spinal cord in rats. Somatosens Mot Res 7(3):315-335.

Long KO, Fisher SK. 1983. The distributions of photoreceptors and ganglion cells in the California ground squirrel, Spermophilus beecheyi. J Comp Neurol 221(3):329-340.

Luethke LE, Krubitzer LA, Kaas JH. 1988. Cortical connections of electrophysiologically and architectonically defined subdivisions of auditory cortex in squirrels. J Comp Neurol 268(2):181-203.

Major DE, Rodman HR, Libedinsky C, Karten HJ. 2003. Pattern of retinal projections in the California ground squirrel (Spermophilus beecheyi): anterograde tracing study using cholera toxin. J Comp Neurol 463(3):317-34

Malach R. 1989. Patterns of connections in rat visual cortex. J Neurosci 9(11):3741-3752.

Mercer JM, Roth VL. 2003. The effects of Cenozoic global change on squirrel phylogeny. Science 299(5612):1568-1572.

Merzenich MM, Kaas JH, Roth GL. 1976. Auditory cortex in the grey squirrel: tonotopic organization and architectonic fields. J Comp Neurol 166(4):387-401.

Miro-Bernie N, Ichinohe N, Perez-Clausell J, Rockland KS. 2006. Zinc-rich transient vertical modules in the rat retrosplenial cortex during postnatal development. Neuroscience 138(2):523-535.

Montero VM. 1993. Retinotopy of cortical connections between the striate cortex and extrastriate visual areas in the rat. Exp Brain Res 94(1):1-15.

Morecraft RJ, Rockland KS, Van Hoesen GW. 2000. Localization of area prostriata and its projection to the cingulate motor cortex in the rhesus monkey. Cereb Cortex 10(2):192-203.

Nahmani M, Erisir A. 2005. VGluT2 immunochemistry identifies thalamocortical terminals in layer 4 of adult and developing visual cortex. J Comp Neurol 484(4):458-473.

Neafsey EJ. 1990. The complete ratunculus: output organization of layer V of the cerebral cortex. Tees BKRC, editor. Cambridge, MA: MIT Press. 197-212 p.

Neafsey EJ, Bold EL, Haas G, Hurley-Gius KM, Quirk G, Sievert CF, Terreberry RR. 1986. The organization of the rat motor cortex: a microstimulation mapping study. Brain Res 396(1):77-96.

Nelson RJ, Sur M, Kaas JH. 1979. The organization of the second somatosensory area (SmII) of the grey squirrel. J Comp Neurol 184(3):473-489.

Olavarria J, Mendez B. 1979. The representations of the visual field on the posterior cortex of Octodon degus. Brain Res 161(3):539-543.

Olavarria J, Montero V. 1990. Elaborate organization of visual cortex in the hamster. Neurosci Res 8(1):40-47.

Olavarria J, Montero VM. 1984. Relation of callosal and striate-extrastriate cortical connections in the rat: morphological definition of extrastriate visual areas. Exp Brain Res 54(2):240-252.

Olavarria J, Montero VM. 1989. Organization of visual cortex in the mouse revealed by correlating callosal and striate-extrastriate connections. Vis Neurosci 3(1):59-69.

Olavarria J, Van Sluyters RC. 1982. The projection from striate and extrastriate cortical areas to the superior colliculus in the rat. Brain Res 242(2):332-336.

Ongur D, Price JL. 2000. The organization of networks within the orbital and medial prefrontal cortex of rats, monkeys and humans. Cereb Cortex 10(3):206-219.

Palomero-Gallagher N, Zilles K. 2004. Isocortex. In: Paxinos G, editor. The Rat Nervous System. London: Elsevier.

Paolini M, Sereno MI. 1998. Direction selectivity in the middle lateral and lateral (ML and L) visual areas in the California ground squirrel. Cereb Cortex 8(4):362-371.

Paxinos G, Franklin KBJ. 2003. The Mouse Brain in Stereotaxic Coordinates: Academic Press.

Paxinos G, Kas L, Ashwell KWS, Watson C. 1999. Chemoarchitectonic Atlas of the Rat Forebrain: Academic Press.

Payne BR, Lomber SG, Macneil MA, Cornwell P. 1996. Evidence for greater sight in blindsight following damage of primary visual cortex early in life. Neuropsychologia 34(8):741-774.

Picanco-Diniz CW, Oliveira HL, Silveira LC, Oswaldo-Cruz E. 1989. The visual cortex of the agouti (Dasyprocta aguti): architectonic subdivisions. Braz J Med Biol Res 22(1):121-138.

Picano-Diniz C. 1987. Organizacao do sistema visual de roedores da Amazonia: topografia das areas visuais da Cutia, Dasyprocta aguti. Doctoral thesis: Universidade Federal do Rio de Janerio.

Polley DB, Read HL, Storace DA, Merzenich MM. 2007. Multiparametric auditory receptive field organization across five cortical fields in the albino rat. J Neurophysiol 97(5):3621-3638.

Preuss, TM. 1995. Do rats have prefrontal cortex? The Rose-Woolsey-Akert program reconsidered. J Cogn. Neurosci. 7: 1-24.

Preuss TM, Stepniewska I, Jain N, Kaas JH. 1997. Multiple divisions of macaque precentral motor cortex identified with neurofilament antibody SMI-32. Brain Res 767(1):148-153.

Qi HX, Preuss TM, Kaas JH. 2007. Somatosensory areas of the cerebral cortex: Architectonic characteristics and modular organization. Basbaum A, How RR, Kaneki A, Shepherd GM, Westheimer G, Kaas JH, editors: Elsevier.

Qi HX, Kaas JH. 2004. Myelin stains reveal an anatomical framework for the representation of the digits in somatosensory area 3b of macaque monkeys. J Comp Neurol 477(2):172-187.

Ray JP, Price JL. 1992. The organization of the thalamocortical connections of the mediodorsal thalamic nucleus in the rat, related to the ventral forebrain-prefrontal cortex topography. J Comp Neurol 323(2):167-197.

Reep RL, Goodwin GS, Corwin JV. 1990. Topographic organization in the corticocortical connections of medial agranular cortex in rats. J Comp Neurol 294(2):262-280.

Reep RL, Chandler HC, King V, Corwin JV. 1994. Rat posterior parietal cortex: topography of corticocortical and thalamic connections. Exp Brain Res 100(1):67-84.

Reid SN, Juraska JM. 1991. The cytoarchitectonic boundaries of the monocular and binocular areas of the rat primary visual cortex. Brain Res 563(1-2):293-296.

Reinoso BS, Pimenta AF, Levitt P. 1996. Expression of the mRNAs encoding the limbic system-associated membrane protein (LAMP): I. Adult rat brain. J Comp Neurol 375(2):274-288.

Remple MS, Reed JL, Stepniewska I, Lyon DC, Kaas JH. 2007. The organization of frontoparietal cortex in the tree shrew (Tupaia belangeri): II. Connectional evidence for a frontal-posterior parietal network. J Comp Neurol. 501(1):121-49

Remple MS, Reed JL, Stepniewska I, Kaas JH. 2006.Organization of frontoparietal cortex in the tree shrew (Tupaia belangeri). I. Architecture, microelectrode maps, and corticospinal connections. J Comp Neurol. 497(1):133-54.

Remple MS, Henry EC, Catania KC. 2003. Organization of somatosensory cortex in the laboratory rat (Rattus norvegicus): Evidence for two lateral areas joined at the representation of the teeth. J Comp Neurol 467(1):105-118.

Robson JA, Hall WC. 1975. Connections of layer VI in striate cortex of the grey squirrel (Sciurus carolinensis). Brain Res 93(1):133-139.

Robson JA, Hall WC. 1977. The organization of the pulvinar in the grey squirrel (Sciurus carolinensis). II. Synaptic organization and comparisons with the dorsal lateral geniculate nucleus. J Comp Neurol 173(2):389-416.

Rosa MG. 1999. Topographic organisation of extrastriate areas in the flying fox: implications for the evolution of mammalian visual cortex. J Comp Neurol 411(3):503-523.

Rosa MG, Krubitzer LA. 1999. The evolution of visual cortex: where is V2? Trends Neurosci 22(6):242-248.

Rosa MGP, Casagrande VA, Preuss TM, Kaas JH. 1997. Visual field represnetation in striate and prestriate cortices of a prosimian primate (Galago garnetti). The American Physiological Society:3193-3217.

Rose M. 1912. Histologische Localization der Grosshirnide der kleinen Saugetire (Rodentia, Insectivora, Chiroptera). JF Phychol U Neur 19:389-479.

Rose M. 1929. Cytoarchitektonischer Atlas der Großhirnrinde der Maus. J Psychol Neurol 35: 65-173.

Rose M. 1930. Cytoarchitektonischer Atlas der Grosshinrinde der Maus. JF Phychol U Neur 40:1-51.

Rutkowski RG, Miasnikov AA, Weinberger NM. 2003. Characterisation of multiple physiological fields within the anatomical core of rat auditory cortex. Hear Res 181(1-2):116-130.

Ryugo DK, Killackey HP. 1974. Differential telencephalic projections of the medial and ventral divisions of the medial geniculate body of the rat. Brain Res 82(1):173-177.

Sanderson KJ, Welker W, Shambes GM. 1984. Reevaluation of motor cortex and of sensorimotor overlap in cerebral cortex of albino rats. Brain Res 292(2):251-260.

Sanides F. 1970. Functional architecture of motor and sensory cortices in primates in the light of a new concept of neocortex evolution. In: Montagna W, editor. The primate brain. New York: Appleton-Century-Crofts. 137-208.

Schober W. 1986. The rat cortex in stereotaxic coordinates. J Hirnforsch 27(2):121-143.

Sereno M, Rodman H, Karten H. Organization of visual cortex in the california ground squirrel; Society for Neuroscice Abstract1991.

Sewards TV, Sewards MA. 2001. Cortical association areas in the gustatory system. Neurosci Biobehav Rev. 25(5):395-407. Review.

Slutsky DA, Manger PR, Krubitzer L. 2000. Multiple somatosensory areas in the anterior parietal cortex of the California ground squirrel (Spermophilus beecheyii). J Comp Neurol 416(4):521-539.

Sripanidkulchai K, Wyss JM. 1986. Thalamic projections to retrosplenial cortex in the rat. J Comp Neurol 254(2):143-165.

Sur M, Nelson RJ, Kaas JH. 1978. The representation of the body surface in somatosensory area I of the grey squirrel. J Comp Neurol 179(2):425-449.

Swanson LW. 1992. Brain Maps: Structure of the Rat Brain, 1st ed. New York: Elsevier.

Swanson LW. 2003. Brain Maps: Structure of the Rat Brain. Academic Press.

Szel A, Rohlich P. 1992. Two cone types of rat retina detected by anti-visual pigment antibodies. Exp Eye Res 55(1):47-52.

Thomas H, Tillein J, Heil P, Scheich H. 1993. Functional organization of auditory cortex in the mongolian gerbil (Meriones unguiculatus). I. Electrophysiological mapping of frequency representation and distinction of fields. Eur J Neurosci 5(7):882-897.

Tiao YC, Blakemore C. 1976. Functional organization in the visual cortex of the golden hamster. J Comp Neurol 168(4):459-481.

Tusa RJ, Rosenquist AC, Palmer LA. 1979. Retinotopic organization of areas 18 and 19 in the cat. J Comp Neurol 185(4):657-678.

Uylings HB, Groenewegen HJ, Kolb B. 2003. Do rats have a prefrontal cortex? Behav Brain Res 146(1-2):3-17.

Van Brederode JF, Mulligan KA, Hendrickson AE. 1990. Calcium-binding proteins as markers for subpopulations of GABAergic neurons in monkey striate cortex. J Comp Neurol 298(1):1-22.

van Groen T, Wyss JM. 1990. Connections of the retrosplenial granular a cortex in the rat. J Comp Neurol. 300(4):593-606.

Van der Gucht E, Hof PR, Van Brussel L, Burnat K and Arckens L. 2007. Neurofilament protein and neuronal activity markers define regional architectonic parcellation in the mouse visual cortex. Cereb Cortex 17(12):2805-819.

van der Gucht E, Vandesande F, Arckens L. 2001. Neurofilament protein: a selective marker for the architectonic parcellation of the visual cortex in adult cat brain. J Comp Neurol 441(4):345-368.

Van Hooser SD, Nelson SB. 2006. The squirrel as a rodent model of the human visual system. Vis Neurosci 23(5):765-778.

Voelker CC, Garin N, Taylor JS, Gahwiler BH, Hornung JP, Molnar Z. 2004. Selective neurofilament (SMI-32, FNP-7 and N200) expression in subpopulations of layer V pyramidal neurons in vivo and in vitro. Cereb Cortex 14(11):1276-1286.

Vogt BA, Vogt L, Farber NB. 2004. Cingulate Cortex and Disease Models. In: Paxinos G, editor. The Rat Nervous System. London: Elsevier.

Vogt BA. 1993. Structural organization of cingulate cortex: areas, neurons, and somatodendritic transmitter receptors. In: Vogt, B.A. and Gabriel, M., Editors, 1993. Neurobiology of Cingulate Cortex and Limbic Thalamus, Birkhäuser, Boston, pp. 19–70.

Vogt BA, Finch DM, Olson CR. 1992. Functional heterogeneity in cingulate cortex: the anterior executive and posterior evaluative regions. Cereb Cortex 2(6):435-443.

Vogt BA, Plager MD, Crino PB, Bird ED. 1990. Laminar distributions of muscarinic acetylcholine, serotonin, GABA and opioid receptors in human posterior cingulate cortex. Neuroscience 36(1):165-174.

Vogt BA, Miller MW. 1983. Cortical connections between rat cingulate cortex and visual, motor, and postsubicular cortices. J Comp Neurol 216(2):192-210.

Vogt BA, Peters A. 1981. Form and distribution of neurons in rat cingulate cortex: areas 32, 24, and 29. J Comp Neurol 195(4):603-625.

Vogt BA, Rosene DL, Peters A. 1981. Synaptic termination of thalamic and callosal afferents in cingulate cortex of the rat. J Comp Neurol 201(2):265-283.

Wagor E. 1978. Pattern vision in the grey squirrel after visual cortex ablation. Behav Biol 22(1):1-22.

Wagor E, Mangini NJ, Pearlman AL. 1980. Retinotopic organization of striate and extrastriate visual cortex in the mouse. J Comp Neurol 193(1):187-202.

Wallace MN. 1983. Organization of the mouse cerebral cortex: a histochemical study using glycogen phosphorylase. Brain Res 267(2):201-216.

Wallace MN, Rutkowski RG, Palmer AR. 2000. Identification and localisation of auditory areas in guinea pig cortex. Exp Brain Res 132(4):445-456.

Wallace MT, Ramachandran R, Stein BE. 2004. A revised view of sensory cortical parcellation. Proc Natl Acad Sci U S A 101(7):2167-2172.

Wang Q, Burkhalter A. 2007. Area map of mouse visual cortex. J Comp Neurol 502(3):339-357.

Wang Y, Kurata K. 1998. Quantitative analyses of thalamic and cortical origins of neurons projecting to the rostral and caudal forelimb motor areas in the cerebral cortex of rats. Brain Res. 781(1-2):135-47.

Weber JT, Casagrande VA, Harting JK. 1977. Transneuronal transport of [3H]proline within the visual system of the grey squirrel. Brain Res 129(2):346-352.

West RW, Dowling JE. 1975. Anatomical evidence for cone and rod-like receptors in the gray squirrel, ground squirrel, and prairie dog retinas. J Comp Neurol 159(4):439-460.

Wise SP, Donoghue, JP. 1986. Motor cortex of rodents. New York: Plenum. 243-269 p.

Wong P, Kaas JH. Architectonic subdivisions of neocortex in the grey squirrel (Sciurus carolinesis); Soc for Neurosci Abstract. 2006.

Wong-Riley M. 1979. Changes in the visual system of monocularly sutured or enucleated cats demonstrable with cytochrome oxidase histochemistry. Brain Res 171(1):11-28.

Woolsey TA, Van der Loos H. 1970. The structural organization of layer IV in the somatosensory region (SI) of mouse cerebral cortex. The description of a cortical field composed of discrete cytoarchitectonic units. Brain Res 17(2):205-242.

Woolsey TA, Welker C, Schwartz RH. 1975. Comparative anatomical studies of the SmL face cortex with special reference to the occurrence of "barrels" in layer IV. J Comp Neurol 164(1):79-94.

Wu CW, Bichot NP, Kaas JH. 2000. Converging evidence from microstimulation, architecture, and connections for multiple motor areas in the frontal and cingulate cortex of prosimian primates. J Comp Neurol 423(1):140-177.

Zilles K. 1990. Organization of the Neocortex. In: Tees BKRC, editor. The Cerebral Cortex of the Rat: MIT Press.

Zilles, K, and Wree A. 1985. Cortex: Areal and laminar structure. In G. Paxions (ed): The Rat Nervous System, Vol. 1:Forebrain and Midbrain. New York: Academic Press, pp. 375-415.

Zilles K, Wree A. 1995. Cortex: Areal and laminar structure. G P, editor. Sydney: Academic Press. 375-415 p.

Zilles K, Wree A, Schleicher A, Divac I. 1984. The monocular and binocular subfields of the rat's primary visual cortex: a quantitative morphological approach. J Comp Neurol 226(3):391-402.

Zilles K, Zilles B, Schleicher A. 1980. A quantitative approach to cytoarchitectonics. VI. The areal pattern of the cortex of the albino rat. Anat Embryol (Berl) 159(3):335-360.

CHAPTER III

ARCHITECTONIC SUBDIVISIONS OF NEOCORTEX IN THE TREE SHREW (*TUPAIA BELANGERI)*

Introduction

The tree shrews are diurnal, arboreal mammals that bear some squirrel-like characteristics. At first glance, tree shrews and squirrels are so similar in appearance that to the natives in South-east Asia, they are one and the same animal, with both species bearing the same name Tupai in the Malay and Indonesian languages. In fact, when a Western naturalist, William Ellis, recorded the first tree shrew in 1780, he mistook it to be a squirrel. It took 40 years after the first recording before taxonomists recognized tree shrews as a separate species in the genus *Tupaia* (Emmons, 2000). Tree shrews are the only members of the order Scandentia that diversified from the rest of the Euarchontoglire clade about 85 million years ago (Murphy et al., 2001a; Huchon et al., 2002). Since then, tree shrews have been established as non-rodent, small mammals that, with flying lemurs, are the closest living relatives of primates (Liu et al., 2001; Murphy et al., 2001 a,b; Springer et al., 2003). Tree shrews possess certain features of the brain that are shared with primates, such as a well developed visual system and a reduced dependence on olfaction (Sorenson, 1970), and were once considered to be primates by Le Gros Clark (1959). While this classification no longer holds, the observation made by Clark, that tree shrews resemble primates, has resulted in tree shrews being the species of choice in many neuroanatomical and electrophysiological experiments. Here, we

This chapter has been published: Wong P, Kaas JH. 2009. Architectonic subdivisions of neocortex in the tree shrew (*Tupaia belangeri*). Anatomical Record 292(7) 994-1027.

describe the architectonic subdivisions of neocortex in tree shrews, so as to establish a reliable areal cortical map that can be used to guide functional studies.

Tree shrews have often been used as animal models in the study of the visual system (e.g. Lund et al., 1985; Fitzpatrick, 1996). They are visually oriented animals with a retina consisting of mostly cones. The laterally placed eyes offer about 60° of binocular overlap (Kaas, 2002). The superior colliculus is exceptionally large compared to primates (Kaas and Huerta, 1988) and more distinctly laminated (Abplanalp, 1970; Lane et al., 1971). Their visual cortex is expansive. Primary visual cortex is relatively large and architectonically distinct, and several extrastriate visual areas have been proposed (Kaas et al., 1972; Sesma et al., 1984; Lyon et al., 1998). Pyramidal cells in primary visual cortex share a similar branching pattern to those found in primates, but are more branched and spinous than those found in galagos and monkeys (Elston et al., 2005). Primary visual cortex of tree shrews contains an orderly arrangement of orientation selective columns similar to those of primates (Bosking et al., 1997), while rodents do not (Van Hooser et al., 2006).

Given that tree shrews are arboreal, and use their forepaws to climb and manipulate food items (Bishop, 1969), as do most primates, their sensorimotor system and cortex is well developed. Tree shrews are found to have at least five somatosensory fields, and a large forepaw representation is apparent in primary somatosensory cortex (Sur et al., 1980). The organization of the motor cortex has also been comprehensively characterized through corticospinal tracing and intracortical microstimulation, and the subdivisions of motor cortex have been defined cytoarchitecturally (Remple et al., 2006). There are two distinct motor fields that have been identified in tree shrews, and these

areas have been found to share common features with the primary and premotor cortical areas of primates (Remple et al., 2006). The auditory cortex of tree shrews is less well studied. However, preliminary cortical mapping results indicate at least one auditory field, presumably the primary auditory cortex, which contains a complete tonotopic representation (Oliver et al., 1978). Architecturally, there are at least two definable regions in the auditory cortex of tree shrews. The first being a core region, that has a densely populated granular layer 4, and the second being a belt region, which has a less densely populated granular layer 4, located dorsal and medial to the core (Casseday et al., 1976).

These various studies reflect an interest in understanding the organization of tree shrew neocortex and future studies may be better guided by a comprehensive architectonic map of tree shrew neocortex. There are three published architectonic maps of tree shrew neocortex to date. The first two were by Clark (1924) and von Bonin (1961), which showed only a few cortical areas. The third, by Zilles (1978), adopted a quantitative approach to determining the borders of cortical areas and defined a number of cortical areas. These earlier studies used the Nissl preparation to reveal cell bodies.

As the repertoire of staining procedures available has since increased, an update to the cortical maps is now timely. In this present study, we use a battery of staining preparations to aid us in the characterization of cortical areas in the tree shrew. In addition to the traditional Nissl and myelin stains, another histochemical preparation, the zinc stain (Danscher, 1981, 1982; Danscher and Stoltenberg, 2005) has proved to be useful in revealing areal borders in the neocortex. This technique reveals free ionic zinc in the synapses of corticocortical terminations, allowing secondary sensory areas to be

distinguished from primary sensory areas since the dense thalamocortical inputs in layer 4 of primary sensory areas lack free ionic zinc (e.g. Valente et al., 2002). Four immunohistochemical stains were also used, including those for neurofilaments (SMI-32), parvalbumin (PV), calbindin (CB) and the vesicle glutamate transporter 2 (VGluT2). The SMI-32 antibody reacts with non-phosphorylated epitopes in neurofilaments M and H that are present in a subset of pyramidal cells (Lee et al., 1988; Campbell and Morrison, 1989). PV preparations reveal a subset of GABAergic, non-pyramidal cells, such as basket and double bouquet interneurons (Condé et al., 1996; DeFelipe, 1997; Hof et al., 1999; Celio, 1986) that contain the calcium-binding parvalbumin protein. PV is also a useful marker that labels afferent cortical terminals from sensory thalamic nuclei (Van Brederode et al., 1990; DeFelipe and Jones, 1991; DeVencia et al., 1998; Hackett et al., 1998; Latawiec et al., 2000; Cruikshank et al., 2001; Wong and Kaas, 2008). CB, another calcium-binding protein, reveals a subset of GABA immunoreactive interneurons that are different from those revealed by PV (Van Berderode et al., 1990). VGluT2 immunostaining reveals thalamocortical terminations (Fujiyama et al., 2001; Kaneko and Fujiyama, 2002; Nahami and Erisir, 2005; Wong and Kaas, 2008).

The use of several staining methods in this study allows us to provide more extensive descriptions of the architectonic subdivisions present in the neocortex of tree shrews. Comprehensive cortical maps with rigorous areal borders are more reliably established when the same borders are detected across different sections stained with different histological and immunohistochemical stains.

Materials and Methods

Animal subjects

The cortical architecture was studied in a total of 8 adult *Tupaia belangeri* that were kindly provided for by David Fitzpatrick at Duke University. All experimental procedures were approved by the Vanderbilt Institutional Animal Care and Use Committee and followed the guidelines published by the National Institute of Health.

Tissue Preparation

The tree shrews were given a lethal dose of sodium pentobarbital (100mg/kg). For visualizing synaptic zinc in the cortex, tree shrews were given 200mg/kg body weight of sodium sulphide with 1cc of herparin in 0.1M phosphate buffer (PB) intravenously. Perfusion was carried out transcardially with phosphate-buffered saline (PBS), followed by 4% paraformaldehyde in 0.1M PB, and 4% paraformaldehyde and 10% sucrose in PB. The brains were removed from the skull, bisected, and post-fixed for 2 to 4 hours in 4% paraformaldehyde and 10% sucrose in PB. The hemispheres were placed in 30% sucrose overnight for cryoprotection before cutting on a freezing microtome into 40μm thick sections in the coronal, parasagittal or horizontal planes. Brain sections were saved in four to five series. In some cases, the brains were artificially flattened, then cut tangentially at 40μm and saved in three series.

Histochemistry

One series of sections from each hemisphere was processed for Nissl substance (with thionin) and another series was processed for myelin, using the Gallyas (1979) silver procedure. In some cases, a third series of sections were processed for cytochrome oxidase (CO) (Wong-Riley, 1979).

Zinc Histochemistry

In tree shrews that were given intravenous injections of sodium sulfide, a series of sections was processed using the protocol outlined by Inchiohe et al. (2003) to visualize synaptic zinc. Brain sections were washed thoroughly with 0.1M PB, followed by 0.01M PB. The zinc-enriched terminals were visualized using the IntenSE M Silver enhancement kit (Amersham International, Little Chalfont Bucks, UK). The developing reagent was a one-to-one cocktail of the IntenSE M kit solution and 50% gum Arabic solution. The development of the sections was terminated, when a dark brown/black signal was seen, by rinsing sections in 0.01M PB. Sections were then mounted and dehydrated in an ascending series of ethanols, (70% for 20min, 95% for 10min, 100% for 10min), cleared in xylene and coverslipped using Permount (Fisher Scientific, Pittsburgh, PA).

Immunohistochemistry

Each case contains one to two series of sections that have been immunostained for SMI-32 (1:2000; Covance Inc. Princeton, NJ), parvalbumin (PV) (1:4000; Sigma-Aldrich, St. Louis, Mo), calbindin (CB) (1:5000; Swant, Bellinzona, Switzerland) or

vesicle glutamate transporter 2 (VGluT2) (1:4000; Chemicon now part of Millipore, Billerica, MA). Sections were incubated in their respective antibodies for 40 to 48 hours at 4°C. Details of the immunohistochemical procedures have been described in Wong and Kaas (2008).

Light microscopy

The architectonic borders were delineated from the brain sections that had undergone the various histochemical and immunohistochemical procedures described above. The locations of architectonic borders were determined by analysis of laminar and cell density changes in the processed sections when viewed at high power using a projection microscope. The Nissl, zinc and VGluT2 preparations were most useful in identifying primary sensory areas, while sensorimotor cortical areas were better distinguished in the Nissl and SMI-32 preparations. Other histological preparations were used for corroborating ambiguous borders. Digital photomicrographs of sections were acquired using a Nikon DXM1200 (Nikon Inc., Melville, NY) camera mounted on a Nikon E800 (Nikon Inc., Melville, NY) microscope, and adjusted for brightness and contrast using Adobe Photoshop (Adobe Systems Inc., San Jose, CA).

Anatomical reconstruction

Areal borders were reconstructed on surface views of the tree shrew brain as described in Wong and Kaas (2008). In brief, architectonic borders were identified and drawn for each outlined brain section using a Bausch and Lomb Microprojector (Bausch & Lomb, Rochester, NY). Adjacent brain sections were aligned based on blood vessels

and other landmarks that were added to the section outlines. Outlines of brain sections with marked borders were imported into Adobe Illustrator (Adobe Systems Inc., San Jose, CA) and aligned using the contour of the outline sections and the landmarks that were drawn. Brain surface views were reconstructed by projecting cortical and areal borders of selected brain sections onto lines appropriate for dorsal lateral, medial, and 45º view, and spacing these lines according to the location on the brain. Typically, the different histological procedures revealed similarly located boundaries between areas, suggesting that functionally relevant borders were being identified.

Results

Our current findings provide further evidence for several previously proposed subdivisions of neocortex in tree shrews (e.g. Zilles, 1978; Lyon et al., 1998; Remple et al., 2006), and evidence for areas that have not been previously described. Some of these proposed areas are shown on a dorsolateral view of the tree shrew brain in Fig. 26F. Descriptions of the cortical areas, by region, are as follows.

Occipital cortex

The occipital region of tree shrews consists of areas 17 and 18, following Brodmann's (1909) terminology, and possibly areas lateral to area 18 that are included here in temporal cortex (Fig. 26-29). Areas 17 and 18 are architectonically distinct, and both fields are found to be coextensive with systematic retinal maps of the primary visual (V1) and secondary visual (V2) areas, respectively (Kaas et al., 1972). The visually responsive region lateral to area 18 has been divided into the temporal dorsal (TD),

temporal anterior (TA) and temporal posterior (TP) regions (Kaas et al., 1972). Area TD lies in the middle portion along the rostral V2 border and shares some characteristics to the middle temporal visual area (MT) of primates, such as dense V1 input into the region, relative location and dense myelination of area TD (Sesma et al., 1984; Kaas and Preuss, 1993; Lyon et al., 1998). Tracer injection studies have shown that area TP has connections with both V1 and V2 (Sesma et al., 1984; Lyon et al., 1998), and area TA has connections with V2 (Lyon et al., 1998).

Primary visual area, Area 17. Area 17, or striate cortex is a very architectonically distinct region with easily identifiable borders at low magnification (Fig. 26). The borders of area 17 are apparent even at low magnification in Nissl, fibers, zinc, CO, SMI-32, PV, and VGluT2 stains, and are observed to be in similar locations (Figs. 26 and 27). Area 17 is bordered rostrolaterally by extrastriate area 18, and extends medially onto the ventral surface of the hemisphere, where it is bordered by cortex known as the prostriata (Fig. 46 Laterally, layer 4 of area 17 tapers off near the 17/18 border (Figs. 26 and 27), where a transition zone of callosal connections with the other cerebral hemisphere may be located (Pritzel et al., 1988; 1990).

In Nissl preparations, layer 4 forms a dark band of densely populated granule cells (Figs. 26A, 27A). A cell-poor cleft in the middle of layer 4 is observed in sagittal sections, closer to the caudal portion of area 17 (Fig. 27A) (Conley et al., 1984; Jain et al., 1994). This cleft divides layer 4 into layers 4a, and 4b, which receives projections from different layers of the geniculate nucleus (Harting et al., 1973; Conley et al., 1984). At higher magnifications (Fig. 28), area 17 has a layer 3 that is broad and divided into three sublayers, with layer 3a and 3c being less densely populated with cells than the

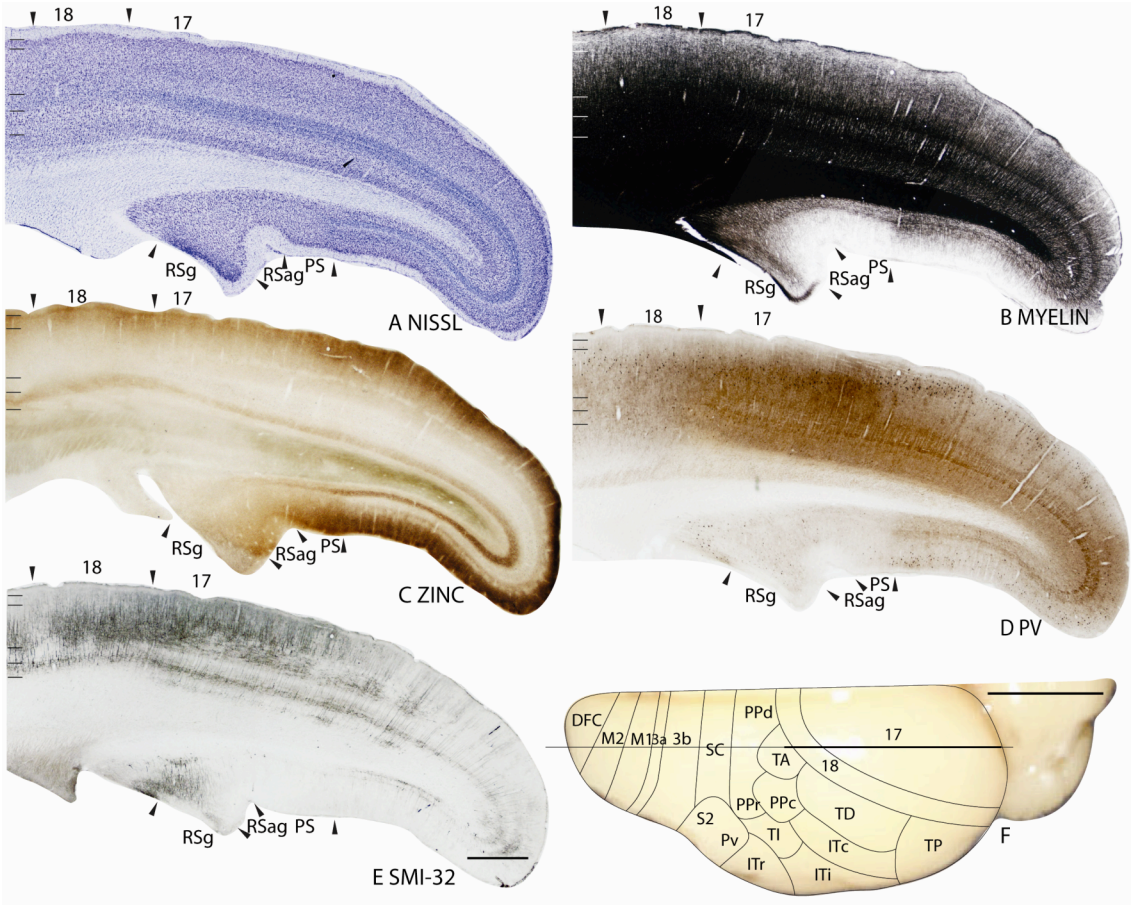

Figure 26. Architectonic characteristics of visual areas 17, 18 and TD. Coronal sections from occipital cortex were processed for (A) Nissl substance, (B) myelin, (C) synaptic zinc, (D) CO, and (E) vesicle glutamate transporter 2 (VGluT2). The architectonic borders of proposed cortical areas are shown on the dorsal view of the tree shrew brain in panel F. The vertical line on the brain shows the level from which the sections were taken for panels A-E. The thicker portion of the line marks the regions illustrated in panels A-E. Occipital areas 17 and 18 are adopted from Brodmann (1909). TD is the temporal dorsal visual area. Arrowheads on the sections illustrated here and in the following figures mark architectonic boundaries. Short lines on the sections indicate cortical layers 1 to 6. See table 1 for abbreviations for other areas. The scale bar for brain sections (panel E) = 0.5mm. The scale bar on the brain (panel F) = 5mm.

middle layer 3b, and a layer 2 that has a dense population of small cells (Fig. 28A). The laminar features of area 17 can also be appreciated in sections processed for myelin, where the outer and inner band of Baillarger in layers 3c and 5 respectively are revealed (Figs. 26B, 27B, 28B). Note that the outer band of Baillarger, also known as the

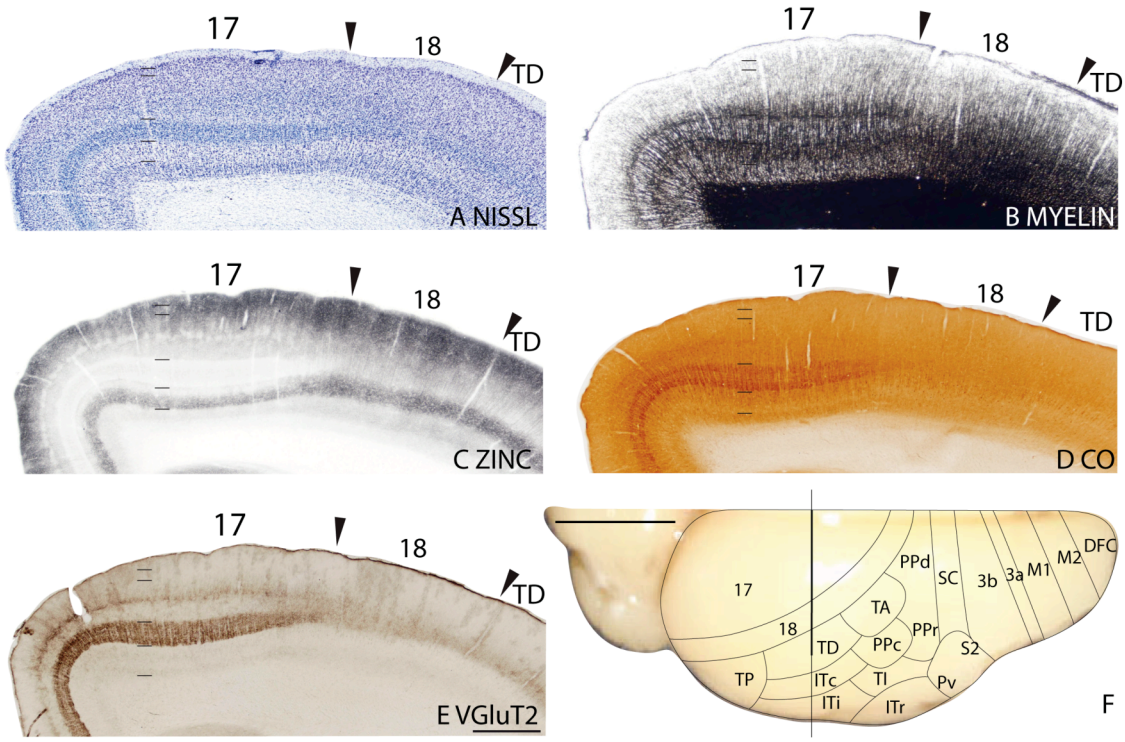

Figure 27. Architectonic characteristics of visual areas and adjoining retrosplenial cortex. Parasagittal sections from occipital cortex were processed for (A) Nissl substance, (B) myelin, (C) synaptic zinc, (D) PV, and (E) neurofilaments with the SMI-32 antibody. The level at which the sagittal sections are taken from is indicated by the horizontal line on the dorsal view of the brain in panel F. The thicker line in panel F marks the regions illustrated in panels A-E. Short lines on the sections indicate the extent of each cortical layers 1 to 6. See table 1 for abbreviations for other areas. The scale bar for brain sections (panel E) = 1mm. The scale bar on the brain (panel F) = 5mm.

stria of Gennari, is coextensive with layer 3C in Nissl stains, and is not in layer 4 as commonly depicted for primates. The two bands of Baillarger are not apparent laterally in area 18, and medially in PS, which is poorly myelinated, allowing the delimitation of the area 17/18 and 17/PS areal borders. In CO preparations, layer 4 is darkly stained (Figs. 26D, 28C), while middle layer 3 is lightly stained (Fig. 26D). Layer 4 is darkly stained for PV in area 17 (Figs. 27E, 28G) and tapers off at the 17/18 border (Fig. 27E). Layers 3a and 3b showed darkly stained cell bodies immunoreactive for PV (Fig. 28G). SMI-32 staining of area 17 is not homogenous, with more pyramidal cells labeled closer to the

rostral border of area 17 (Fig. 27E). At higher magnifications, the SMI-32 stain revealed dark bands of pyramidal neurons in layers 3 and 5, with some staining in inner layer 6, and no SMI-32 immunopositive cell bodies in layer 4 (Fig. 28D). Layers 1, 2, and 3a of area 17 express high levels of CB, with a dense population of CB-immunoreactive cell bodies (Fig. 28H).

Layer 4 of area 17 expresses very little synaptic zinc, standing out as a white band (Figs. 26C, 27C, 28E), and layers 1 to 3b and 5b stain darker than the rest of the cortical layers in area 17 (Fig. 28E). The adjacent area 18 and PS express more synaptic zinc in layer 4 (Figs. 26C, 27C). Layers 3, especially inner layer 3, and 6 show higher levels of zinc stain than layer 4, but lower levels than the corresponding layers of the adjacent cortices. The lower levels of zinc staining in layers 3 and 6 suggest that there are a greater proportion of thalamic terminations in these layers than in adjoining areas of cortex. The lateral geniculate nucleus of tree shrews has major projections to layer 4 and minor projections to layers 3b, 3c and 6 (Conley et al., 1984). In coronal sections and at higher magnification, the zinc stain also reveals a patchy pattern in layer 3b (Figs. 26C, 28E).

In artificially flattened cortex, a pattern of myelin-poor patches surrounded by myelin-rich regions is observed in layer 3 (Figs. 29A, 29B). In addition, there are circular regions, resembling ‘walls’, darkly stained for zinc, surrounding zinc-poor centers (Fig. 29D). In VGluT2 stained sections, layer 4 is darkly stained in area 17 compared to the adjoining cortical areas (Fig. 26E). Small, dark patches of VGluT2 staining seem to correspond to the zinc-poor centers in layer 3c (Fig. 28F). The patchy staining pattern is observed in sections of flattened cortex through layer 3 (Fig. 29C). This suggests that

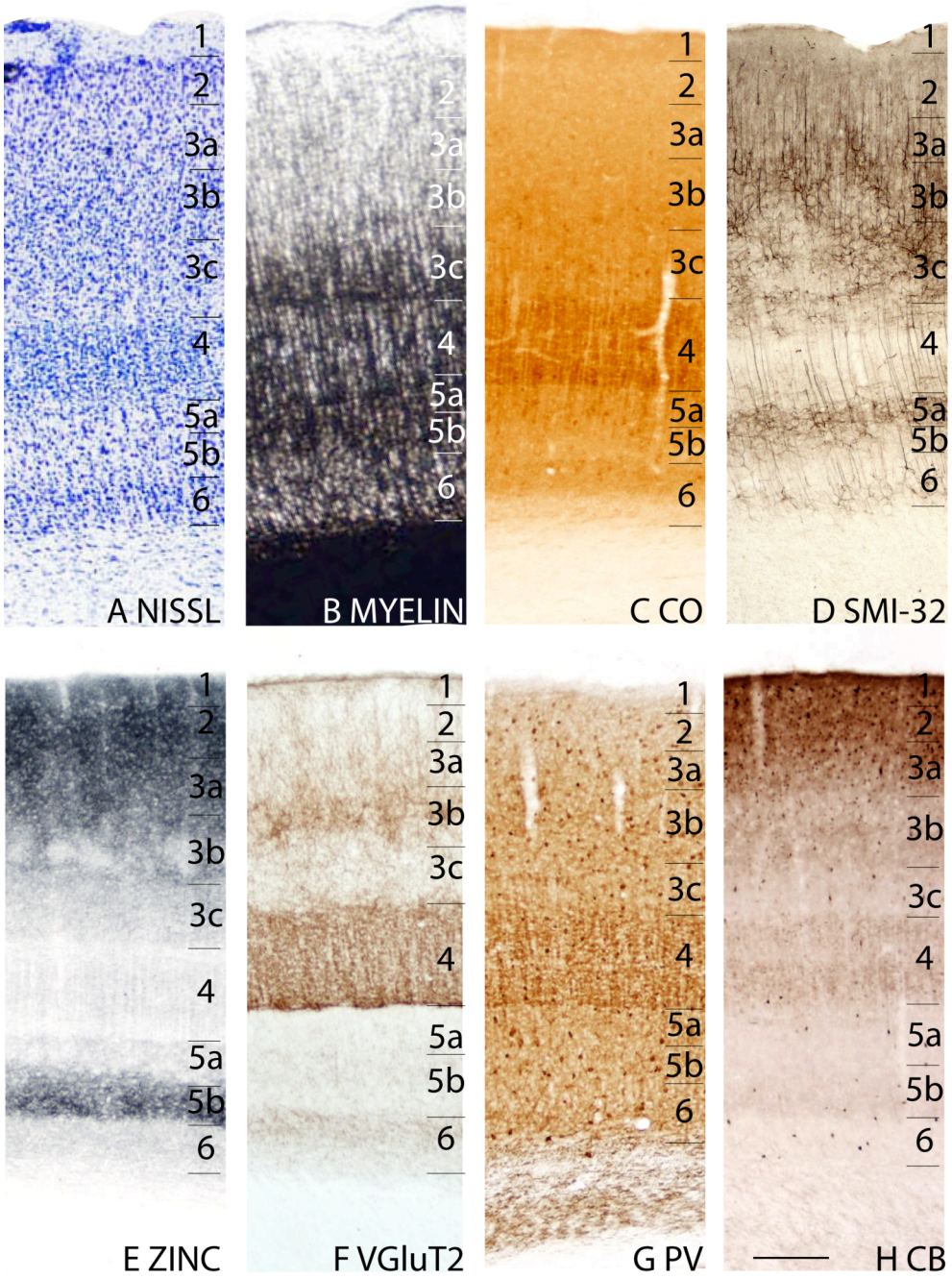

Figure 28. The laminar characteristics of area 17 at higher magnification. The sublayers of layer 3 are apparent in the Nissl, synaptic zinc, VGluT2 and CB preparations. Layer 5 has two sublayers, 5a and 5b, that are apparent in Nissl, CO, SMI-32 and zinc preparations. Scale bar = 0.25mm.

thalamocortical and corticocortical projections follow some form of modular organization in layer 3b of the tree shrew's primary visual cortex, whereby thalamic projections are

clustered in patches surrounded by 'walls' of corticocortical projections. This is reminiscent of the projections of the koniocellular layers of the lateral geniculate layer to layer 3 of area 17 in primates (e.g. Weber et al., 1983; see Casagrande and Kaas, 1994, for review), and the 'honeycomb' structure that has been described in the layers 1 and 2 of visual cortex in rats (Ichinohe et al., 2003). It is also interesting to note that the VGluT2-rich patches and zinc-poor patches are smaller in size compared to the myelin-poor patches (Fig. 29).

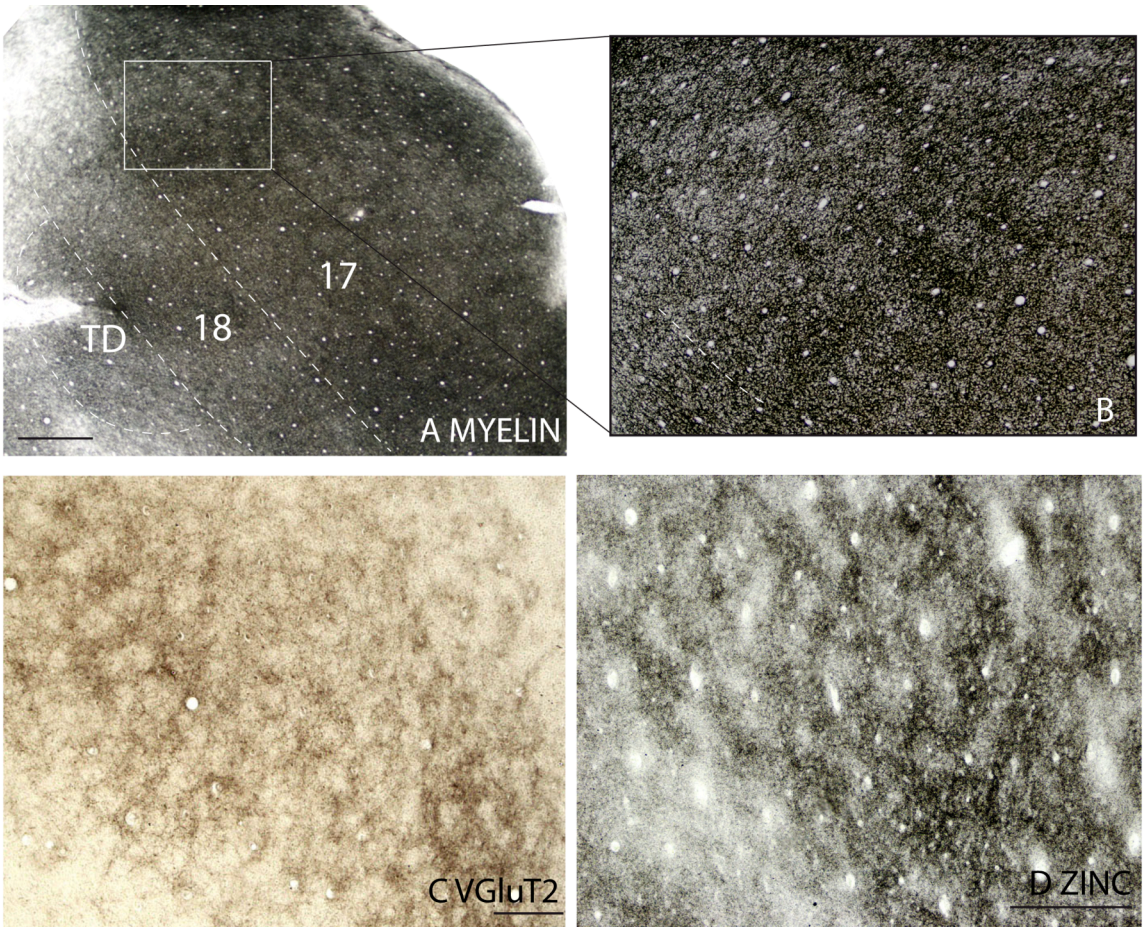

Figure 29. Patchy staining pattern of area 17. A. A myelin stained section cut parallel to the surface of an artificially flattened cerebral hemisphere. Dashed lines show the approximate location of the cortical borders. The boxed region in A is shown in B at higher magnification. C and D are from a different case and show the patchy staining pattern of area 17 in VGluT2 and zinc preparations. Scale bar in panel A = 0.5mm, for panel B and C = 0.5mm, for panel D = 250μm.

Second visual area, Area 18. Area 18 in the tree shrews lies along the lateral border of the primary visual area, V1 or area 17, and is approximately one-third the size of area 17 (Sesma et al., 1984). Electrophysiological recordings revealed that area 18 is coextensive with the second visual area, V2, and contains a representation of the contralateral visual hemifield that is an approximate mirror reversal of that in area 17 (Kaas et al., 1972).

The laminar pattern of area 18 is less distinct than area 17. As shown in Nissl preparations (Figs. 26A, 27A), layers 4 and 6 in area 18 are less densely packed with granular cells compared to area 17. Layer 5 is more sparsely populated with cells than the three cortical areas TA, TD and TP that lie lateral to V2 (Figs. 31A, 33A). In sections stained for myelin, the distinct outer and inner bands of Baillarger that are present in area 17 are absent in area 18, although area 18 has a moderately high level of myelination (Figs. 26B, 27B) that is higher than the cortical areas along its lateral border (Figs. 29B, 31B). In sections stained for zinc, area 18 shows increased staining in layer 4, suggesting less thalamic and more corticocortical inputs are present. Layer 5 is thicker and more darkly stained compared to area 17 (Fig. 26C). The intensity of zinc staining in layer 4 of area 18 is higher than in area TD (Figs. 26C, 32C, 33C), but is lower than in areas TA and TP (Fig. 31C, not shown). As such, area TD likely receives proportionally more thalamic inputs than areas 18, TA and TP, while area TA and TP receives proportionately the most cortical inputs. Layer 4 of area 18 shows lower levels of CO staining compared to area 17 (Fig. 26D).

Layers 4 and 6 express less PV (Fig. 27D) and VGluT2 (Fig. 26E) in area 18 than area 17. In SMI-32 preparations, area 18 shows a higher density of pyramidal cells in

layer 3 compared to area 17 (Fig. 27E). Additionally, the SMI-32 immunoreactive pyramidal cells in 5 of area 18 are larger and have shorter apical dendrites than those in area 17 (Fig. 27E).

Temporal visual cortex

Originally identified as area 19 by Kaas et al. (1972), the strip of cortex lateral to area 18 has since been divided into three architectonically distinct areas, TA, TD and TP (Sesma et al., 1984; Lyon et al., 1998). These three areas receive projections from area 17, with TD receiving the densest inputs, followed by TP, then TA with the fewest inputs (Sesma et al., 1984; Lyon et al., 1998). In sections processed for the Cat-301 antibody, both TD and TA expressed more of the antigen for Cat-301 than TP (Jain et al., 1994).

Temporal anterior area, TA. In the Nissl stain, area TA has a thinner layer 4 and a more densely packed layer 5 with larger pyramidal cells than area 18 (Fig. 30A). Area TA is less well myelinated than both area 18 and TD. There are higher levels of synaptic zinc in TA, with a thicker, more darkly stained layer 5 compared to area 18 (Fig. 30C). In CO preparations, layer 4 is somewhat darker stained in area TA than in area 18, but is lighter stained than in the ventrally located posterior parietal caudal area (PPc) (not shown).

Layer 4 of area TA has much lower immunoreactivity levels for both PV (Fig. 30D) and VGluT2 than the adjoining areas (not shown). SMI-32 immunostaining reveals darkly stained pyramidal cells in layers 3 and 5 of area TA with layer 5 being more densely packed with pyramidal cells than the adjoining area 18 (Fig. 30E). The pyramidal cells in layer 3 have shorter apical dendrites compared to those in area 18. The

distribution of SMI-32 immunopositive pyramidal cells in layers 3 and 5 of TA is similar to that of PPd (Fig. 30E).

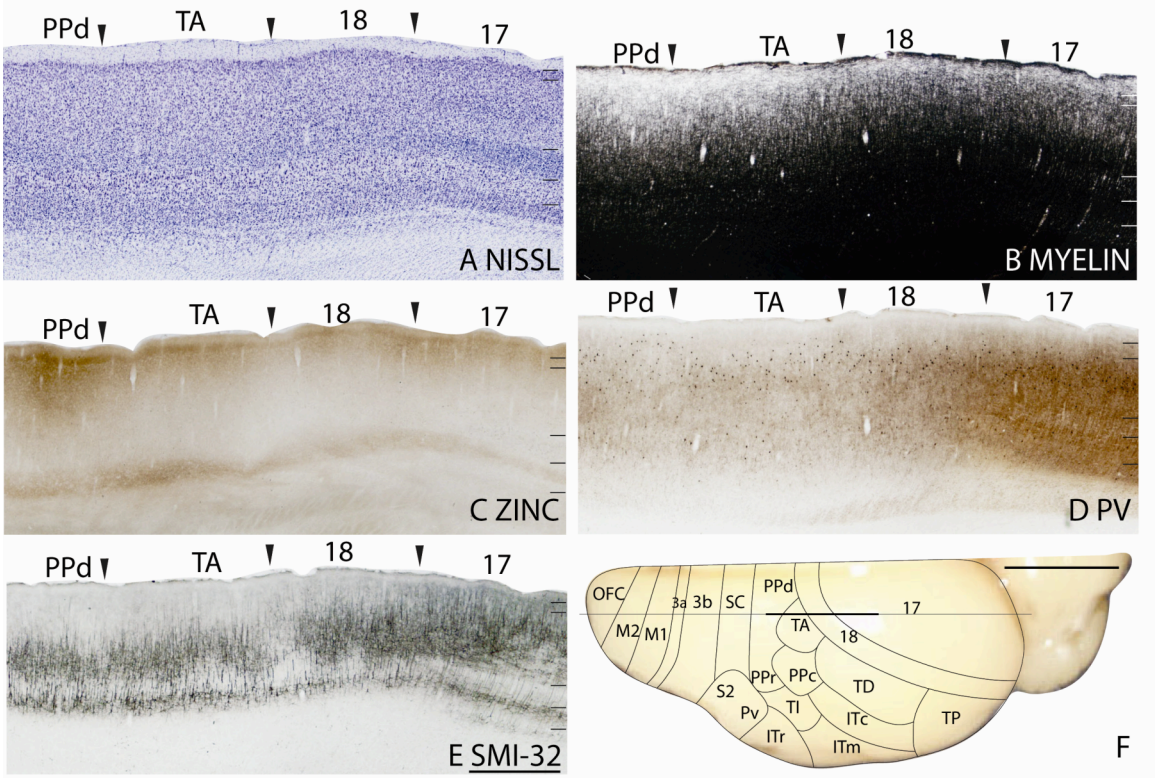

Figure 30. Architectonic characteristics of visual and temporal visual areas. The level at which the sagittal sections are taken from is indicated by the horizontal line on the dorsal view of the brain in panel F. The thicker line in panel F marks the regions illustrated in panels A-E. The extent of each cortical layers 1 to 6 is indicated by the short horizontal lines on panels A-E. The scale bar for brain sections (panel E) = 1mm. The scale bar on the brain (panel F) = 5mm.

Temporal dorsal area, TD. Area TD is about 6mm long and 2 to 3 mm wide (Sesma et al., 1984). Based on its relative location, connection pattern with area 17, myeloarchitecture, and Cat-301 immunostaining characteristics, area TD has been proposed as a possible homologue of the primate MT (Sesma at al., 1984; Kaas and Preuss, 1993; Jain et al., 1994; Northcutt and Kaas, 1995).

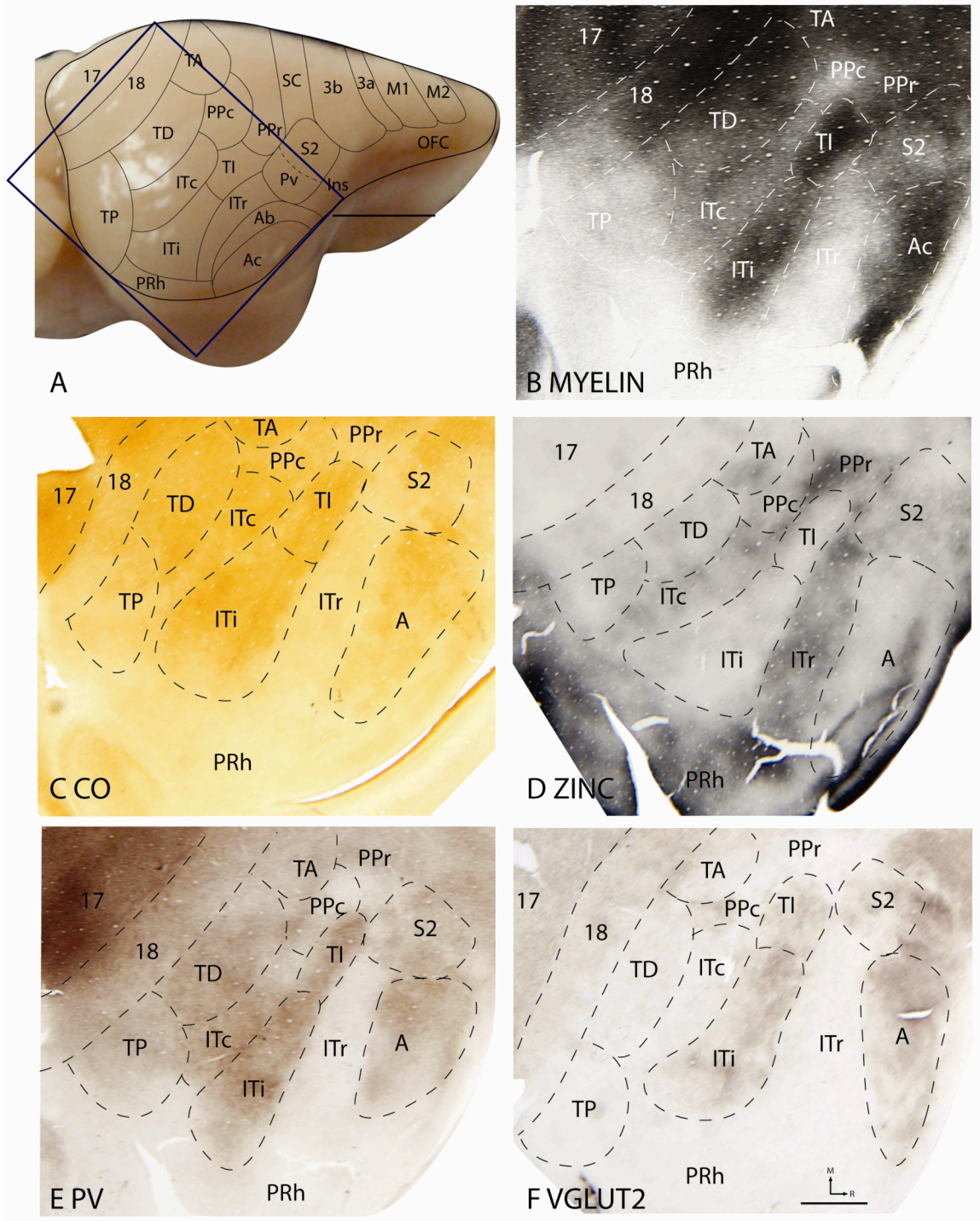

Figure 31. Architectonic characteristics of temporal and inferior temporal cortex in flattened preparations. A. Architectonic borders of proposed cortical areas are shown on the lateral view of the tree shrew brain. The box indicates the regions that are illustrated in panels B to F. Sections in panels B to F are cut parallel to the surface of an artificially flattened cerebral hemisphere and show the topographic organization of the areas in the temporal and inferior temporal cortex. Scale bar in panel A = 5mm, in panel F = 2mm.

Near the area 18/TD border, sections processed for Nissl bodies reveal a reasonably well-developed layer 4 in area TD that is thicker than in area 18 (Figs. 26A, 32A), but much less populated with granule cells than in area 17 (Figs. 26A, 32A). Layer 5 of area TD was packed with pyramidal cells that were larger than those in area 18 (Fig. 26A), but smaller than those in the inferior temporal caudal area (ITc). The distribution densities of cells do not seem to be homogeneous in area TD. Away from the 18/TD border, the density of cells in layer 4 increases (Fig. 32A). Area TD is slightly more myelinated than area TA (not shown), TP (Fig. 32B) and ITc (Fig. 31B), but is less myelinated than area 18 (Figs. 26B, 32B). As observed in the Nissl stain, the myelination level of area TD is not uniform and increases gradually away from the 18/TD border (Fig. 32B). In the zinc stain, layers 3 and 5 of area TD are more intensely stained compared to area 18 (Figs. 26C, 33A) and are similarly stained to that of TP (Fig. 33A). The distribution of free ionic zinc in layer 4 of area TD is lower than in areas 18 and TP (Fig. 33A). In flattened cortex, layer 4 of area TD has higher levels of CO activity than area 18, and similar levels to ITc (Fig. 31C).

In PV preparations, two bands of PV immunopositive terminations, reflecting thalamic inputs, are observed, one dark band in layer 4 and a lighter band in layer 6. Layers 4 and 6 of area TD are more immunoreactive for PV than either area 18 or TP. The immunoreactivity of layer 4 for PV increases away from the 18/TD border (Fig. 32C). TD stains poorly for VGluT2, with layer 4 being less intensely stained for VGluT2 than in area 18 (Figs. 26E, 31F). There is no noticeable difference between the levels of VGluT2 staining in TD and TP (Fig. 31F). SMI-32 staining in TD is less than in ITc (Fig. 35K), but is darker than in TP (not shown). The pyramidal cells in layers 3 and 5 of area

TD stain darker for the SMI-32 antibody compared to area 18, however, they have shorter apical dendrites (Fig. 33C). As the staining pattern gradually changes somewhat from medial to lateral, it is possible that TD represents the visual field from central to peripheral vision.

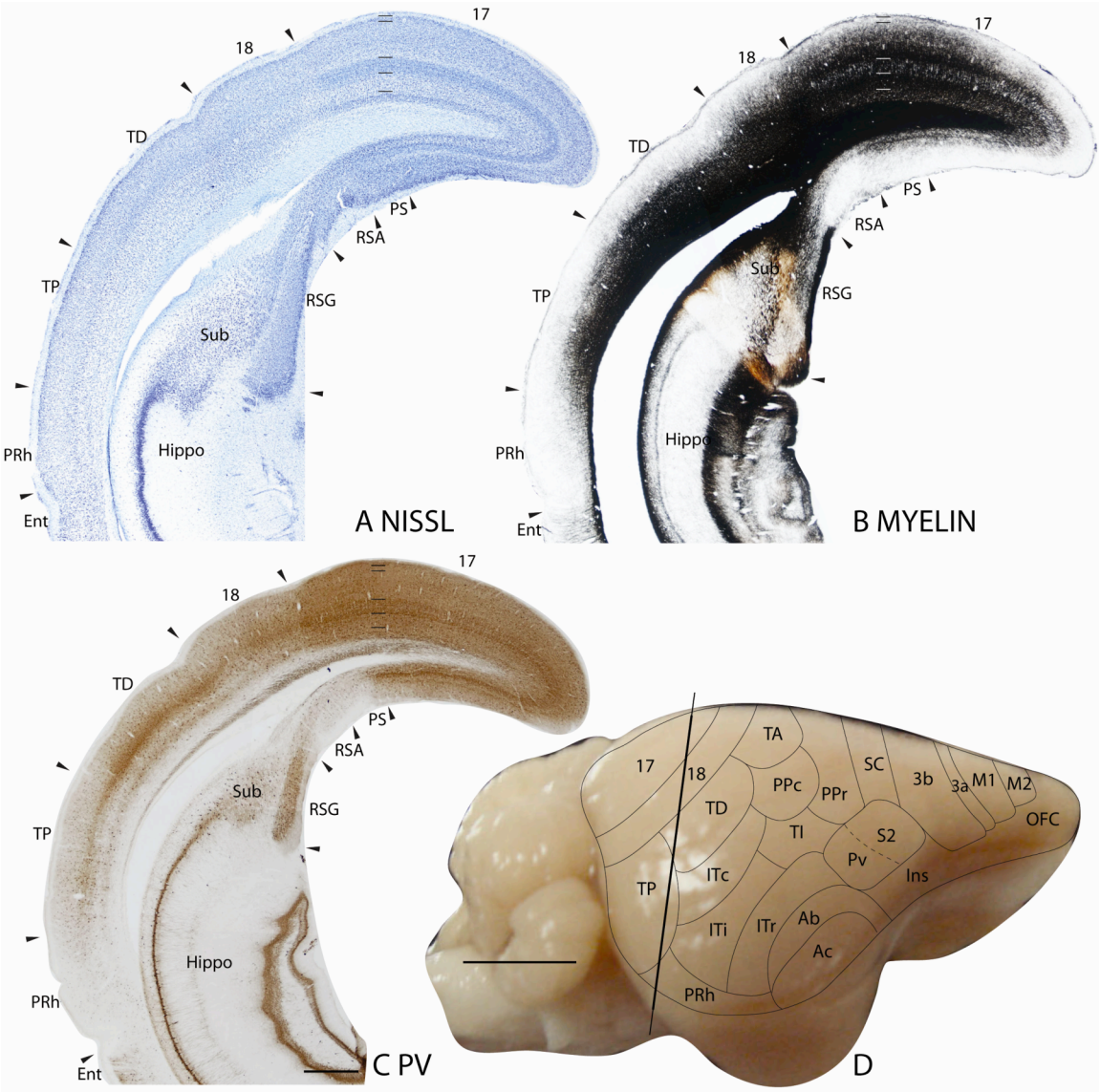

Figure 32. Architectonic characteristics of occipital and temporal visual areas. The location from which the coronal sections are taken from is indicated by the vertical line on the lateral view of the brain in panel D. The thicker portion of the line indicates the region that is illustrated in panels A to C. The scale bar for brain sections (panel C) = 1mm. The scale bar on the brain (panel D) = 5mm.

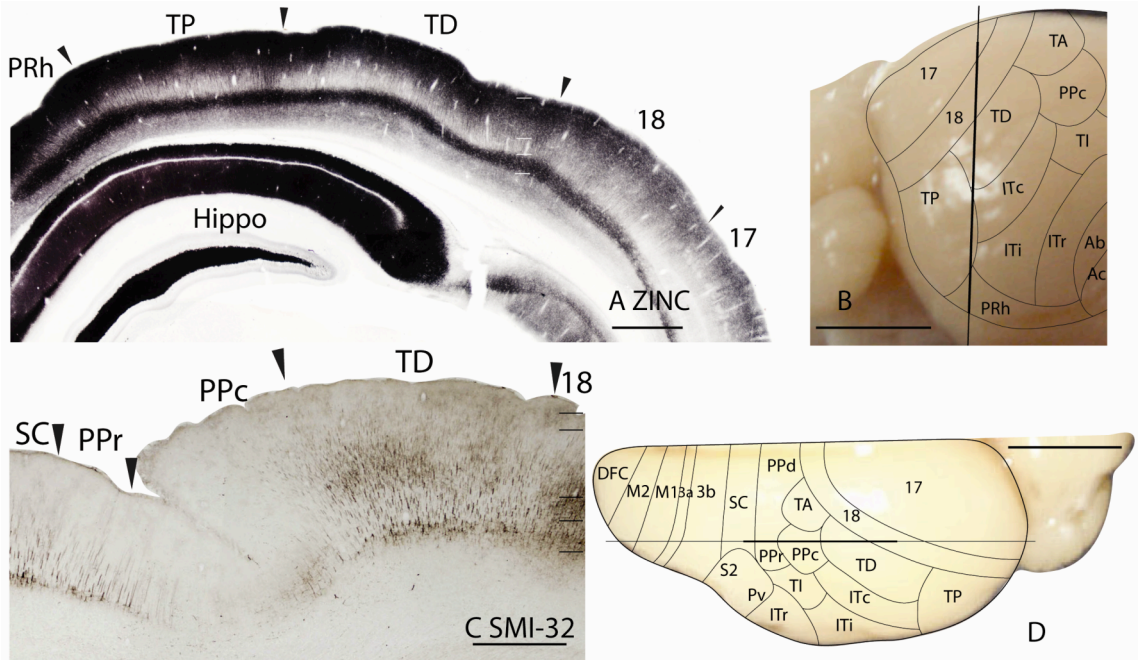

Figure 33. Architectonic characteristics of the temporal dorsal area. A. A coronal section stained for synaptic zinc. The level at which this section is taken from is indicated by the vertical line on the lateral view of the tree shrew brain. C. A parasagittal section stained for the SMI-32 antibody to reveal neurofilaments. The horizontal line on the dorsal view of the tree shrew brain in D indicates the location from which the section in panel C is taken from. The scale bar for brain sections (panels A and C) = 1mm. The scale bar on the brain (panels B and D) = 5mm.

Temporal posterior area, TP. Area TP covers an area of approximately 10mm^2 (Sesma et al., 1984), and as revealed by the Nissl stain, is less densely populated with cells in layers 2 and 3 than the adjoining area 18 (Fig. 32A). Layer 4 of TP is more densely populated by granule cells than the adjoining ITi (Fig. 34B). TP is less myelinated than both area 18 and TD (Fig. 32B). The myelination levels of TP and ITi are similar (Fig. 34C). The TP/PRh border is distinctly marked by the lack of myelination in PRh (Fig. 34C). In CO preparations, layer 4 of area TP stains darker than layer 4 of area 18 (not shown), and is lighter stained than layer 4 of ITi (Fig. 34C) and ITc (not shown). There is an overall increase in the intensity of zinc staining across the cortical

Figure 34. Architectonic characteristics of the temporal posterior and inferior temporal areas. Cortical areas are shown on a lateral view of the ventral hemisphere in panel A. The thicker portion of the horizontal line across the brain indicates the location of the horizontal brain sections illustrated in panels B to E. The scale bar for brain sections (panel E) = 0.5mm. The scale bar on the brain (panel F) = 5mm.

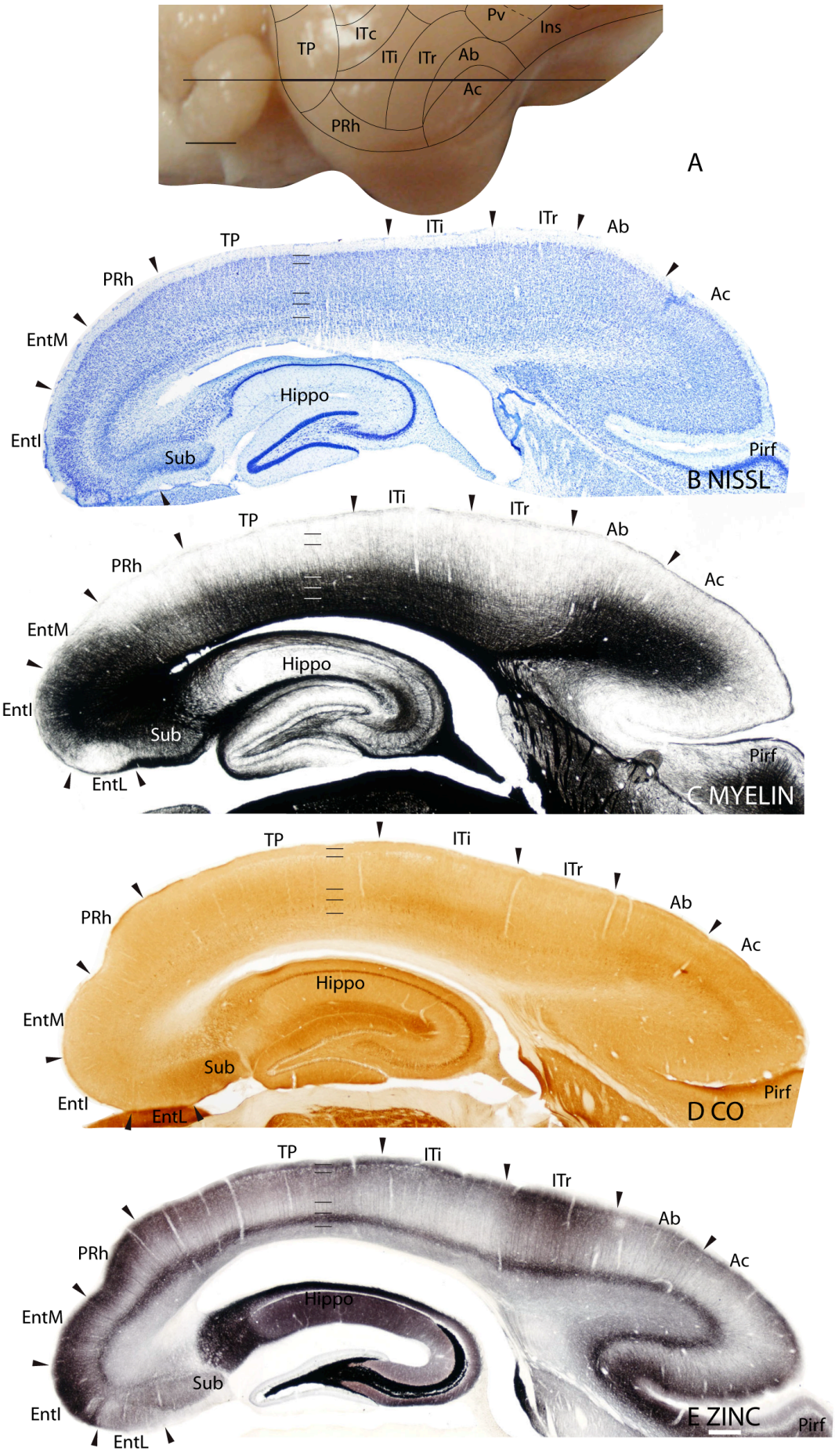
TP
ITc
ITi
ITr
Ab
Pv
Ins
Ac
PRh
A
TP
ITi
ITr
Ab
PRh
Ac
EntM
Hippo
EntI
Sub
Pirf
B NISSL
TP
ITi
ITr
Ab
PRh
Ac
EntM
Hippo
EntI
Sub
Pirf
EntL
C MYELIN
TP
ITi
ITr
Ab
PRh
Ac
Hippo
EntM
Sub
EntI
Pirf
EntL
D CO
TP
ITi
ITr
Ab
PRh
Ac
Hippo
EntM
Sub
EntI
Pirf
EntL
E ZINC

layers of area TP compared to the adjoining area 18, TD (Fig. 32E), ITi (Fig. 34E) and ITc (not shown). However, the level of zinc staining in TP is still lower than that of PRh (Figs. 32E, 34E).

In PV preparations, there is one thin but distinct band of PV immunopositive terminations in layer 4 of TP, and a faint band in layer 6. TP is lightly stained for the PV antibody compared to TD, but more darkly stained than PRh (Fig. 32C). TP stains poorly for both SMI-32 and VGluT2 (not shown).

Temporal inferior area, TI. Ti has a well developed layer 4 that is densely populated with cells in Nissl stained sections (Figs. 35G, 36A). Layer 5 of TI is more densely populated with cells than ITr (Figs. 35G, 36A) and ITc (Fig. 35G), and has smaller cells compared to PPc (Fig. 36A). In the myelin stain, TI is more densely myelinated than the surrounding areas (Figs. 31B, 35H, 36B), with a band of myelinated fibers in inner layer 3 (Fig. 35H). In flattened cortex stained for CO, TI is a darkly stained oval (Fig. 31C). In coronal sections, two bands of CO staining, in layers 4 and 6, are present in TI, and absent in PPc and ITr (Fig. 36D). Layer 4 of TI stains poorly for the zinc stain, as such, the borders of TI with the surrounding cortical areas are distinct in the zinc stain (Figs. 31D, 35I, 36C).

TI stains darkly for PV with a band of PV immunopositive terminations in layer 4, and also note the scattering of PV positive cells (Fig. 35J). In flattened cortex, TI is a darkly stained oval in PV preparations (Fig. 31E). TI also stains darkly for VGluT2 compared to the surrounding areas in flattened cortex (Fig. 31F), and in coronal sections, has a dense band in layer 4, and a lighter band in layer 6 (Fig. 36E). In SMI-32

preparations, layer 5 of TI has darkly stained SMI-32 immunopositive pyramidal neurons (Fig. 35J).

Inferior temporal cortex

The organization of inferior temporal (IT) cortex in tree shrews has not been extensively studied. Zilles (1978) considered IT cortex of tree shrews to be as a single area, area temporalis 3 (Te3). More recently, Remple et al., (2007) divided IT cortex into at least three areas, the temporal inferior area (TI), the temporal posterior inferior area (TPI), and, the rest of IT cortex surrounding these two areas, the temporal inferior ventral (TIV) area. In this study, IT cortex has been divided into four areas, inferior temporal rostral (ITr), inferior temporal intermediate (ITi), inferior temporal caudal (ITc), and TI. ITi is similar to TPI of the Remple et al. (2007) study.

Inferior temporal rostral area, ITr. In Nissl preparations, layer 4 of ITr is less densely packed with granule cells than layer 4 of auditory cortex (Fig. 34B), TI (Fig. 36A), and ITi (Fig. 35A). However, layer 4 of ITr is more distinct than layer 4 of PRh (Fig. 35A). ITr is less myelinated (Figs. 34C, 35B, 36B) than the cortical areas surrounding it, except for PRh (Figs. 34D, 35C, 36C), and this is observed in artificially flattened cortex as well (Fig. 31B). ITr expresses more free ionic zinc, especially in layer 4, compared to the auditory cortex (Fig. 34E), TI (Fig. 36C), and ITi (Figs. 34D, 35C). Compared to PRh, ITr expresses less free ionic zinc across all the cortical layers, with the greatest difference in layer 4 (Fig. 35C). At higher magnification, CO staining is observed in layer 5 of ITr, but very little CO staining is present in layers 4 and 6 (Fig. 36C). ITr expresses less CO protein than the surrounding cortical areas (Fig. 6C), such as

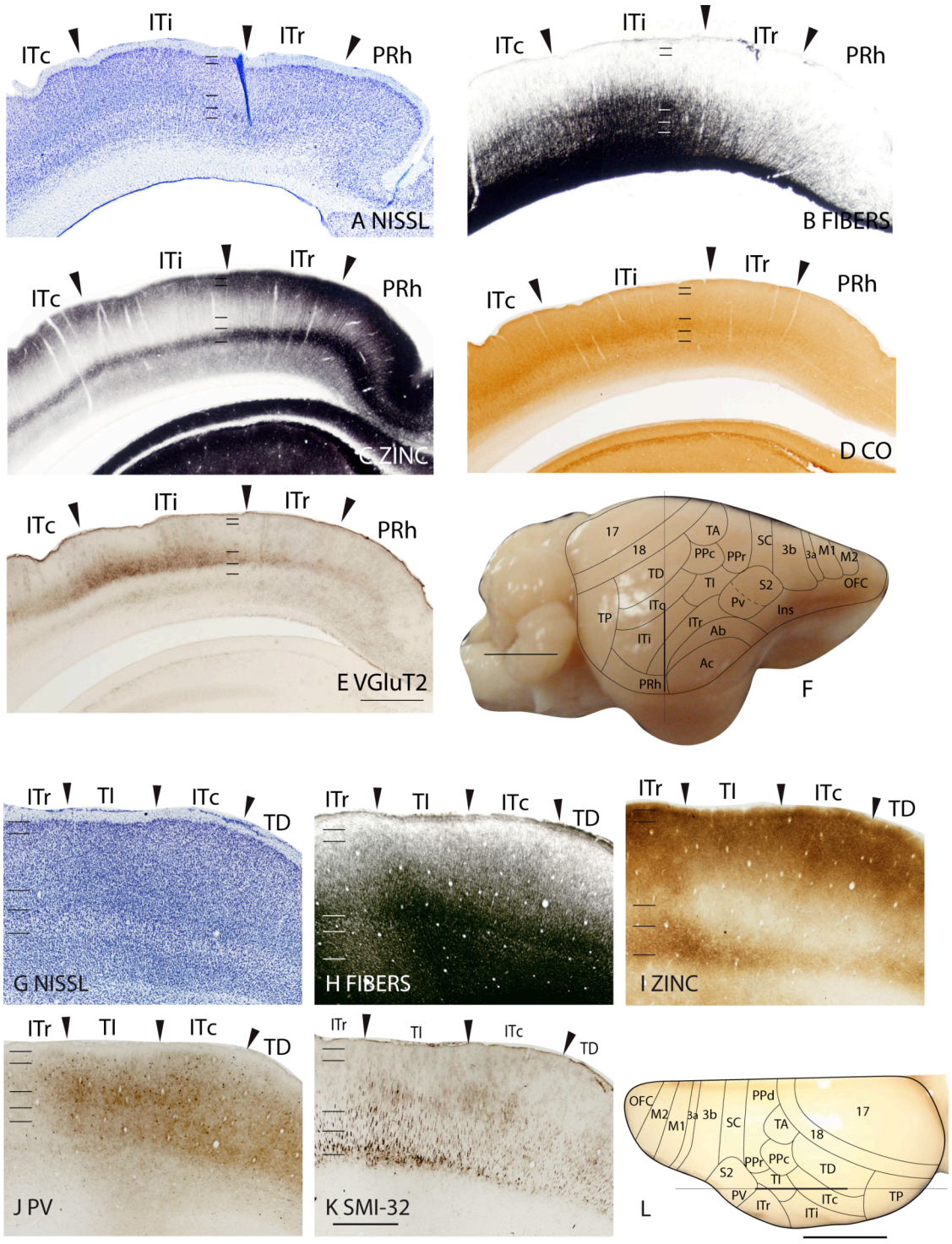

Figure 35. Architectonic characteristics of the inferior temporal areas. Panels A to E are coronal sections taken from the approximate location indicated by the vertical line on the lateral view of the tree shrew brain in panel F. Panels G to K are parasagittal sections take from the approximate location indicated by the horizontal line on the dorsal view of the tree shrew brain in panel L. The scale bar for brain sections (panels E and K) = 1mm. The scale bar on the brain (panels F and L) = 5mm.

Ti (Fig. 36D), auditory cortex (Fig. 34D) and ITi (Figs. 34D, 35D), and is more darkly stained for CO than PRh (Figs. 34D, 35D).

ITr stains poorly for PV (Fig. 31E) and VGluT2 (Fig. 31F) compared to the surrounding cortical areas. Sections stained for SMI-32 revealed a sparse population of pyramidal cells in layer 5 (Fig. 35K).

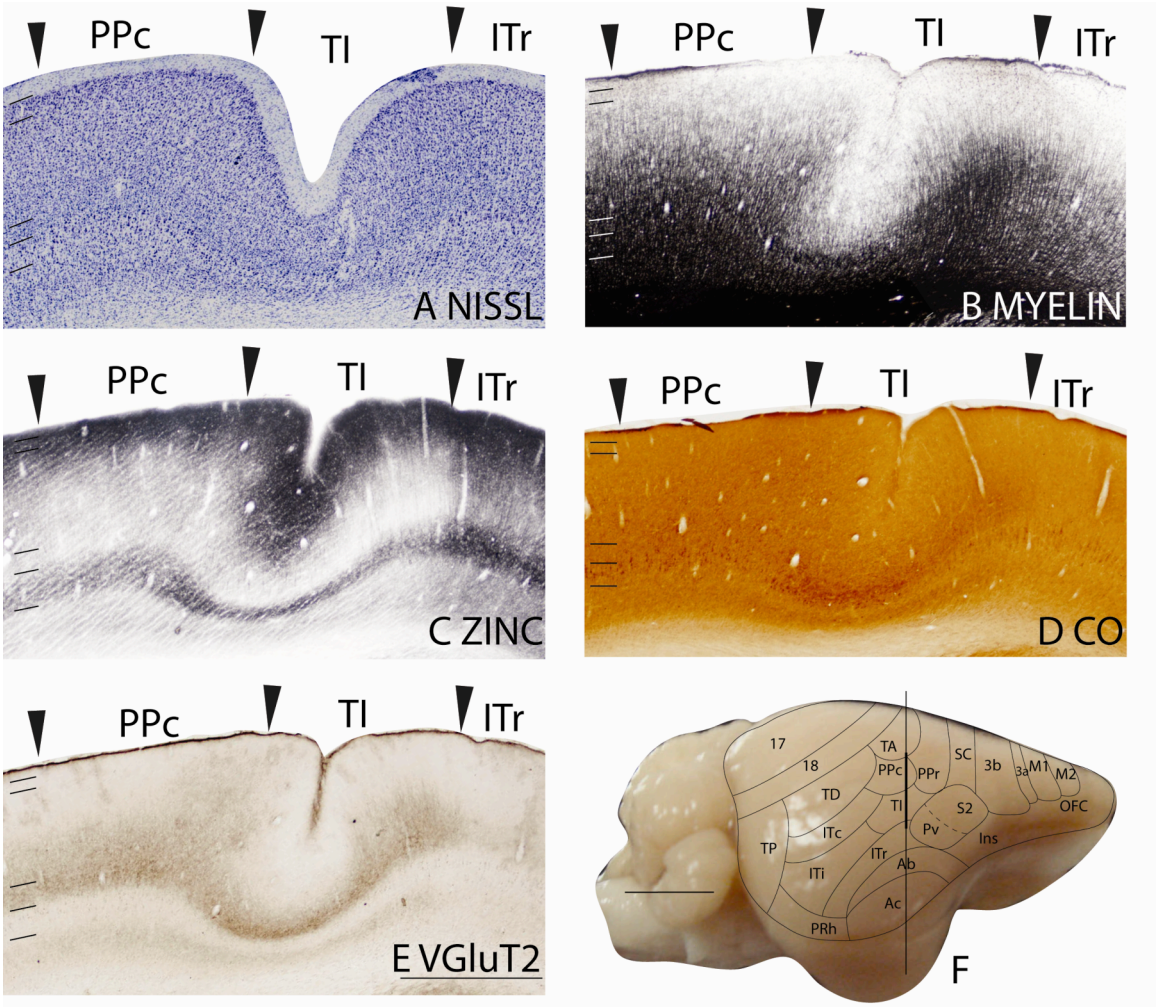

Figure 36. Architectonic characteristics of the termporal intermediate area and adjoining areas. Cortical areas are shown on a lateral view of the right hemisphere in panel F. The thicker part of the vertical line across the brain indicates the location of the coronal brain sections illustrated in panels A to E. The scale bar for brain sections (panel E) = 1mm. The scale bar on the brain (panel F) = 5mm.

Inferior temporal intermediate area, ITi. In Nissl preparations, ITi has a thicker and more densely packed layer 4 than ITr, and a thicker, but less densely packed layer 4 than ITc (Fig. 35A). Layer 5 of ITi is sparsely populated and the size of cells is smaller compared to both ITc and ITr (Fig. 35A). Layer 4 of ITi is thicker but more sparsely populated than the adjoining TP, and layer 5 is thinner and populated with smaller cells than in TP (Fig. 34B). In myelin preparations, ITi is more myelinated than the bordering areas, ITc and ITr (Fig. 35B), and has a similar level of myelination compared to TP (Fig. 34C). In flattened cortex, ITi stands out as a darkly myelinated oval (Fig. 31B). ITi expresses more CO protein than both ITr and TP (Figs. 34D, 35D), and expresses a similar level of CO to ITc (Fig. 35D). In flattened cortex, ITi is an oval region that stains darker for CO than the surrounding regions (Fig. 31C). ITi expresses less free ionic zinc than ITr across all the cortical layers, and this is most obvious in layer 4 (Figs. 34D, 35C). The zinc staining in ITi is slightly lower than that in both TP (Fig. 34E) and ITc (Fig. 35C). In flattened cortical sections stained for zinc, ITi is a light patch surrounded by darker stained areas (Fig. 31D).

ITi stains darker for PV than ITr and TP, and to a lesser extent, ITc as well (Fig. 31E). In VGluT2 preparations, layer 4 of ITi is thicker and darker stained than TP (Fig. 31F), ITc, and ITr (Fig. 35E). ITi stains poorly with the SMI-32 antibody (not shown).

Inferior temporal caudal area, ITc. In Nissl preparations, ITc has a thinner layer 4 compared to ITi (Fig. 35A) and TD (Fig. 35G), and a less densely populated layer 4 than in TI (Fig. 35G). Layer 5 of ITc is less populated with cells than TI (Fig. 10G), and more populated with cells than ITi (Fig. 35A) and TD (Fig. 35G). ITc has lower levels of myelination compared to the surrounding areas TD, TI, and ITi (Figs. 31B, 35B, 35H).

ITc expresses similar levels of CO to TD (Fig. 31C), and less CO than TI and ITi (Figs. 31C, 35D). In the zinc stain, ITc expresses more free zinc ions than TI (Figs. 6D, 10I) and ITi (Figs. 31D, 35C), especially in the upper cortical layers. ITc expresses less free zinc ions, especially in layer 4, than TD (Figs. 31D, 35I).

In PV preparations, more labeled cells are observed in layers 2 and 3 than in layers 4, 5 and 6 (Fig. 35J). ITc stains less intensely for PV immunopositive terminals then both ITi and TI (Figs. 31E, 35J). Layer 4 of ITc stains less intensely for VGluT2 than layer 4 of both ITi (Figs. 31F, 35E) and TI (Fig. 31F). In SMI-32 immunostained sections, ITc has a sparser distribution of SMI-32 labeled pyramidal cells compared to TI (Fig. 35K).

Auditory cortex

The auditory cortex of tree shrews contains a primary auditory core (Ac) of one or more primary auditory areas (Casseday et al., 1976; Diamond et al., 1970; Oliver and Hall, 1975; 1978), and a bordering auditory belt (Ab), which wraps around the mediorostral border of the primary auditory core (Oliver and Hall, 1978). Ac extends ventrally into the rhinal fissure, where it abuts the ectorhinal cortex (Ect).

Primary auditory core (Ac). The primary auditory core is characterized by a thick layer 4 that is densely populated by small granule cells in the Nissl stain, and by a layer 5 that contains medium-sized pyramidal cells in the outer sublayer of layer 5 (Fig. 37A). Ac is well myelinated, with distinct outer and inner bands of Baillarger that are absent in Ect (Fig. 37B). In CO preparations, layer 4 of Ac stains darker than the surrounding

Figure 37. Architectonic characteristics of the auditory areas. Cortical areas are shown on a lateral view of the right hemisphere in panel F. The thicker part of the vertical line across the brain indicates the location of the coronal brain sections illustrated in panels A to E. Short horizontal lines on panels A to F indicate the extent of the 6 cortical layers. The scale bar for brain sections (panel E) = 1mm. The scale bar on the brain (panel F) = 5mm.

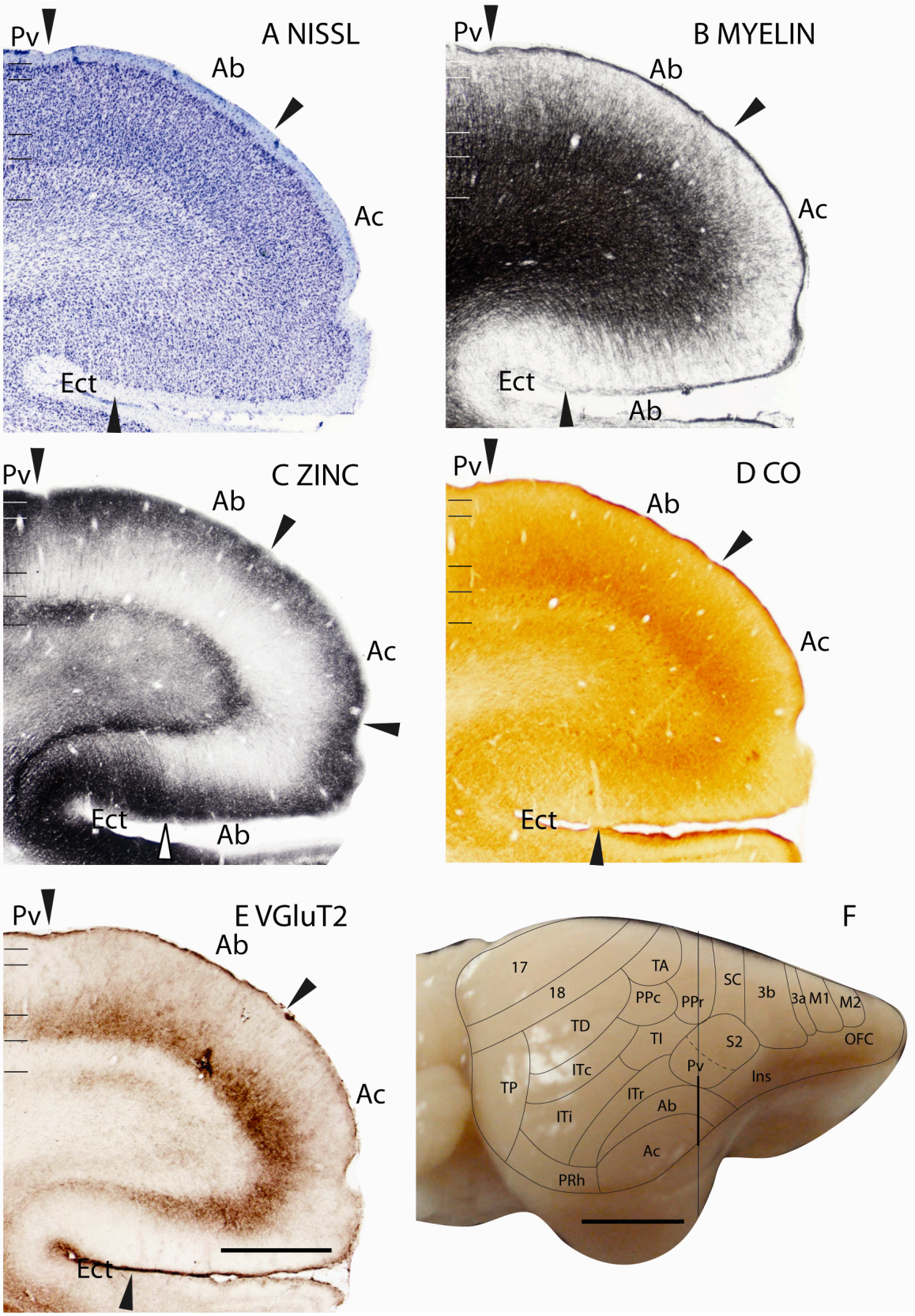
A NISSL
Pv
Ab
Ac
Ect
B MYELIN
Pv
Ab
Ac
Ect
Ab
C ZINC
Pv
Ab
Ac
Ect
Ab
D CO
Pv
Ab
Ac
Ect
E VGluT2
Pv
Ab
Ac
Ect
F
17
18
TA
PPc
PPr
SC
3b
3a
M1
M2
TD
TI
S2
OFC
ITc
Pv
Ins
TP
ITr
Ab
ITi
Ac
PRh

areas, Ab and Ect (Fig. 37D). Layer 4 of Ac stains poorly for free zinc ions, and as such shows up as a white band, providing a sharp ventral border with Ect (Fig. 37C).

In VGluT2 preparations, layer 4 of Ac is a wide band that is more intensely stained compared to the surrounding areas, Ab and Ect (Fig. 37E). Neurons stained for PV are present throughout the cortical layers in Ac (Fig. 38A). Layer 4 of Ac stains darkly for PV immunopositive terminations and this staining terminates at the Ac/Ect border (Fig. 38A). Small SMI-32 immunopositive pyramidal neurons densely populate layer 3, and a few SMI-32 stained pyramidal cells are observed in layer 5 of Ac (Fig. 38B).

Auditory belt (Ab). Ab has a thinner layer 4 then Ac, but is thicker than in Pv (Fig. 37A). In the Nissl stain, the granule cells in layer 4 of Ab are larger and more darkly stained than those in Ac, and in layer 3, the cells are larger in Ab than in Ac (Fig. 37A). Ab is more heavily myelinated than Pv, and has similar myelination levels to Ac (Fig. 37B). Like Ac, Ab expresses low levels of free zinc ions in layer 4; as such, layer 4 of Ab is a white band in zinc stained sections (Fig. 37C). Layer 4 of Ab stains more darkly for CO than in Pv, and is more lightly stained and thinner than in Ac (Fig. 37D).

In VGluT2 preparations, layer 4 of Ab stains darkly for VGluT2 immunopositive terminations compared to the adjoining Pv, and is thinner and less intense in staining compared to Ac (Fig. 37E). Layer 4 of Ab stains darkly for PV immunopositive terminations, and darkly stained neurons are present throughout the cortical layers (Fig. 38A). The Ab/ITr border is marked by a decrease in PV staining in layer 4 of ITr. The Ab/Ac border is not distinct in the PV stain, although PV staining in layer 4 of Ab is more diffuse than in Ac (Fig. 38A). In sections stained for the SMI-32 antibody, Ab has

similar staining characteristics to Ac, with a dense population of SMI-32 immunopositive pyramidal cells in layer 3, and some stained pyramidal cells in layer 5 (Fig. 38B).

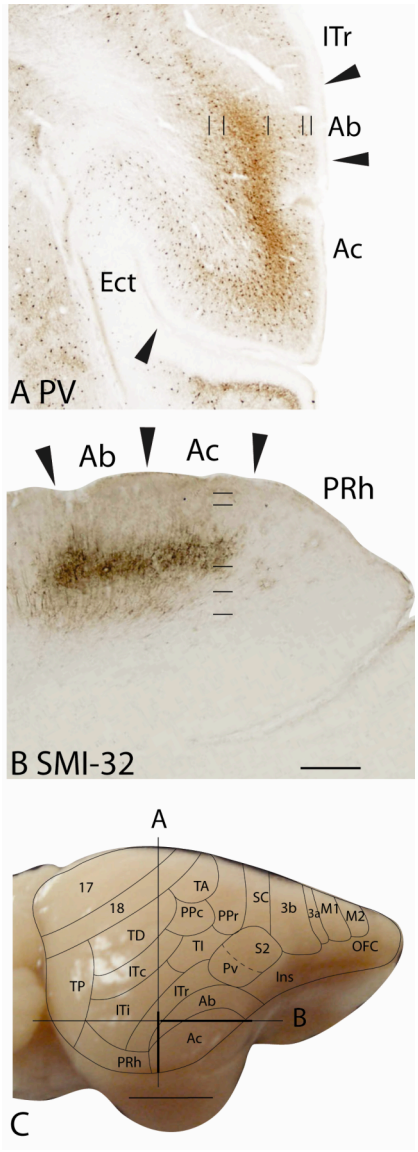

Figure 38. Architectonic characteristics of the auditory areas in PV and SMI-32 preparations. Cortical areas are shown on a lateral view of the right hemisphere in panel C. The vertical line indicates the location from which the coronal section in panel A is taken, and the horizontal line indicates the location from which the horizontal section in panel B is taken. The scale bar for brain sections (panel B) = 0.5mm. The scale bar on the brain (panel F) = 5mm.

Parietal cortex

The parietal cortex in tree shrews consists of six main areas. Three of these areas are in the anterior parietal cortex: the primary somatosensory area (3b(S1)), the adjoining strip of the transitional area, area 3a, and the somatosensory caudal area (SC). In the lateral ventral cortex, there are the second somatosensory (S2) and the parietal ventral (Pv) areas. The sixth area is the posterior parietal area, which has been subdivided into the posterior parietal dorsal (PPd), posterior parietal rostral (PPr), and posterior parietal caudal (PPc) areas.

Primary somatosensory area, 3b(S1). Area 3b(S1) in tree shrews contains the complete representation of the body, and extends over the medial wall where it abuts the cingulate cortex (Sur et al., 1981)(for example see Fig. 18D). In Nissl preparations, 3b(S1) has a koniocellular appearance, with a layer 4 that is more densely populated with small granule cells than the surrounding cortical areas, and a layer 5 that is populated with medium sized pyramidal cells (Figs. 39A, 41 A, 42A). In some sections, the thickness of layer 4 in 3b(S1) is not constant throughout the area, and this is observed in the myelin stain as well. 3b(S1) is well myelinated, with two distinct bands of Baillarger, compared to the adjacent areas SC (Fig. 39B), 3a (Figs. 41B, 42B), and the dorsal cingulate area (CGd)(Fig. 41B). However, in favorable sections, the myelinated bands are discontinuous (Fig. 41B). In the zinc stain, 3b(S1) expresses less free zinc ions throughout the cortical layers than the surrounding areas, especially layer 4 of 3b(S1), which appears as a white band, allowing 3b(S1) to be delineated from the adjacent areas such as 3a (Figs, 41C, 42C), SC, and CGd (Figs. 39C, 41C), where layer 4 of those areas stain darker in the zinc stain. The varying thickness of layer 4 in 3b(S1) is observed in the

zinc stain as well, forming a 'scallop' pattern that is absent in the adjoining insular area (Fig. 41C). The non-uniform thickness of layer 4 that is observed in the Nissl, myelin, zinc, and VGluT2 stain may be due to the presence of different representations of body part in a single section. Layer 4 of 3b(S1) expresses more CO than the adjoining SC and CGd (Fig. 39D), and some darkly stained cell bodies are present in layer 5 (Fig. 39D, 41D).

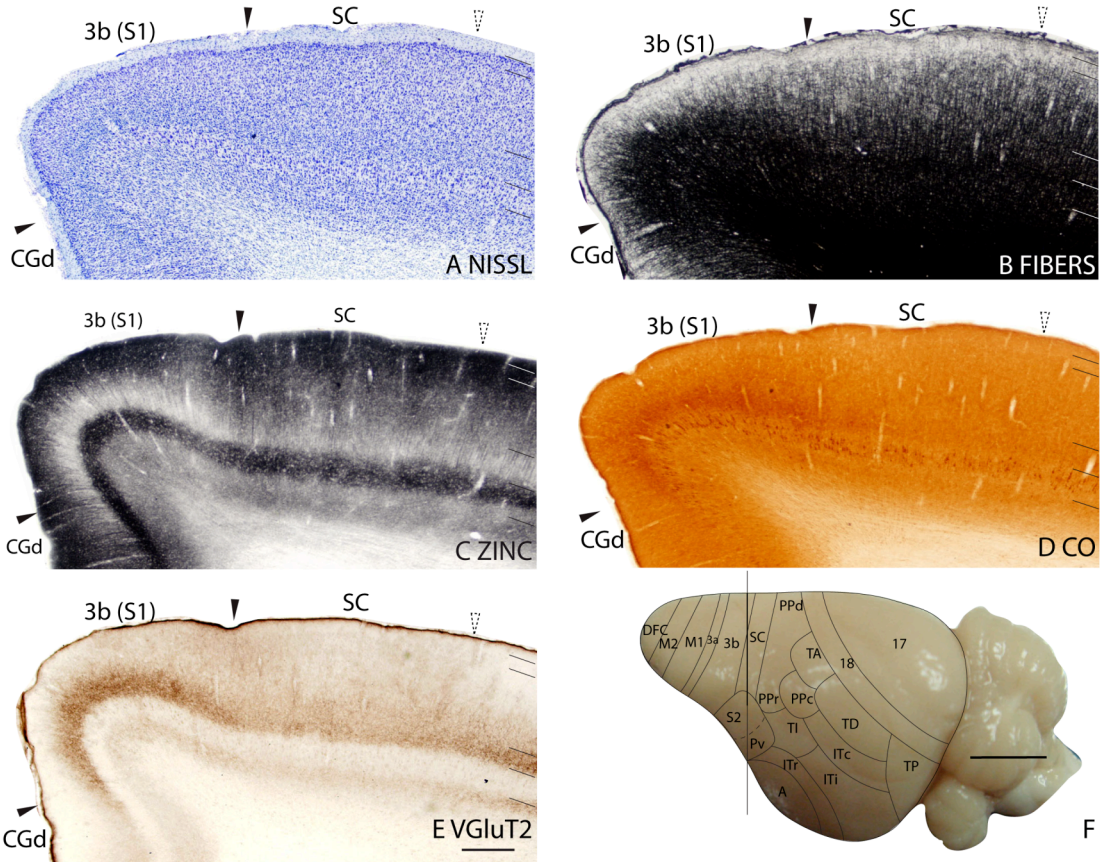

Figure 39. Architectonic characteristics of the primary somatosensory cortex. Cortical areas are shown on a dorsolateral view of the right hemisphere in panel F. The vertical line across the cortex (panel F) indicates the location where the coronal brain sections in panels A to E were obtained. Short horizontal lines on panels A to E indicate the extent of the 6 cortical layers. Solid arrows mark the extent of 3b(S1). Dotted arrows indicate the approximate location of the border between SC and S2. The scale bar for brain sections (panel E) = 0.5mm. The scale bar on the brain (panel F) = 5mm.

In the VGluT2 stain, layer 4 of 3b(S1) is darkly stained compared to the surrounding areas SC, CGd (Fig. 39E), and 3a (Figs. 39E, 41E), and the staining is not uniform throughout its extent (Fig. 41E). A lighter stained band is observed in layer 6. Layer 4 of 3b(S1) stains darkly for PV immunopositive terminations, and a concentration of PV immunopositive cells is observed in the upper cortical layers (Fig. 42D). In SMI-32 preparations, two bands of pyramidal neurons are labeled in layers 3 and 5 (Fig. 42E). These SMI-32 immunopositive neurons are not as densely packed as those in SC (Fig. 42E) and are smaller than those in 3a (Fig. 42E).

Area 3a. In Nissl preparations, Area 3a has a layer 4 that is thinner than in 3b(S1) and is thicker than in M1 (Figs. 41A, 42A). Layer 5 of 3a is populated with pyramidal cells that are larger than those in 3b(S1), but smaller than in M1 (Figs. 41A, 42A). Although 3a is not as well myelinated as 3b(S1) (Figs. 41B, 42B), an outer band of Baillarger, which is lighter than that in 3b(S1), is present in 3a, and absent in M1 (Fig. 42B). Layer 4 of 3a stains darker in the zinc stain than in 3b(S1), and 3a expresses more free zinc ions throughout the cortical layers compared to M1 and 3b(S1) (Figs. 16C, 42C). In CO preparations, darkly stained cell bodies are present in layer 5 of 3a (Fig. 41D).

In VGluT2 immunostained sections, layer 4 of 3a has reduced staining compared to layer 4 of 3b(S1), and has darker staining than layer 4 of M1 (Fig. 41E). No VGluT2 staining is observed in layer 6 of 3a. There are few PV immunopositive neurons present in area 3a, and the PV immunopositive terminations that are present in 3b(S1) are absent in 3a (Fig. 42D). In SMI-32 preparations, layer 3 of 3a has fewer, though larger, stained pyramidal neurons than layer 3 of 3b(S1) (Fig. 42E). SMI-32 immunopositive neurons in

layer 5 of 3a are larger than those in 3b(S1), but smaller and have shorter apical dendrites than those in M1 (Fig. 42E).

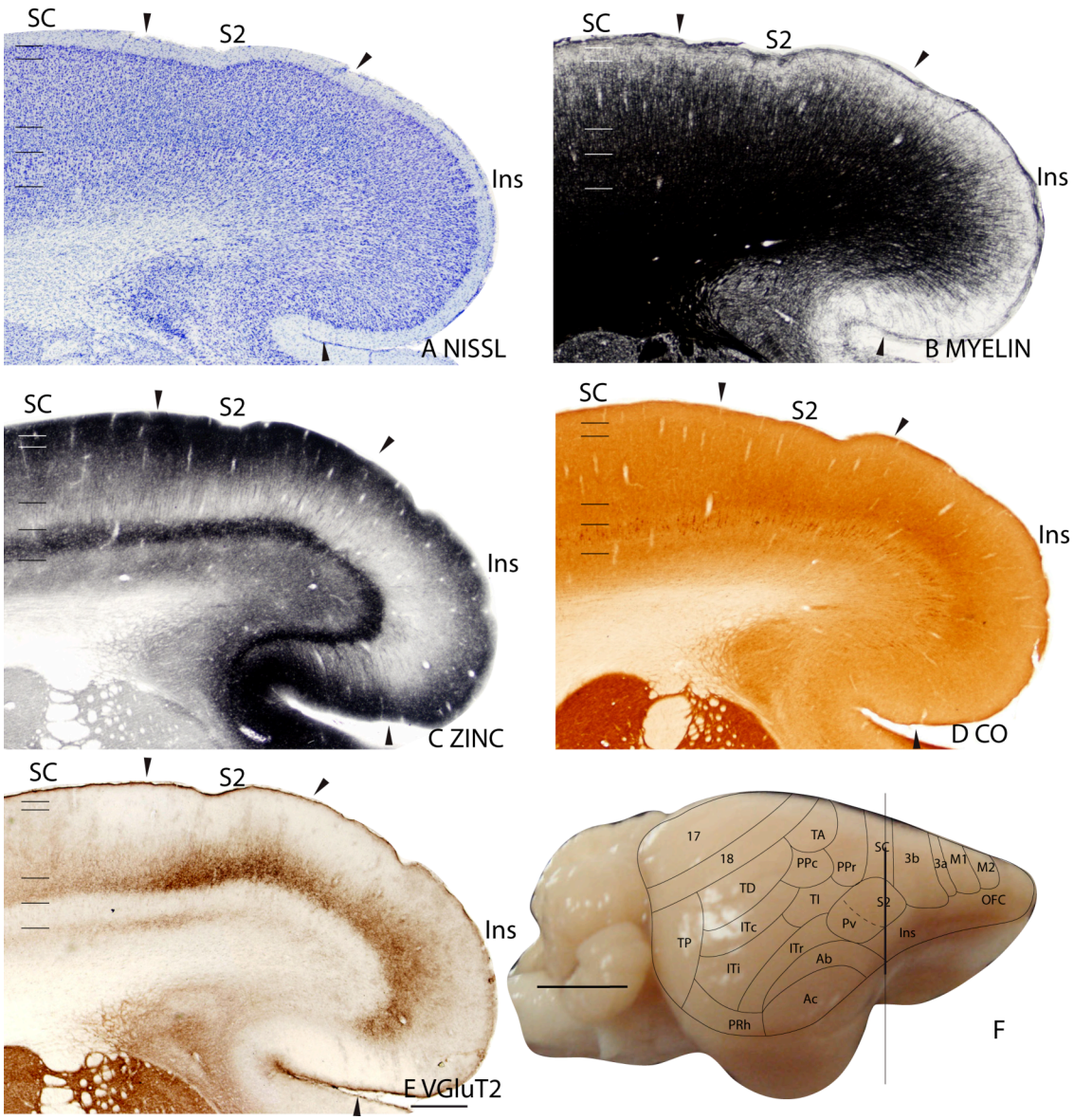

Figure 40. Architectonic characteristics of the secondary somatosensory cortex and insular cortex. Cortical areas are shown on a lateral view of the right hemisphere in panel F. The vertical line across the cortex (panel F) indicates the location where the coronal brain sections in panels A to E were obtained. The extent of each cortical layers 1 to 6 is indicated by the short horizontal lines on panels A-E. The scale bar for brain sections (panel E) = 0.5mm. The scale bar on the brain (panel F) = 5mm.

Somatosensory caudal area, SC. In Nissl stained sections, SC has a moderately packed layer 4 that is thinner than layer 4 of 3b(S1) (Figs. 39A, 42A). Layer 4 of SC is also thinner and packed with smaller cells than layer 4 of S2 (Fig. 40A). Layer 5 of SC is moderately populated with pyramidal cells that are larger than those in 3b(S1) (Figs. 39A, 42A) and PPd (Fig. 42G), but smaller than those in S2 (Fig. 40A). In the myelin stain, SC lacks distinct bands of Baillarger, and has reduced myelination compared to 3b(S1) (Figs. 39B, 42B). SC is also not as well myelinated as S2 (Fig. 40B), but has similar levels of myelination to PPd (Fig. 42H). In the zinc stain, SC stains darker,

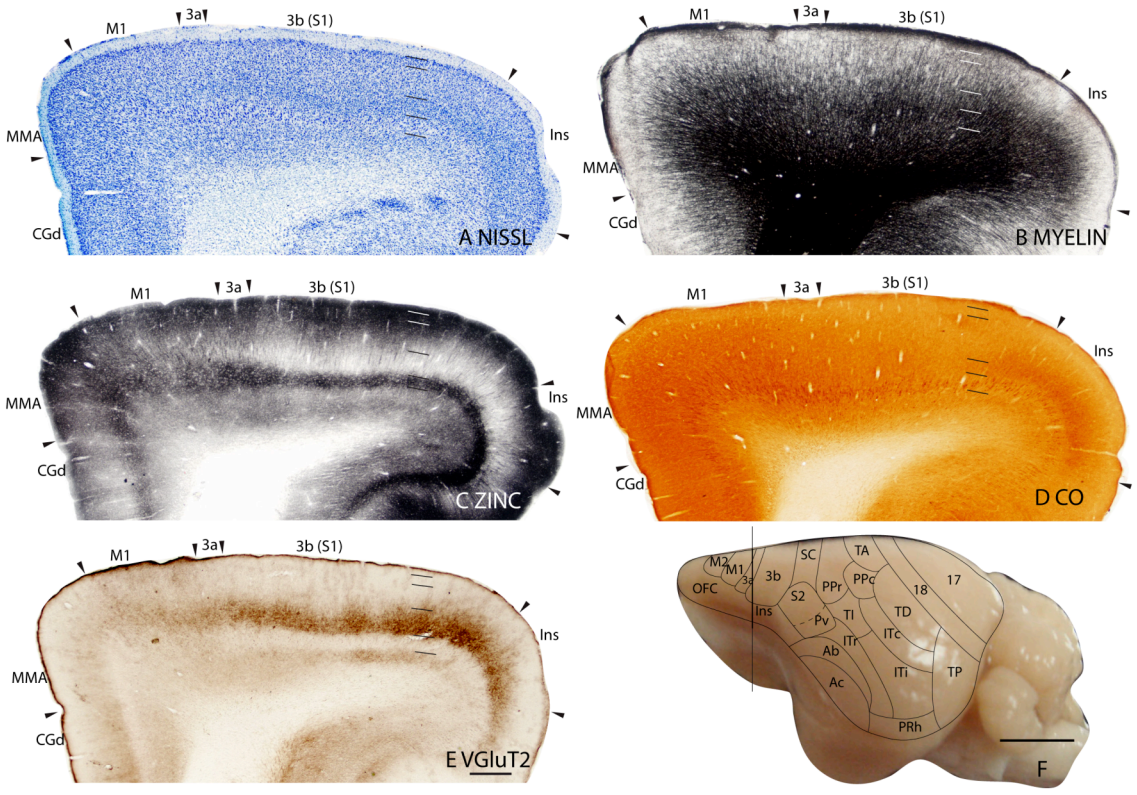

Figure 41. Architectonic characteristics of primary somatosensory and motor areas. Cortical areas are shown on a lateral view of the left hemisphere in panel F. The vertical line across the cortex (panel F) indicates the location where the coronal brain sections in panels A to E were obtained. Short horizontal lines on panels A to E indicate the extent of the 6 cortical layers. The scale bar for brain sections (panel E) = 0.5mm. The scale bar on the brain (panel F) = 5mm.

especially in layer 4, compared to both 3b(S1) (Figs. 39C, 42C) and S2 (Fig. 40C), and stains at a similar level to PPd (Fig. 42I). Layer 4 of SC expresses less CO than layer 4 of 3b(S1) (Fig. 39D) and S2 (Fig. 40D), and layer 5 of SC is populated with CO-stained cells (Figs. 39D, 40D).

SC stains lighter in the VGluT2 stain compared to 3b(S1) (Fig. 39E) and S2 (Fig. 40E). A faint band of VGluT2 staining that is present in layer 6 of SC is absent in S2 (Fig. 40E). In PV preparations, PV immunopositive terminations in SC do not form a dark band in layer 4 as they do in 3b(S1) (Fig. 42D). There is a sparse distribution of PV immunostained cell bodies in SC, and there is no distinct difference in PV staining between SC and PPd (Fig. 42J). Layer 3 of SC is more densely populated with SMI-32 immunopositive neurons compared to 3b(S1), and in layer 5, the SMI-32 immunopositive pyramidal neurons are larger and more darkly stained than those in 3b(S1) (Fig. 42E) and PPd (Fig. 42K).

Second somatosensory, S2, and parietal ventral, Pv areas. S2 in tree shrews contains a topographic map of the contralateral body surface, and cortex caudal and lateral to S2, which corresponds to Pv, is also responsive to somatosensory stimulation (Sur et al., 1981). Remple et al. (2006), distinguished Pv from S2 in the Nissl stain, where in Pv, layer 5 was thinner and more densely packed compared to S2. In the other stains used, S2 and Pv have similar patterns of staining. Results presented here for S2 also apply to Pv, as we did not distinguish an architectonic border between the two fields.

In Nissl stained sections, S2 has a well-developed layer 4 that is thinner than that of 3b(S1), and thicker than that of SC. Layer 5 of S2 is populated with pyramidal cells

that are larger than the adjoining insular (Ins) area (Fig. 40A), but are smaller than in 3b(S1). S2 is more highly myelinated than SC, but is less myelinated than Ins (Fig. 40B).

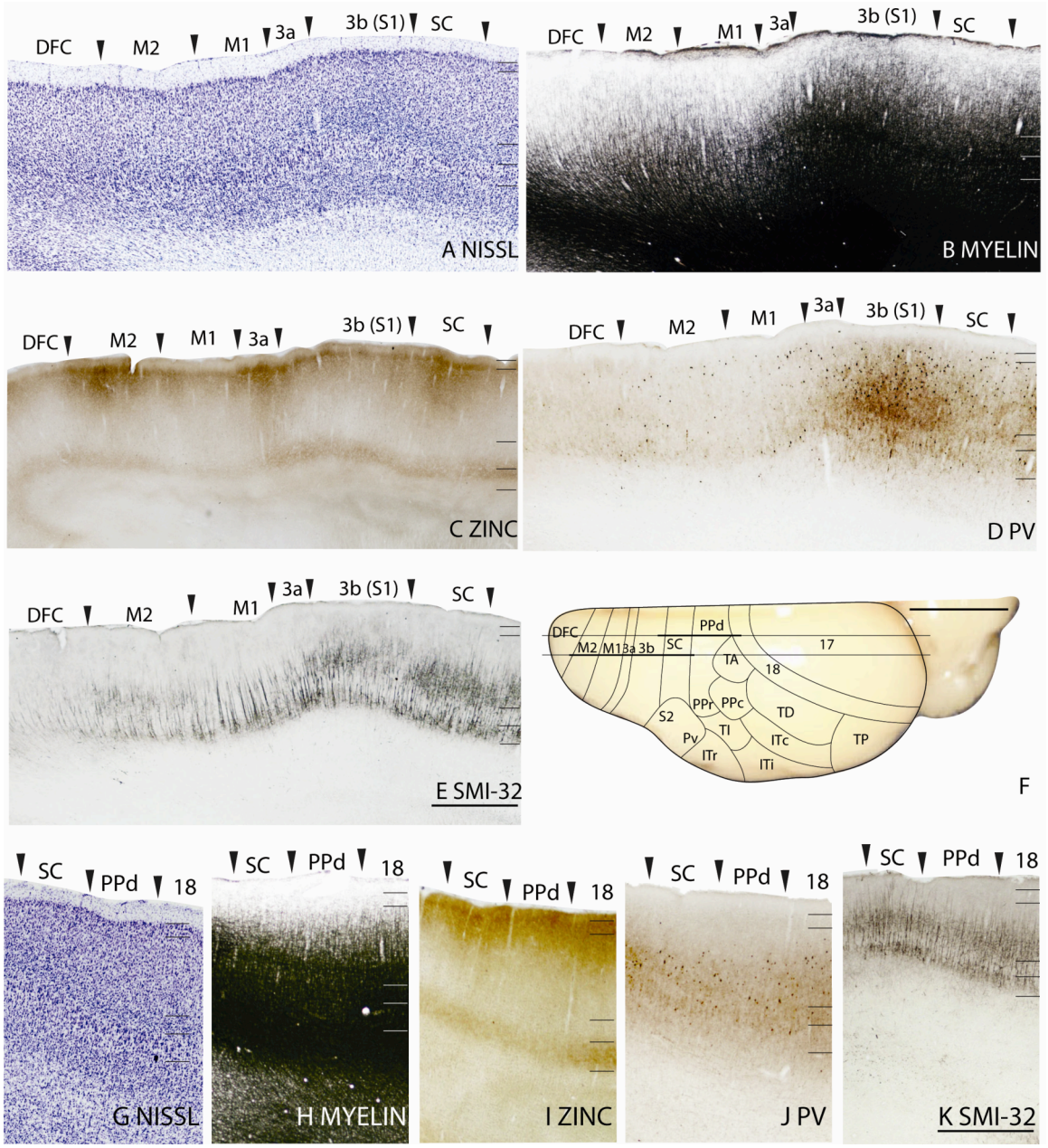

Figure 42. Architectonic characteristics of somatosensory and motor areas. Cortical areas are shown on a dorsal view of the left hemisphere in panel F. The lateral most horizontal line across the cortex (panel F) indicates the location where the sagittal brain sections in panels A to E were obtained. The horizontal line across the cortex (panel F) that is close to the medial wall indicates the location where the sagittal brain sections in panels G to K were obtained. The scale bar for brain sections (panels E and K) = 1mm. The scale bar on the brain (panel F) = 5mm.

No bands of Baillarger are observed in S2 (Fig. 40B). In the zinc stain, layer 4 of S2 is lighter stained than in SC (Fig. 40C), but is darker stained than in 3b(S1) and Ins (Fig. 40B). Layers 1 to 3 of S2 also express more free zinc ions than Ins (Fig. 40C). Layer 4 of S2 is thinner and stains less intensely for CO than layer 4 of Ins (Fig. 40D).

In VGluT2 preparations, a band of VGluT2 immunostained terminations in layer 4 of S2 is thinner and darker than in Ins, and thicker and darker than in SC (Fig. 40E). No VGluT2 immunostaining is observed in layer 6 of S2. Layer 4 of S2 has reduced staining of PV immunopositive terminations compared to 3b(S1) and Ins, and has higher staining compared to SC (not shown). In SMI-32 preparations, the pyramidal cells in layer 3 of S2 are less darkly stained and the pyramidal cells in layer 5 are smaller than those in 3b(S1) (not shown).

Posterior parietal area, PP. The posterior parietal area has been divided into three regions, PPr, PPc and PPd, where each of these regions has different connections patterns with the motor cortex (Remple et al., 2007). Although areas PPd and PPr have dissimilar connection patterns with the motor cortex, they have similar architectonic characteristics, and we were unable to reliably determine the architectonic border between them. As such, they were drawn as a single architectonic field in our summary diagrams.

In Nissl stained sections, layer 4 of PPd is thicker and more populated with granule cells than the adjoining TA (Fig. 5A), but is neither as well-developed nor as populated with granule cells as compared to area infraradiata dorsalis (IRd) along the medial wall (Fig. 45A). Layer 5 of PPd has a similar packing density of pyramidal cells compared to TA (Fig. 30A), and a reduced packing density compared to area 18 and SC

(Fig. 42G). Pyramidal cells in layer 5 are larger than those in area 18 and SC (Figs. 30A, 42G), and similarly sized to those in TA (Fig. 30A). PPd also has a higher packing density of cells in layers 1 to 3 compared to TA (Fig. 30A). In myelin preparations, PPd has similar myelination levels as SC (Fig. 42H), and is less myelinated than area 18, TA (Fig. 30B), and IRd (Fig. 45B). PPd expresses free zinc ions throughout the cortical layers. Layers 1 to 3 are darker in the zinc stain than the corresponding layers in TA (Fig. 30C), and layer 5 stains lighter for free zinc ions than IRd (Fig. 45D). In CO preparations, layer 4 of PPd is not darkly stained, and layer 5 is populated with darkly stained cell bodies (Fig. 45F).

PPd shows reduced staining for VGluT2 immunopositive terminals compared to the surrounding areas, such as SC and area 18, except for IRd, where the staining intensities in layer 4 are similar (Fig. 45E). In PV preparations, the staining intensities of PPd, TA (Fig. 30D), and SC (Fig. 42J) are similar. The PPd/IRd border is distinct in PV stained sections, as PV immunopositive terminations are absent in layer 4 of PPd and are present in layer 4 of IRd (Fig. 45C). PPd and TA have similar staining characteristics in the SMI-32 stain, where there is dense staining in layer 3, and layer 5 is populated with medium-sized pyramidal cells (Fig. 30E). The SMI-32 immunostained pyramidal cells in layer 3 of PPd have smaller apical dendrites than in area 18 (Figs. 30E, 142K), and in layer 5, PPd is more densely populated with SMI-32 immunopositive pyramidal cells than area 18 (Figs. 30E, 42K).

In Nissl stained sections, layer 4 of PPc is populated by small granule cells, and layer 5 is populated by medium sized pyramidal cells that are mainly in outer layer 5 (Fig. 36A). PPc has reduced myelination compared to TD and TI, and no bands of

Baillarger are observed (Figs. 31B, 36B). In the zinc stain, PPc stains darker for zinc than TI (Fig. 36C), and stains at similar intensity to ITc and TA (Fig. 31D). CO staining in layer 4 of PPc is lower than in TI, and in layer 5, darkly stained cell bodies are present (Fig. 36D).

Layer 4 of PPc shows diffuse and less intense staining for VGluT2 antibody compared to TI (Fig. 36E). PPc also stains less intensely for PV compared to the surrounding areas (Fig. 31E), and a sparse population of SMI-32 immunostained pyramidal cells is observed in layer 5 of PPc (not shown).

Frontal cortex

Here, the frontal cortex in tree shrews is divided into four areas, the primary motor area (M1), the secondary motor area (M2), the dorsal frontal cortex (DFC), and the orbital frontal cortex (OFC).

Primary motor cortex, M1. M1 is a narrow strip, approximately 1mm wide, that has a complete body and orofacial representation (Remple et al., 2006). In the Nissl stain, M1 has a poorly developed layer 4, and a well-developed layer 5, where inner layer 5 is populated with large pyramidal cells (Figs. 41A, 42A). M1 is less well myelinated than 3a, with no distinct band of Baillarger (Figs. 41B, 42B), and has similar levels of myelination to M2 (Fig. 42B). In the zinc stain, the staining intensity is lower in M1 than in M2 (Fig. 42C) and MMA (Fig. 41C), and higher, especially in layer 4, than in 3a and 3b(S1) (Figs. 41C, 42C). M1 does not express high levels of CO in layer 4 (Fig. 41D), although darkly stained cell bodies are observed in layer 5.

In VGluT2 preparations, layer 4 of M1 stains poorly compared to 3a, but is darker stained than MMA (Fig. 41E). No VGluT2 staining is observed in layer 6 of M1. In the PV stain, M1 stains poorly for PV immunopositive terminations, and is sparsely populated with PV immunopositive neurons (Fig. 42D). M1 has large, densely stained SMI-32 pyramidal neurons in layer 5, with thick apical dendrites that extend to layer 3 (Fig. 42E). No SMI-32 immunopositive neurons were present in layer 3 of M1.

Secondary motor cortex, M2. M2 is delineated from M1 by a thinner layer 5 that is less densely packed with pyramidal neurons than in M1 (Fig. 42A). The M2/DFC border is marked by the return of a granular layer 4 and smaller layer 5 pyramidal cells in DFC (Figs. 42A, 43A). In myelin preparations, M2 is more myelinated than DFC (Figs. 42B, 43B), and less myelinated than OFC (Fig. 43B). M2 expresses higher levels of free zinc ions throughout the cortical layers compared to the adjacent cortical areas such as M1 (Fig. 42C), DFC (Figs. 42C, 44A), and OFC (Fig. 44A). In CO preparations, the rostral border of M2 with DFC is not distinct, except for the larger sized, darkly stained cell bodies in layer 5 of M2 than in layer 5 of DFC (Fig. 44C). The M2/OFC border is distinct in CO preparations, as a band of dark CO staining is present in layer 4 of OFC and absent in M2 (Fig. 44C).

M2 expresses low levels of VGluT2 staining, resulting in a distinct M2/OFC border (Fig. 44B). The rostral border of M2 with DFC is not as distinct in VGluT2 preparations, as both cortical areas stain at similar intensities (Fig. 44B). No VGluT2 staining is observed in layer 6 of M2. PV staining in M2 is lower than in DFC and OFC (Fig. 43C), and is similar to that of M1 (Fig. 43D). SMI-32 immunoreactive pyramidal cells in layer 5 of M2 were smaller than those in M1, and had thinner apical dendrites

(Fig. 43E). No SMI-32 immunoreactive pyramidal cells is observed in layer 3 of M2. The M2/DFC border is marked by a transition to a sparser population of small SMI-32 immunoreactive cells, with poorly stained cell bodies and thin apical dendrites (Fig. 43E).

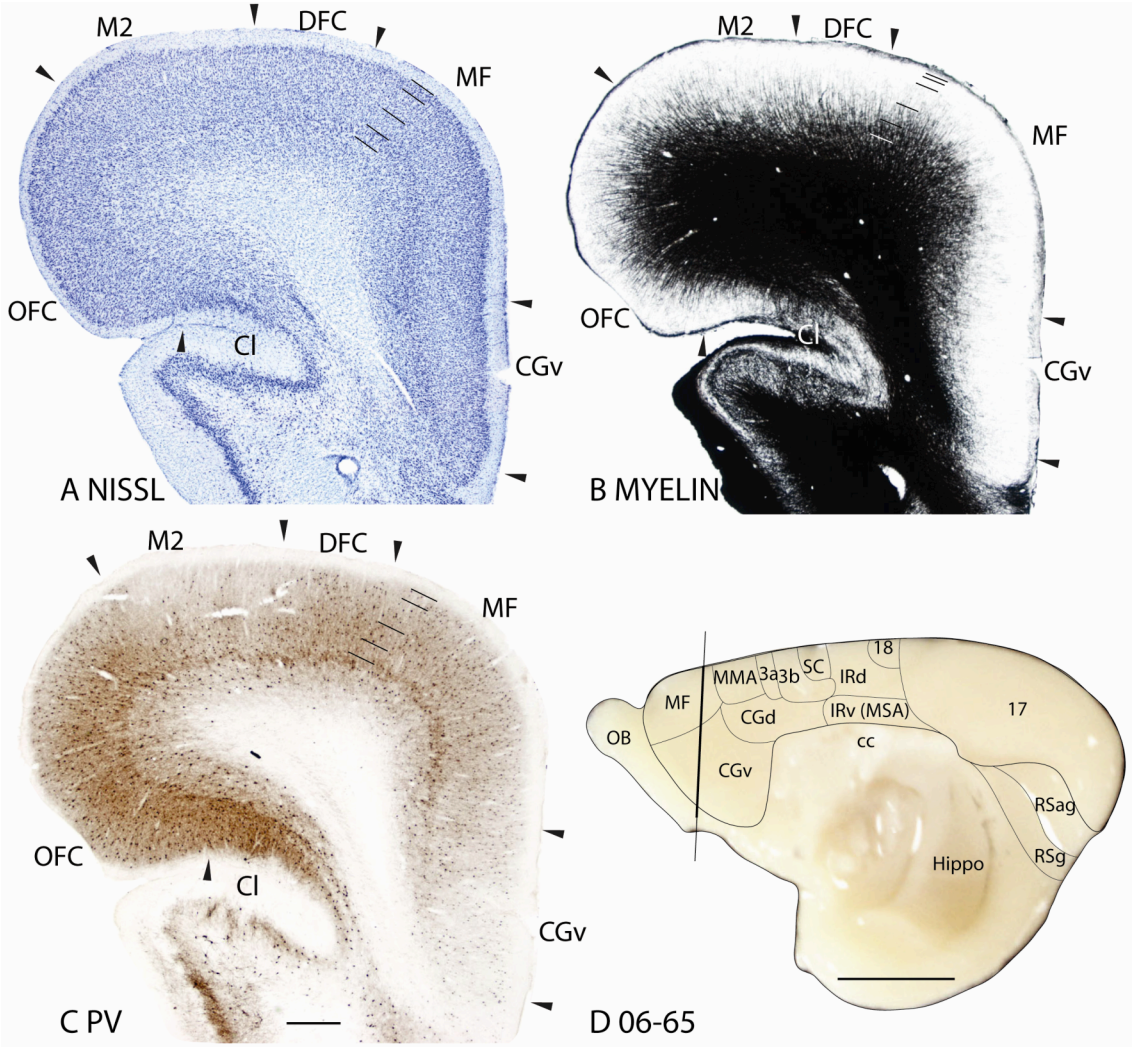

Figure 43. Architectonic characteristics of the medial frontal and cingulate areas. Cortical areas are shown on the medial view of the right hemisphere (panel D). The vertical line across the cortex (panel D) indicates the location where the coronal brain sections in panels A to C were obtained. The extent of each cortical layers 1 to 6 is indicated by the short horizontal lines on panels A to C. The scale bar for brain sections (panel E) = 0.5mm. The scale bar on the brain (panel F) = 5mm.

Dorsal frontal cortex, DFC. In Nissl stained sections, DFC has a thin granular 4 (Figs. 42A, 43A). DFC also has a lower cell packing density throughout the cortical layers, resulting in a paler appearance of DFC compared to the medial frontal (MF) area (Fig. 43A). In myelin preparations, DFC has reduced myelination compared to the surrounding areas such as M2 and MF (Figs. 42B, 43B). DFC has lower expression of free zinc ions compared to M2, especially in layer 4 (Fig. 44A). However, the zinc staining of layer 4 in DFC is not homogenous as it reduces towards the DFC/MF border, which is marked by the transition to increased zinc stain in layer 4 of MF (Fig. 43A). There is no band of CO staining in layer 4 of DFC, although there are darkly stained cell bodies in layer 5 (Fig. 44C). This allows for the demarcation of the DFC/MF border, where there is a band of CO staining in layer 4 of MF (Fig. 44C).

VGluT2 expression in DFC is similar to that of M2 and MF; as such the borders of DFC are not distinct in the VGluT2 stain (Fig. 44B). In PV preparations, a thin, PV stained band is observed in layer 6 of DFC (Fig. 43C). Layers 3 to 5 of DFC stains darker for PV immunopositive terminals compared to M2 and MF, and DFC has a larger population of PV immunopositive neurons than M2 (Fig. 43C). In SMI-32 preparations, DFC does not have stained pyramidal cells in layer 3, and has a sparse population of poorly stained pyramidal cells bodies in layer 5 that have thin apical dendrites (Fig. 42E).

Orbital frontal cortex, OFC. In Nissl preparations, OFC is overall more densely populated with cells than M2, giving it a darker appearance than M2 (Fig. 43A). OFC has a well-developed layer 4 that is populated with small granule cells (Fig. 43A). Layer 5 of OFC has a lower cell packing density, and is populated with smaller pyramidal cells than layer 5 of M2 (Fig. 43A). The ventral border of OFC is marked by a transition to poorly

laminated cortex with a thick, densely populated layer 2/3 in the claustral cortex (Cl) (Fig. 43A). OFC is more myelinated than the surrounding cortical areas M2 and Cl (Fig. 43B). In zinc preparations, layer 4 of OFC stains poorly, standing out as a white band. As a result, a distinct dorsal border with M2 and ventral border with Cl is seen in the zinc stain, as layer 4 both of the adjoining areas expresses higher levels of free zinc ions (Fig. 44A). Layer 4 of OFC stains darkly in CO preparations, expressing higher levels of CO protein than the surrounding areas M2 and Cl (Fig. 44C).

OFC has a darkly stained VGluT2 immunopositive band in layer 4 that terminates at the OFC/M2 and OFC/Cl borders (Fig. 44B). In PV preparations, OFC has darker PV staining compared to M2, with an increased population of PV immunoreactive neurons throughout the cortical layers. OFC also has a band of PV immunopositive terminations in layer 4 and a thinner band in layer 6 (Fig. 43C). The upper cortical layers of OFC are less darkly stained than in Cl (Fig. 43C). In SMI-32 preparations, there are no immunostained pyramidal cell bodies, and some short immunostained dendrites in OFC (not shown).

Medial cortex

The cortical areas along the medial wall of the tree shrew neocortex can be divided into rostral, middle and caudal regions. The rostral region consists of the medial frontal (MF), the dorsal cingulate (CGd), the ventral cingulate (CGv), and the medial motor (MMA) areas. In tree shrews, the somatosensory cortex, including areas 3a, 3b(S1) and SC, wraps onto the medial wall to occupy part of the middle region, and the rest

consists of the infraradiata areas. The caudal region, largely occupied by area 17, also includes area 18, prostriata (PS), and the retrosplenial areas.

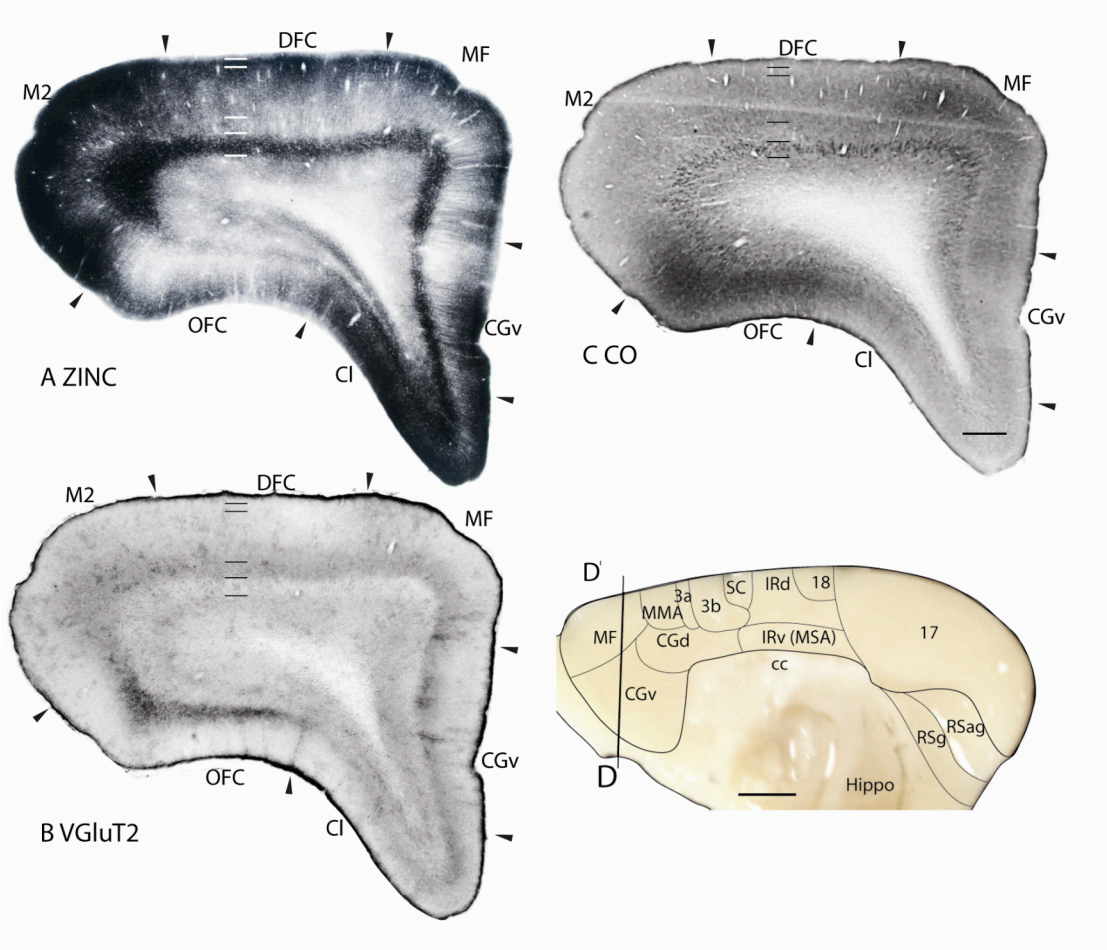

Figure 44. Architectonic characteristics of the medial frontal and cingulate ventral area. Cortical areas are shown on the medial view of the right hemisphere (panel D). The vertical line across the cortex (panel D) indicates the location where the coronal brain sections in panels A to C were obtained. Short horizontal lines on panels A to E indicate the extent of the 6 cortical layers. The scale bar for brain sections (panel C) = 0.5mm. The scale bar on the brain (panel D) = 2.5mm.

Medial frontal area, MF. In Nissl preparations, MF has a well-developed layer 4 that is more densely populated with granule cells than in DFC, and a layer 5 that is less densely populated with cells than in CGv (Fig. 43A). MF is also more heavily myelinated than DFC and CGv (Fig. 43B). In the zinc stain, MF expresses more free zinc ions in

layer 4 than DFC, with a higher density of zinc stained 'strings' running through layer 4 (Fig. 44A). MF has a band of CO staining in layer 4 that is absent in both DFC and CGv (Fig. 44C), and darkly stained cell bodies in layer 5.

The borders of MF in the VGluT2 stain are not distinct as the adjoining cortical areas, DFC and CGv, stain with similar intensities to MF for the VGluT2 stain (Fig. 44B). In PV preparations, a thin band of PV stain is present in layer 6, and darkly stained PV immunopositive cell bodies are present throughout the cortical layers (Fig. 43C). There is no distinct difference between DFC and MF in the PV stain, whereas the MF/CGv border is marked by a transition to a sparser distribution of PV immunopositive cell bodies and the absence of PV stain in layer 6 of CGv.

Cingulate ventral area, CGv. CGv has a less densely populated, and a thinner layer 4 than MF in Nissl stained sections (Fig. 43A). The upper cortical layers 2 and 3 are populated with larger cells than in MF, although this changes in the ventral portion of CGv, where the cells that populate layer 2 and 3 are reduced in size (Fig. 43A). Layer 5 of CGv is thick and densely populated with cells. In myelin preparations, CGv is less myelinated then MF (Fig. 43B). The pattern of zinc staining in CGv is not homogenous. At the dorsal border of CGv, layer 4 stains very poorly for the zinc stain, and the staining increases towards the ventral border of CGv (Fig. 44A). CGv stains poorly for CO (Fig. 44C). The variable staining patterns in the Nissl and zinc stains suggest the possibility for further subdividing CGv.

CGv stains poorly in the VGluT2 stain (Fig. 44B). In the PV stain, no dense bands of PV immunopositive terminations are observed, and only a scattering of small PV immunopositive cell bodies are present (Fig. 43C).

Cingulate dorsal area, CGd. CGd is densely populated with cells throughout the cortical layers, giving it a dark appearance in the Nissl stain (Fig. 41A). Layer 4 in CGd is very thin and not well developed, and layer 5 is densely populated with small pyramidal cells. The 3b(S1)/CGd border is marked by the reduction in the thickness of layer 4 in CGd (Fig. 39A). CGd is less heavily myelinated than MMA (Fig. 41B), and 3b(S1) (Fig. 39B). In the zinc stain, CGd stains more intensely than 3b(S1) (Fig. 39C), especially in layer 4, where CGd expresses more free zinc ions than layer 4 of 3b(S1). CGd expresses less free zinc ions than MMA, as such CGd has a lighter appearance than MMA in zinc stained sections (Fig. 41C). In CO preparations, the CGd/3b(S1) border is marked by the reduction of CO staining in CGd (Fig. 39D).

CGd has reduced expression of VGluT2 immunopositive terminals compared to 3b(S1), resulting in a distinct 3b(S1)/CGd border (Fig. 39E). The CGd/MMA border is not as distinct, although CGd stains more intensely for VGluT2 than MMA (Fig. 41E). In the PV stain, the dorsal border of CGd with 3b(S1) is marked by a transition to reduced PV staining in CGd, and the absence of PV immunopositive terminals in layer 4 of CGd (not shown). The PV staining pattern of CGd is similar to that of CGv.

Medial motor area, MMA. MMA is adjacent to M1 along the medial wall, and has projections to M1 and M2 (Remple et al., 2007). MMA does not have a distinct granular layer 4, and has a thick layer 5 that is densely populated with pyramidal cells (Fig. 41A). The upper cortical layers 2 and 3 of MMA are densely populated with cells, giving it a darker appearance than the adjacent M1 (Fig. 41A). MMA is as heavily myelinated as M1, and is more heavily myelinated than CGd (Fig. 41A). In the zinc stain, MMA expresses more free zinc ions throughout its cortical layers than both CGd and M1 (Fig.

41C). MMA stains poorly for CO, and it is difficult to define the MMA/CGd and M1/MMA borders in CO preparations (Fig. 41D)

In VGluT2 preparations, layer 4 of MMA stains less densely than the surrounding areas (Fig. 41E), and PV expression in terminals is weak, with a sparse scattering of PV immunopositive neurons (not shown).

Infraradiata dorsal area, IRd. In Nissl preparations, layer 4 of IRd is sparsely populated with medium sized cells, and layer 5 is sparsely populated with small pyramidal cells (Fig. 45). IRd is myelinated at similar levels to PPd, and is more heavily myelinated than the infraradiata ventral area (IRv) (Fig. 45B). In the zinc stain, IRd expresses more free zinc ions in layers 4 and 5 compared to PPd (Fig. 45D). The borders of IRd are not as obvious in the CO stain as the CO expression of IRd, and the adjoining PPd and IRv are similar (Fig. 45F).

Reduced VGluT2 staining intensity in IRd marks the IRd/IRv border (Fig. 45E). However, IRd has similar levels of VGluT2 staining to PPd, as such the IRd/PPd border is not distinct in VGluT2 preparations (Fig. 45E). In PV preparations, IRd is more darkly stained than PPd, and layer 4 of IRd is more darkly stained with PV immunopositive terminals than layer 4 of PPd (Fig. 45C).

Infraradiata ventral area, IRv. In Nissl stained sections, IRv has a thin layer 4, and a layer 5 that is more densely populated with small cells than IRd (Fig. 45A). IRv is less heavily myelinated than IRd, and an outer band of Baillarger is present (Fig. 45B). The upper cortical layers 2 and 3, and layer 5 of IRv stains darker in the zinc stain than the corresponding layers in IRd (Fig. 45D). The ventral border of IRv is marked by a reduced expression of free zinc ions. IRv stains lightly for CO (Fig. 45F).

In VGluT2 preparations, two immunostained bands are present in IRv, a darker band in layer 4 and a lighter band in layer 6 (Fig. 45E). Layer 4 of IRv stains darker for VGluT2 than layer 4 of IRd. The absence of the two bands in adjoining cortex marks the ventral border of IRv (Fig. 45E). PV immunostaining in layer 4 of IRv is more diffuse than in IRd, and layers 2 and 3 of IRv do not stain as darkly for PV, giving IRv a paler appearance than IRd (Fig. 45C). IRv expresses more PV staining than the adjoining cortex, allowing the delineation of the ventral border of IRv (Fig. 45C).

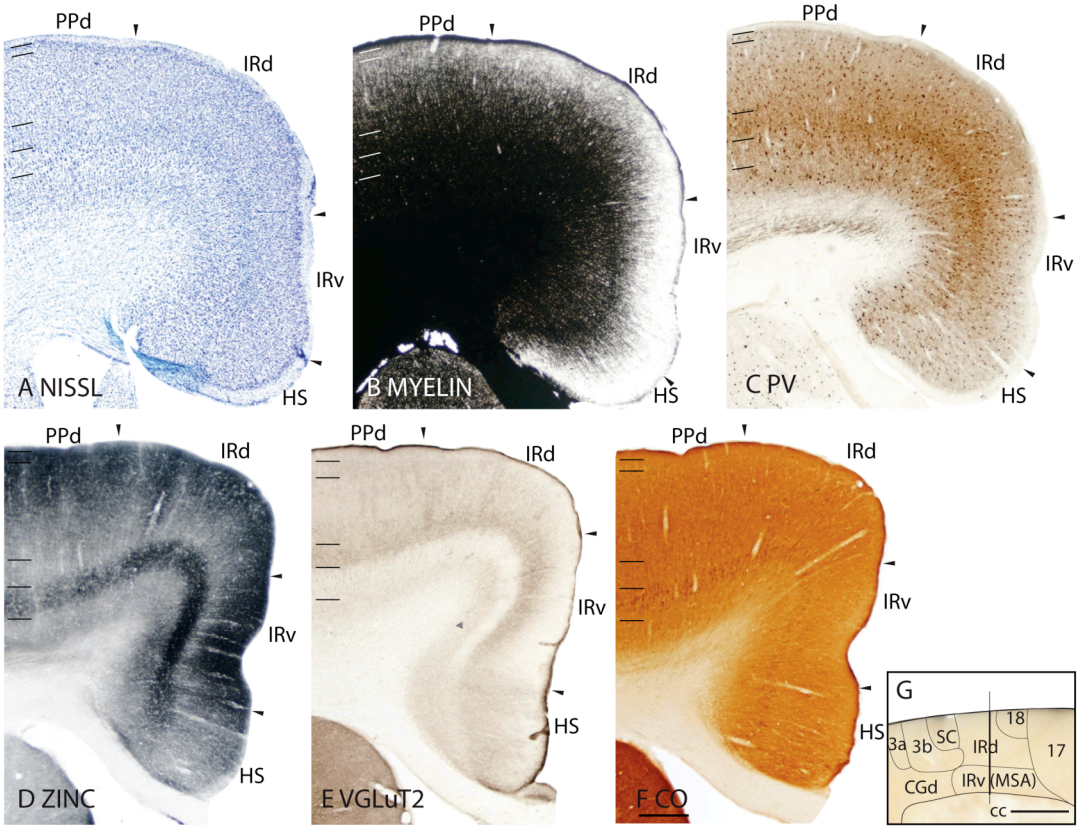

Figure 45. Architectonic characteristics of the infraradiata areas. Cortical areas are shown on the medial view of the right hemisphere (panel G). The vertical line across the cortex (panel G) indicates the location where the coronal brain sections in panels A to F were obtained. The extent of each cortical layers 1 to 6 is indicated by the short horizontal lines on panels A to F. The scale bar for brain sections (panel F) = 0.5mm. The scale bar on the brain (panel G) = 2.5mm.

Prostriata, PS. Prostriata runs between the ventromedial edge of area 17 and the retrosplenial agranular (RSag) area, where there is a slope in the cortex. In Nissl preparations, the area 17/PS border is marked by a disappearance of a well-developed granular layer 4 in PS (Fig. 26A). Layer 2 of PS is more densely packed with cells than in RSag (Fig. 26A). PS is more lightly myelinated than area 17, and, to a lesser extent, RSag (Figs. 26B, 46A). PS expresses higher levels of free zinc ions throughout the cortical layers compared to the adjoining area 17 and RSag (Figs. 26C, 46B). The absence of a dark CO-stained band in layer 4 marks the transition to PS from area 17 (Fig. 46C).

PS shows almost no VGluT2 staining (Fig. 46D). In PV preparations, a scattering of PV immunopositive cell bodies is observed (Fig. 46E), and no staining of PV immunopositive terminations is observed (Figs. 26D, 46E). There are no SMI-32 immunostained cell bodies present in PS (Fig. 26E).

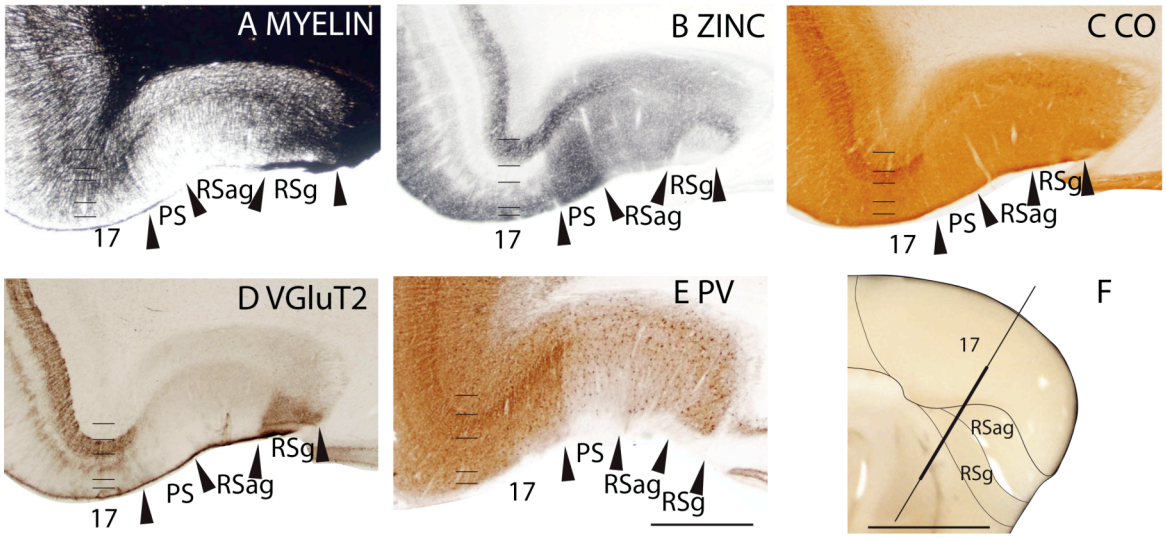

Figure 46. Architectonic characteristics of the retrosplenial areas. Cortical areas are shown on the medial view of the right caudal hemisphere (panel F). The vertical line across the cortex (panel F) indicates the location where the coronal brain sections in panels A to E were obtained. The scale bar for brain sections (panel E) = 0.5mm. The scale bar on the brain (panel F) = 5mm.

Retrosplenial agranular area, RSag. In Nissl preparations, RSag is not well laminated. It has lower cell packing density, and as a result has a paler appearance than the adjoining PS and retrosplenial granular (RSg) areas (Fig. 26A). RSag is lightly myelinated compared to RSg, but is more heavily myelinated than PS (Fig. 46A). In zinc preparations, RSag is more lightly stained than PS, especially in layer 5, and is more darkly stained in layers 1 to 3 than in RSg (Figs. 26C, 46B). CO expression in RSag is poor, and there is no distinct different in staining pattern between RSag and PS (Fig. 46C).

RSag does not have visibly detectable levels of VGluT2 (Fig. 46D) and SMI-32 (Fig. 26E) immunoreactivity. In PV preparations, RSag has a similar staining pattern to PS, and has a lighter appearance in layers 1 to 3 when compared to RSg (Fig. 46E).

Retrosplenial granular area, RSg. In Nissl preparations, darker staining of layer 2/3 in RSg marks the RSag/RSg border (Fig. 26A). Similar to RSag, RSg does not have well developed laminar properties. RSg is more heavily myelinated than RSag (Figs. 26B, 46A). The upper cortical layers 1 to 3 of RSg stains less intensely in the zinc stain than RSag, and no darkly stained band is observed in layer 5 (Fig. 46B). In CO preparations, RSg has poor CO expression (Fig. 46C). However, a denser population of CO stained cell bodies in layer 5 is present in RSg than in RSag (Fig. 46C).

The upper cortical layers 2/3 of RSg stain darkly for VGluT2, providing a sharp border between RSg and RSag (Fig. 46D). In PV preparations, RSg has more darkly stained PV immunopositive cell bodies than RSag, and RSg has an overall darker appearance than RSag (Fig. 46E). Closer to the rostral border of RSag, SMI-32

immunopositive dendrites are present in the middle layers, and a few SMI-32 immunopositive cell bodies are present in layer 5 of RSag (Fig. 26E).

Remaining cortical areas

Insular area, Ins. In Nissl preparations, Ins has a well-developed layer 4 that is populated by granule cells that are small than those in S2 (Fig. 40A). Layer 5 of Ins is more sparsely populated with cells than both 3b(S1) and S2, giving it a paler appearance than the adjoining areas (Figs. 26A, 41A). Ins is as heavily myelinated as S2 (Fig. 40B), and is less heavily myelinated than 3b(S1) (Fig. 41B). In zinc preparations, Ins expresses lower levels of free zinc ions throughout the cortical layers than S2 (Fig. 40C). The difference in free zinc ion expression between S2 and Ins is most distinct in layer 4 (Fig. 40C). Ins expresses higher levels of free zinc ions compared to 3b(S1), especially in layer 5 (Fig. 41C). In CO preparations, layer 4 of Ins stains more intensely than in S2 (Fig. 40D).

Layer 4 of Ins contains VGluT2 immunopositive terminations, and no staining is observed in layer 6 (Figs. 40E, 41E). VGluT2 expression in layer 4 of Ins is lower and the staining is more diffuse than in S2 (Fig. 40E), whereas the VGluT2 expression in layer 4 of Ins is less intense than in 3b(S1) (Fig. 41E). In PV preparations, PV staining in layer 4 of Ins is more intense than in S2, and less intense than in 3b(S1)(not shown).

Perirhinal area, Prh. In Nissl stained sections, Prh does not have a well-developed layer 4 and has a low cell population density, giving it a pale appearance (Figs. 32A, 33B, 35A). It is also poorly myelinated compared to the adjoining areas TP, ITr, and the entorhinal cortex (Figs. 32B, 34C, 35B). In zinc preparations, Prh stains more

intensely compared to the surrounding areas such as TP (Fig. 34E), and ITr (Fig. 35C), whereas it stains at similar intensity to the entorhinal cortex (Fig. 9E). Prh stains poorly in the CO stain (Figs. 34D, 35D). In the three immunostains used, Prh has low immunoreactivity for all three, VGluT2 (Fig. 35E), PV (Fig, 32C), and SMI-32 (not shown).

Discussion

In the present study, we used a battery of histological procedures to reveal and characterize the architectonic subdivisions of tree shrew neocortex that have known or presumed functional significance. Previous architectonic studies of tree shrews (Clark, 1924; von Bonin and Bailey, 1961; Zilles et al., 1978) have been limited, and were completed too early to take advantage of the many immunohistochemical and other architectonic procedures that are now available to help characterize cortical areas. There has been a longstanding (e.g. Clark, 1924) and persisting interest in cortical organization of tree shrews (e.g. Kaas et al., 1972; Sesma et al., 1984; Lyon et al., 1998; Remple et al., 2006), as they are close relatives of primates (Liu et al., 2001; Murphy et al., 2001 a,b; Springer et al., 2003), and insights into cortical organization in tree shrews should inform theories of forebrain evolution in primates. As the differences between areas reflect functional specializations, we discuss the functional implications of the architectonic differences across cortical fields. Most notably, previous findings indicate that cortical areas with layer 4 terminations that have dense expression of VGluT2 and PV, and little synaptic zinc are likely to be dominated by thalamic rather than cortical inputs (Van Brederode et al., 1990; DeFelipe and Jones, 1991; DeVencia et al., 1998; Hackett et al.,

1998; Latawiec et al., 2000; Cruikshank et al., 2001; Fujiyama et al., 2001; Kaneko and Fujiyama, 2002; Valente et al., 2002; Nahami and Erisir, 2005; Wong and Kaas, 2008). Areas of high metabolic activity, typically sensory areas, express high levels of CO, especially in layer 4. Such areas are likely to have a well developed layer 4 of granule cells that is densely myelinated. In brain sections cut parallel to the brain surface, several of the histological preparations revealed a patchy pattern in some areas of cortex, suggesting that these areas have a modular organization.

Here we discuss our results and conclusions for each major cortical region of the tree shrews in the context of previous architectonic and experimental studies of cortical organization in tree shrews, and, to a limited extent, in other mammals.

Occipital cortex

The occipital cortex of tree shrews includes two architectonically distinct fields, areas 17 and 18, which correspond to visual areas V1 and V2 of other mammals. Areas lateral to area 18 include visual areas TA, TP and TD, which also may be considered as parts of occipital cortex, but they are discussed here as parts of dorsal temporal cortex.

Area 17 has such pronounced sensory features that it was easily identified as such in early architectonic studies (Clark, 1924; von Bonin and Bailey, 1961). These and a number of subsequent investigators (see Lund et al., 1985), were impressed with the very distinct layer 4 of granule cells, which is divided by a narrow, cell poor cleft into inner and outer halves (Figs. 1 and 2), now identified as sublayers 4a and 4b (Lund et al., 1985). Both Clark (1924), and von Bonin and Bailey (1961) considered the possibility that the 4a and 4b divisions of layer 4 in tree shrews are homologous to the outer and

inner sublayers of layer 4 of primates (sublayers 4Cα and 4Cβ of Brodmann's (1909) terminology), as they considered tree shrews to be primates. We now know that 4a and 4b in tree shrews do not correspond to 4Cα and 4Cβ sublayers of primates, and they represent different evolutionary specializations of layer 4. In primates, layer 4Cα receives inputs from the magnocellular layers of the lateral geniculate nucleus, while layer 4Cβ receives inputs from the parvocellular layers (Casagrande and Kaas, 1994). In tree shrews, sublayers 4a and 4b each receive inputs from a mixture of lateral geniculate layers (Conley et al., 1984), and neurons in sublayer 4a are distinguished by responding to the onset of light, while neurons in 4b responded to the offset of light (Norton et al., 1985; Kretz et al., 1986). Sublayers of layer 4 are also apparent in CO preparations, with the middle portion of layer 4 expressing less CO (Fig. 26; also see Lund et al., 1985). In our preparations, layer 4 of tree shrews is also characterized by dense expressions of PV and VGluT2, reflecting dense inputs from the lateral geniculate nucleus of the sensory thalamus (Diamond et al., 1970; Hasting et al., 1973). The very poor zinc staining of layer 4 indicates that this layer is dominated by thalamic rather than cortical inputs. Additionally, layer 4 of tree shrews, as well as cats and monkeys, expresses very little of the antigen for the Cat-301 antibody (Jain et al., 1994).

Layer 3 of tree shrews also has sublayers, with a cell sparse inner subdivision of layer 3, which is most obvious in Nissl preparations (Fig. 28A). Clark (1924) speculated that this inner portion of layer 3 might correspond to a fiber dense band, the stria of Gennari, and our brain sections stained for myelin clearly indicate that the outer band of Baillarger, or the stria of Gennari, is in the inner portion of layer 3 that is sublayer 3c (also see Rockland et al., 1982). This result is in conflict with most current interpretations

of layers 3 and 4 in primates, which place the stria of Gennari in sublayer 4B of Brodmann (1909). Thus, the present results add to previous evidence that the laminar pattern of area 17 of monkeys has been misinterpreted, and that Brodmann's layer 4B of monkeys corresponds to layer 3C of tree shrews, galagos, and other mammals (see Casagrande and Kaas, 1994 for review). Note that sublayer 3b of tree shrews and cats expresses more of the antigen for Cat 301 than adjoining layers, as does the sublayer typically defined as layer 4B of macaques (Jain et al., 1994).

In addition to sublayer 3c, sublayers 3a and 3b have been distinguished in Nissl material from area 17 of tree shrews (e.g. Lund et al., 1985; Jain et al., 1994; Wong-Riley and Norton, 1988). Layer 3b is somewhat more densely packed with cells than sublayers 3c and 3a. In the present study, we also found that sublayer 3b is distinguished from sublayers 3a and 3c by a patchy pattern of zinc poor regions and a dense expression of VGluT2 (Fig. 28). Both of these features suggest the existence of more inputs from the thalamus in layer 3b than in adjoining sublayers, and likely some input from the lateral geniculate nucleus, and such inputs from the lateral geniculate nucleus to layer 3b have been demonstrated (Hubel, 1975; Conley et al., 1984; Usrey et al., 1992). Our material also indicates that sublayer 3a expresses less PV and much more CB than sublayer 3b (Fig. 28). Finally, we were able to divide layer 5 into two distinct sublayers, 5a as a band of SMI-32 immunoreactive pyramidal cells and 5b with a dense expression of synaptic zinc (Fig. 28). As sublayer 3a also has considerable synaptic zinc, sublayers 3a and 5b are likely dominated by cortical inputs, perhaps those intrinsic to area 17.

We also observed architectonic features of area 17 in brain sections cut parallel to the artificially flattened cortex. In layer 3, an uneven distribution of myelin-light patches

was surrounded by myelin-dark regions (Fig. 29), as previously reported by Lyon et al., (1998). In addition, synaptic zinc and VGluT2 were distributed in a patchy formation that was also apparent in layer 3b of transverse brain sections (Fig. 28). This modular pattern within area 17 of tree shrews is reminiscent of the CO-dark blobs of area 17 of primates, although tree shrews do not have CO blobs (e.g., Wong-Riley and Norton, 1988). However, the patchy pattern may reflect a pattern of VGluT2-rich terminals of the lateral geniculate nucleus inputs that are surrounded by walls of zinc-enriched terminals of intrinsic connections (Rockland et al., 1982; Sesma et al., 1984; Bosking et al., 1997). The CO blobs of primates receive inputs from the koniocellular layers of the lateral geniculate nucleus (see Casagrande and Kaas, 1994).

Area 18 of the present study corresponds to the area 18 that was shown to be coextensive with the second visual area, V2 by Kaas et al., (1972), a visual area common to nearly all mammals (Rosa and Krubitzer, 1999). In Nissl preparations, area 18 of tree shrews has less dense cell packing in layers 4 and 6 than in area 17 and in areas along the lateral border of area 18, such that the overall laminar pattern of area 18 is less distinct. Surprisingly, area 18 was not recognized by Clark (1924), who divided cortex lateral to area 17 into a large parietal area, of which includes several of our subdivisions of cortex. Likewise, von Bonin (1961) did not subdivide cortex lateral to V1. More recently, Zilles et al. (1978) defined an area Oc2 as equivalent to area 18 and V2 in tree shrews. Oc2 of Zilles et al. (1978) closely corresponds to area 18 of the present study. Here, we show that area 18 expresses less PV and VGluT2 in axonal terminations, and more synaptic zinc in layer 4 and 6 than area 17. These observations are consistent with the evidence that area 18 receives more cortical inputs, including dense, topographically organized

inputs from area 17 (Sesma et al., 1984; Lyon et al., 1998). The distributions of myelinated fibers in area 18 does not form distinct outer and inner bands of Baillarger, as in area 17, and in surface view preparations, area 18 appears to have an alternating pattern of myelin-light and myelin-dense bands or ovals. Cusick et al. (1985) found that the myelin-dense ovals corresponded to locations with dense clusters of callosally projecting neurons and callosal terminations. Thus, there is evidence for a modular organization in area 18 of tree shrews. Squirrels also have a similar pattern of myelin-dense and myelin-light modules in area 18 (Kaas et al., 1989), and monkeys have a modular pattern of myelin-dense and myelin-light bands in area 18 (e.g. Tootell et al., 1983; Krubitzer and Kaas, 1989). Area 18 of tree shrews is also distinguished by a greater expression of the antigen for Cat-301 in layer 3 than in adjoining cortex (Jain et al., 1994), and lower levels of CO in layer 4 than area 17 (Jain et al., 1994; present study). Thus, area 18 of tree shrews can be identified in a number of preparations.

Temporal visual cortex

In the present study, we have retained the three divisions of temporal cortex along the outer border of V2 that were described as differing in V1 projections by Sesma et al (1984). In brief, a temporal dorsal area (TD) receives dense projections from V1, a more posterior region, the temporal posterior area (TP) receives a second pattern of dense projections from V1, while a more anterior region, the temporal anterior area (TA) receives only sparse inputs from V1. All three areas have connections with V2, and with each other, but only sparse connections with more ventral portions of the temporal lobe (Lyon et al., 1998). Other visual inputs come from the visual pulvinar (Lyon et al., 2003).

Area TA and TD project to the forelimb portion of primary motor cortex (Remple et al., 2007), and thus can be considered visuomotor in function. Neurons in the region of TD were found to be responsive to visual stimuli, although the receptive fields were large and difficult to delineate (Kaufman and Somjen, 1979). Lesions of temporal cortex including much of TP, TD and ITc regions produce impairments in visual learning (Killackey et al., 1971).

The architectonic borders of TA, TP and TD are subtle. Previous studies have shown that TD is more densely myelinated than TA and TP (Sesma et al., 1984; Lyon et al., 1998), and that TA and TD express higher levels of the antigen for the Cat-301 antibody than TP (Jain et al., 1994). Higher levels of Cat-301 staining have been associated with structures having larger neurons with thicker, more rapidly conducting axons (e.g. Hockfield et al., 1983; Hendry et al., 1984)), while sensory areas are typically more densely myelinated than other fields (e.g. Hopf, 1964). Our present results also show that TD is more densely myelinated than TA and TP. In addition, TD has a more developed, thicker layer 4 than TA and TP, as well as more VGluT2 and PV immunopositive terminations, indicating the presence of thalamic inputs, and more synaptic zinc, indicating the presence of cortical terminations. The relative position of TD across from central V2 and V1, the dense inputs from both of these areas, together with pulvinar inputs and dense myelination, have lead to the hypothesis that TD is a homologue of primate area MT (Sesma et al., 1984; Kaas and Preuss, 1993; Jain et al., 1994; Northcutt and Kaas, 1995). If so, MT may have originated as a visual area adjacent to V2 (area 18), with the DL-V4 complex emerging later in evolution.

Inferior temporal cortex

We have included in the inferior temporal region of tree shrew cortex, area ITc, ITi, and ITr, located in a caudodorsal to rostroventral sequence. We also include the temporal inferior area, TI, of Lyon et al. (1998) because of its position, and because TI, together with other divisions of inferior temporal cortex, receives inputs from a posterior division of the visual pulvinar, PP (Lyon et al., 2003). While visual functions of inferior temporal cortex have not been physiologically demonstrated, connections with the visual pulvinar, and at least a few connections with cortical visual areas (Lyon et al., 1998), suggest that the inferior temporal areas of tree shrews are higher-order visual or multisensory areas, as they are in other mammals (Wong et al., 2008). Large lesions that include the IT region are followed by impairments in visual behavior (Killackey et al., 1971).

TI was previously described as being more myelinated than surrounding cortex (Lyon et al., 1998). We found that TI expresses lower levels of zinc and higher levels of CO than surrounding cortex, perhaps as a result of inputs from the pulvinar (Lyon et al., 2003). Of the three other inferior temporal areas, ITi has the most features of a sensory area with thalamic input, including a well developed layer 4, higher myelination, low levels of synaptic zinc, more CO expression, and more PV and VGluT2 immunopositive terminations. ITi (TPI of Lyon et al., 1998) has more visual input from the TD-TP region of Lyon et al. (1998), as well as from two nuclei of the visual pulvinar with superior colliculus inputs (Lyon et al., 2003). Thus, ITi is likely to have visual functions. In contrast, ITr and ITc do not have architectonic features of a core sensory area, but rather the appearance of an association or higher-order processing area. Thus, ITr and ITc have

low myelination, a high expression of synaptic zinc, and low levels of PV and VGluT2 staining. ITr may be involved in auditory functions, as ITr is in the region identified as non-primary auditory cortex by Oliver and Hall (1978) based on connections with the dorsal division of the medial geniculate complex and the suprageniculate, as well as the visual pulvinar. There also appears to be some connections with motor cortex (Remple et al., 2007). Overall, the relative position, architectonic features, and cortical and subcortical connections of ITr of tree shrews are reminiscent of the temporal intermediate area of squirrels (Wong and Kaas, 2008; Wong et al., 2008). By position next to higher-order visual areas TP and TD, ITc is likely to have visual functions.

Auditory cortex

The auditory cortex of tree shrews contains at least one core sensory area and a surrounding belt region (Oliver and Hall, 1975; Casseday et al., 1976; Oliver and Hall, 1978). The core region (Ac) can be identified by being the target of topographically organized projections from the ventral subdivision of the medial geniculate nucleus, in addition to diffuse projections from the posterior nucleus and the medial (magnocellular) subdivision of the medial geniculate nucleus (Oliver and Hall, 1975; Casseday et al., 1976; Oliver and Hall, 1978). The surrounding auditory belt region (Ab) receives inputs from the other subdivisions of the medial geniculate nucleus, such as the medial (magnocellular) and dorsal subdivision (Casseday et al., 1976; Oliver and Hall, 1975; Oliver and Hall, 1978) and the posterior nucleus (Diamond et al., 1970; Harting et al., 1973), and is differentiated from the core by the lack of inputs from the ventral subdivision of the medial geniculate (Oliver and Hall, 1975; Casseday et al., 1976; Oliver

and Hall, 1978). Both Ac and Ab have a koniocellular appearance, such as a darkly stained granular layer 4 in Nissl preparations and dense myelination (Diamond et al., 1970; Oliver and Hall, 1975; Casseday et al., 1976; Oliver and Hall, 1978), and can be differentiated cytoarchitectonically by the thinner layer 4 and a less densely packed layer 3 in Ab (Oliver and Hall, 1978). These findings are congruent with our present results. Both Ac and Ab are poorly populated by zinc-enriched terminals. In addition, layer 4 of Ac stains more intensely than layer 4 of Ab in VGluT2 and PV preparations, as expected of primary sensory cortex.

Parietal cortex

Tree shrews have as many as eight parietal cortical areas; the primary somatosensory area 3b or S1, the secondary somatosensory area (S2) and parietal ventral area (Pv), the transitional area 3a, the somatosensory caudal area (SC), and the posterior parietal dorsal (PPd), posterior parietal rostral (PPr), and posterior parietal caudal (PPc) areas. Of these eight areas, area 3b(S1) is the largest and has a topographic representation of the contralateral body surface (Lende, 1970; Sur et al., 1980; 1981). The somatotopic organization of the contralateral body surface begins with the head representation laterally, proceeding to the hand, arm, rostral trunk, and over the medial wall to the tail, caudal trunk and foot in a lateromedial progression (Lende, 1970; Sur et al., 1980; 1981). This topographic pattern is similar to the primary somatosensory areas of other mammals (see Kaas, 1983 for review). As expected of primary sensory areas, area 3b(S1) has a koniocellular appearance with a layer 4 that is densely packed with granule cells, expresses low levels of free zinc ions, and is densely packed with VGluT2 and PV

immunopositive thalamocortical terminals. This suggests that layer 4 receives proportionately more inputs from the thalamus than from other cortical areas. As with primary somatosensory cortex of other mammals, area 3b(S1) in tree shrews receives input from the ventroposterior nucleus (Diamond et al., 1970; Garraghty et al., 1991). As has been reported in other studies, the architectonic features of area 3b(S1) are not uniform throughout (Sur et al., 1980; 1981; Cusick et al., 1985). In particular, the lateral part of area 3b(S1), where the face representation is located, has a thicker layer 4 (Sur et al., 1980). The non-uniform staining of 3b(S1) is also observed in sections stained for free zinc ions, VGluT2 and myelin. In favorable sections, the myelinated bands of Baillarger are discontinuous, which may be related to the discontinuities in the cortical representations of body parts, including the septa that invaginate 3b(S1), where the neurons have high response thresholds (Sur et al., 1980; Cusick et al., 1985).

Area 3b(S1) is bordered rostrally by area 3a, a narrow band of cortex where neurons are activated by taps to the body and non-cutaneous stimuli (Sur et al., 1980; Kaas, 1983). Area 3a receives topographically organized projections from area 3b(S1) and primary motor cortex (M1) (Remple et al., 2007). Area 3a is distinguished from area 3b(S1) by a reduction in thickness of layer 4, larger pyramidal cells in layer 5, reduction in myelination, increased expression levels of free zinc ions and reduction in VGluT2 and PV staining. From the relative position and architectonic characteristics, area 3a in tree shrews is likely to be homologous to the intermediate sensorimotor area of Sanides and Krishnamurti (1967), postcentralis 2 region of Zilles (1978), and area 3a of rodents such as grey squirrels (Gould et al., 1989; Wong and Kaas, 2008), and primates (Sur et al., 1980; see Slutsky et al., 2000 and Krubitzer et al., 2004 for review).

The cortical area caudal to area 3b(S1), the caudal somatosensory area SC, was previously identified as the posterior somatic field (Sur et al., 1980). SC is characterized by a moderately populated layer 4, larger pyramidal cells in layer 5 in comparison to 3b(S1), and a reduced myelination level with no distinct bands of Baillarger. In layer 4, SC has higher expression levels of free zinc ions and lower expression of VGluT2 and PV immunopositive thalamocortical terminations compared to 3b(S1), suggesting an increase in proportion of corticocortical over thalamocortical inputs. Area SC is responsive to more intense somatic stimuli (Sur et al., 1980) and has a rudimentary somatotopic map of the contralateral body (Remple et al., 2006; 2007). SC has dense, topographic connections with other somatosensory areas, such as 3a, 3b(S1), S2 and PV, and projections to motor cortex (Remple et al., 2007), as does the parietal medial area of squirrels (Krubitzer et al., 1986; Slutsky et al., 2000; Wong and Kaas, 2008) and rats (Donoghue and Parham, 1983; Reep et al., 1990; 1994; Wang and Kurata, 1998). It is also probable that SC of tree shrews is related to area 1/2 of galagos (Wu and Kaas, 2003), and area 1 of New World monkeys (Remple et al., 2007).

Areas S2 and Pv lie caudal and ventral to area 3b(S1). This region of cortex was previously considered to be a single, larger area that extends down into the rhinal fissure (Lende et al. 1970). Remple et al. (2006) established that S2 and Pv correspond to two separate, mirror image representations of the contralateral body surface, as with other mammals. Pv was also distinguished from S2 by a thinner and more densely packed layer 5 in Nissl preparations. In the histochemical and immunohistochemical stains used here, S2 and Pv have similar architectonic characteristics, and as such, we did not define an architectonic border between the two areas. S2 and Pv are distinguished by the presence

of a well-developed layer 4 that is thinner than that of 3b(S1) and higher levels of myelination than the dorsally adjoining SC. Layer 4 of S2 and PV expresses higher levels of free zinc ions, and lower levels of VGluT2 and PV immunopositive terminations. This suggests an increased proportion of corticocortical inputs over thalamocortical inputs, presumably due to the dense, somatopically organized inputs from 3b(S1) (Sur et al., 1981; Weller et al., 1987). The somatotopic organizations of S2 and Pv in tree shrews are similar to those in squirrels (Nelson et al., 1979; Krubitzer et al., 1986) and rats (Walker and Sinha, 1972; Remple et al. 2003). Additionally, the architectonic characteristics of S2 and Pv in tree shrews are similar to those of grey squirrels (Krubitzer et al., 1986; Wong and Kaas, 2008).

The posterior parietal cortex of tree shrews is subdivided into three cortical areas, the posterior parietal rostral area (PPr), equivalent to the posterior parietal ventral area of Remple et al (2007), the posterior parietal caudal area (PPc), and the posterior parietal dorsal (PPd) area. PPc has the architectonic characteristics of an association cortex, with a thin layer 4 populated by small granule cells, lower myelination levels compared to the surrounding cortical areas and lower expression of CO. In zinc preparations, layer 4 of PPc expresses higher levels of free zinc ions compared to TI, and in VGluT2 and PV preparations, layer 4 of PPc expresses low levels of VGluT2 and PV immunopositive terminations. This suggests a dominance of corticocortical inputs into layer 4 of PPc. PPc is likely to have a role in visuomotor processing, as it is interconnected with visual areas including area 18, TD, TP and TA (Lyon et al., 1998), and projects to the secondary motor area (M2) (Remple et al., 2007). The visual and premotor connections of PPc in

tree shrews are similar to that of posterior parietal cortex in primates, suggesting some homology between the two regions.

The architectonic differences between PPr and PPd were not distinct, and an architectonic border between these two cortical fields was not reliably delimited. PPr and PPd are likely to be involved in the integration of visual and somatosensory information as they receive projections from visual areas, including area 18 and TA, and somatosensory areas, such as 3b(S1), S2, and Pv (Remple et al., 2007). This is reflected in the architectonic appearance of PPr and PPd as they show the characteristics of higher-order, association areas, such as the absence of a well-developed granular layer 4 and lower myelination levels. Additionally, layer 4 of PPr and PPd is densely populated with zinc-enriched terminals, and sparsely populated with VGluT2 and PV immunopositive thalamocortical terminals, which suggests the presence of a larger proportion of corticocortical inputs. PPr and PPd can be teased apart by their connection patterns, as PPr projects topographically to the primary motor area (M1) (Remple et al., 2007).

Frontal cortex

In frontal cortex of tree shrews, we have identified a primary motor cortex, M1, that has the general architectonic features of motor cortices, such as a poorly developed layer 4, a layer 5 that is populated with large SMI-32 immunopositive pyramidal cells, and poor myelination. This architectonically defined field corresponds to the electrophysiologically defined primary motor cortex that has a topographic arrangement of contralateral body movements (Remple et el., 2006). Layer 4 of M1 stains darkly in zinc preparations and poorly for VGluT2 and PV immunopositive terminations, similar to

the agranular motor cortex in grey squirrels (Wong and Kaas et al., 2008). This suggests that larger proportion of inputs into layer 4 of M1 originates from other cortical areas rather than from thalamic nuclei. Anatomical tracing studies have shown that M1 has dense connections with M2, which is rostral to M1, and receives inputs somatosensory areas such as 3b(S1), the posterior parietal cortex, and temporal visual areas such as TA and TD (Remple et al., 2007). Neurons in M2 have a higher current threshold than those in M1 (Remple et al., 2006). Architectonically, M2 is differentiated from M1 by a less densely packed layer 5 with smaller-sized SMI-32 immunopositive pyramidal cells in layer 5. The general connectivity pattern of M2 is similar to M1. Differences include denser projections from PPc and ITr (TIV) to M2 than to M1 (Remple et al., 2007).

The combined extent of both M1 and M2 is comparable to the praecentralis 1 region that was distinguished in tree shrew by Zilles (1978). M1 of tree shrews has similar neuron response properties, organization and architectonic characteristics of primary motor cortex of other mammals, such as the lateral agranular cortex of rats (Donoghue and Wise, 1982; Neafsey et al., 1986; Wise and Donoghue, 1986; Brecht et al., 2004). The organizations, architectures and locations of M1 and M2 in tree shrews bear some similarity to the motor and premotor areas in prosimians and primates (Wise, 1985; Matelli et al., 1986; Barbas and Pandya, 1987; Stepniewska et al., 1993; Wu et al., 2000; Fang et al., 2005). As such, it has been proposed that M2 of tree shrews may be homologous to the premotor cortex of primates (Remple et al., 2006).

We have divided the frontal pole of tree shrews into two main architectonically distinct cortical regions, the dorsal frontal cortex (DFC) and the orbital frontal cortex (OFC), much like the division of the frontal pole in rats and rabbits into the medial and

lateral frontal polar areas (Ray and Price, 1992; Uylings et al., 2003; Gabbott et al., 2005; Leal-Campanario et al., 2007). However, the frontal areas of tree shrews have a distinct granular layer, and as such, have a closer resemblance to the frontal polar region of squirrels (Wong and Kaas, 2008), and the prefrontal cortex of galagos (Preuss and Goldman-Rakic, 1989; 1991) and other primates (Preuss et al., 1997), than the agranular prefrontal cortex of rats (Öngür and Price, 2000). In addition, layer 4 of OFC, and to a lesser extent of DFC, has a lower expression of zinc-enriched corticocortical terminations and a higher expression of VGluT2 and PV immunopositive thalamocortical terminations, which suggests the present of a dominant population of thalamocortical inputs into the area. In galagos, the lateral frontal lobe and orbital prefrontal cortex receives inputs from the mediodorsal nucleus of the thalamus, and the posterolateral cortex receives inputs from the ventral thalamic complex (Markowitsch et al., 1980). However, the frontal polar region of tree shrews is not as complex as that of galagos (Preuss and Goldman-Rakic, 1989; 1991) and other primates (Preuss et al, 1997). Both DFC and OFC of tree shrews have a sparse to almost absent population of SMI-32 immunopositive pyramidal cells, whereas layer 3 of granular prefrontal cortex of galagos and macaques is populated by a specialized type of spinous pyramidal cells that have been suggested to play a role in the evolution of intellectual complexity in primates (Elston et al., 2005). The frontal polar region of tree shrews may have a more complex organization complex than the scheme proposed here, and may be subdivided into more cortical areas, as we have not attempted to make fine architectonic distinctions. Studies of cortical connections might be useful in further subdividing the region.

Medial cortex

The medial frontal area (MF) of tree shrews approximately corresponds to area praecentralis 3 of Zilles (1978). MF has a well-developed layer 4 and a sparsely populated layer 5, and bears an architectonic resemblance to the pre-SMA region in galagos (Wu et al., 2000) that has been identified as the granular medial and medial frontal region of galagos by Preuss and Goldman-Rakic (1991) and area F6 of monkeys (Matelli et al., 1991). MF is also in the approximate location of the frontal and rostral cingulate area of grey squirrels, but unlike MF, the rostral cingulate region of grey squirrels does not have a well-developed layer 4 and is poorly myelinated (Wong and Kaas, 2008). MF expresses moderate levels of free zinc ions and has a sparse distribution of VGluT2 and PV immunopositive terminations, indicating that there is a dominance of corticocortical inputs over thalamocortical inputs. Studies of connections would be needed to confirm this deduction.

The medial motor area (MMA) adjoins M1 along the medial wall and was identified as a region that has dense, topographically organized projections to M1 and M2 (Remple et al., 2007). MMA is likely to have representations of the face and forelimb, although there has been little success in eliciting movements from MMA in microstimulation studies (Remple et al., 2006; 2007). Architectonically, MMA shares some characteristics with M1, such as a poorly developed layer 4, a thick layer 5 that is densely populated with pyramidal cells, and similar myelination levels. MMA expresses high levels of zinc-enriched terminals and low levels of VGluT2 and PV immunopositive thalamocortical terminals. This suggests that MMA receives stronger inputs from other cortical areas compared to thalamic nuclei.

Cingulate cortex of tree shrews is subdivided into the dorsal cingulate (CGd), ventral cingulate (CGv), infraradiata dorsal (IRd) and infradiata ventral (IRv) areas. Various nomenclatures have been used for the cingulate cortical areas, depending on investigator and the species studied. For example, in rats, the anterior cingulate dorsal area of Jones et al. (2007) corresponds to area 24 and part of 32 of Kreig (1946), 24b and 24b' of Vogt and Peters (1981) and Cg1 of Zilles and Wree (1995), and is homologous to area 24 of Brodmann (1909) and IRcα and IRbα of Rose (1931) in rabbits (see Jones et al., 2005; Zilles 2004 for review). In this study, we partly use the nomenclature used by Zilles (1978) for tree shrews. CGd and CGv correspond to the anterior cingularis ventralis of Zilles (1978), and IRd and IRv were retained from Zilles (1978).

CGd does not have a well-developed layer 4 and is distinguished from CGv as CGd has a higher cell packing density and a more homogenous appearance. The architectonic appearance of CGv varies along its dorsoventral extent, especially in the Nissl and zinc preparations, suggesting the possibility for further subdivisions. Both CGv and CGd have reduced staining of VGluT2 and PV immunopositive terminations in layer 4, indicating that these areas receive proportionately less thalamocortical input than adjacent cortical areas such as area 3b(S1). Unlike in rats (Zilles, 1990; Jones et al., 2005) and squirrels (Wong and Kaas, 2008), where the cingulate regions occupy the dorsal extent of the rostral medial wall, the frontal cingulate areas in tree shrews are displaced ventrally by the somatosensory areas, 3a, 3b(S1) and SC, much as in primates (e.g. Wu and Kaas, 2003).

IRd shares some architectonic features of the cingulate cortex in rats (Zilles, 1990; Vogt et al., 2004), such as the poorly developed layer 4 and moderate myelination.

In rats, the cingulate cortex receives diffuse projections from the mediodorsal, ventromedial, and anteromedial nuclei of the thalamus (Domesick, 1969), and has extensive connections with various cortical areas, including the visual and motor cortex (Vogt and Miller, 1983). In tree shrews, IRd expresses high levels of zinc-enriched terminals and low levels of VGluT2 and PV immunopositive terminals, indicating that inputs into IRd originate predominantly in other cortical areas.

IRv is in the approximate location of the medial somatosensory area (MSA) of Remple et al. (2007). Neurons in MSA have larger receptive fields than neurons in 3b(S1) and MSA sends dense projections to both M1 and M2 (Remple et al., 2007). Architectonically, IRv has a thin layer 4 and is less heavily myelinated than IRd, with a thin, distinct outer band of Baillarger. IRv expresses high levels of zinc-enriched terminals, and moderate levels of VGluT2 and PV immunopositive terminals, indicating that inputs into IRv originate from the thalamus, as well as other cortical areas.

Area prostriata (PS) is a limbic area that was identified in primates by Sanides (1970) and is visual in function, representing the peripheral vision of the contralateral visual hemifield. This area has been identified in cats as the splenial visual area (see Rosa, 1999 for review), and is comparable to the posteromedial visual area in rats and mice (Wang and Burkhalter, 2007), medial area 18b (Krieg, 1946; Caviness, 1975), and Oc2MM (Zilles and Wree, 1995). In tree shrews, PS has a poorly developed layer 4, does not have a well-defined laminar pattern, and is poorly myelinated, similar to the prostriata of primates (Allman and Kaas, 1971) and grey squirrels (Wong and Kaas, 2008). Area PS is likely to have a larger proportion of corticocortical, rather than thalamocortical, inputs,

as it expressed high levels of free zinc ions and a near absence of VGluT2 and PV immunopositive terminations.

The retrosplenial cortex has been subdivided in to granular (RSg) and agranular areas (RSag) in a previous study by Zilles (1978). Both RSg and RSag do not have well-defined laminar patterns. RSg is characterized by a densely populated layer 2/3 and is moderately myelinated, whereas RSag has a low cell packing density and is lightly myelinated. Layer 2/3 of RSag expresses higher levels of zinc-enriched corticocortical terminations and lower levels of VGluT2 and PV immunopositive thalamocortical terminations compared to RSg. This suggests that a higher proportion of the inputs into layer 2/3 of RSag originate from other cortical areas, whereas a high proportion of inputs into layer 2/3 of RSg originate from nuclei in the thalamus.

Remaining cortical areas

The insular cortex (Ins) defined here is distinctly laminated and has a well-developed granular layer 4. The low expression of zinc-enriched corticortical terminations in layer 4 of Ins suggests that this layer has few corticortical inputs. Layer 4 of Ins expresses high levels of VGluT2 and PV immunopositive terminations, indicating the presence of dense inputs from the thalamus. In primates, the granular posterior portion of the insular has a dense population of thalamocortical terminations (Jones and Burton, 1976). Anatomical tract tracing studies in primates have shown that Ins has dense connections with the auditory cortex, temporal cortex, and the parvocellular subdivision of the medial geniculate nucleus (Augustine, 1985; Mesulam and Mufson, 1985). In addition, electrophysiological studies have shown the presence of auditory responsive

units in the insular (Sudakov et al., 1971). Ins of tree shrews approximately corresponds in location to the parietal insular cortex of rats (Shi and Cassell, 1998), as both regions lie ventral to 3b(S1) and S2. In rats, the granular zone of insular cortex is involved in viscerosensory modalities (Kosar et al., 1986; Cechetto and Saper, 1986; Sewards and Sewards, 2001). Similar to the posterior insular cortex in primates, part of the granular insular zone of rats receives strong inputs from S2 (Shi and Cassell, 1997), as well as from 3b(S1) and the posterior thalamic nucleus (Shi and Cassell, 1998). Much of this somatosensory zone of granular insular cortex is in the region of somatosensory area Pv as defined by Remple et al. (2003) in rats, and this would correspond to the Pv area of tree shrews rather than the insular cortex.

Perirhinal area (PRh) is retained from Zilles and Wree (1985), and corresponds to areas 35 and 36 of Brodmann (1909), the posterior region of area 35 of Krieg (1946), and the ectorhinal and perirhinal areas of Swanson (2003). As with other mammals, such as grey squirrels (Wong and Kaas, 2008), and rats (Burwell, 2001; Palomero-Gallagher and Zilles, 2004), PRh is poorly myelinated and has a poorly defined lamination pattern. The dark staining in zinc preparations suggests that a large proportion of inputs to PRh is from other areas of cortex. PRh has been suggested to have a role in memory processes, as it has connections with the hippocampal formation (Burwell and Amaral, 1998; Palomero-Gallagher and Zilles, 2004; Furtak et al., 2007). In addition, PRh in rats has connections with the anterior thalamic nuclei (Palomero-Gallagher and Zilles, 2004), and the piriform, frontal, temporal and insular cortical areas (Furtak et al., 2007).

Table 1: Abbreviations

3b(S1)	Primary somatosensory area
Ab	Auditory belt area
Ac	Auditory core area
CB	Calbindin
cc	Corpus callosum
CGd	Cingulate dorsal area
CGv	Cingulate ventral area
Cl	Claustral cortex
CO	Cytochrome oxidase
DFC	Dorsal frontal cortex
Ect	Ectorhinal cortex
Ent	Entorhinal cortex
EntI	Entorhinal intermediate area
EntL	Entorhinal lateral area
EntM	Entorhinal medial area
Hippo	Hippocampal cortex
HS	Hippocampus supracommissuralis
Ins	Insular cortex
IRd	Infraradiata dorsalis
IRv	Infraradiata ventral area
ITc	Inferior temporal caudal area
ITi	Inferior temporal intermediate area
ITr	Inferior temporal rostral area
M1	Primary motor area
M2	Secondary motor area
MF	Medial frontal cortex
MMA	Medial motor area
MT	Middle temporal visual area
OB	Olfactory bulb
OFC	Orbital frontal cortex
PB	Phosphate buffer
PBS	Phosphate buffer with saline
Pirf	Piriform cortex
PPc	Posterior parietal caudal area
PPd	Posterior parietal dorsal area
PPr	Posterior parietal rostral area
PRh	Perirhinal area
PS	Prostriata
PV	Parvalbumin
Pv	Parietal ventral area
Rsag	Retrosplenial agranular area
RSg	Retrosplenial granular area
S2	Secondary somatosensory area

SC	Somatosensory caudal area
Sub	Subiculum
TA	Temporal anterior area
TD	Temporal dorsal area
TI	Temporal inferior area
TIV	Temporal inferior ventral area
TP	Temporal posterior area
TPI	Temporal posterior inferior area
V1	Primary visual area
V2	Secondary visual area
VGluT2	Vesicle Glutamate Transporter 2

References

Abplanalp P. 1970. Some subcortical connections of the visual system in tree shrews and squirrels. Brain Behav Evol 3(1):155-168.

Allman JM and Kaas JH. 1971. Representation of the visual field in striate and adjoining cortex of the owl monkey (Aotus trivirgatus). Brain Res 35(1):89-106.

Augustine JR. 1985. The insular lobe in primates including humans. Neurol Res 7(1):2-10.

Barbas H and Pandya DN. 1987. Architecture and frontal cortical connections of the premotor cortex (area 6) in the rhesus monkey. J Comp Neurol 256(2):211-228.

Bishop A. 1964. Use of the hand in lower primates. In Evolutionary and genetic biology of primates. J. Buettner-Janusch, eds. New York: Academic Press. 133-225.

Bonin GV. 1960. The isocortex. In Primatologia, G. Hofer, A.H. Schultz, and D. Starck, eds. Basel and New York: Karger.

Bosking WH, Zhang Y, Schofield B and Fitzpatrick D. 1997. Orientation selectivity and the arrangement of horizontal connections in tree shrew striate cortex. J Neurosci 17(6):2112-127.

Brecht M, Krauss A, Muhammad S, Sinai-Esfahani L, Bellanca S and Margrie TW. 2004. Organization of rat vibrissa motor cortex and adjacent areas according to cytoarchitectonics, microstimulation, and intracellular stimulation of identified cells. J Comp Neurol 479(4):360-373.

Brodmann K. 1909. Brodmann's 'Localisation in the Cerebral Cortex'. L.J. Garey, eds. London: Eldred Smith-Gordon.

Burwell RD and Amaral DG. 1998. Cortical afferents of the perirhinal, postrhinal, and entorhinal cortices of the rat. J Comp Neurol 398(2):179-205.

Burwell RD. 2001. Borders and cytoarchitecture of the perirhinal and postrhinal cortices in the rat. J Comp Neurol 437(1):17-41.

Campbell MJ and Morrison JH. 1989. Monoclonal antibody to neurofilament protein (SMI-32) labels a subpopulation of pyramidal neurons in the human and monkey neocortex. J Comp Neurol 282(2):191-205.

Casseday HJ, Diamond IT and Harting JK. 1976. Auditory pathways to the cortex in Tupaia glis. J Comp Neurol 166(3):303-340.

Caviness VSJ. 1975. Architectonic map of neocortex of the normal mouse. J Comp Neurol 164(2):247-263.

Cechetto DF and Saper CB. 1987. Evidence for a viscerotopic sensory representation in the cortex and thalamus in the rat. J Comp Neurol 262(1):27-45.

Celio MR. 1986. Parvalbumin in most gamma-aminobutyric acid-containing neurons of the rat cerebral cortex. Science 231(4741):995-97.

Chapin JK and Lin CS. 1984. Mapping the body representation in the SI cortex of anesthetized and awake rats. J Comp Neurol 229(2):199-213.

Conde F, Lund JS and Lewis DA. 1996. The hierarchical development of monkey visual cortical regions as revealed by the maturation of parvalbumin-immunoreactive neurons. Brain Res Dev Brain Res 96(1-2):261-276.

Conley M, Fitzpatrick D and Diamond IT. 1984. The laminar organization of the lateral geniculate body and the striate cortex in the tree shrew (Tupaia glis). J Neurosci 4(1):171-197.

Cruikshank SJ, Killackey HP and Metherate R. 2001. Parvalbumin and calbindin are differentially distributed within primary and secondary subregions of the mouse auditory forebrain. Neuroscience 105(3):553-569.

Cusick CG and Kaas JH. 1988. Cortical connections of area 18 and dorsolateral visual cortex in squirrel monkeys. Vis Neurosci 1(2):211-237.

Cusick CG, MacAvoy MG and Kaas JH. 1985. Interhemispheric connections of cortical sensory areas in tree shrews. J Comp Neurol 235(1):111-128.

Danscher G and Stoltenberg M. 2005. Zinc-specific autometallographic in vivo selenium methods: tracing of zinc-enriched (ZEN) terminals, ZEN pathways, and pools of zinc ions in a multitude of other ZEN cells. J Histochem Cytochem 53(2):141-153.

Danscher G. 1981. Histochemical demonstration of heavy metals. A revised version of the sulphide silver method suitable for both light and electronmicroscopy. Histochemistry 71(1):1-16.

DeFelipe J and Jones EG. 1991. Parvalbumin immunoreactivity reveals layer IV of monkey cerebral cortex as a mosaic of microzones of thalamic afferent terminations. Brain Res 562(1):39-47.

DeFelipe J. 1997. Types of neurons, synaptic connections and chemical characteristics of cells immunoreactive for calbindin-D28K, parvalbumin and calretinin in the neocortex. J Chem Neuroanat 14(1):1-19.

Diamond IT, Snyder M, Killackey H, Jane J and Hall WC. 1970. Thalamo-cortical projections in the tree shrew (Tupaia glis). J Comp Neurol 139(3):273-306.

Domesick VB. 1969. Projections from the cingulate cortex in the rat. Brain Res 12(2):296-320.

Donoghue JP and Parham C. 1983. Afferent connections of the lateral agranular field of the rat motor cortex. J Comp Neurol 217(4):390-404.

Elston GN, Elston A, Casagrande V and Kaas JH. 2005. Areal specialization of pyramidal cell structure in the visual cortex of the tree shrew: a new twist revealed in the evolution of cortical circuitry. Exp Brain Res 163(1):13-20.

Emmons LH. 2000. Tupai: A field study of Bornean tree shrews . Berkeley, CA: Univ. of California Press.

Fang PC, Stepniewska I and Kaas JH. 2005. Ipsilateral cortical connections of motor, premotor, frontal eye, and posterior parietal fields in a prosimian primate, Otolemur garnetti. J Comp Neurol 490(3):305-333.

Fujiyama F, Furuta T and Kaneko T. 2001. Immunocytochemical localization of candidates for vesicular glutamate transporters in the rat cerebral cortex. J Comp Neurol 435(3):379-387.

Furtak SC, Wei SM, Agster KL and Burwell RD. 2007. Functional neuroanatomy of the parahippocampal region in the rat: the perirhinal and postrhinal cortices. Hippocampus 17(9):709-722.

Gabbott PL, Warner TA, Jays PR, Salway P and Busby SJ. 2005. Prefrontal cortex in the rat: projections to subcortical autonomic, motor, and limbic centers. J Comp Neurol 492(2):145-177.

Gallyas F. 1979. Silver staining of myelin by means of physical development. Neurol Res 1(2):203-09.

Garraghty PE, Florence SL, Tenhula WN and Kaas JH. 1991. Parallel thalamic activation of the first and second somatosensory areas in prosimian primates and tree shrews. J Comp Neurol 311(2):289-299.

Gould HJ3, Whitworth RHJ and LeDoux MS. 1989. Thalamic and extrathalamic connections of the dysgranular unresponsive zone in the grey squirrel (Sciurus carolinensis). J Comp Neurol 287(1):38-63.

Hackett TA, Stepniewska I and Kaas JH. 1998. Subdivisions of auditory cortex and ipsilateral cortical connections of the parabelt auditory cortex in macaque monkeys. J Comp Neurol 394(4):475-495.

Harting JK, Diamond IT and Hall WC. 1973. Anterograde degeneration study of the cortical projections of the lateral geniculate and pulvinar nuclei in the tree shrew (Tupaia glis). J Comp Neurol 150(4):393-440.

Hendry SH, Hockfield S, Jones EG and McKay R. 1984. Monoclonal antibody that identifies subsets of neurones in the central visual system of monkey and cat. Nature 307(5948):267-69.

Hockfield S, McKay RD, Hendry SH and Jones EG. 1983. A surface antigen that identifies ocular dominance columns in the visual cortex and laminar features of the lateral geniculate nucleus. Cold Spring Harb Symp Quant Biol 48 Pt 2877-889.

Hof A. 1964. In Localisation in the cerebral cortex from the anatomical point of view Madison: The university of Wisconsin Press. 5-16.

Hof PR, Glezer ,I, Conde F, Flagg RA, Rubin MB, Nimchinsky EA and Vogt Weisenhorn DM. 1999. Cellular distribution of the calcium-binding proteins parvalbumin, calbindin, and calretinin in the neocortex of mammals: phylogenetic and developmental patterns. J Chem Neuroanat 16(2):77-116.

Huchon D, Madsen O, Sibbald MJ, Ament K, Stanhope MJ, Catzeflis F, de Jong WW and Douzery EJ. 2002. Rodent phylogeny and a timescale for the evolution of Glires: evidence from an extensive taxon sampling using three nuclear genes. Mol Biol Evol 19(7):1053-065.

Humphrey AL and Norton TT. 1980. Topographic organization of the orientation column system in the striate cortex of the tree shrew (Tupaia glis). I. Microelectrode recording. J Comp Neurol 192(3):531-547.

Ichinohe N and Rockland KS. 2004. Region specific micromodularity in the uppermost layers in primate cerebral cortex. Cereb Cortex 14(11):1173-184.

Jain N, Preuss TM and Kaas JH. 1994. Subdivisions of the visual system labeled with the Cat-301 antibody in tree shrews. Vis Neurosci 11(4):731-741.

Jones BF, Groenewegen HJ and Witter MP. 2005. Intrinsic connections of the cingulate cortex in the rat suggest the existence of multiple functionally segregated networks. Neuroscience 133(1):193-207.

Kaas JH and Catania KC. 2002. How do features of sensory representations develop? Bioessays 24(4):334-343.

Kaas JH and Huerta MF. 1988. Subcortical visual system of primates. Comparative Primate Biology; Neurosciences 4:327-391.

Kaas JH, and Preuss TM. 1993. Archontan affinities as refleted in the visual system. In Mammalian Phylogeny, F. Szalay, M. Novacek, and M. McKenna, eds. New York: Springer Verlag. 115-128.

Kaas JH, Hall WC, Killackey H and Diamond IT. 1972. Visual cortex of the tree shrew (Tupaia glis): architectonic subdivisions and representations of the visual field. Brain Res 42(2):491-96.

Kaas JH, Lin CS and Wagor E. 1977. Cortical projections of posterior parietal cortex in owl monkeys. J Comp Neurol 72(3):387-408.

Kaneko T and Fujiyama F. 2002. Complementary distribution of vesicular glutamate transporters in the central nervous system. Neurosci Res 42(4):243-250.

Kaufman PG and Somjen GG. 1979. Receptive fields of neurons in area 17 and 18 of tree shrew (Tupaia glis). Brain Res Bull 4:319-325.

Killackey H, Snyder M and Diamond IT. 1971. Function of striate and temporal cortex in the tree shrew. J Comp Physiol Psychol 74(1):Suppl 2:1-229.

Kosar E, Grill HJ and Norgren R. 1986. Gustatory cortex in the rat. I. Physiological properties and cytoarchitecture. Brain Res 379(2):329-341.

Krieg WJS. 1946. Connections of the cerebral cortex. I. The albino rat. A. Topography of the cortical areas. J Comp Neurol 84:221-275.

Krubitzer LA and Kaas JH. 1989. Cortical integration of parallel pathways in the visual system of primates. Brain Res 478(1):161-65.

Krubitzer LA, Huffman KJ, Disbrow E and Recanzone G. 2004. Organization of area 3a in macaque monkeys: contributions to the cortical phenotype. J Comp Neurol 471(1):97-111.

Krubitzer LA, Sesma MA and Kaas JH. 1986. Microelectrode maps, myeloarchitecture, and cortical connections of three somatotopically organized representations of the body surface in the parietal cortex of squirrels. J Comp Neurol 250(4):403-430.

Lane RH, Allman JM and Kaas JH. 1971. Representation of the visual field in the superior colliculus of the grey squirrel (Sciurus carolinensis) and the tree shrew (Tupaia glis). Brain Res 26(2):277-292.

Latawiec D, Martin KA and Meskenaite V. 2000. Termination of the geniculocortical projection in the striate cortex of macaque monkey: a quantitative immunoelectron microscopic study. J Comp Neurol 419(3):306-319.

Le Gros Clark WE. 1959. The Antecedents of Man. Edinburgh: Edinburgh University Press.

Le Gros Clark WE. 1924. On the brain of the tree-shrew (Tupaia mior). Proc Acad Soc (Lond) 77:1179-1309.

Leal-Campanario R, Fairen A, Delgado-Garcia JM and Gruart A. 2007. Electrical stimulation of the rostral medial prefrontal cortex in rabbits inhibits the expression of conditioned eyelid responses but not their acquisition. Proc Natl Acad Sci U S A 104(27):11459-464.

Lee VM, Carden MJ, Schlaepfer WW and Trojanowski JQ. 1987. Monoclonal antibodies distinguish several differentially phosphorylated states of the two largest rat neurofilament subunits (NF-H and NF-M) and demonstrate their existence in the normal nervous system of adult rats. J Neurosci 7(11):3474-488.

Lende RA. 1970. Cortical localization in the tree shrew (Tupaia). Brain Res 18(1):61-75.

Liu FG, Miyamoto MM, Freire NP, Ong PQ, Tennant MR, Young TS and Gugel KF. 2001. Molecular and morphological supertrees for eutherian (placental) mammals. Science 291(5509):1786-89.

Lund JS, Fitzpatrick D, and Humphrey AL. 1985. The striate visual cortex of the tree shrew. In Visual cortex, E.G. Jones, and A. Peters, eds. New York: Plenum Press. 157-205.

Lyon DC, Jain N and Kaas JH. 1998. Cortical connections of striate and extrastriate visual areas in tree shrews. J Comp Neurol 401(1):109-128.

Lyon DC, Jain N and Kaas JH. 2003. The visual pulvinar in tree shrews II. Projections of four nuclei to areas of visual cortex. J Comp Neurol 467(4):607-627.

Markowitsch HJ, Pritzel M, Wilson M and Divac I. 1980. The prefrontal cortex of a prosimian (Galago senegalensis) defined as the cortical projection area of the thalamic mediodorsal nucleus. Neuroscience 5(10):1771-79.

Matelli M, Camarda R, Glickstein M and Rizzolatti G. 1986. Afferent and efferent projections of the inferior area 6 in the macaque monkey. J Comp Neurol 251(3):281-298.

Matelli M, Luppino G and Rizzolatti G. 1991. Architecture of superior and mesial area 6 and the adjacent cingulate cortex in the macaque monkey. J Comp Neurol 311(4):445-462.

Mesulam MM, and Mufson EJ. 1985. The insula of Reil in man and monkey. Architectonics, connectivity and function. In Cerebral Cortex, E.G. Jones, and A. Peters, eds. New York: Plenum Press. 179-226.

Murphy WJ, Eizirik E, Johnson WE, Zhang YP, Ryder OA and O'Brien SJ. 2001a. Molecular phylogenetics and the origins of placental mammals. Nature 409(6820):614-18.

Murphy WJ, Eizirik E, O'Brien SJ, Madsen O, Scally M, Douady CJ, Teeling E, Ryder OA, Stanhope MJ, et al.. 2001b. Resolution of the early placental mammal radiation using Bayesian phylogenetics. Science 294(5550):2348-351.

Nahmani M and Erisir A. 2005. VGluT2 immunochemistry identifies thalamocortical terminals in layer 4 of adult and developing visual cortex. J Comp Neurol 484(4):458-473.

Neafsey EJ, Bold EL, Haas G, Hurley-Gius KM, Quirk G, Sievert CF and Terreberry RR. 1986. The organization of the rat motor cortex: a microstimulation mapping study. Brain Res 396(1):77-96.

Nelson RJ, Sur M and Kaas JH. 1979. The organization of the second somatosensory area (SmII) of the grey squirrel. J Comp Neurol 184(3):473-489.

Northcutt RG and Kaas JH. 1995. The emergence and evolution of mammalian neocortex. Trends Neurosci 18(9):373-79.

Norton TT, Rager G and Kretz R. 1985. ON and OFF regions in layer IV of striate cortex. Brain Res 327(1-2):319-323.

Oliver DL and Hall WC. 1978. The medial geniculate body of the tree shrew, Tupaia glis. II. Connections with the neocortex. J Comp Neurol 182(3):459-493.

Oliver DL and Hall WC. 1975. Subdivisions of the medial geniculate body in the tree shrew (Tupaia glis). Brain Res 86(2):217-227.

Ongur D and Price JL. 2000. The organization of networks within the orbital and medial prefrontal cortex of rats, monkeys and humans. Cereb Cortex 10(3):206-219.

Palomero-Gallagher N, and Zilles K. 2004. Isocortex. In The Rat Nervous System. G. Paxinos, eds. London: Elsevier. 729-757.

Preuss TM and Goldman-Rakic PS. 1991. Architectonics of the parietal and temporal association cortex in the strepsirhine primate Galago compared to the anthropoid primate Macaca. J Comp Neurol 310(4):475-506.

Preuss TM and Goldman-Rakic PS. 1989. Connections of the ventral granular frontal cortex of macaques with perisylvian premotor and somatosensory areas: anatomical evidence for somatic representation in primate frontal association cortex. J Comp Neurol 282(2):293-316.

Preuss TM, Stepniewska I, Jain N and Kaas JH. 1997. Multiple divisions of macaque precentral motor cortex identified with neurofilament antibody SMI-32. Brain Res 767(1):148-153.

Ray JP and Price JL. 1992. The organization of the thalamocortical connections of the mediodorsal thalamic nucleus in the rat, related to the ventral forebrain-prefrontal cortex topography. J Comp Neurol 323(2):167-197.

Reep RL, Goodwin GS and Corwin JV. 1990. Topographic organization in the corticocortical connections of medial agranular cortex in rats. J Comp Neurol 294(2):262-280.

Remple MS, Henry EC and Catania KC. 2003. Organization of somatosensory cortex in the laboratory rat (Rattus norvegicus): Evidence for two lateral areas joined at the representation of the teeth. J Comp Neurol 467(1):105-118.

Remple MS, Reed JL, Stepniewska I and Kaas JH. 2006. Organization of frontoparietal cortex in the tree shrew (Tupaia belangeri). I. Architecture, microelectrode maps, and corticospinal connections. J Comp Neurol 497(1):133-154.

Remple MS, Reed JL, Stepniewska I, Lyon DC and Kaas JH. 2007. The organization of frontoparietal cortex in the tree shrew (Tupaia belangeri): II. Connectional evidence for a frontal-posterior parietal network. J Comp Neurol 501(1):121-149.

Rockland KS, Lund JS and Humphrey AL. 1982. Anatomical binding of intrinsic connections in striate cortex of tree shrews (Tupaia glis). J Comp Neurol 209(1):41-58.

Rosa MG and Krubitzer LA. 1999. The evolution of visual cortex: where is V2? Trends Neurosci 22(6):242-48.

Rose M. 1931. Cytoarchitektonischer atlas der grosshinrinde der Maus. J Psychol Neurol 43:353-430.

Sanides F and Krishnamurti A. 1967. Cytoarchitectonic subdivisions of sensorimotor and prefrontal regions and of bordering insular and limbic fields in slow loris (Nycticebus coucang coucang). J Hirnforsch 9(3):225-252.

Sesma MA, Casagrande VA and Kaas JH. 1984. Cortical connections of area 17 in tree shrews. J Comp Neurol 230(3):337-351.

Sewards TV and Sewards MA. 2001. Cortical association areas in the gustatory system. Neurosci Biobehav Rev 25(5):395-407.

Shi CJ and Cassell MD. 1998. Cortical, thalamic, and amygdaloid connections of the anterior and posterior insular cortices. J Comp Neurol 399(4):440-468.

Shi CJ and Cassell MD. 1997. Cortical, thalamic, and amygdaloid projections of rat temporal cortex. J Comp Neurol 382(2):153-175.

Slutsky DA, Manger PR and Krubitzer L. 2000. Multiple somatosensory areas in the anterior parietal cortex of the California ground squirrel (Spermophilus beecheyii). J Comp Neurol 416(4):521-539.

Sorenson M. 1970. Behaviour of tree shrews. Primate Behaviour 1:141-193.

Springer MS, Murphy WJ, Eizirik E and O'Brien SJ. 2003. Placental mammal diversification and the Cretaceous-Tertiary boundary. Proc Natl Acad Sci U S A 100(3):1056-061.

Stepniewska I, Preuss TM and Kaas JH. 1993. Architectonics, somatotopic organization, and ipsilateral cortical connections of the primary motor area (M1) of owl monkeys. J Comp Neurol 330(2):238-271.

Sudakov K, MacLean PD, Reeves A and Marino R. 1971. Unit study of exteroceptive inputs to claustrocortex in awake, sitting, squirrel monkey. Brain Res 28(1):19-34.

Sur M, Weller RE and Kaas JH. 1981a. The organization of somatosensory area II in tree shrews. J Comp Neurol 201(1):121-133.

Sur M, Weller RE and Kaas JH. 1981b. Physiological and anatomical evidence for a discontinuous representation of the trunk in S-I of tree shrews. J Comp Neurol 201(1):135-147.

Sur M, Weller RE and Kaas JH. 1980. Representation of the body surface in somatosensory area I of tree shrews, Tupaia glis. J Comp Neurol 194(1):71-95.

Swanson L. 2003. Brain Maps: Structure of the Rat Brain. Academic Press.

Tootell RB, Silverman MS, De Valois RL and Jacobs GH. 1983. Functional organization of the second cortical visual area in primates. Science 220(4598):737-39.

Usrey WM, Muly EC and Fitzpatrick D. 1992. Lateral geniculate projections to the superficial layers of visual cortex in the tree shrew. J Comp Neurol 319(1):159-171.

Uylings HB, Groenewegen HJ and Kolb B. 2003. Do rats have a prefrontal cortex? Behav Brain Res 146(1-2):3-17.

Valente T, Auladell C and Perez-Clausell J. 2002. Postnatal development of zinc-rich terminal fields in the brain of the rat. Exp Neurol 174(2):215-229.

Van Brederode JF, Mulligan KA and Hendrickson AE. 1990. Calcium-binding proteins as markers for subpopulations of GABAergic neurons in monkey striate cortex. J Comp Neurol 298(1):1-22.

Van Hooser SD and Nelson SB. 2006. The squirrel as a rodent model of the human visual system. Vis Neurosci 23(5):765-778.

de Venecia RK, Smelser CB and McMullen NT. 1998. Parvalbumin is expressed in a reciprocal circuit linking the medial geniculate body and auditory neocortex in the rabbit. J Comp Neurol 400(3):349-362.

Vogt BA and Miller MW. 1983. Cortical connections between rat cingulate cortex and visual, motor, and postsubicular cortices. J Comp Neurol 216(2):192-210.

Vogt BA and Peters A. 1981. Form and distribution of neurons in rat cingulate cortex: areas 32, 24, and 29. J Comp Neurol 195(4):603-625.

Vogt BA, Vogt L, and Farber NB. 2004. Cingulate Cortex and Disease Models. In The Rat Nervous System. G. Paxinos, eds. London: Elsevier. 704-727.

Walker C and Sinha MM. 1972. Somatotopic organization of Smll cerebral neocortex in albino rat. Brain Res 37(1):132-36.

Wang Q and Burkhalter A. 2007. Area map of mouse visual cortex. J Comp Neurol 502(3):339-357.

Wang Y and Kurata K. 1998. Quantitative analyses of thalamic and cortical origins of neurons projecting to the rostral and caudal forelimb motor areas in the cerebral cortex of rats. Brain Res 781(1-2):135-147.

Wassle H, Regus-Leidig H and Haverkamp S. 2006. Expression of the vesicular glutamate transporter vGluT2 in a subset of cones of the mouse retina. J Comp Neurol 496(4):544-555.

Weber JT, Huerta MF, Kaas JH and Harting JK. 1983. The projections of the lateral geniculate nucleus of the squirrel monkey: studies of the interlaminar zones and the S layers. J Comp Neurol 213(2):135-145.

Weller RE, Sur M and Kaas JH. 1987. Callosal and ipsilateral cortical connections of the body surface representations in SI and SII of tree shrews. Somatosens Res 5(2):107-133.

Wise SP. 1985. The primate premotor cortex: past, present, and preparatory. Annu Rev Neurosci 81-19.

Wise SP, and Donoghue JP. 1986. Motor cortex of rodents. New York: Plenum.

Wong P and Kaas JH. 2008. Architectonic subdivisions of neocortex in the gray squirrel (Sciurus carolinensis). Anat Rec (Hoboken) 291(10):1301-333.

Wong P, Gharbawie OA, Luethke LE and Kaas JH. 2008. Thalamic connections of architectonic subdivisions of temporal cortex in grey squirrels (Sciurus carolinensis). J Comp Neurol 510(4):440-461.

Wong-Riley M. 1979. Changes in the visual system of monocularly sutured or enucleated cats demonstrable with cytochrome oxidase histochemistry. Brain Res 171(1):11-28.

Wong-Riley MT and Norton TT. 1988. Histochemical localization of cytochrome oxidase activity in the visual system of the tree shrew:normal patterns and the effect of retinal impulse blockage. J Comp Neurol 272(4):562-578.

Wu CW, Bichot NP and Kaas JH. 2000. Converging evidence from microstimulation, architecture, and connections for multiple motor areas in the frontal and cingulate cortex of prosimian primates. J Comp Neurol 423(1):140-177.

Zilles K. 2004. Architecture of the human cerebral cortex. In The human nervous system, G. Paxinos, and J. Mai, eds. Elsevier. 997-1055.

Zilles K. 1990. Organization of the Neocortex of the rat. In The Cerebral Cortex of the Rat, B. Tees, and R.C. Kolb, eds. MIT Press. 21-34.

Zilles K. 1978. A quantitative approach to cytoarchitectonics: 1. The areal pattern of the cortex of Tupaia Belangeri. Anat Embryol (Berl) 153195-212.

Zilles K, and Wree A. 1995. In Cortex: Areal and laminar structure. G. Paxinos, eds. Sydney: Academic Press. 649-685.

CHAPTER IV

ARCHITECTONIC SUBDIVISIONS OF NEOCORTEX IN THE GALAGO (*OTOLEMUR GARNETTI)*

Introduction

Galagos are prosimian primates that represent a branch of the primate evolution that gave rise to anthropoids about 50 million years ago (Simons and Rasmussen, 1994; Martin, 2004). The brain weights of prosimian primates are smaller relative to body weights than in anthropoid primates (Jerison, 1979; Stephan et al., 1981; Preuss and Goldman-Rakic, 1991a, 1991c). They have also retained many anatomical features of early primates, whereas these anatomical features have been modified during the course of anthropoid evolution (Martin, 1990; Fleagle, 1999). As such, it can be assumed that features of neocortical organization in early primates will be conserved to a greater degree in prosimians than in anthropoids (Preuss and Goldman-Rakic, 1991a). Here, we describe the architectonic subdivisions of neocortex in the galago, so as to establish a reliable areal cortical map that can be used to guide functional studies, and can also be compared to cortical maps of anthropoid primates, such as macaque monkeys, to identify features that are similar or different.

Galagos have often been used in studies of visual, auditory, somatosensory and motor cortex (e.g. Allman et al., 1973; Raczkowski and Diamond, 1978; Symonds and Kaas, 1978; Wall et al., 1982; Weller and Kaas, 1982; Xu et al., 2004). The retinotopic organization of V1 in galagos is similar to monkeys, and mammals in general, containing a complete representation of the visual field (Rosa et al., 1997), with the lower visual

hemifield represented dorsally and upper visual hemifield represented ventrally (Weller and Kaas, 1982; Rosa et al., 1997). The temporal lobe of galagos contains several well differentiated areas (Zilles et al., 1979) and share several common areas present in the macaque monkey, including auditory associated, multisensory and visual associated areas (Preuss and Goldman-Rakic, 1991a). Area 3b(S1), the primary somatosensory area of galagos, contains a single systematic representation of the cutaneous body surface (Carlson and Welt, 1980; Sur et al., 1980; Carlson and Welt, 1981), receives topographically organized input from the ventroposterior nucleus, and projects to the ventrally located secondary somatosensory area (S2)(Kaas, 1982; Burton and Carlson, 1986). Area 3a lies rostral to area 3b(S1) and is likely homologous to area 3a of monkeys that contains a systematic representation (Kaas et al., 1979) and is responsive to muscle spindle receptor activation (Krubitzer and Kaas, 1990b).

There are several cytoarchitectural cortical maps of galagos to date, mostly based on the traditional Nissl stain for cell bodies, or myelin (von Bonin, 1942; von Bonin, 1945; von Bonin and Bailey, 1961; Kanagasuntheram et al., 1966; Zilles et al., 1979; Preuss and Goldman-Rakic, 1991a). As the repertoire of staining procedures available has increased, an updated cortical map using a battery of staining preparations to characterize the cortical areas in the galago is now timely. For the present study, in addition to the traditional Nissl, myelin and cytochrome oxidase stains, we use another histochemical preparation, the zinc stain (Danscher, 1981; Danscher, 1982; Danscher and Stoltenberg, 2005) that has been useful in revealing areal borders in the neocortex. This histochemical procedure reveals unbound ionic zinc in the synaptic vesicles of cortical neuron terminations and synaptic clefts. Thalamocortical terminations do not

contain free ionic zinc and are as such distinguished from corticocortical terminations. Primary sensory areas are distinguished from secondary sensory areas due to the lack of zinc staining in layer 4 of primary sensory areas, where dense thalamocortical inputs terminate (e.g. Valente et al., 2002). In addition, three immunohistochemical stains for parvalbumin (PV) and vesicle glutamate transporter 2 (VGluT2) were employed. The PV antibody reveals a subset of GABAergic, nonpyramidal cells, such as basket and double bouquet interneurons (Celio, 1986; Conde et al., 1996; DeFelipe, 1997; Hof et al., 1999), that contain the calcium-binding PV protein. More importantly for the present study, PV is a useful marker that labels afferent cortical terminals from sensory thalami nuclei (Van Brederode et al., 1990; DeFelipe and Jones, 1991; Hackett et al., 1998; de Venecia et al., 1998; Latawiec et al., 2000; Wong and Kaas, 2008; Wong and Kaas, 2009a, b). VGluT2 preparations reveal thalamocortical and not corticocortical terminations (Fujiyama et al., 2001; Kaneko and Fujiyama, 2002; Wong and Kaas, 2008; Hackett and de la Mothe, 2009; Wong and Kaas, 2009a, b).

The use of a battery of staining procedures, we are able to provide more detailed descriptions of the architectonic subdivisions present in the neocortex of galagos. When borders in similar locations are detected across adjacent series of sections stained with different histological and immunohistochemical stains, comprehensive cortical maps with rigorous areal borders are more reliably established.

Materials and Methods

Animal subjects

The cortical architecture was studied in a total of six adult *Otolemur garnetti*. All experimental procedures were approved by the Vanderbilt Institutional Animal Care and Use Committee and followed the guidelines published by the National Institute of Health.

Tissue Preparation

The galagos were given a lethal dose of sodium pentobarbital (100mg/kg). For visualizing synaptic zinc in the cortex, galagos were given 200mg/kg body weight of sodium sulfide with 1cc of heparin in 0.1M phosphate buffer (PB), pH 7.2, intravenously. Perfusion was carried out transcardially with phosphate-buffered saline (PBS), pH 7.2, followed by 4% paraformaldehyde in 0.1M PBS and 4% paraformaldehyde and 10% sucrose in PBS. The brains were removed from the skull, bisected and post-fixed for 2 to 4 hours in 4% paraformaldehyde and 10% sucrose in PBS. The hemispheres were placed in 30% sucrose overnight for cryoprotection before cutting on a freezing microtome into 40μm thick sections in the coronal, parasagittal or horizontal sections. Brain sections were saved in four to five series. In some cases, the brains were artificially flattened, then cut tangentially to the pia at 40μm, and saved in three series.

Histochemistry

One series of sections from each hemisphere was processed for Nissl substance (with thionin) and another series was processed for myelin, using the (Gallyas, 1979)

silver procedure. In some cases, a third series of sections were processed for cytochrome oxidase (CO)(Wong-Riley, 1979).

Zinc Histochemistry

In galagos that were given IV injections of sodium sulfide, a series of sections was processed using the protocol outlined by Ichinohe et al. (2003) to visualize synaptic zinc. Brain sections were washed thoroughly with 0.1M PB, followed by 0.01M PB. The zinc-enriched terminals were visualized using the IntenSE M Silver enhancement kit (Amersham International, Little Chalfont Bucks, UK). The developing reagent was a one-to-one cocktail of the IntenSE M kit solution and 50% gum Arabic solution. The development the sections was terminated when a dark brown/black signal was seen by rinsing sections in 0.01M PB. Sections were then mounted and dehydrated in an ascending series of ethanols, (70% for 20min, 95% for 10min, 100% for 10min), cleared in xylene and coverslipped using Permount.

Immunohistochemistry

Each case contains one to two series of sections that have been immunostained for parvalbumin (PV) (1:4000; Sigma-Aldrich, St. Louis, Mo), or vesicle glutamate transporter 2 (VGluT2) (1:4000; Chemicon now part of Millipore, Billerica, MA). Sections were incubated in their respective antibodies for 40 to 48 hours at 4°C. Details of the immunohistochemical procedures have been described in Wong and Kaas (2008).

Light microscopy

The architectonic borders were delineated from the brain sections that have undergone the various histochemical and immunohistochemical procedures described above. The locations of architectonic borders were determined by analysis of laminar and cell density changes in the processed sections when viewed at high power using a projection microscope. The Nissl, zinc and VGluT2 preparations were most useful in identifying primary sensory areas, while sensorimotor cortical areas were better distinguished in the Nissl and SMI-32 preparations. Other histological preparations were used for corroborating ambiguous borders. Digital photomicrographs of sections were acquired using a Nikon DXM1200 (Nikon Inc., Melville, NY) camera mounted on a Nikon E800 (Nikon Inc., Melville, NY) microscope and adjusted for brightness and contrast using Adobe Photoshop (Adobe Systems Inc., San Jose, CA).

Anatomical reconstruction

For further details on how the anatomical reconstruction is done, please refer to Wong and Kaas (2008). In brief, architectonic borders were identified and drawn for each outlined brain sections using a Bausch and Lomb Microprojector (Bausch & Lomb, Rochester, NY). Adjacent brain sections were aligned based on blood vessels and other landmarks that were added to the section outlines. The different histological procedures revealed similarly located boundaries between areas, suggesting that functionally relevant borders were being identified. Outlines of brain sections were imported into Adobe Illustrator (Adobe Systems Inc., San Jose, CA) and aligned using the contour of the outline sections and the landmarks that were drawn. For coronal and horizontal sections,

the distances of the architectonic borders from the midline were measured. Positions of sagittal sections were aligned on a dorsal view of the brain. The surface views of the brain were reconstructed by projecting cortical and areal borders of brain sections onto lines appropriate for dorsal, lateral, medial and 45-degree angle view, and spacing these lines according to the location on the brain. In general, different histological procedures revealed similarly located boundaries between areas, suggesting that functionally relevant borders were being identified. In instances where architectonic borders were not clearly defined, but functional borders from microelectrode mapping and anatomical studies were well established, the locations of these functional borders were placed on the summary illustration to better guide future studies. The two types of borders are distinguished in the results.

Results

The present results provide further evidence for the presence of several previously proposed subdivisions of neocortex in galagos, as well as providing an interpretation of cortical organization that differs somewhat from previous depictions (von Bonin, 1942; von Bonin, 1945; von Bonin and Bailey, 1961; Kanagasuntheram et al., 1966; Zilles et al., 1979; Preuss and Goldman-Rakic, 1991a). The proposed areas are outlined on views of the galago brain in figures that follow. For abbreviations, refer to Table 1.

An overview of cortical organization based on brain sections cut parallel to the surface of flattened cortex

Brain sections that contain all regions of flattened cortex in single sections nicely indicate the relative positions of cortical areas, and often the extents of cortical borders, but they also need to be interpreted carefully as cortical layers stain differently, and such sections typically contain regions involving different layers. This is apparent in the myelin and zinc-stained sections of figure 1, as the border of area 17 with area 18 is clear, whereas regional differences in staining within area 17 are apparent as the sections course from layer 3 to layer 4 (Fig. 47). Thus, in zinc preparations, layer 4 stains lightly over much of area 17, whereas darker regions correspond to layer 3 (Fig. 47B). In the myelin stained section, darker areas correspond to the myelin dense inner layers of area 17, while lighter regions correspond to superficial layers. Given this caution, area 3b(S1) is overall more myelinated then adjoining cortex, as is the auditory core (A). The middle temporal area, MT, is also more myelinated. In contrast, the middle layers of these areas, 17, MT, A and 3b(S1), all have reduced levels of free ionic zinc. Descriptions of cortical areas, region by region, follow.

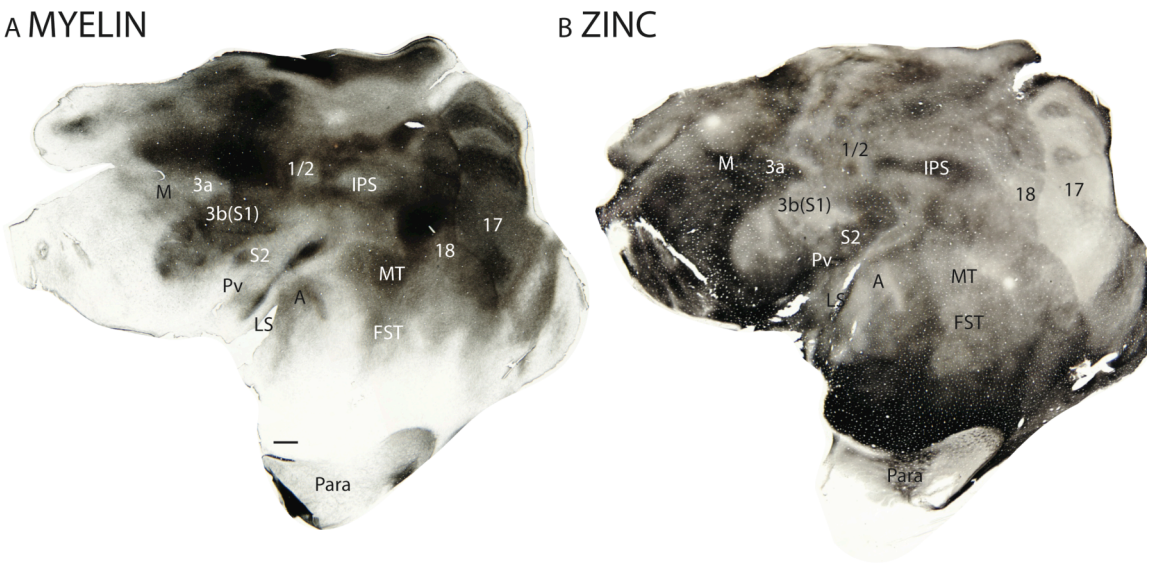

Figure 47. Architectonic characteristics galago cortex in flattened preparations stained for myelin (A) and for synaptic zinc (B). Scale bar in panel A = 2mm.

Occipital cortex

Area 17 (V1). Area 17 in galagos, which is co-extensive with the primary visual area (V1), occupies the caudal most extent of the dorsolateral surface of occipital cortex and extends over the medial wall to occupy both banks of the calcrine sulcus. Area 17, with an approximate surface area of approximately 200mm^2 (Rosa et al., 1997), has distinct architectonic characteristics that allow it to be easily distinguished from the rostrolaterally adjoining extrastriate area 18 (V2) and the medially bordering prostriata (PS). The cortical borders of area 17 are apparent even at low magnification in Nissl, CO, myelin, zinc, PV and VGluT2 stains, and the borders across adjacent main sections of different preparations are in similar locations (Fig. 48).

Figure 48. Architectonic characteristics of visual areas 17, 18, 19d and DM. Sagittal sections from occipital cortex were processed for (A) Nissl substance, (B) myelin, (C) CO, (D) synaptic zinc, (F) parvalbumin (PV) and (F) vesicle glutamate transporter 2 (VGluT2). The architectonic borders of proposed cortical areas are shown on the dorsal view (G) and medial view (H) of the galago brain. The horizontal line on the brain shows the level from which the sections were taken for panels A-F. The thicker portion of the line marks the regions illustrated in panels A-F. Occipital areas 17, 18 and 19 are adopted from Brodmann (1909). DM is the dorsal medial visual area. Arrowheads on the sections illustrated here and in the following figures mark architectonic boundaries. Short lines on the sections indicate cortical layers 1 to 6. See table 1 for abbreviations for other areas. The scale bar for brain sections (panel E) = 1mm. The scale bar on the brain (panel F) = 2.5mm.

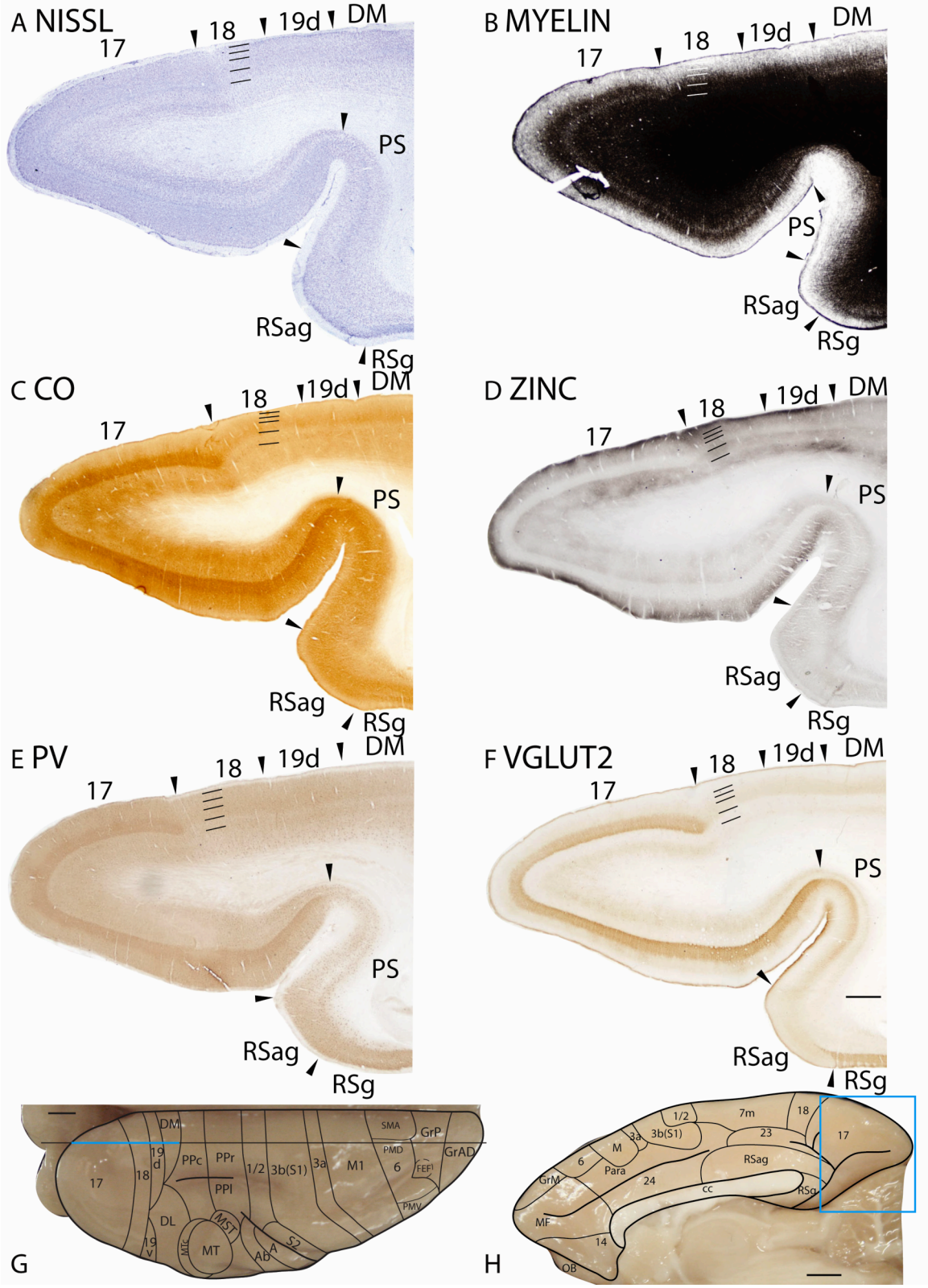
A NISSL
17
18
19d
DM
PS
RSag
RSg
B MYELIN
17
18
19d
DM
PS
RSag
RSg
C CO
17
18
19d
DM
PS
RSag
RSg
D ZINC
17
18
19d
DM
PS
RSag
RSg
E PV
17
18
19d
DM
PS
RSag
RSg
F VGLUT2
17
18
19d
DM
PS
RSag
RSg
G
DM
19d
17
18
PPc
PPr
PPl
1/2
3b(S1)
3a
M1
SMA
GrP
PMD
6
FEF
GrAD
PMV
DL
MST
MTc
MT
A
Ab
S2
19v
H
1/2
7m
18
3a
3b(S1)
23
17
M
6
Para
RSag
GrM
24
cc
RSg
MF
14
OB

In Nissl preparations, area 17 has a banded appearance, with darkly stained layers 4 and 6, and paler layer 3 and 5 (Fig. 48A). Area 17 is densely myelinated (Fig. 48B; 50B). Layer 4 of area 17 is darkly stained band for CO and layers 1, 2, 5 and 6 are lighter stained (Fig. 48C). In zinc preparations, layer 4 of area 17 stands out as a white band as it expresses very little synaptic zinc (Fig. 48D), suggesting that the main projections to this cortical layer is from the thalamic nuclei rather than other cortical areas. Layers 1 to 3 and layers 5 are more darkly stained, likely because these cortical layers receive corticocortical connections that contain free ionic zinc in their terminations. Layer 4 of area 17 stains darkly for PV (Fig. 48E) and VGluT2 (Fig. 48F) immunopositive terminations, reflecting dense terminations from thalamic nuclei. A second, faint band of VGluT2 immunopositive terminations is observed in layer 6 (Fig. 48F), possibly reflecting the collaterals of axons that terminate more extensively in layer 4 (Casagrande and Kaas, 1994).

Layer 3 of area 17 is subdivided into a number of ovals that are histologically distinct from surrounding matrix, corresponding to the well-known CO rich “blobs” and CO poor “interblobs” (Casagrande and Kaas, 1994; Preuss and Kaas, 196; Condo and Casagrande, 1990). In flattened preparations through layer 3 of area 17, a patchy pattern with myelin-poor clusters is observed within a myelin-rich background (Fig. 49B). Flattened sections of area 17 at a comparable cortical depth stained for CO showed darkly stained patches of CO-rich ovals within a CO-poor region (Fig. 49C). In zinc preparations, there are circular regions of dark staining surrounding zinc-poor patches (Fig. 49D). These results are consistent with the evidence that thalamocortical and corticocortical projections follow a modular organization in layer 3 of the galago visual

cortex, with the thalamic projections from lateral geniculate K cells forming clusters in a background of corticocortical projections. These patches of thalamocortical terminations in layer 3 stain darkly in VGluT2 (Fig. 49E) and PV (Fig. 49F) preparations.

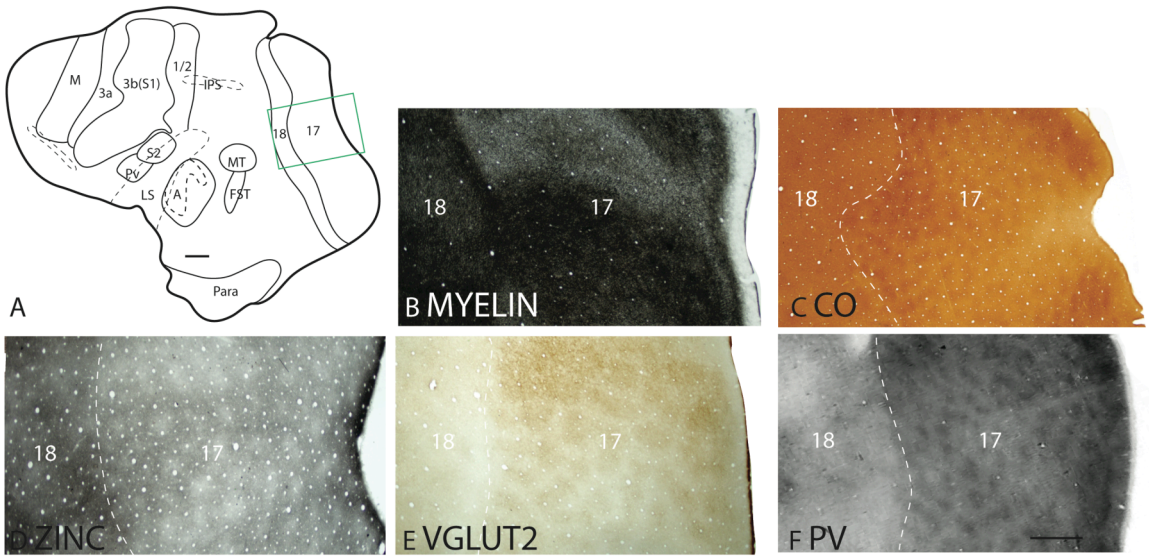

Figure 49. Patchy staining pattern of area 17. The boxed region in A is shown in panels B to F at higher magnification. A myelin (B), CO (C), synaptic zinc (D) VGluT2 (E) and PV (F) stained section cut parallel to the surface of an artificially flattened cerebral hemisphere. Cytochrome oxidase rich regions, known as CO blobs are observed in area 17 of the galago neocortex (C). Dashed lines show the approximate location of the cortical borders. Scale bar in panel A = 4mm, in panel F = 1mm.

In coronal sections stained for Nissl bodies viewed at higher magnifications, layers 4 and 6 of area 17 are densely populated with cells, contributing to their dark appearance (Fig. 50A). Middle layer 3, primarily composed of small pyramidal cells, has clusters of darkly stained cells (Fig. 50A) that are likely to be co-extensive with the cytochrome oxidase blobs (Fig. 50C) and the PV-immunopositive thalamocortical terminations (Fig. 50D). At higher magnifications, darkly CO-stained cells are present in layer 5 of area 17 (Fig. 50C). PV-immunopositive cell bodies are present in all layers,

with a lower concentration in the infragranular layers 5 and 6 (Fig. 50D). Furthermore, area 17 is densely myelinated with distinct inner and outer bands of Baillarger (Fig. 48B) that tend to merge in darkly stained sections (Fig. 50B).

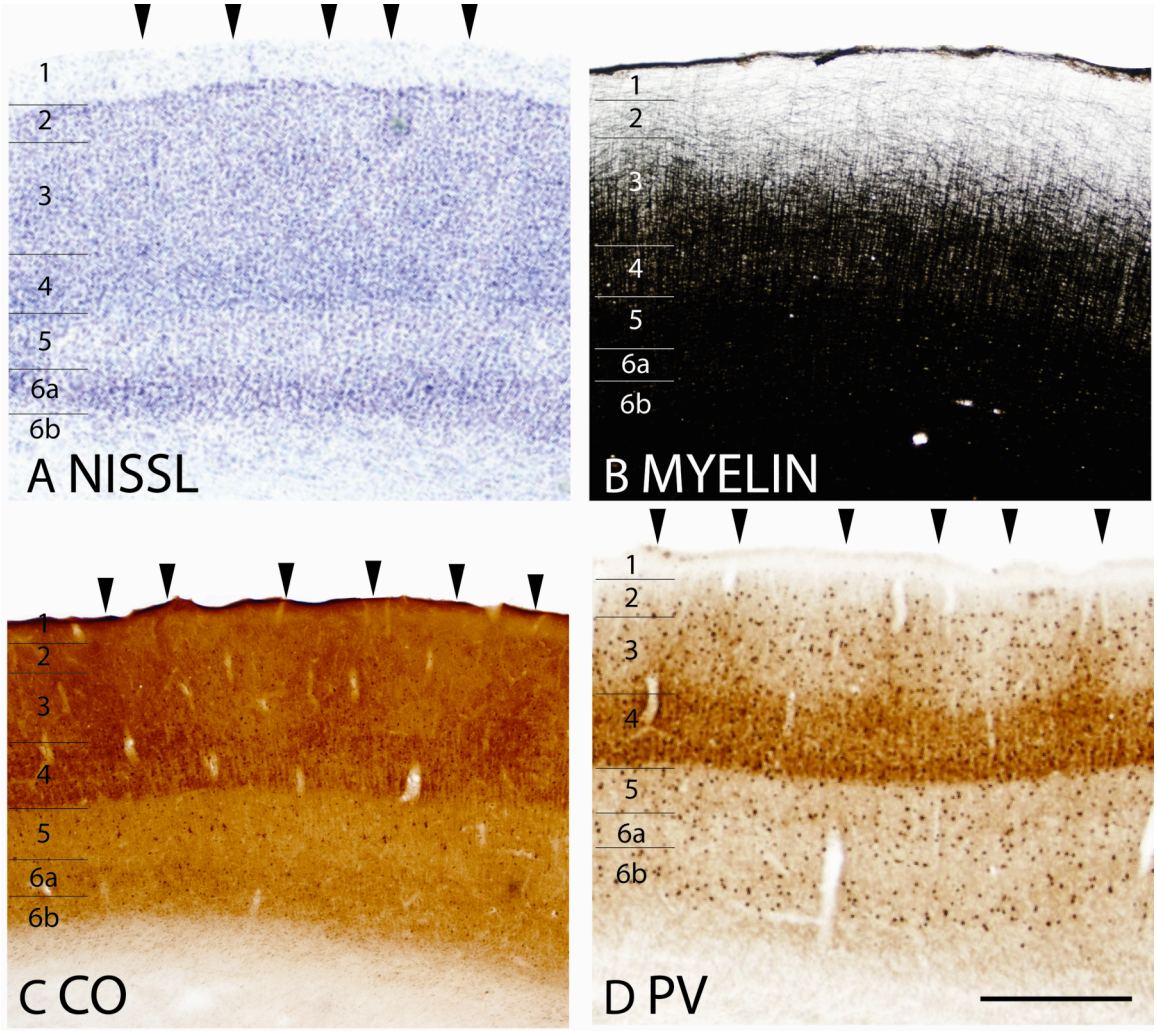

Figure 50. The laminar characteristics of area 17 at higher magnification. The arrowheads in panels A, C and D indicate the locations of CO blobs in layer 3. Layer 6 has two sublayers, 6a and 6b, that are apparent in Nissl, and PV preparations. Scale bar = 0.5mm.

Area 18 (V2). Area 18 of galagos lies along most of the lateral border of area 17 and is approximately one-third the surface area of area 17, with a maximum width of

3mm (Rosa et al., 1997). Co-extensive with the secondary visual area (V2), area 18 contains a representation of the contralateral visual hemifield, with the lower visual field represented dorsally and the upper visual field represented ventrally (Rosa et al., 1997).

The area 17/18 border is distinct due to the less conspicuous laminar pattern of area 18. In Nissl preparations, layers 4 and 6 of area 18 is less darkly stained and less densely populated cells, resulting in a muted banded appearance compared to area 17 (Fig. 48A). Area 18 is densely myelinated, but the outer and inner bands of Baillarger that are present in area 17 are not distinct in area 18 (Fig. 48B). Layer 4 of area 18 is also less metabolically active than layer 4 of area 17, as evidenced by the reduction in staining intensity for CO (Fig. 48C). A band of CO staining is apparent in layer 4 and a faint band of CO staining is present in inner layer 5 of area 18 (Fig. 48C). Area 18 exhibits darker staining than area 17 throughout the cortical layers in zinc preparations (Fig. 48D). The increased intensity of zinc staining is especially prominent in layer 4 as area 17 transitions to area 18 (Fig. 48D). Inner layer 5 of area 18, which corresponds to the faint CO-dense band, is more lightly stained than outer layer 5 in zinc preparations (Fig. 48D). Area 18 lacks the dense PV- and VGluT2- immunopositive terminations that are present in layer 4 of area 17 (Fig. 48F). In addition, the faint band of VGluT2 staining present in layer 6 of area 17 is absent in area 18 (Fig. 48F). Thus, a thalamic input to layer 4 is absent of greatly reduced. The reduction in staining intensity in VGluT2 preparations and the increased staining intensity in zinc preparations in layer 4 of area 18 suggest that corticocortical inputs dominate.

In tangent sections along layer 3, area 18 has a more homogenous myelination pattern (Fig. 49B) and lacks the CO rich patches or ‘blobs’ that are present in area 17

(Fig. 49C). Area 18 stains darker and more evenly for the zinc stain (Fig. 3D), and lighter for the VGluT2 (Fig. 49E) and PV (Fig. 49F) stains compared to area 17.

Area 19 dorsal (V3d) and area 19 ventral (V3v). Early studies of extra-striate areas of galagos did not include a third visual area, V3 or area 19 (Rosa et al., 1997; Beck and Kaas, 1998a; Collins et al., 2001), whereas others included other visual areas, dorsomedial (DM) and dorsolateral (DL) visual areas, in area 19 (e.g. Raczkowski and Diamond, 1978). Areas V3d (19d) and V3v (19v) were first differentiated from DM and DL in galagos by (Lyon and Kaas, 2002a) in studies of V1 projections. While area 19 has been used inconsistently as a term for visual regions of cortex (e.g. Brodmann, 1909), the term has been associated with V3 in cats (Hubel and Wiesel, 1965), and area 19 is used here as the architectonic term for V3.

Areas 19d and 19v have previously been described as regions that are moderately myelinated and stain dark for CO in flattened preparations of cortex (Lyon and Kaas, 2002a). As expected, areas 19d and 19v resemble each other. Here, we observe that area 19d has a thicker granular layer 4 than area 18 (Fig. 48A) in Nissl preparations and area 19d has a lighter appearance than DM (Fig. 48A). Sections stained for myelinated fibers show that area 19d is darkly myelinated, but lacks distinct inner and outer bands of Baillarger (Fig. 48B). Area 19d stains slightly dark for CO than area 18, but is lighter than DM (Fig. 48C). In zinc preparations, the upper cortical layers, layer 5 and inner layer 6 of area 19d stain darkly (Fig. 48D). Overall, area 19d is more darkly stained for free ionic zinc in the synapses than both areas 18 and DM (Fig. 48D). Area 19d stains more intensely in PV preparations than 18 and DM (Fig. 48E). Layer 4 of area 19d is

more darkly stained for VGluT2 immunopositive terminations than layer 4 of area 18, and is stained at similar intensities to layer 4 of DM (Fig. 48F).

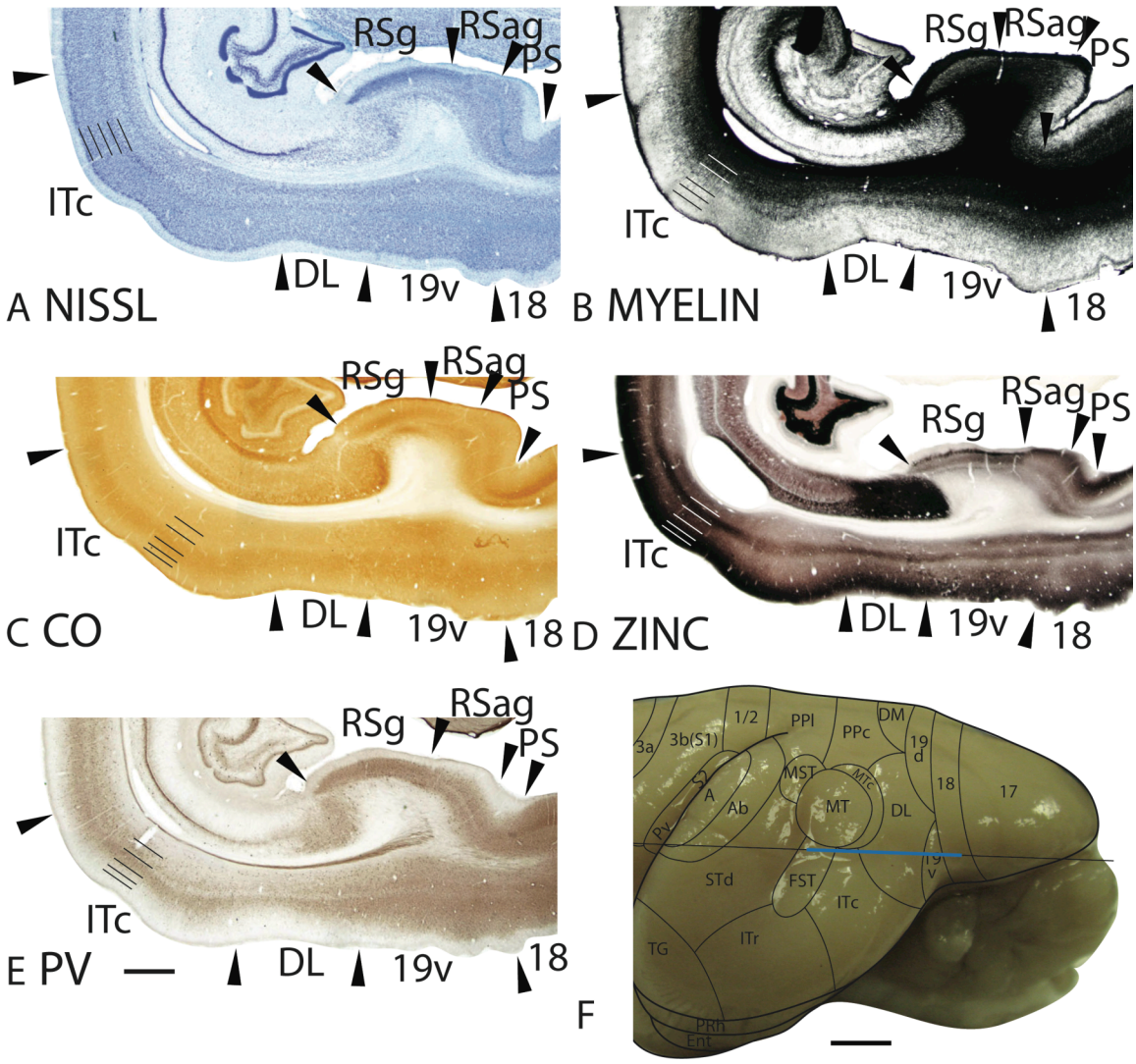

Figure 51. Architectonic characteristics of visual and temporal visual areas. The level at which the horizontal sections are taken from is indicated by the horizontal line on the dorsal view of the brain in panel F. The thicker line in panel F marks the regions illustrated in panels A-E. The extent of each cortical layers 1 to 6 is indicated by the short horizontal lines on panels A-E. The scale bar for brain sections (panel E) = 1mm. The scale bar on the brain (panel F) = 2.5mm.

Area 19v is discontinuous with area 19d, with DL separating them. In Nissl preparations, area 19v has a thin, darkly stained layer 4 that is thicker than that of DL (Fig. 51A) and area 18 (Fig. 51A). Area 19v is less myelinated than area 18 and more myelinated than area DL (Fig. 51B). In CO preparations, area 19v is moderately stained (Fig. 51C). The upper cortical layers, layer 5 and inner layer 6 of area 19v is darkly stained for zinc, whereas layer 4 and outer layer 6 stains lighter, giving area 19v a banded appearance in zinc preparations (Fig. 51D). Additionally, Area 19v stains as darkly as area 18, and layer 4 of area 19v is lighter stained than layer 4 of DL in the zinc stain (Fig. 51D). In PV preparations, area 19v stains moderately for PV-immunopositive terminations, with lower intensity in layer 5 (Fig. 51E). The PV staining in area 19v is not homogenous, tapering off towards the 19v/DL border (Fig 51E). In VGluT2 preparations, a moderately stained band is present in layer 4 of area 19v and this band is darker, but thinner than that of area 18 (Fig. 52D).

Dorsomedial (DM) and dorsolateral (DL) visual areas. The dorsomedial visual area, DM, has a thin layer 4 that is densely packed with granule cells and as such, is darkly stained in the Nissl stain (Fig. 48A; 53A). DM is moderately myelinated (Fig. 48B; 53B). Furthermore, DM has higher myelination levels than DL (Fig. 7B) and lower myelination level than area 19d (Fig. 48B). Layer 4 of DM expresses moderate levels of CO, with two bands of CO staining, in layers 4 and 6 (Fig. 48C; 53C). In zinc preparations, DM stains with lower intensity compared to area 19d (Fig. 48D), and DL (Fig. 53D). DM stains darker in PV preparations than DL (Fig. 53E) and stains lighter than area 19d (Fig. 48E). In favorable sections, DM has two intensely stained bands of PV immunopositive terminations, one in layer 4 and another in outer layer 6 (Fig. 53E).

Layer 4 of DM stains at similar levels to area 19d (Fig. 48F) and DL (Fig. 53F) for VGluT2 immunopositive terminations.

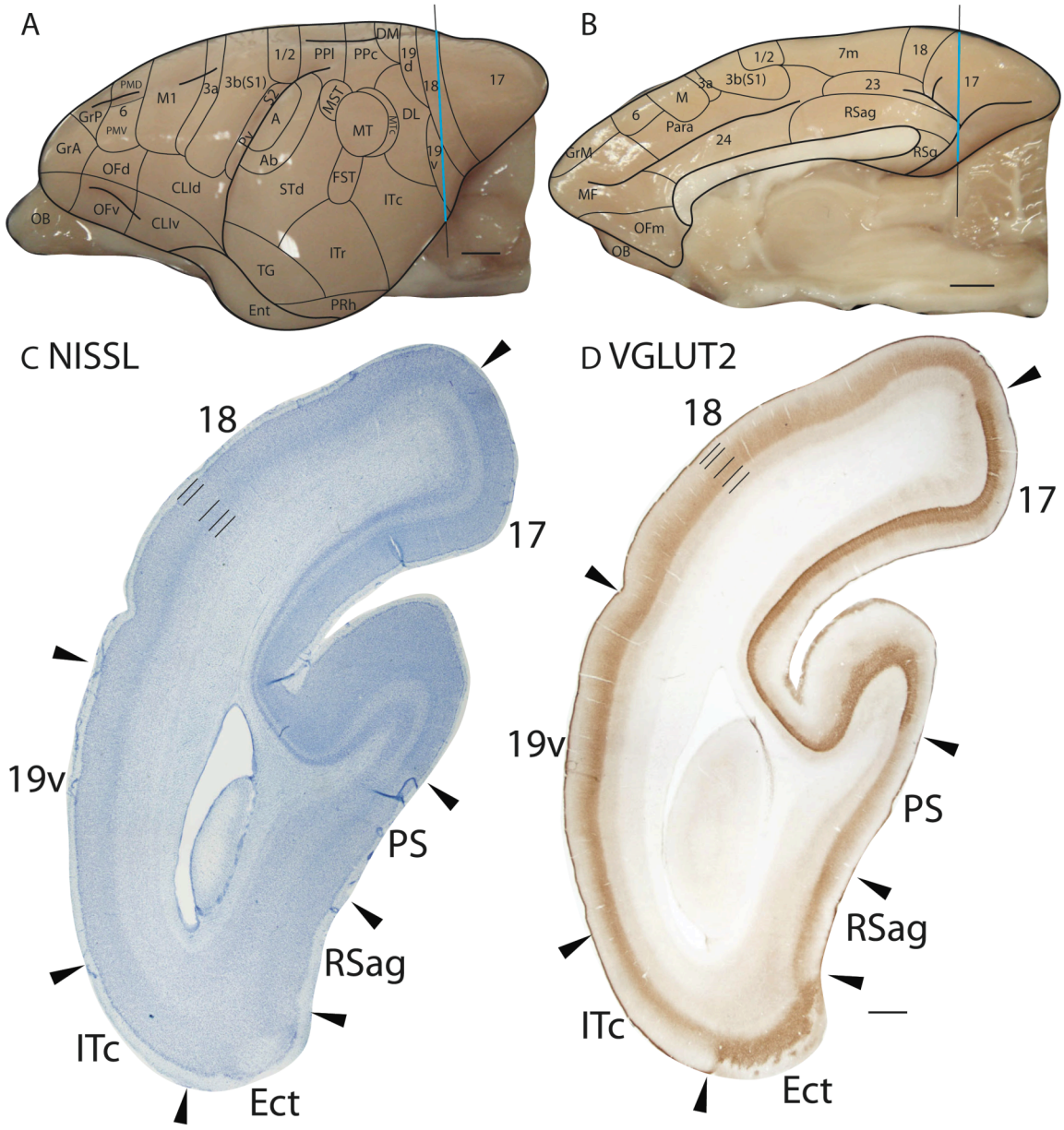

Figure 52. Architectonic characteristics of visual areas and adjoining retrosplenial cortex. Coronal sections from occipital cortex were processed for (A) Nissl substance and (B) VGluT2. The level at which the coronal sections are taken from is indicated by the vertical line on the lateral and medial view of the brain in panels A and B respectively. The thicker line in panel A and B marks the regions illustrated in panels C and D. Short lines on the sections indicate the extent of each cortical layers 1 to 6. See table 1 for abbreviations for other areas. The scale bar for brain (panels A and B) = 2.5mm. The scale bar on the brain section (panel D) = 1mm.

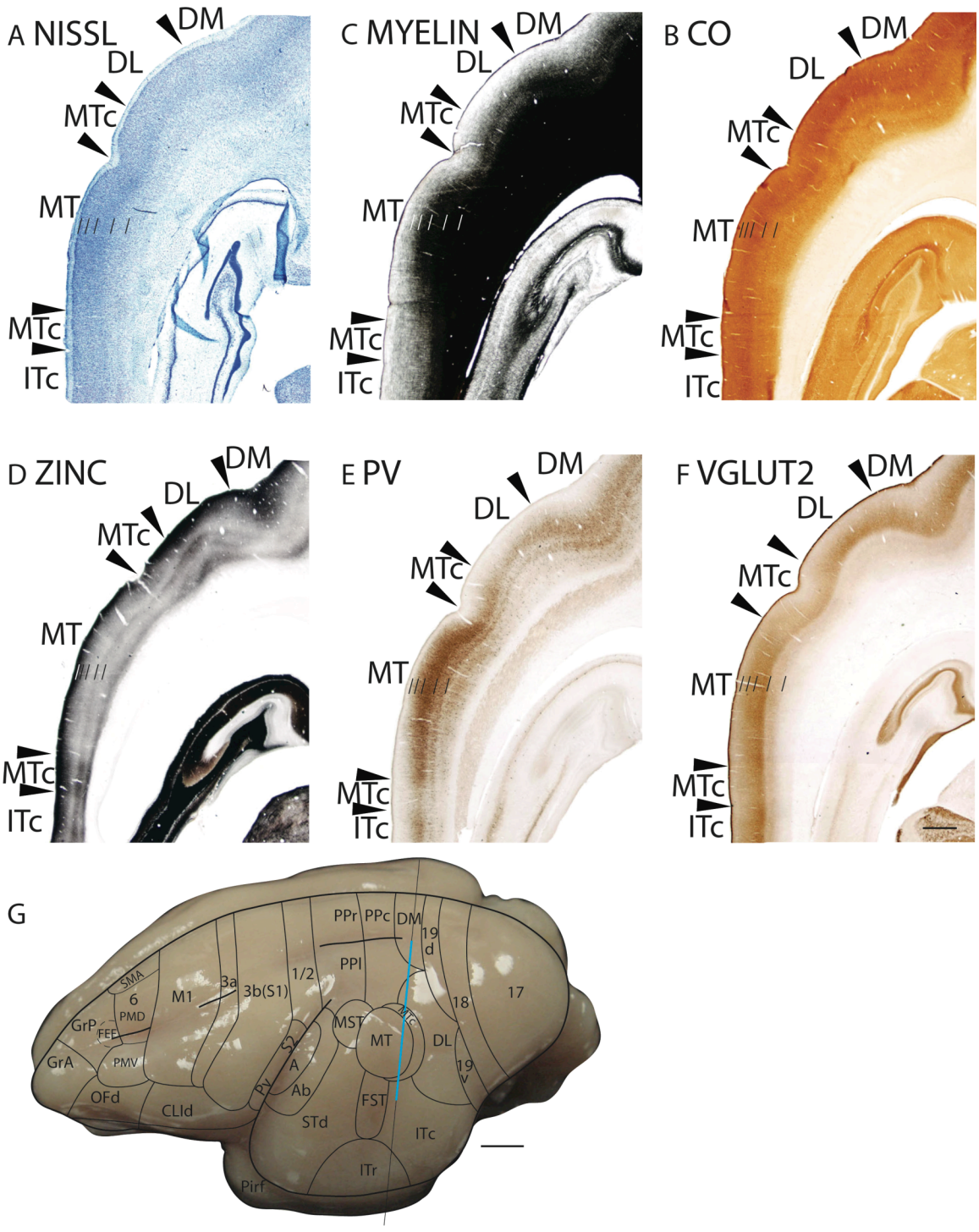

Figure 53. Architectonic characteristics of middle temporal cortex. The level at which the coronal sections are taken from is indicated by the vertical line on the dorsolateral view of the brain in panels G. The thicker line in panel G marks the regions illustrated in panels A to F. Short lines on the sections indicate the extent of each cortical layers 1 to 6. See table 1 for abbreviations for other areas. The scale bar for brain (panel G) = 1mm. The scale bar on the brain section (panel F) = 2.5mm.

The dorsolateral visual area, DL, surrounds at least the caudal portion of the middle temporal visual area (MT) in galagos and is likely to have projections to the inferior temporal area of cortex (Wall et al., 1982). In Nissl preparations, layer 4 of DL is moderately stained and densely populated with granule cells, and is thinner than layer 4 of MT (Fig. 53A) and 19v (Fig. 51A). Furthermore, the supragranular layers of DL are paler in appearance than those of MT (Fig. 53A). DL is less myelinated than the adjoining DM, MT and 19v, and has a distinct outer band of Baillarger (Fig. 51B; 53B). Both layer 4 and 6 of DL are moderately stained in CO preparations (Fig. 51C; 53C). In zinc preparations, DL expresses moderate levels of free ionic zinc, and is more darkly stained than MT, DM (Fig. 53D) and 19v (Fig. 51D). DL is lightly stained in PV preparations compared to the adjoining MT, DM and 19v, but two thin and faint bands of PV immunopositive terminations, in layers 4 and outer 6, are observed (Fig. 51E; 53E). In VGluT2 preparations, a single, lightly stained band is present in layer 4 of DL (Fig. 53F).

Temporal cortex

The temporal cortex of galagos is rather large and can be broadly divided into three regions. First are the temporal extrastriate areas, which consists of the middle temporal visual area (MT), the crescent surrounding MT (MTc), the middle superior temporal area (MST) and the fundus of the superior temporal area (FST). Second is the inferior temporal region is a large region that is further divided into the rostral (ITr) and caudal (ITc) areas. Third are the auditory association areas, which include the primary auditory cortex (A1), the rostral auditory area (R), and the auditory belt (Ab).

Figure 54. Architectonic characteristics of middle temporal cortex. The level at which the coronal sections are taken from is indicated by the vertical line on the dorsolateral (G) and medial (H) views of the brain. The thicker line in panels G and H marks the regions illustrated in panels A to F. Short lines on the sections indicate the extent of each cortical layers 1 to 6. See table 1 for abbreviations for other areas. The scale bar for brain (panels G and H) = 2.5mm. The scale bar on the brain section (panel F) = 1mm.

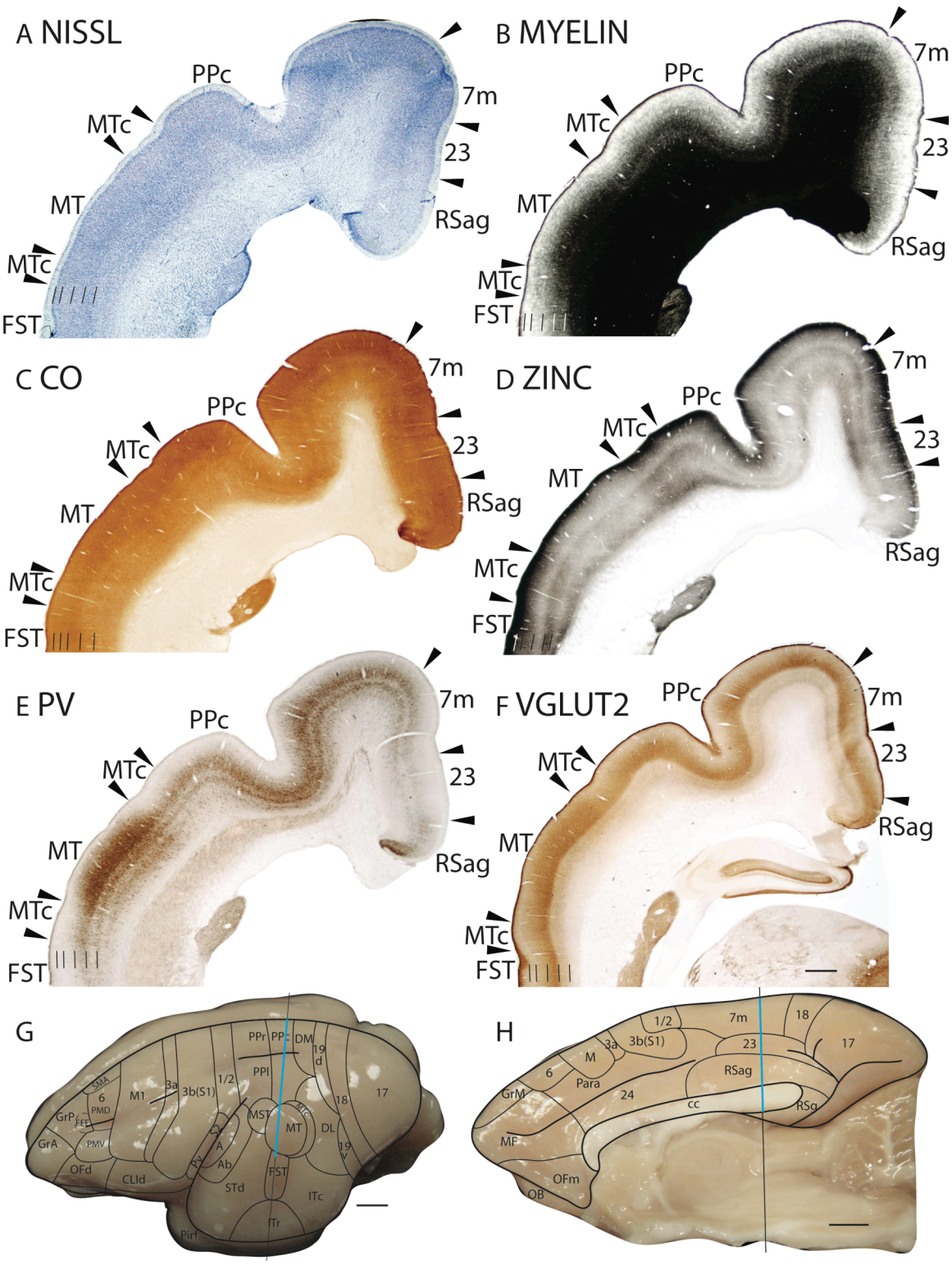
A NISSL
PPc
MTc
MT
MTc
FST
7m
23
RSag
B MYELIN
PPc
MTc
MT
MTc
FST
7m
23
RSag
C CO
PPc
MTc
MT
MTc
FST
7m
23
RSag
D ZINC
PPc
MTc
MT
MTc
FST
7m
23
RSag
E PV
PPc
MTc
MT
MTc
FST
7m
23
RSag
F VGLUT2
PPc
MTc
MT
MTc
FST
7m
23
RSag
G
PPr
PPc
DM
19 d
PPl
1/2
3a
3b(S1)
M1
SMA
6
PMD
FEF
GrP
GrA
PMV
OFd
CLId
MST
MT
DL
18
17
19 v
A
Ab
STd
FST
ITc
ITr
PirF
H
1/2
7m
18
3a
3b(S1)
23
17
M
6
Para
RSag
GrM
24
cc
RSg
MF
OFm
OB

Temporal extrastriate areas – Middle temporal visual area (MT) and the crescent of the middle temporal visual area (MTc). In galagos, MT is complete exposed on the surface as galagos lack a superior temporal sulcus. It has been defined as an oval region that is highly myelinated and has a surface area of approximately 18mm^2 (Allman et al., 1973; Beck and Kaas, 1998a; Xu et al., 2004). MT and the adjoining areas, such as the crescent of MT (MTc) and MST are perhaps best appreciated in sections that were cut tangentially to the pia, as the full extent of these areas are present in a single section (Fig. 55). In CO preparations, both MT and MST are darkly stained, and MTc is stained as a series of CO-dense puffs along the caudal portion of MT (Fig. 55A). MT is also darkly stained in VGluT2 preparations, whereas MST and MTc are lighter stained, which makes the border of MT distinct (Fig. 55B). In PV preparations, the dense PV immunopositive terminations in MT have a somewhat patchy distribution (Fig. 55C). MST and MTc are less densely populated by PV-immunopositive terminations than MT (Fig. 55C).

Area MT has many architectonic features of a sensory area of cortex. In coronal sections, MT has a more darkly stained layer 4 that is densely populated with granule cells than adjoining areas (Fig. 53A; 54A) in Nissl preparations. At higher magnification, layer 5 of MT is sparsely populated by larger pyramidal cells (Fig. 56A). In myelin preparations, MT is densely myelinated (Fig. 53B; 54B; 56B). Layer 4 of MT also stains darkly for CO (Kaskan and Kaas, 2007), although this is not especially evident in figs 5C and 8C. Throughout the cortical layers, MT stains lighter for synaptic zinc than surrounding areas (Fig. 53D; 54D). However, MT is more darkly stained for free synaptic zinc, especially in layer 4, than area 17. This is consistent with the evidence that MT receives a large amount of corticocortical inputs, a large portion of which originates from

area 17 (Kaskan and Kaas, 2007). The PV immunostain is perhaps one of the best markers for MT, as MT stains darkly for PV immunopositive terminations and has a tri-banded appearance (Fig. 53E; 54E). A large concentration of PV immunopositive terminations is present in layers 3 and 4, followed by a second, thinner band in inner layer 5, likely 5b, and a third, faint band is present in middle layer 6, likely layer 6B (Fig. 56C). In VGluT2 preparations, a thick, darkly stained band of VGluT2 immunopositive terminations is present in layers 3 and 4 of MT (Fig. 53F; 54F; 56D). The higher expression of VGluT2 immunopositive terminations by MT (Fig. 53F; 54F) suggests that MT receives more thalamic inputs than the adjoining cortical areas. Much of this input comes from the visual pulvinar (Wong et al., in press).

MTc has a thinner, less densely populated layer 4 than MT (Fig. 53A; 54A) in Nissl preparations and is less densely myelinated (Fig. 53B; 54B). MTc expresses moderate amounts of CO and is less darkly stained for CO than MT (Fig. 53C; 54C). In zinc preparations, MTc stains more darkly for synaptic zinc, especially in the upper cortical layers, layer 5 and inner layer 6 (Fig. 53D; 54D). Layers 4 and outer 6 of MTc are faintly stained for PV immunopositive terminations, and overall, MTc stains fainter than MT in PV preparations (Fig. 53E; 54E; 55C). In VGluT2 preparations, a thin, faintly stained band is present in layer 4 of MTc (Fig. 53F; 54F), and MTc is lighter stained than MT (Fig. 55B). In sections cut tangentially to the pia, MTc contains several CO-dense puffs (Fig. 55A; Kaskan and Kaas, 2007).

Figure 55. Architectonic characteristics of middle temporal cortex in flattened preparations stained for CO (A), VGluT2 (B) and PV (C). Dashed lines show the approximate location of the cortical borders. The scale bar on the brain section (panel C) = 1mm.

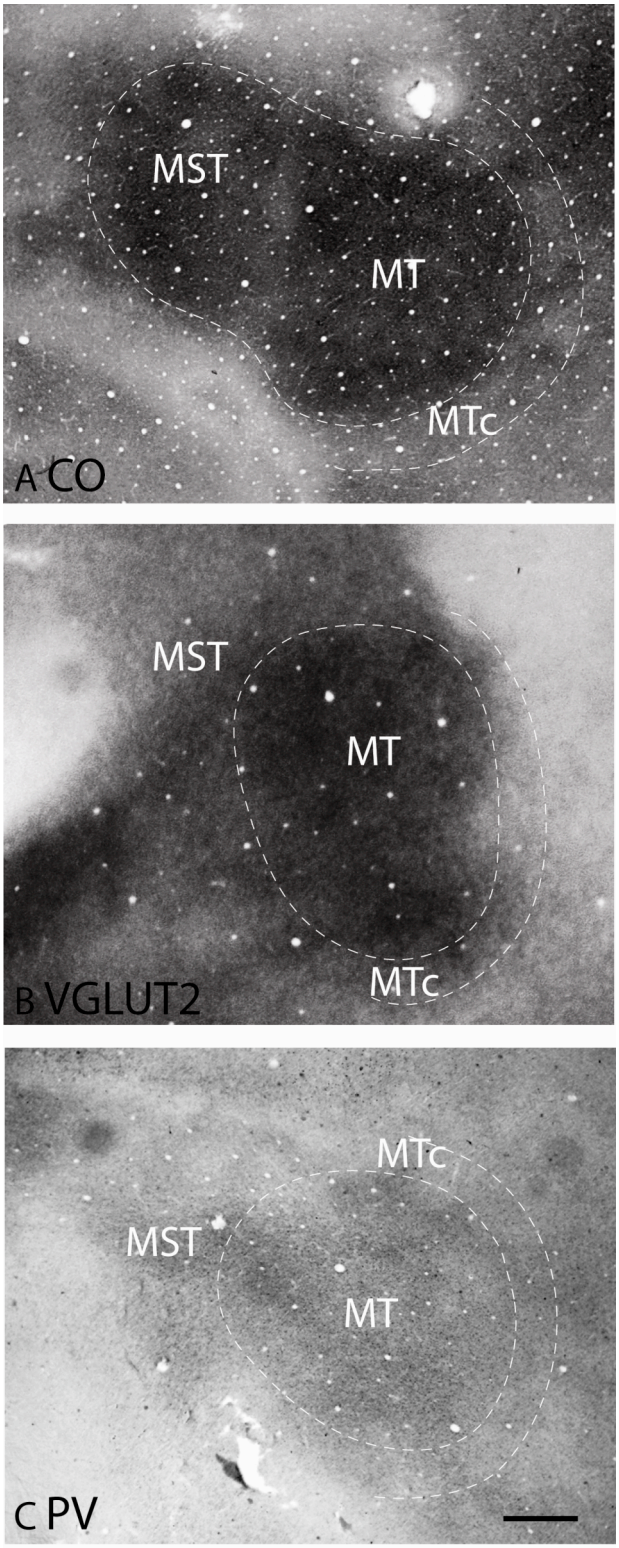
MST
MT
MTc
A CO
MST
MT
MTc
B VGLUT2
MTc
MST
MT
C PV

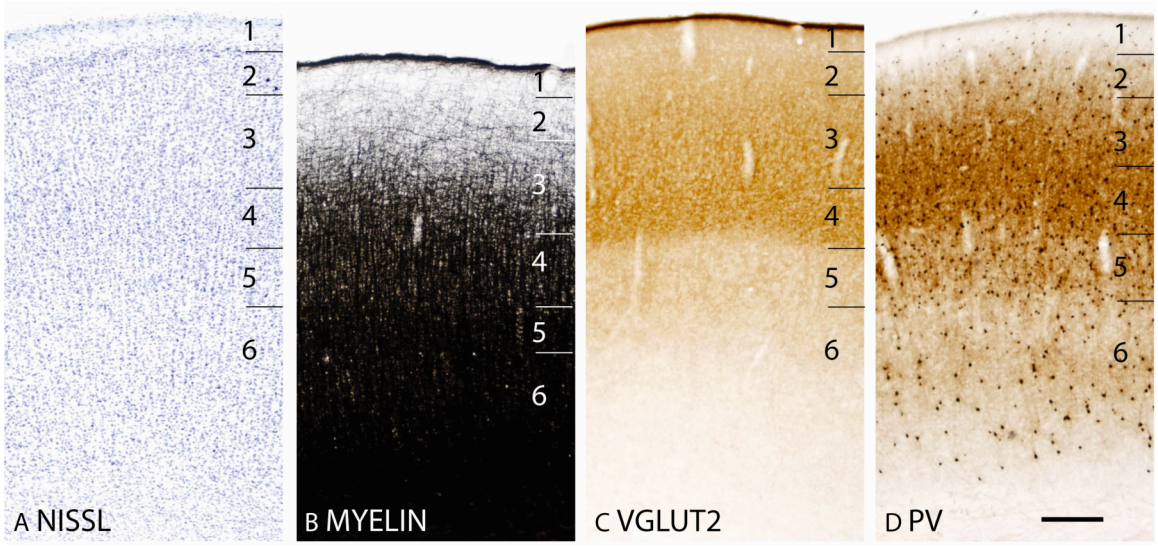

Figure 56. The laminar characteristics of MT at higher magnification. Scale bar = 0.25mm.

The middle superior temporal area (MST) and the fundal area of the superior temporal sulcus (FST). In sections cut tangentially to the pia, MST stains at similar levels for CO to MT (Fig. 55A). In PV and VGluT2 preparations, MST is more lightly stained than MT (Fig. 55B; 55C). In Nissl preparations, FST does not have the well-defined lamination of MT, with no distinct granular layer 4 (Fig. 55A; 57A) and FST is less densely myelinated than MT (Fig. 54B). FST stains lighter for CO than MT (Fig. 54C). In zinc preparations, FST has a banded appearance as the upper cortical layers 1 to 3, and layers 5 and innermost 6 are darkly stained, whereas layers 4 and upper 6 are lighter stained (Fig. 54D; 57D). FST is poorly stained for PV compared to MT, with a faint band of PV immunopositive terminations in layer 4 (Fig. 54E). FST expresses lower levels of VGluT2 terminations than MT (Fig. 54F).

Figure 57. Architectonic characteristics of inferior temporal cortex. The level at which the coronal sections are taken from is indicated by the vertical line on the lateral view of the brain in panels G. The thicker line in panel G marks the regions illustrated in panels A to F. Short lines on the sections indicate the extent of each cortical layers 1 to 6. See table 1 for abbreviations for other areas. The scale bar for brain (panel G) = 2.5mm. The scale bar on the brain section (panel F) = 1mm.

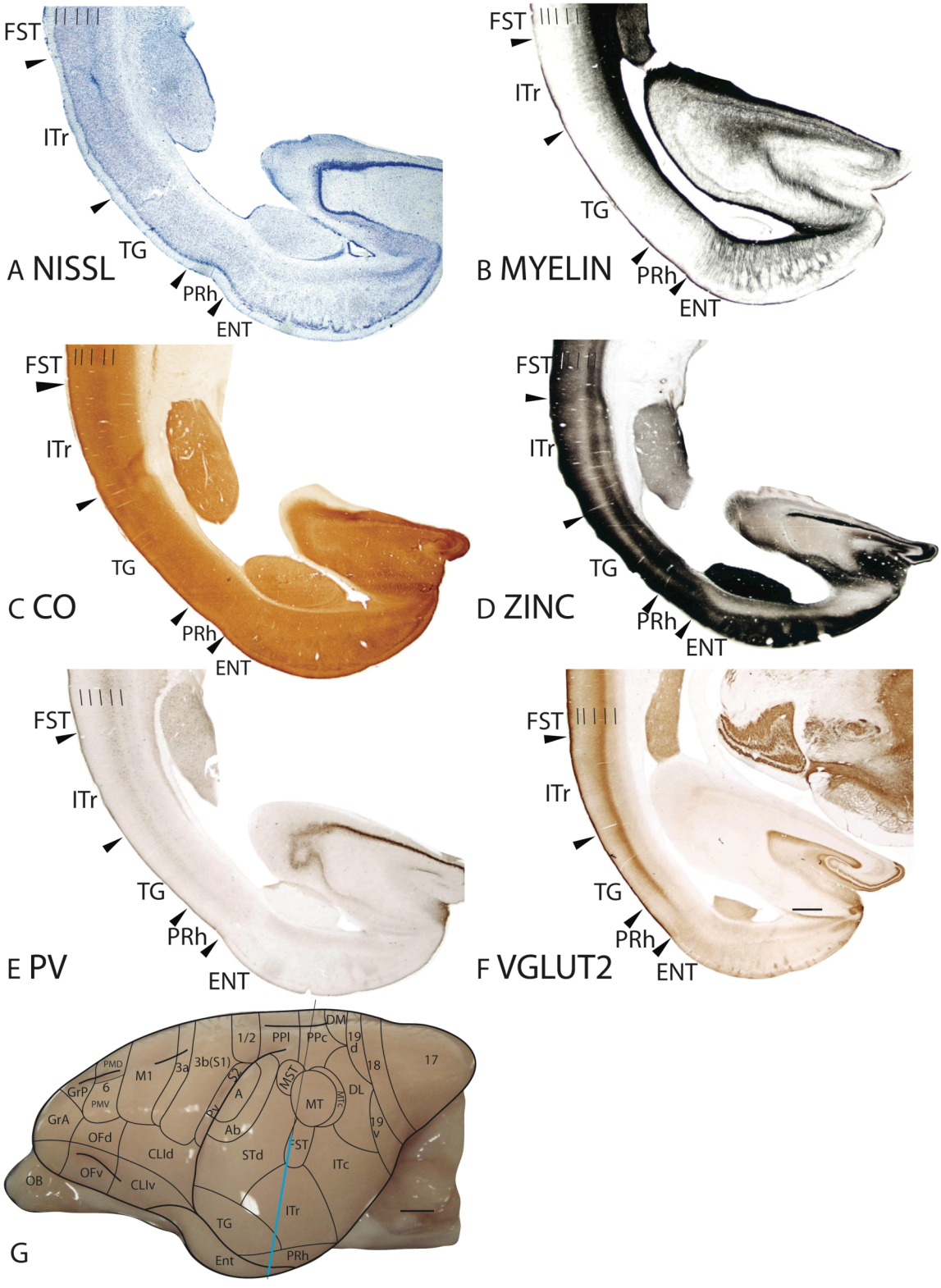
FST
ITr
TG
PRh
ENT
A NISSL
B MYELIN
C CO
D ZINC
E PV
F VGLUT2
G
DM
1/2
PPl
PPc
19 d
18
17
PMD
M1
3a
3b(S1)
6
PMV
GrP
GrA
OFd
CLId
OFv
CLIv
OB
Ab
A
MST
MT
DL
19 v
STd
ITc
Ent

Inferior temporal rostral (ITr) and inferior temporal caudal (ITc) areas. Previous architectonic studies have identified two to three areas within the inferior temporal cortex of galagos (Zilles et al., 1979; Preuss and Goldman-Rakic, 1991a). Here, we have identified two cortical areas, the inferior temporal rostral (ITr) and caudal (ITc) areas.

In Nissl preparations, ITr has a thin, darkly stained band in layer 4 and a pale layer 5 (Fig. 57A). Throughout the cortical layers, ITr is more darkly stained than the pole of the temporal cortex, the a*rea temporopolaris* (TG) (Fig. 57A). In myelin preparations, ITr is more densely myelinated than TG and is as densely myelinated as FST (Fig. 57B). ITr stains more darkly for CO than TG, and is stains at similar intensity to FST (Fig. 57C). Layers 4 and inner 6 of ITr expresses lower levels of free ionic zinc than the other cortical layers, giving ITr a banded appearance in the zinc stain (Fig. 57D). Compared to FST and TG, ITr expresses less zinc throughout the cortical layers, with the greatest difference in layers 4 and inner 6 of ITr (Fig. 57D). ITr stains poorly for PV immunopositive termination, and has a scattered population of PV immunopositive cell bodies in layer 4 that tapers off towards the ITr/TG border (Fig. 57E). In VGluT2 preparations, ITr has a darkly stained band in layer 4 that tapers off towards the ITr/TG border (Fig. 57F).

Throughout the cortical layers, ITc is more densely packed with cells than the ventrally adjoining perirhinal cortex (PRh), giving ITc a darker appearance than PRh in Nissl preparations (Fig. 58A). ITc is moderately myelinated and is more densely myelinated than PRh (Fig. 58B). In CO preparations, layer 4 of ITc is darkly stained (Fig. 58C). In zinc preparations, layer 4 and, to a lesser extent, inner layer 6 of ITc expresses less free ionic zinc than the other cortical layers, giving ITc a banded appearance (Fig.

58D). Furthermore, ITc expresses less synaptic zinc than PRh (Fig. 58D). ITc has a scattering of darkly stained PV immunopositive cell bodies in layers 3 to 5 and a dark band of PV immunopositive terminations in layer 4 (Fig. 58E). The poor PV staining in PRh provides a distinct ITc/PRh border. In VGluT2 preparations, ITc has a darkly stained band in layer 4 (Fig. 58F). Additionally, layers 3 and 5 of ITc, but less so for layer 6, express a moderate amount of VGluT2 immunopositive terminations (Fig. 58F).

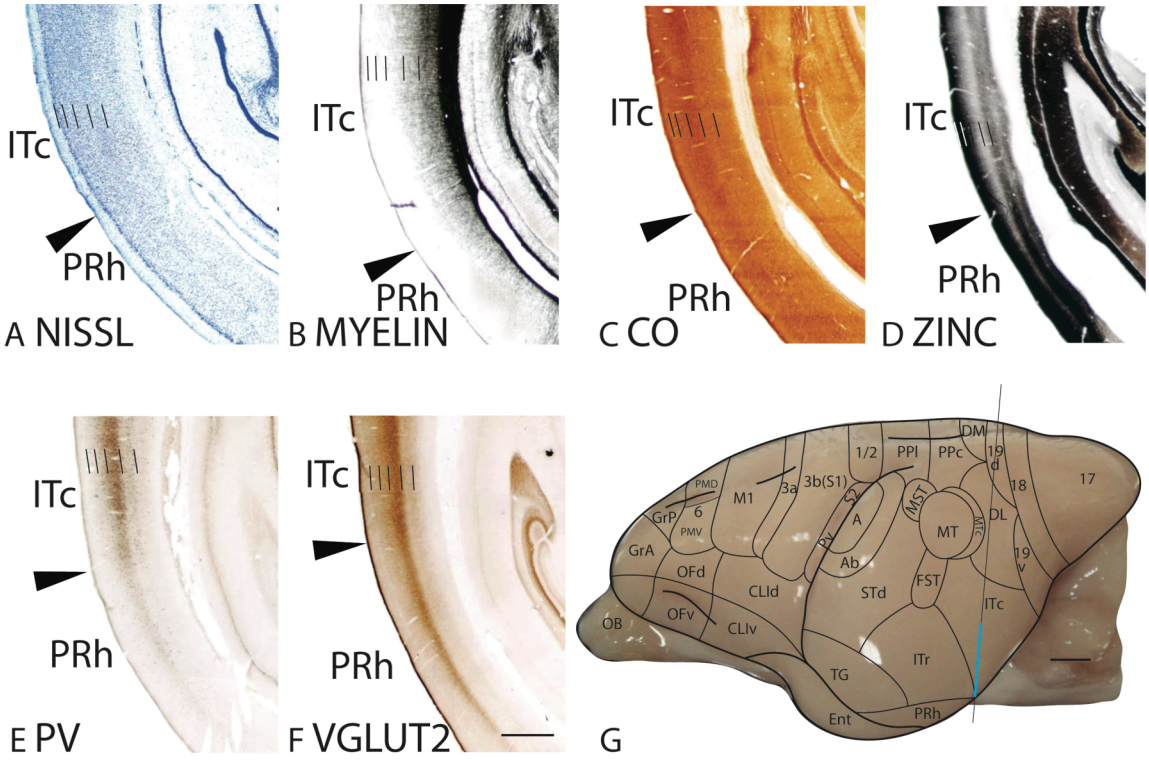

Figure 58. Architectonic characteristics of inferior temporal cortex. The level at which the coronal sections are taken from is indicated by the vertical line on the dorsolateral view of the brain in panels G. The thicker line in panel G marks the regions illustrated in panels A to F. Short lines on the sections indicate the extent of each cortical layers 1 to 6. See table 1 for abbreviations for other areas. The scale bar for brain (panel G) = 2.5mm. The scale bar on the brain section (panel F) = 1mm.

Throughout the cortical layers, ITc expresses more VGluT2 immunopositive terminations than PRh. The presence of darkly stained bands of PV and VGluT2

immunopositive terminations, and relatively poor zinc staining in layer 4 of ITc suggests a predominance of thalamocortical over corticocortical inputs to this layer.

Auditory associated areas – Primary auditory (A) and auditory belt (Ab) areas. The primary auditory region, A, includes primary auditory cortex, A1, and the rostral primary area, R, of Brugge (1982). These two representations of ton frequencies were not distinguished architectonically in the present study and are included together in the auditory field, A. A portion of area A is on the surface of the temporal lobe and another portion is on the caudal bank of the lateral sulcus (Fig. 47). Sectioning artificially flattened cortex tangential to the pia is a way to appreciate much of the borders of area A (Fig. 59). This involves unfolding the lateral sulcus and it is difficult to keep all of area A on the same plane. The hooked shape of area A in the flattened sections in figure 59 is likely to be due to uneven flattening, as area A is likely to be ovalish in shape (Brugge, 1982). In flattened sections, area A is a densely myelinated region, surrounded by a myelin-poor region, the auditory belt (Fig. 59B). Area A also expresses higher levels of CO than the surrounding cortex, suggesting that area A is more highly metabolically active (Fig. 59C). Sections through layer 4 of area A stain poorly for free ionic zinc (Fig. 59D), consistent with the evidence that primary auditory cortex receives dense thalamic inputs from the medial geniculate complex and few layer 4 corticocortical terminations, at least in other primates (Luethke et al., 1989). Furthermore, area A is darkly stained for PV (Fig. 59E) and VGluT2 (Fig. 59F) immunopositive terminations, indicating a higher population of thalamocortical terminations in layer 4 of area A than in surrounding cortex.

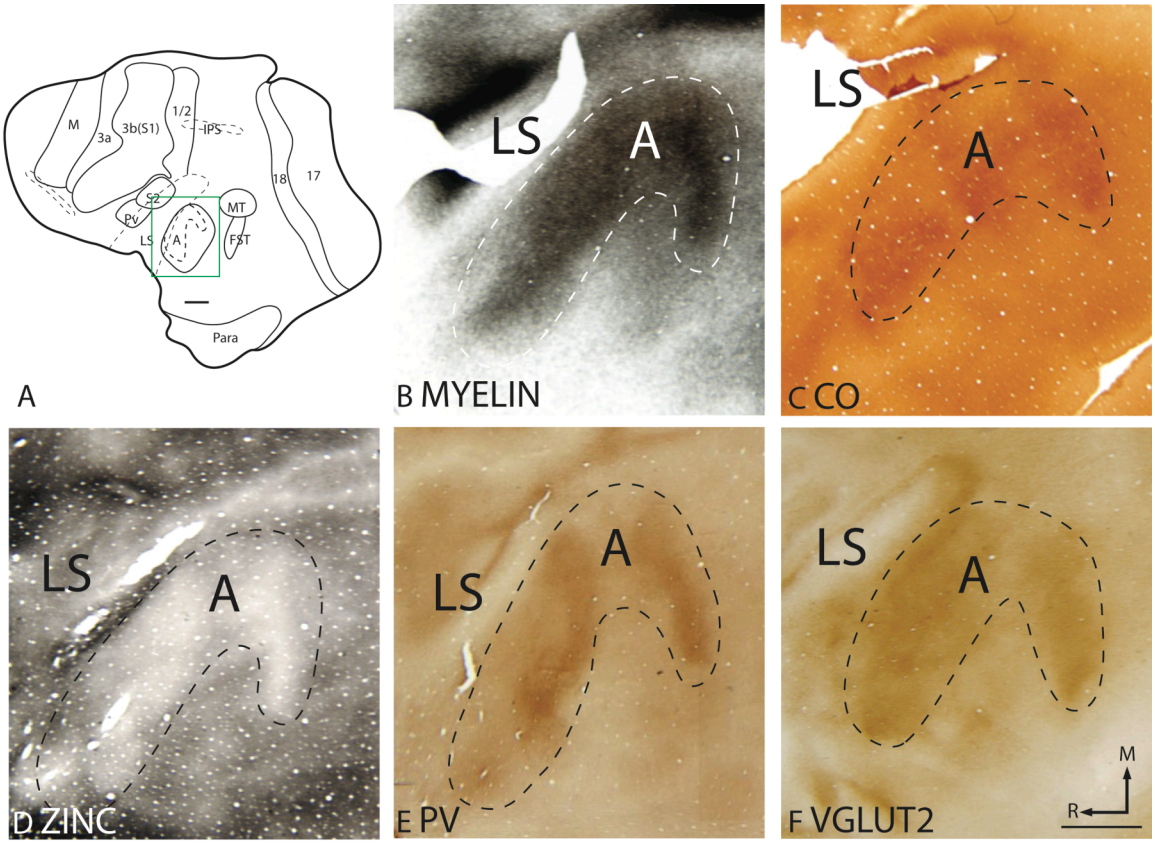

Figure 59. Architectonic characteristics of auditory cortex in flattened preparations. The boxed region in A is shown in panels B to F at higher magnification. Dashed lines show the approximate location of the cortical borders. The scale bar on the brain (panel A) = 4mm, on brain section (panel F) = 2mm.

In Nissl preparations, layer 4 of area A is densely populated with granule cells, and layer 5 is more sparsely populated with larger pyramidal cells (Fig. 60A; 61A). Area A is densely myelinated (Fig. 60B; 61B) and has a layer 4 that is darkly stained in CO preparations (Fig. 60C). Layer 4 of area A stains poorly for free ionic zinc compared to layer 4 of the adjoining Ab (Fig. 60D). In PV preparations, a darkly stained band of PV immunopositive terminations is present in layer 4 of area A (Fig. 60E; 61C), with a scattering of darkly stained PV immunopositive cell bodies in the upper cortical layers (Fig. 61C). In addition, layer 4 of area A is also darkly stained for VGluT2

immunopositive terminations (Fig. 61D). The presence of dense populations of PV and VGluT2 immunopositive terminations and the near absence of terminations containing free ionic zinc suggests the predominating input to layer 4 of area A is from the thalamic nuclei, likely the ventral subdivision of the medial geniculate (Luethke et al., 1989; de la Mothe et al., 2006), rather than from other cortical areas.

In monkeys, a narrow belt of secondary auditory areas surrounds the primary core auditory areas (Kaas and Hackett, 2000). These areas are not uniform in architectonic appearance (Hackett et al., 1998), but they can be difficult to distinguish from each other. Here, we identify a narrow, lateral auditory belt and a narrow medial auditory belt, the main divisions defined in monkeys. Connectional studies with tracer injections have suggested that lateral Ab (identified as A II in Conley et al., 1991) has connections with secondary nuclei of the medial geniculate body and none with the ventral subdivision of the medial geniculate body. Architectonically, layer 4 of lateral Ab is paler and less densely packed with cell bodies than layer 4 of area A (Fig. 60A). Lateral Ab is less myelinated (Fig. 60B) and expresses lower staining for CO (Fig. 60C) than area A. Lateral Ab stains darker in zinc preparations than area A, especially in layer 4 (Fig. 60D). In PV (Fig. 60E) and VGluT2 (not shown) preparations, lateral Ab is lighter stained for PV and VGluT2 immunopositive terminations than area A. The increased expression of free ionic zinc, and decreased expression of PV and VGluT2 immunopositive terminations in layer 4 of lateral Ab suggests that lateral Ab receives a higher proportion of corticocortical than thalamocortical inputs. It is possible that some of these inputs originate from area A.

Figure 60. Architectonic characteristics of auditory cortex. The level at which the horizontal sections are taken from is indicated by the horizontal line on the lateral view of the brain in F. The thicker line in panel F marks the regions illustrated in panels A to E. Short lines on the sections indicate the extent of each cortical layers 1 to 6. See table 1 for abbreviations for other areas. The scale bar for brain (panel F) = 2.5mm. The scale bar on the brain section (panel E) = 1mm.

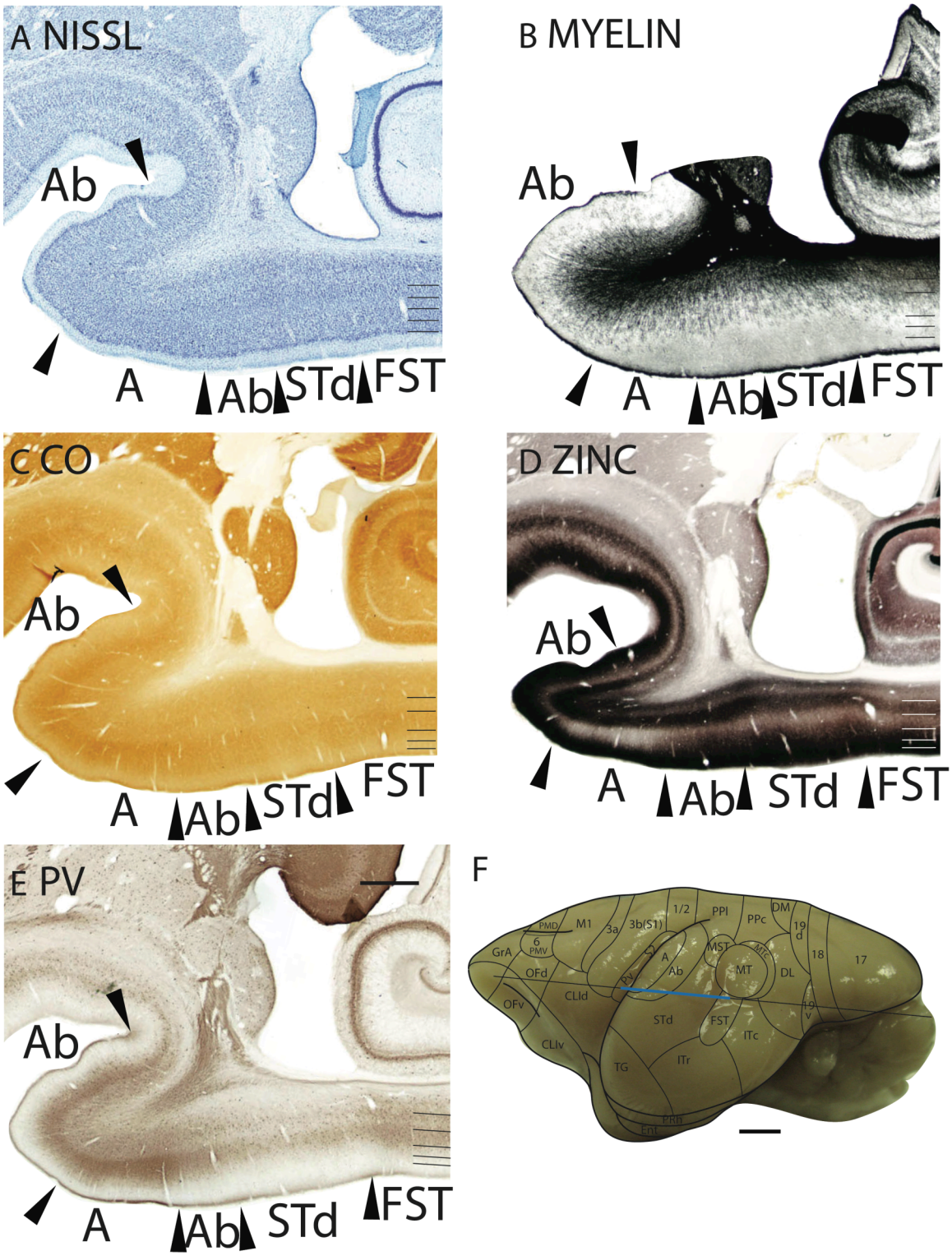
A NISSL
Ab
A
Ab
STd
FST
B MYELIN
Ab
A
Ab
STd
FST
C CO
Ab
A
Ab
STd
FST
D ZINC
Ab
A
Ab
STd
FST
E PV
Ab
A
Ab
STd
FST
F
PMD
M1
3a
3b(S1)
1/2
PPl
PPc
DM
19
d
6
PMV
GrA
OFd
CLId
OFv
CLIv
TG
STd
FST
ITc
ITr
PRh
Ent
A
Ab
MST
MTc
MT
DL
18
17
19
v

Medial Ab has a thinner granular layer 4 in Nissl preparations (Fig. 60A) and is moderately myelinated (Fig. 60B). Additionally, medial Ab expresses lower staining for CO (Fig. 60C) than area A. The border between medial Ab and area A is distinct in zinc preparations as medial Ab stains darker in zinc preparations than area A, especially in layer 4 (Fig. 60D). In PV (Fig. 60E) and VGluT2 (not shown) preparations, medial Ab is moderately stained, and the population of PV and VGluT2 immunopositive terminations is less dense than that in area A. This indicates that medial Ab receives a higher proportion of corticocortical inputs and lower proportions of thalamocortical inputs than area A.

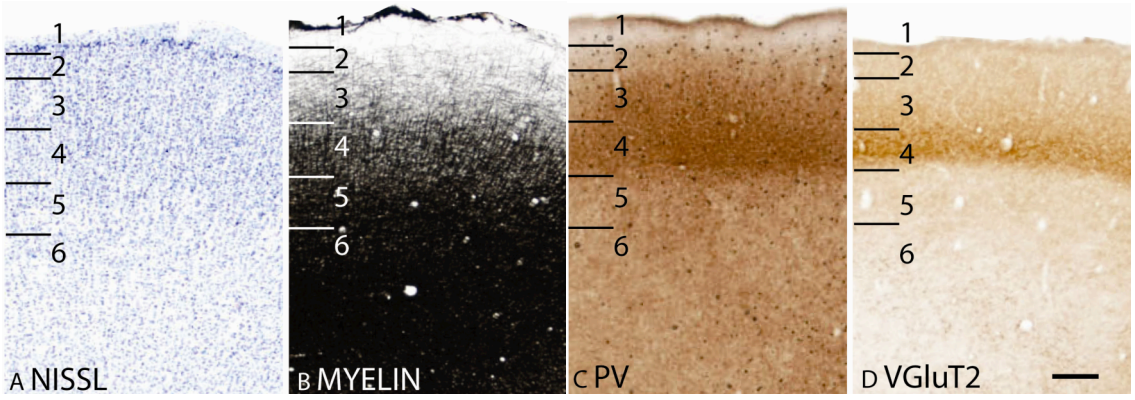

Figure 61. The laminar characteristics of primary auditory area at higher magnification. Scale bar = 1mm.

Remaining temporal areas – Area temporopolaris (TG) and superior temporal dorsal area (STd). The temporal pole was identified as area TG by von Bonin and Bailey (1947) and as area 38 by Brodmann (1909). We have retained area TG as the nomenclature of the temporal pole in galagos to be consistent with Preuss and Goldman-Rakic, 1991a). Area TG is bordered dorsally by ITr and STd, and ventrally by PRh. In Nissl preparations, TG is differentiated from ITr by the lack of a darkly stained layer 4 in TG, and from PRh by the overall paler appearance of TG compared to PRh (Fig. 57A). In

myelin preparations, TG is less densely myelinated than ITr and more densely myelinated than PRh (Fig. 57B). Layer 4 of TG is lighter stained in CO preparations than ITr (Fig. 57C). Layer 4 of TG is more lightly stained than the other cortical layers, giving TG a banded appearance in zinc preparations (Fig. 57D). Throughout the cortical layers, TG stains darker than ITr, and lighter than PRh for the zinc stain (Fig. 57D). The TG/PRh border is distinct in zinc preparations as the lighter zinc-stained layer 4 of TG terminates at the border (Fig. 57D). TG is poorly stained in PV preparations and does not have any visible staining for PV immunopositive terminations or cell bodies (Fig. 57E). In VGluT2 preparations, TG has a darkly stained band of VGluT2 immunopositive terminations in layer 4 (Fig. 57F). This VGluT2 immunopositive band is thinner than that in ITr and thicker than that in PRh.

The superior temporal dorsal area (STd) is bordered rostrally by Ab and caudally by ITr and FST. The dorsal border of STd with the posterior parietal cortex is not clear and is left unmarked. STd is bordered ventrally by TG. In Nissl preparations, STd has a thin layer 4, and broad layers 5 and 6 (Fig. 60A). Additionally, layers 4 and outer 6 of STd are pale in appearance (Fig. 60A). STd is moderately myelinated and layer 6 of STd is more myelinated than Ab and FST (Fig. 60B). STd expresses less CO and is as such less darkly stained in CO preparations that the adjoining Ab and FST (Fig. 60C). Layers 1 to 3 and 5 of STd are darkly stained for free ionic zinc (Fig. 60D). Throughout the cortical layers, STd is more lightly stained than Ab and more darkly stained than FST in zinc preparations (Fig. 60D). STd is lightly stained in PV (Fig. 60E) and VGluT2 (not shown) preparations. In sections stained for PV, two faint bands of PV immunopositive

terminations with a scattering of darkly stained PV immunopositive cell bodies are observed in layers 4 and outer 6 of STd (Fig. 60E).

Parietal cortex

The parietal cortex of galagos can be divided into anterior, lateral and posterior regions. The anterior region consists of areas involved in early stages of cortical processing of somatosensory inputs, and includes the primary somatosensory area, 3b(S1), a rostrally adjoining strip of transition cortex, area 3a, and a caudally adjoining area termed here, area 1/2. Posterior parietal cortex, identified by Brodmann (1909) in a prosimian lemur as area 7, includes all the parietal areas caudal to area 1/2, with some of the cortex buried in the intraparietal sulcus (IPS). The lateral somatosensory cortex in the lateral sulcus includes the second somatosensory area, S2, and the adjoining parietal ventral area, Pv.

Primary somatosensory area, 3b(S1). Microelectrode mapping studies (Carlson and Welt, 1980; Sur et al., 1980) have shown that the primary somatosensory area in galagos contain a complete, inverted representation of the contralateral cutaneous surface, with the oral and face representations located ventrally, followed by the hand, trunk, foot, leg then tail dorsally. This area is coextensive with the architectonically defined area 3b(S1) that has a koniocellular appearance. In Nissl preparations, area 3b(S1) has a thick, darkly stained layer 4 that is densely packed with granule cells (Fig. 62A; 65A). Furthermore, layer 4 of area 3b(S1) does not maintain a constant thickness throughout the coronal plane (Fig. 62A), being generally thicker in hand and face representations than medially for trunk and foot representations. Thinner regions also correspond to

discontinuities in the representation of the body surface, such as between the hand and face representations. At higher magnifications, layer 3 is densely packed with medium-sized pyramidal cells, whereas layer 5 is sparsely populated with larger pyramidal cells (Fig. 63A). Area 3b(S1) is densely myelinated (Fig. 62B; 65B), with poorly defined inner and outer bands of Baillarger (Fig. 63B). In CO preparations, layer 4 of area 3b(S1) is darkly stained, suggesting that this area is metabolically active (Fig. 62C; 65C). Fainter bands of CO staining are present in inner layer 3, likely 3b and 3c, and layer 6 (Fig. 63C). The architectonic borders of area 3b(S1) are distinct in zinc preparations as the poor staining layer 4 terminates at the medial boundary with the paralimbic area (Para), at the ventral boundary with the claustral region (Fig. 16D), and at the caudal boundaries with areas 1/2 and S2/Pv (Fig. 65D). In PV preparations, area 3b(S1) stains darker than the surrounding paralimbic and claustral regions (Fig. 62E). A dense, discontinuous band of PV immunopositive terminations is present in layer 4 (Fig. 62E) and, to a lesser extent, layers 3, 5 and 6 of area 3b(S1) (Fig. 62E; 63E; 65E). Layers 3b, 3c and 4 of area 3b(S1) are also highly populated with darkly PV stained cell bodies, whereas layers 5 and 6 are less densely populated with PV immunopositive cell bodies (Fig. 63E). In VGluT2 preparations, two stained bands area observed in area 3b(S1). A thick darkly stained band of VGluT2 immunopositive terminations in layer 4 also extends up into inner layer 3 (Fig. 62F; 63F; 65F). A fainter VGluT2 immunostained band is present in layer 6 (Fig. 62F; 63F). The dense populations of PV and VGluT2 immunopositive terminations, and sparse population of terminations containing free ionic zinc in layer 4 of area 3b(S1) suggests a larger proportion of inputs to layer 4 originate from the ventroposterior nucleus of the thalamus rather than from other cortical areas.

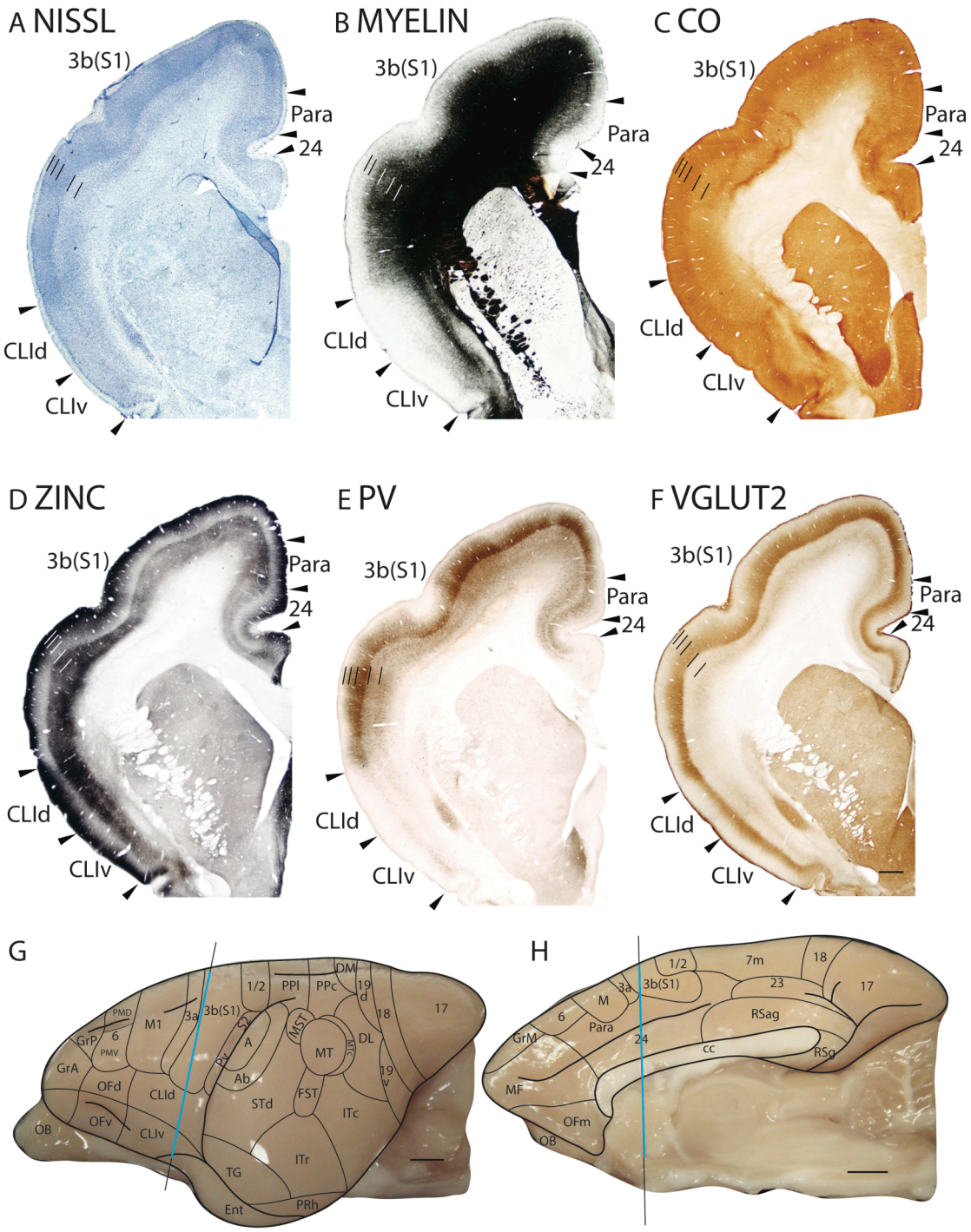

Figure 62. Architectonic characteristics of somatosensory cortex. The level at which the coronal sections are taken from is indicated by the vertical line on the lateral (G) and medial (H) of the brain. The thicker line in panels G and H marks the regions illustrated in panels A to F. Short lines on the sections indicate the extent of each cortical layers 1 to 6. See table 1 for abbreviations for other areas. The scale bar for brain (panels G, H) = 2.5mm. The scale bar on the brain section (panel F) = 1mm.

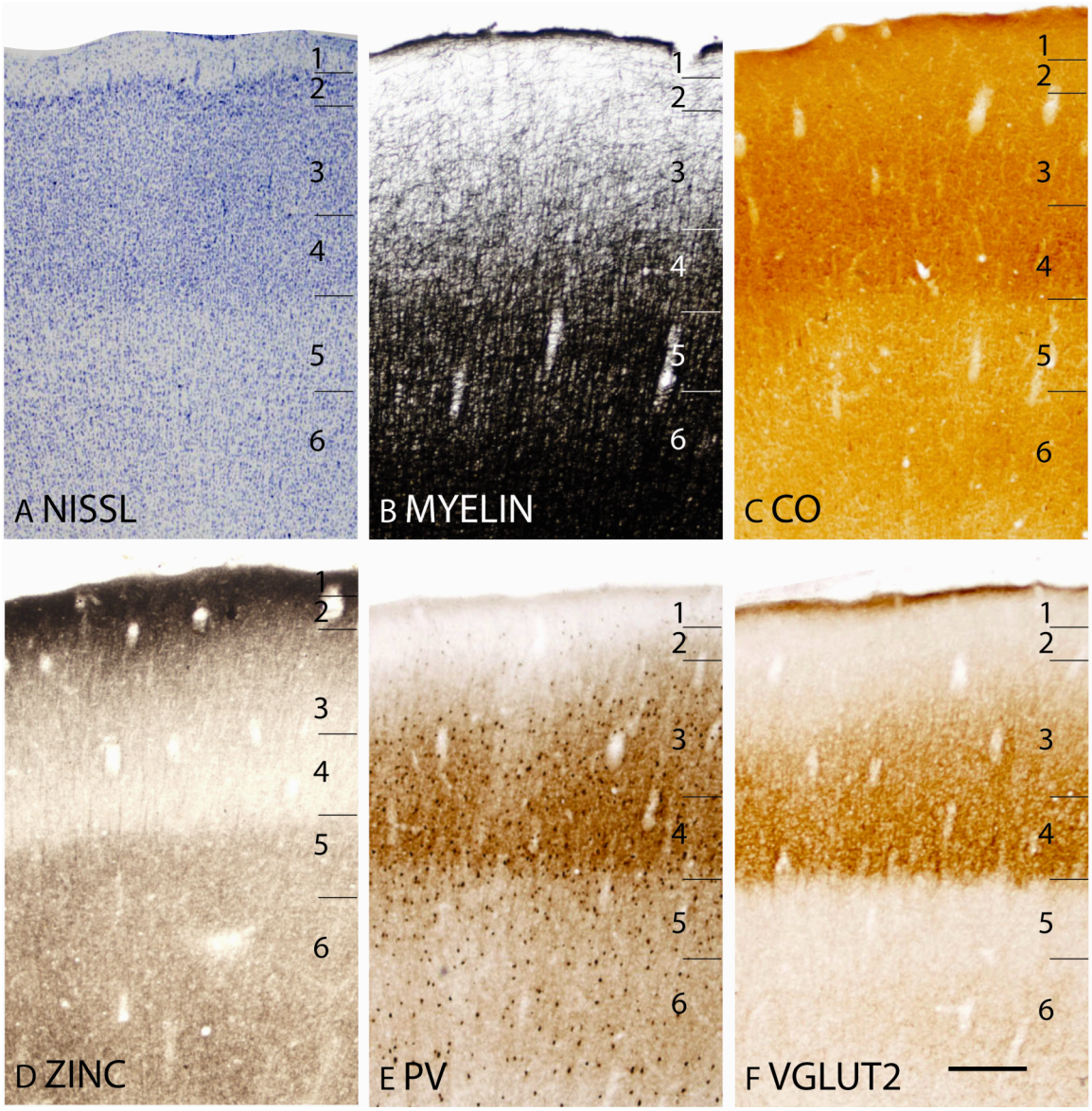

Figure 63. The laminar characteristics of primary somatosensory area at higher magnification. Scale bar = 0.25mm.

The full extent and heterogeneous appearance of area 3b(S1) can be appreciated in artificially flattened cortex that has been sectioned tangentially to the cortical surface (Fig. 64). Area 3b(S1) is more highly myelinated (Fig. 64A) and expresses more CO (Fig. 64B) than the surrounding cortical areas. In addition, sections through layer 4 show that area 3b(S1) is more poorly stained for free ionic zinc than the surrounding cortical area

(Fig. 64C). However, the staining patterns in the myelin, CO and zinc preparations are patchy. The patchy staining pattern is partly due to the flattening process as the sectioning plane goes in and out of layer 4. In addition, the patchy pattern reflects the discontinuous representation of the cutaneous surface (Nelson et al., 1980; Jain et al., 2001; Kaas et al., 2006), with each patch corresponding to a particular region of the cutaneous surface.

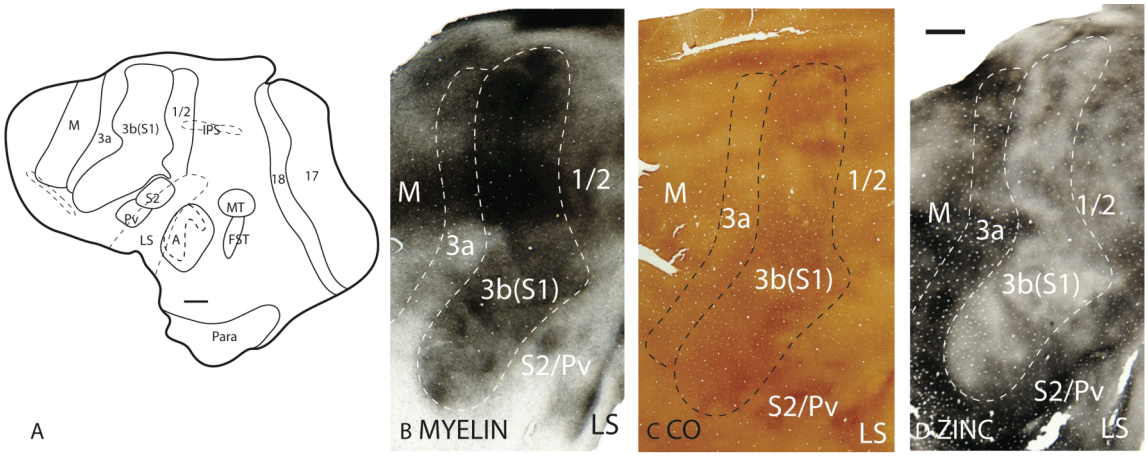

Figure 64. Architectonic characteristics of somatosensory cortex in flattened preparations. The boxed region in A is shown in panels B to D at higher magnification. Dashed lines show the approximate location of the cortical borders. The scale bar on the brain (panel A) = 4mm, on brain section (panel D) = 2mm.

Figure 65. Architectonic characteristics of somatosensory cortex. The level at which the coronal sections are taken from is indicated by the vertical line on the lateral (G) and medial (H) of the brain. The thicker line in panels G and H marks the regions illustrated in panels A to F. Short lines on the sections indicate the extent of each cortical layers 1 to 6. See table 1 for abbreviations for other areas. The scale bar for brain (panels G, H) = 2.5mm. The scale bar on the brain section (panel F) = 1mm.

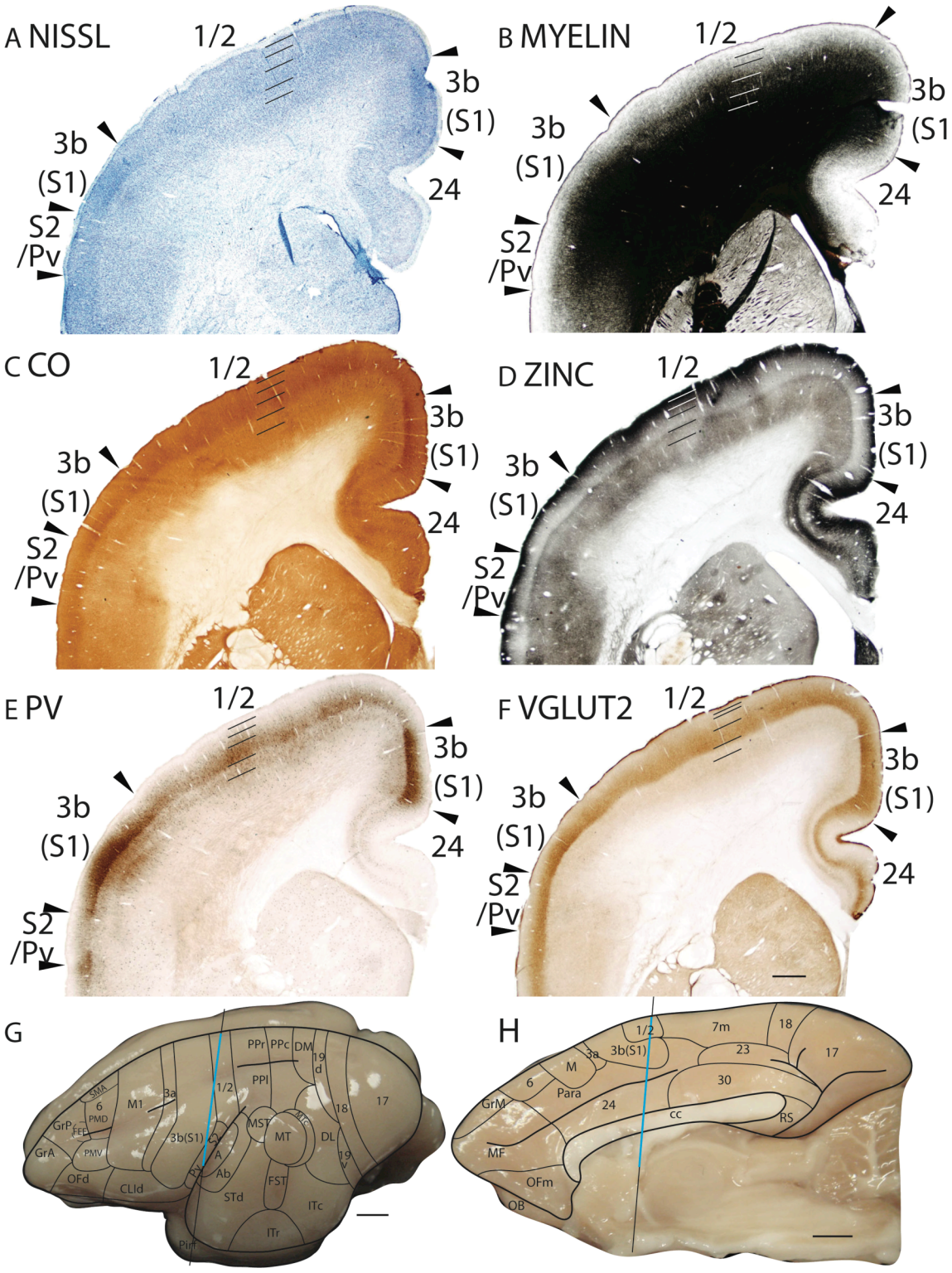
A NISSL
1/2
3b
(S1)
3b
(S1)
S2
/Pv
24
B MYELIN
1/2
3b
(S1)
3b
(S1)
S2
/Pv
24
C CO
1/2
3b
(S1)
3b
(S1)
S2
/Pv
24
D ZINC
1/2
3b
(S1)
3b
(S1)
S2
/Pv
24
E PV
1/2
3b
(S1)
3b
(S1)
S2
/Pv
24
F VGLUT2
1/2
3b
(S1)
3b
(S1)
S2
/Pv
24
G
PPr
PPc
DM
19
d
PPl
1/2
SMA
6
PMD
M1
3a
GrP
FEF
GrA
PMV
3b(S1)
A
Ab
MST
MTc
MT
18
DL
19
v
17
OFd
CLld
STd
FST
ITc
ITr
Pirf
H
1/2
7m
18
3a
3b(S1)
23
17
M
6
Para
30
GrM
24
cc
RS
MF
OFm
OB

Area 3a. In Nissl preparations, area 3a has a thinner layer 4 than area 3b(S1) and a layer 5 that is populated with larger and darker staining cells (Fig. 66B). Area 3a is less densely myelinated than area 3b(S1) with no distinct inner or outer bands of Baillarger (Fig. 66C). Layer 4 of area 3a stains less intensely for CO than layer 4 of area 3b(S1) (Fig. 66D). In zinc preparations, area 3a stains darker than area 3b(S1) (Fig. 66E), suggesting that area 3a receives more corticocortical inputs than area 3b(S1). Layer 4 of area 3a has reduced staining for PV (Fig. 66F) and VGluT2 (not shown) immunopositive terminations than area 3b(S1), providing further evidence that area 3a receives proportionately less thalamocortical inputs to layer 4 than area 3b(S1). In artificially flattened sections that were cut tangentially to the cortical surface, area 3a is a strip of cortex that lies along the length of the rostral border of area 3b(S1) (Fig. 64). In these sections, area 3a is a more lightly myelinated strip of cortex (Fig. 18A) and stains lighter for CO (Fig. 64B) than area 3b(S1). Furthermore, area 3a is more darkly stained for free zinc ions than area 3b(S1) in sections through layer 4 of the cortex (Fig. 64C).

Area 1/2. The identity of the band of somatosensory cortex just caudal to area 3b(S1) is not established, but it is in the position of area 1 or area 1 plus 2. There is a tradition of referring to this region as area 1/2 (Sanides and Kristanamurti, 1967; see Wu and Kaas, 2003). The region of cortex that we have identified as area 1/2 corresponds to area 1/2 of Wu and Kaas (2003), and overlaps with the posterior somatosensory area (area 2-5) identified by (Preuss and Goldman-Rakic, 1991a). Connectional studies using tracer injections have shown that area 1/2 of galagos has dense connections with area 3b(S1) as well as areas S2 and Pv of lateral somatosensory cortex (Wu and Kaas, 2003).

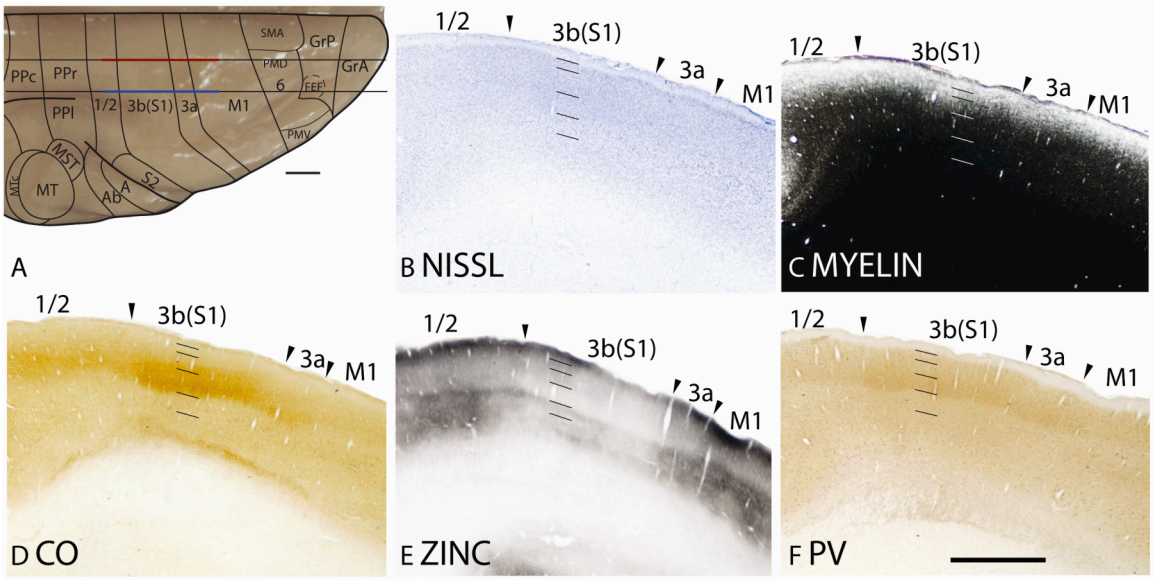

Figure 66. Architectonic characteristics of somatosensory cortex. The level at which the sagittal sections are taken from is indicated by the horizontal line on the dorsal view (A) of the brain. The thicker line in panel A marks the regions illustrated in panels B to F. Short lines on the sections indicate the extent of each cortical layers 1 to 6. See table 1 for abbreviations for other areas. The scale bar for brain (panel A) = 2.5mm. The scale bar on the brain section (panel F) = 1mm.

In Nissl preparations, area 1/2 has a paler appearance than area 3b(S1) and layer 4 of area 1/2 is less densely packed with cells in comparison to area 3b(S1) (Fig. 65A; 66B). Area 1/2 is moderately myelinated and is less myelinated than area 3b(S1)(Fig. 65B; 66C). The lower myelination density of area 1/2 is also observed in sections that were cut tangentially to the pia (Fig. 18A). Layer 4 of area 1/2 has a CO-stained band that is less intensely stained than that in area 3b(S1) (Fig. 65C; 66D). The lowered CO staining of area 1/2 is observed in flattened sections as well (Fig. 64B). Area 1/2 expresses higher levels of zinc staining, especially in layer 4, than area 3b(S1) (Fig. 65D; 66E). The increased zinc staining intensity of area 1/2 is also observed in sections cut tangentially to the cortical surface, through layer 4 (Fig. 64C). Layer 4 of area 1/2 stains moderately for PV immunopositive terminations and a fainter band in layer 5 is observed

(Fig. 65E; 66F). Additionally, PV immunopositive cell bodies are present in layers 3 to 5 and, to a lesser extent, layer 6. Compared to area 3b(S1), area 1/2 expresses lower levels of PV staining (Fig. 65E; 66F). There is a diffuse band of VGluT2 staining in layer 4 of area 1/2 that is less intensely stained than that in layer 4 of area 3b(S1)(Fig. 65F). The increased intensity of zinc staining and lowered intensities of PV and VGluT2 staining in area 1/2 in comparison to area 3b(S1), likely reflect a proportionately greater corticocortical inputs, and proportionately smaller thalamocortical inputs than area 3b(S1).

Secondary somatosensory (S2) and parietal ventral (Pv) areas. The secondary somatosensory (S2) and parietal ventral (Pv) areas lie on the rostral bank toward the borders of the lateral sulcus, where they extend into the depths. Connectional studies using tracer injections have shown that S2 and Pv have topographic connections with area 3b(S1)(Wu and Kaas, 2003). S2 and Pv have a topographic representation of the cutaneous surface and the neurons in both areas have larger receptive fields than those in area 3b(S1) (Burton and Carlson, 1986; Garraghty et al., 1991; Wu and Kaas, 2003). Architectonically, S2 and Pv have similar characteristics. As such we did not distinguish an architectonic border between the two fields and the results presented here for S2 also apply to Pv.

In Nissl preparations, S2 has a paler staining layer 4 that is less densely populated by granule cells than area 3b(S1)(Fig. 65A). Furthermore, S2 has a paler appearance than the ventrally adjoining claustral area (CLI)(Fig. 65A). S2 is moderately myelinated (Fig. 65B). Compared to the dorsally adjacent area 3b(S1), S2 is less densely myelinated, and compared to the ventrally adjacent CLI, S2 is more densely myelinated (Fig. 65B). In CO

preparations, S2 expresses less CO than the adjoining areas 3b(S1) and CLI (Fig. 65C). Throughout the cortical layers, S2 stains darker in zinc preparations than the surrounding areas 3b(S1) and CLI (Fig. 65D). In PV preparations, S2 does not have the distinct band of PV immunopositive terminations that is present in the surrounding cortical areas 3b(S1) and CLI (Fig. 65E). Furthermore, a scattering of PV immunostained cell bodies is present in S2 (Fig. 65E). S2 expresses moderate levels of VGluT2 immunopositive terminations in layer 4, which is lower than that in area 3b(S1) and thinner than that in CLI (Fig. 65F).

In artificially flattened sections that were cut tangentially to the pia, S2 has a lower level of myelination (Fig. 64A) and expression of CO (Fig. 64B) compared to area 3b(S1). Additionally, in sections through layer 4, S2 is more darkly stained for free ionic zinc than area 3b(S1)(Fig. 64C). The staining of S2 in flattened sections is patchy in appearance and this may be due to the presence of different representations of body parts in a single section.

Posterior parietal region. The posterior parietal region covers most of the IPS region and extends over the medial wall as area 7m. Divided into at least three areas, the posterior parietal region includes the posterior parietal rostral (PPr), lateral (PPl), and caudal (PPc) areas. The region we define as the posterior parietal cortex closely matches area 7 of (Preuss and Goldman-Rakic, 1991a), which is divided into six fields. The rostral portion of the posterior parietal cortex, which likely includes PPr and PPl, produces complex movements in the galagos when stimulated by microelectrode (Stepniewska et al., 2005b), whereas the caudal region, which is likely to be co-extensive with PPc, seems to receive visual inputs from areas such as V1 (Lyon and Kaas, 2002c).

Figure 67. Architectonic characteristics of posterior parietal cortex. The level at which the coronal sections are taken from is indicated by the vertical line on the dorsolateral view of the brain (A). The thicker line in panel A marks the regions illustrated in panels B to G. Short lines on the sections indicate the extent of each cortical layers 1 to 6. See table 1 for abbreviations for other areas. The scale bar for brain (panel A) = 2.5mm. The scale bar on the brain section (panel G) = 1mm.

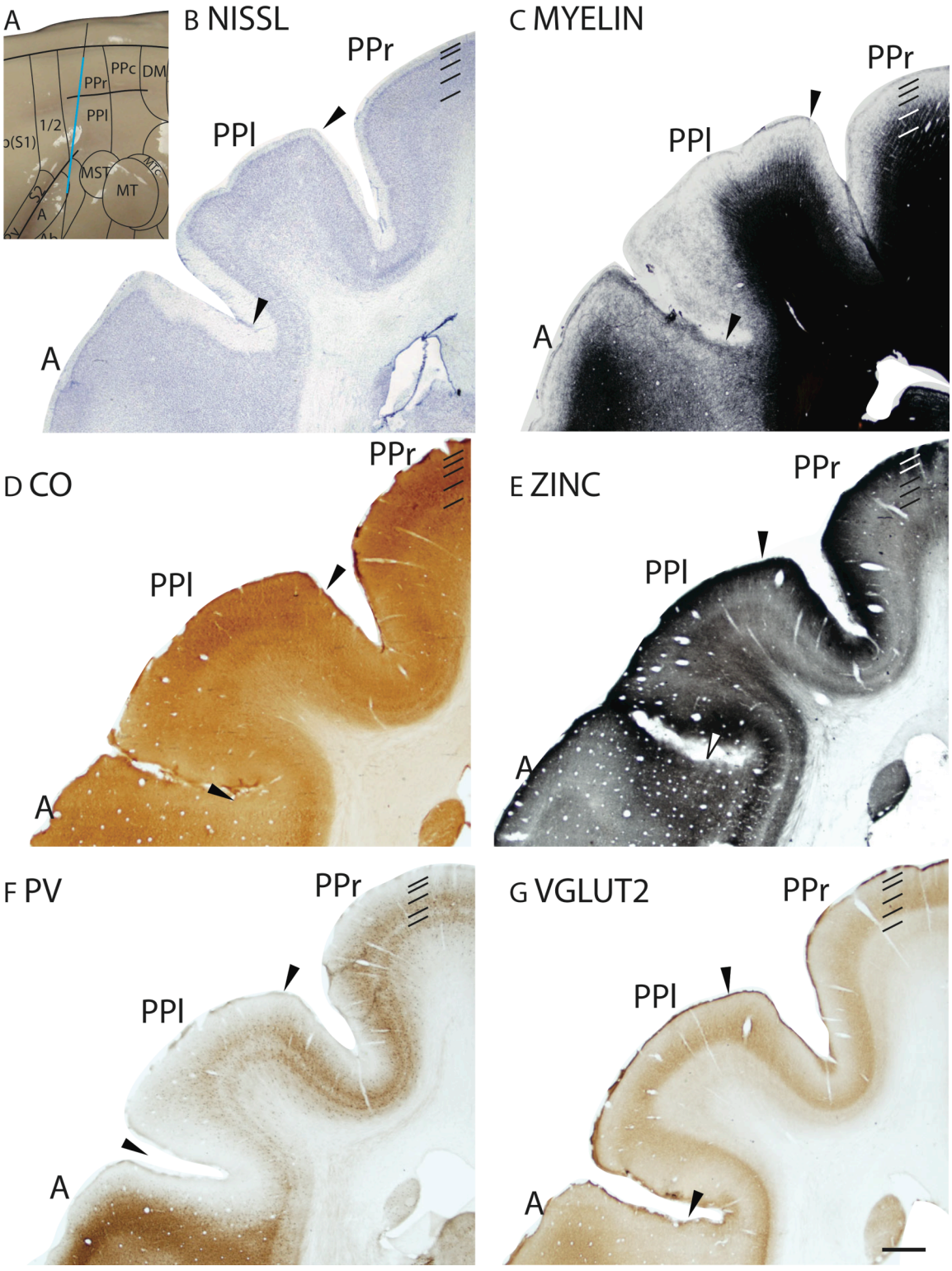
A
B NISSL
C MYELIN
D CO
E ZINC
F PV
G VGLUT2
PPr
PPl
PPc
DM
1/2
MST
MT
MTc
A

The architectonic appearance of PPl and PPr are similar, with subtle differences. In Nissl preparations, PPl has a paler appearance than PPr (Fig. 67B). Layer 4 of PPl is less densely populated with granule cells and layer 4 of PPr is thin, but more densely populated with granule cells (Fig. 67B). PPl and PPr have similar myelination densities (Fig. 67C). In CO preparations, layer 4 of PPl and PPr are moderately stained, with a second faint and thin band in layer 6 (Fig. 67D). Throughout the cortical layers, PPl is more darkly stained for free ionic zinc than PPr, and both PPl and PPr are more intensely zinc-stained than the auditory core, area A (Fig. 67E). There are two PV immunopositive bands in layers 4 and outer 6 of PPl and PPr (Fig. 67F). In addition, PPc is more intensely stained than PPl, with a larger population of PV immunostained cell bodies and PV immunopositive terminations (Fig. 67F). PPl and PPr are moderately stained for VGluT2 immunopositive terminations, with PPr containing a more diffusely stained band in layer 4 (Fig. 67G).

Architectonically, PPc has a moderately populated granular layer 4 than is less densely populated than layer 4 of area 7 (Fig. 54A). In myelin preparations, PPc is moderately myelinated with a distinct outer band of Baillarger, and is more highly myelinated than area 7m (Fig. 54B). PPc has two CO stained bands, in layers 4 and 6, and is less darkly CO stained than area 7m (Fig. 54C). PPc has similar CO expression levels to PPr and PPl (not shown). PPc stains less darkly for synaptic zinc than the adjoining areas MTc and 7m (Fig. 54D). In PV preparations, PPc is moderately stained for PV immunopositive terminations, with a darker thicker band in layer 4 and a thinner band in layer 6 (Fig. 54E). PPc is more darkly PV stained than MTc and area 7m (Fig. 54E). Further more, PPc is more darkly stained for PV immunopositive terminations than

PPr and PPl (not shown). In VGluT2 preparations, PPc is more darkly stained than MTc and area 7m (Fig. 54F), as well as PPr and PPl (not shown).

Medial area 7 (7m). In Nissl preparations, layer 4 of area 7m is darkly stained and densely populated with granule cells (Fig. 54A). Area 7m is moderately myelinated with a distinct outer band of Baillarger (Fig. 54B). There are two bands of CO staining in area 7m, a thicker and darker staining band in layer 4 and a thinner and lighter staining band in outer layer 6 (Fig. 54C). Area 7m stains darker than area 23 and lighter than DM in CO preparations (Fig. 54C). In zinc stained sections, area 7m has a banded appearance, with layers 1 to 3, 5 and inner 6 staining darker than layers 4 and outer 6 (Fig. 54D). Area 7m stains darker than DM and lighter than area 23 in zinc preparations (Fig. 54D). Layers 4 and outer 6 of area 7m stains moderately for PV immunopositive terminations and area 7m is sparsely populated with moderately stained cell bodies (Fig. 54E). Area 7m stains lighter than DM and darker than area 23 in PV preparations (Fig. 54E). In VGluT2 preparations, layer 4 is moderately stains and is less intensely stained than layer 4 of DM (Fig. 54F). Furthermore, a thin, faintly stained band of VGluT2 immunopositive terminations is present in outer layer 6 (Fig. 54F).

Claustral cortex

The claustral cortex, or area claustralis isocorticalis (Cli) of Zilles et al. (1979) in galagos is located rostral to the lateral sulcus and ventral to area 3b(S1). This region has been also referred to as insular cortex, although this cortex is not comparable in location to insular cortex of anthropoid primates. Rather, it is more rostral and over the region of

the claustrum. We have identified two areas, the dorsal claustral area (CLId) and ventral claustral area (CLIv).

In Nissl preparations, the border between area 3b(S1) and CLId is distinct as the thick granular layer 4 of area 3b(S1) terminates at the boundary with CLId (Fig. 62A). Throughout the cortical layers, CLId has a paler appearance and is more sparsely populated with cells than area 3b(S1)(Fig. 62A). The CLId/CLIv border is not distinct in Nissl preparations, although CLIv stains darker in for Nissl bodies away from the border with 3b(S1) (Fig. 62A). Both CLId and CLIv are poorly myelinated (Fig. 62B). The poor myelination of CLId provides for a distinct area 3b(S1)/CLId border (Fig. 62B). Both CLId and CLIv stain moderately in CO preparations, with a diffuse CO-stained band in layer 4, although CLIv is more darkly stained away from the CLId/CLIv border (Fig. 62C). The architectonic border between CLId and CLIv is perhaps most distinct in zinc preparations as the intense zinc staining in CLId terminates at the CLId/CLIv border (Fig. 62D). The difference in zinc staining intensities is most marked in layer 4, as layer 4 of CLIv is paler in appearance than CLId (Fig. 62D). This suggests that layer 4 of CLIv receives proportionately less corticocortical inputs using free ionic zinc than layer 4 of CLId. Both CLId and CLIv are poorly stained in PV preparations (Fig. 62E). Layers 4 of CLId and CLIv stain moderately for VGluT2 immunopositive terminations, with the band in layer 4 of CLIv being thicker and more darkly stained than that in CLId (Fig. 62F).

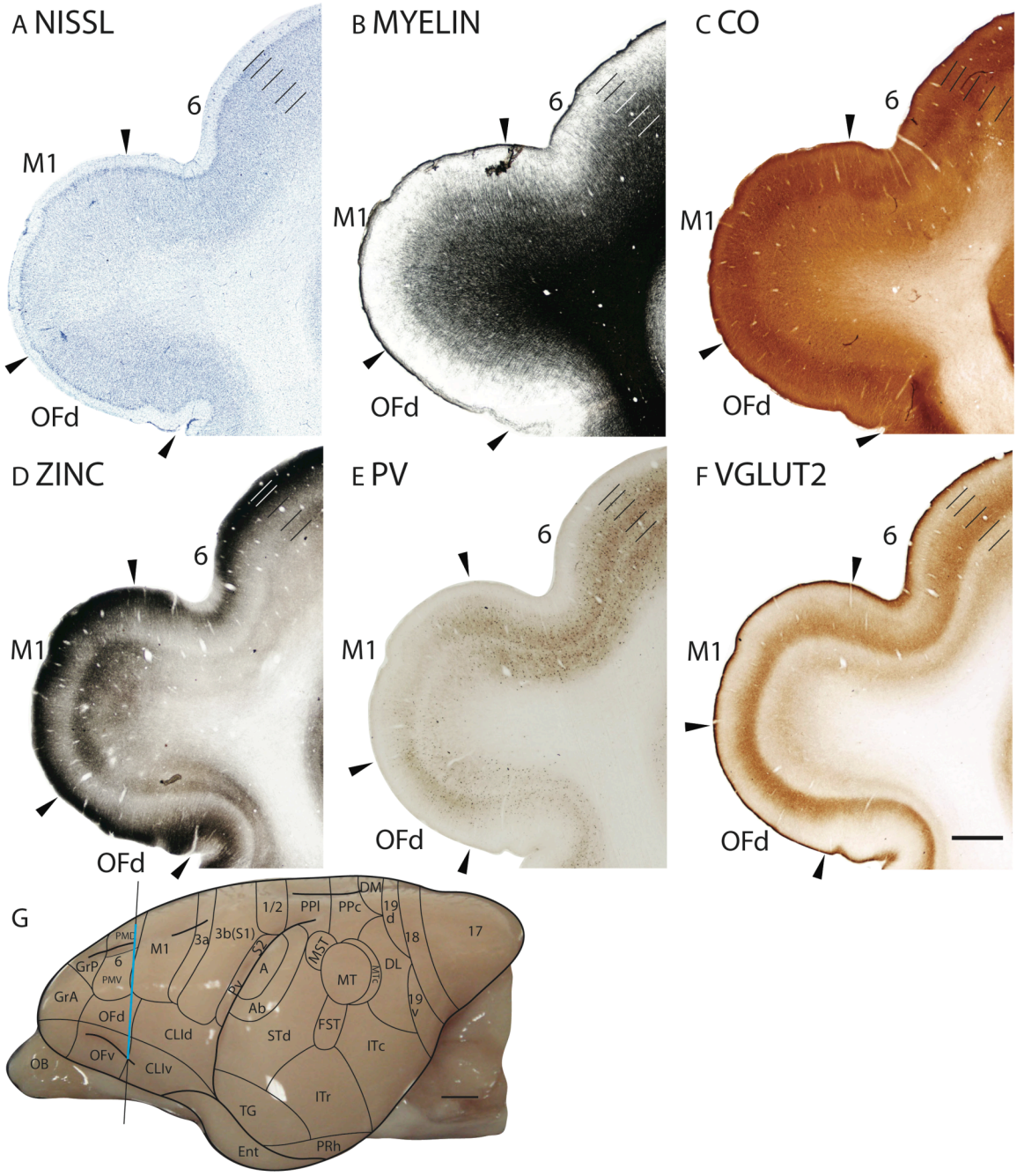

Figure 68. Architectonic characteristics of frontal cortex. The level at which the coronal sections are taken from is indicated by the vertical line on the lateral view of the brain (G). The thicker line in panel G marks the regions illustrated in panels A to F. Short lines on the sections indicate the extent of each cortical layers 1 to 6. See table 1 for abbreviations for other areas. The scale bar for brain (panel G) = 2.5mm. The scale bar on the brain section (panel F) = 1mm.

Frontal cortex

Frontal cortex of galagos is divided into the motor, granular frontal, orbital frontal and the medial frontal regions. The motor region consists of primary motor cortex (M1) and area 6, also known as the premotor and supplementary motor areas. There are at least three areas in the granular frontal region, the granular anterior (GrA), posterior (GrP), and medial (GrM) areas. The orbital frontal region consists of the dorsal (OFd), ventral (OFv) and medial (OFm) areas. There is a possibility of the medial frontal region consisting of more than one cortical area, but due to the lack of clear architectonic and functional evidence, we have left it as a single, medial frontal (MF) area.

Primary motor cortex (M1). In Nissl preparations, M1 has a paler appearance than the rostrally adjoining area 6 and ventrally adjoining claustral region (Fig. 68A). M1 lacks a distinct granular layer 4 and has a thick layer 5 that is populated with large pyramidal cells (Fig. 68A). In myelin preparations, M1 is moderately myelinated and has similar myelination levels to the dorsal claustral area (CLId) and area 6 (Fig. 68B). Layers 2 to 4 of M1 stain moderately for CO (Fig. 68C). The band of CO staining in M1 is thicker but paler than that in area 6 and OFd (Fig. 68C). In zinc preparations, M1 has a banded appearance, with layers 1 to 3 and layer 5 staining darker than layers 4 and 6 (Fig. 68D). Additionally, there are zinc stained 'threads' running through layer 4 of M1 (Fig. 22D). Compared to the adjoining cortical areas, M1 stains more intensely in sections stained for zinc, with layer 4 and 6 expressing more free ionic zinc than the surrounding cortical areas (Fig. 68D). The increased zinc staining in M1 suggests that M1 receives proportionately more corticocortical inputs that use free ionic zinc in the synapses. M1 stains poorly in PV preparations, with a faint band of PV immunopositive terminations in

layer 4 and a scattering of darkly stained cell bodies in layer 5 (Fig. 68E). In VGluT2 preparations, M1 has a moderately stained band in layer 4 and a faint band in layer 6 (Fig. 68F). Compared to the surrounding cortical layers, M1 expresses less VGluT2 immunopositive terminations in layers 4 and 6 (Fig. 68F).

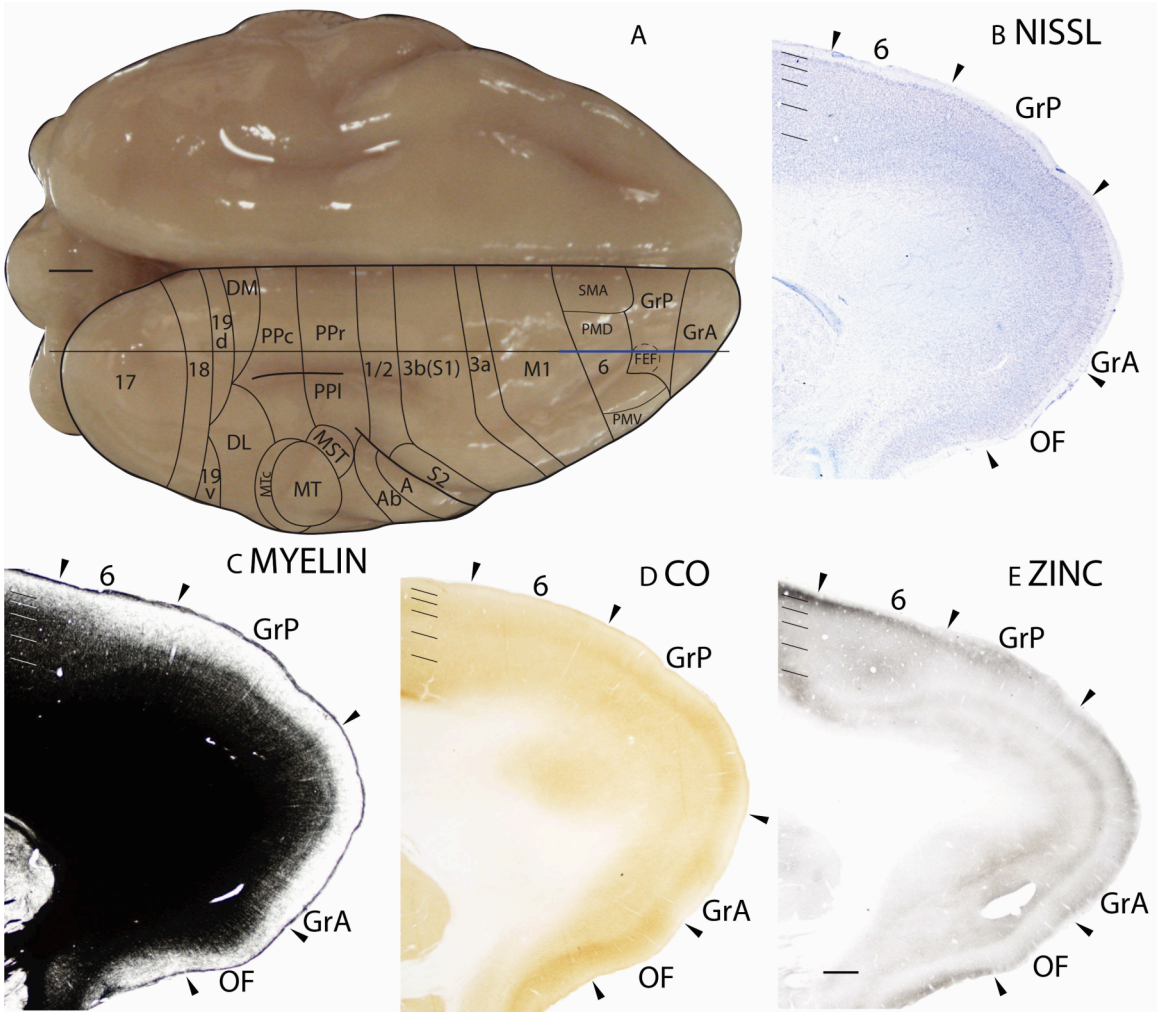

Figure 69. Architectonic characteristics of frontal cortex. The level at which the coronal sections are taken from is indicated by the horizontal line on the dorsal view of the brain (A). The thicker line in panel A marks the regions illustrated in panels B to E. Short lines on the sections indicate the extent of each cortical layers 1 to 6. See table 1 for abbreviations for other areas. The scale bar for brain (panel A) = 2.5mm. The scale bar on the brain section (panel E) = 1mm.

Area 6. Studies of connections using tracer injections and microstimulation have identified up to four areas within area 6, including dorsal (PMd) and ventral (PMv) premotor areas, the supplementary motor area (SMA) and the frontal eye field (FEF) (Wu et al., 2000; Fang et al., 2006; Fang et al., 2008). Although these areas have different connectional and response properties, differences in their architectonic properties are subtle. Their borders, as defined by microelectrode mapping and connectional studies are included on the cortical maps of the brain, and they are described here as a single architectonic field, area 6.

In Nissl preparations, area 6 stains darker than M1 throughout the cortical layers (Fig. 68A). The M1/area 6 border is marked by a more densely populated layer 2, the reappearance of a moderately populated layer 4 with granule cells, and a thinner layer 5 populated with smaller pyramidal cells in area 6 (Fig. 68A). Area 6 is moderately myelinated and the M1/area 6 border is not clearly demarcated in myelin preparations (Fig. 68B). There are two CO stained bands in area 6, a moderately stained band in layer 4 and a lighter stained band in layer 6 (Fig. 68C). In zinc preparations, layer 4 is the most lightly stained, then layer 6, followed by layer 5 (Fig. 68D). Layers 1 to 3 of area 6 are darkly stained in zinc preparations (Fig. 68D). Compared to M1, area 6 expresses less free ionic zinc throughout the cortical layers (Fig. 68D). The M1/area 6 boundary is distinct in PV preparations as area 6 stains darker than M1 (Fig. 68E). There are two bands of PV immunopositive terminations, in layers 4 and 6, of area 6 (Fig. 68E). Darkly stained, PV immunopositive cell bodies are also concentrated in layers 4 and 6 of area 6 (Fig. 68E). Layer 4 of area 6 is moderately stained for VGluT2 immunopositive terminations, with some staining extending up into inner layer 3 (Fig. 68F). Additionally,

a faint band of VGluT2 immunopositive terminations is present in layer 6 of area 6 (Fig. 68F). Area 6 has increased staining for PV and VGluT2 immunopositive terminations, and decreased expression of free ionic zinc compared to M1. This suggests that area 6 receives a proportionately more thalamocortical terminations and less corticocortical terminations than M1.

Granular frontal posterior area (GrP). The granular frontal posterior area (GrP) is bordered caudally by area 6 and ventrally by the orbital frontal region. In Nissl preparations, a thicker granular layer, a thin, darkly stained outer layer 5 and a paler inner layer 5 in GrP marks the area 6/GrP border, (Fig. 69B). Furthermore, GrP has a darker appearance than the dorsal orbital frontal area (OFd) in Nissl stained sections (Fig. 70A). GrP is moderately myelinated with a distinct outer band of Baillarger (Fig. 69C; 70B). In CO preparations, a moderately stained band is present in layer 4 of GrP (Fig. 69D; 70C). GrP, especially layer 4, stains lightly in zinc preparations compared to the granular frontal anterior (GrA)(Fig. 69E) and medial (GrM)(Fig. 70D) areas. In PV preparations, GrP stains moderately for PV immunopositive terminations in layers 3 and 4, with a scattering of moderately stained PV immunopositive cell bodies in layers 3 to 5 (Fig. 70E). Layer 4 is moderately stained and layer 6 is faintly stained for VGluT2 immunopositive terminations (Fig. 70F). GrP less intensely stained than GrM (Fig. 70F) and more intensely stained than GrA (not shown) in VGluT2 preparations.

Granular frontal anterior area (GrA). The granular frontal anterior area (GrA) lies rostral to GrP and extends under to the ventral cortex to border the ventral orbital frontal area (OFv). GrA has a thinner, more sparsely populated granular layer 4 and a thin, darkly stained layer 5 in Nissl preparations (Fig. 69B). In myelin preparations, GrA

has similar myelination levels to GrP and lower myelination levels than OFv, with a less distinct outer band of Baillarger than GrP (Fig. 69C). GrA stains less intensely for CO (Fig. 69D) and more intensely for free ionic zinc (Fig. 69E) than both GrP and OFv. In PV preparations, GrA stains more lightly than GrP and similarly to OFv (not shown). Layer 4 of GrA is faintly stained in VGluT2 preparations, and GrA expresses less VGluT2 immunopositive terminations than both GrP and OFv (not shown).

Granular frontal medial area (GrM). The granular frontal medial area is bordered dorsally by GrP and ventrally by the medial frontal area (MF). In Nissl preparations, GrM has a less densely populated layer 4 than GrP and a layer 5 that is populated by medium-sized, darkly stained cells (Fig. 70A). GrM is moderately myelinated and is not densely populated with vertically running myelinated fibers, unlike GrP and MF (Fig. 70B). Layers 3 and 4 of GrM stain darkly for CO and overall, GrM stains lighter than MF (Fig. 70C). In zinc preparations, GrM is darker stains throughout the cortical layers than GrP and MF (Fig. 70D). Layers 3, 4 and 6 of GrM are less intensely stained for free ionic zinc than layers 1, 2 and 5 (Fig. 70D). PV staining in GrM is not homogenous (Fig. 70E). The dorsal portion is being poorly stained for PV immunopositive terminations and cell bodies, whereas the ventral portion is being moderately stained in layer 4 for PV immunopositive terminations and is populated by darkly stained PV immunopositive cell bodies (Fig. 70E). Compared to GrP and MF, GrM stains less intensely in PV preparations (Fig. 70E). A moderately stained band of VGluT2 immunopositive terminations is present in layer 4 of GrM and extends up to layer 3 (Fig. 70F). GrM expresses more VGluT2 immunopositive terminations than GrP and MF (Fig. 70F).

Figure 70. Architectonic characteristics of frontal cortex. The level at which the coronal sections are taken from is indicated by the vertical line on the lateral (G) and medial (H) views of the brain. The thicker line in panels G and H marks the regions illustrated in panels A to F. Short lines on the sections indicate the extent of each cortical layers 1 to 6. See table 1 for abbreviations for other areas. The scale bar for brain (panel G, H) = 2.5mm. The scale bar on the brain section (panel F) = 1mm.

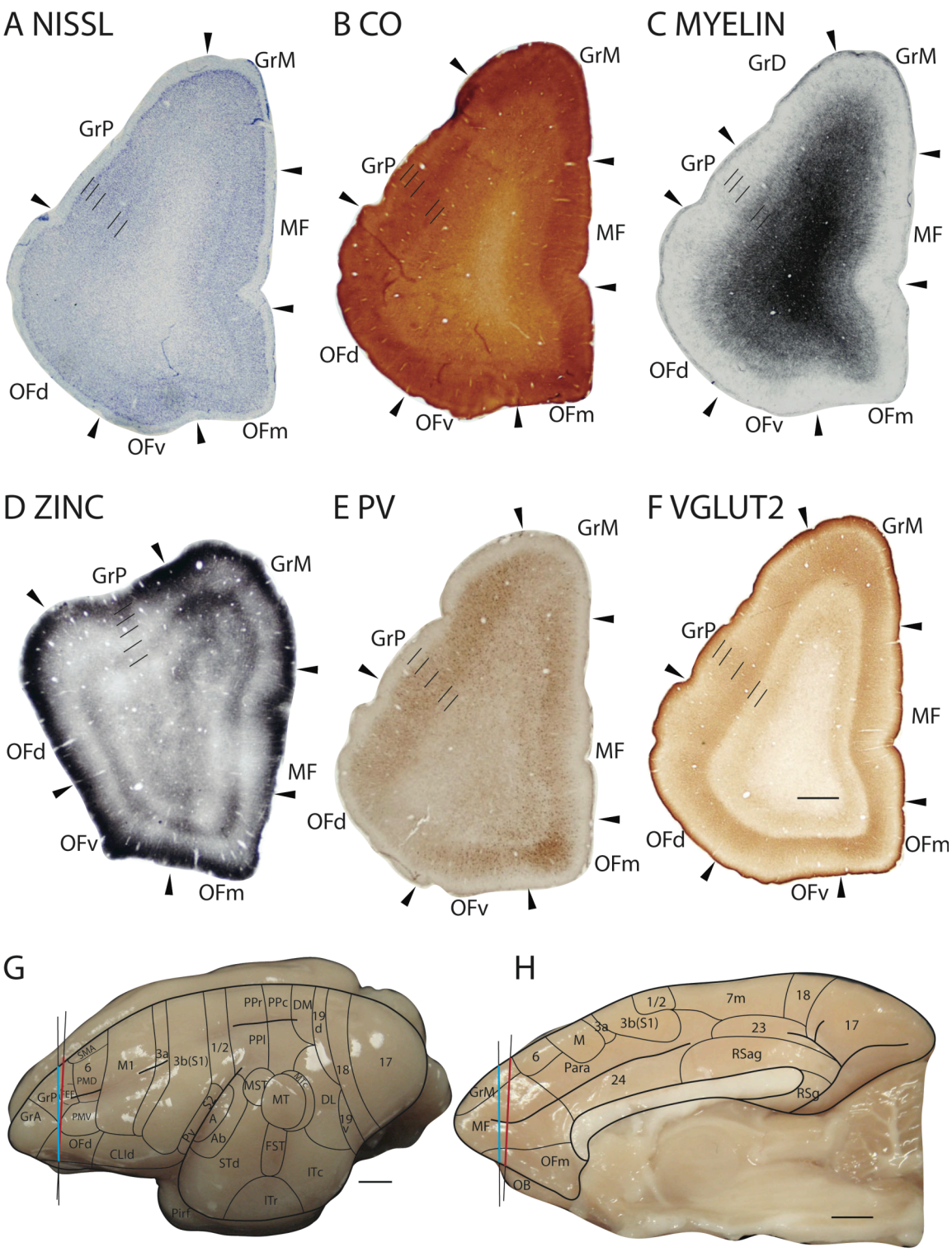
A NISSL
GrM
GrP
MF
OFd
OFv
OFm
B CO
GrM
GrP
MF
OFd
OFv
OFm
C MYELIN
GrD
GrM
GrP
MF
OFd
OFv
OFm
D ZINC
GrP
GrM
OFd
MF
OFv
OFm
E PV
GrM
GrP
MF
OFd
OFm
OFv
F VGLUT2
GrM
GrP
MF
OFd
OFm
OFv
G
PPr
PPc
DM
19 d
PPl
1/2
3a
3b(S1)
M1
SMA
6
PMD
PEF
PMV
GrP
GrA
OFd
CLId
MST
MT
MTc
DL
18
17
19 v
FST
STd
ITc
ITr
Pirf
H
1/2
7m
18
3a
3b(S1)
23
17
M
6
Para
RSag
24
RSg
GrM
MF
OFm
OB

Orbital frontal dorsal area (OFd). The orbital frontal dorsal area is bordered dorsally by M1 and GrP, and ventrally by the orbital frontal ventral area (OFv). In Nissl preparations, OFd has a darker appearance than M1 (Fig. 68A) and a lighter appearance than GrP (Fig. 70A). OFd has a moderately thick layer 4 that is populated by granule cells and a thinner layer 5 than M1 (Fig. 68A; 70A). OFd is moderately myelinated and has no distinct bands of Baillarger (Fig. 68B; 70B). Layer 4 of OFd stains darker for CO than M1 (Fig. 68C) and GrP (Fig. 70C). In zinc preparations, OFd, especially layers 4 to 6, is less intense stained than M1 (Fig. 68D) and more intensely stained than GrP (Fig. 70D). OFd stains at similar levels to OFv in zinc preparations (Fig. 70D). OFd is lightly stained in PV preparations. Layer 4 has a thin, faint band of PV immunopositive terminations, and layers 4, 5 and 6 are sparsely populated with darkly stained PV immunopositive cell bodies (Fig. 68E; 70E). In VGluT2 preparations, Layer 4 of OFd is moderately stained and layer 6 is faintly stained. OFd stains more intensely than M1 (Fig. 68F) and similarly to GrP (Fig. 70F) in VGluT2 preparations.

Orbital frontal ventral area (OFv). The orbital frontal ventral area (OFv) is bordered dorsally by OFv and medially by the orbital frontal medial area (OFm). In Nissl preparations, OFv is darkly stained compared to the adjoining cortical areas OFv and OFm. The upper cortical layers of OFv is populated with medium-sized, darkly stained cells, layer 4 is thin and layer 5 is populated with darkly staining cells (Fig. 23B; 24A). OFv has a higher myelination density than GrA (Fig. 69C) and has similar myelination density to OFd (Fig. 70B). In CO preparations, OFv stains more intensely than GrA (Fig. 69D) and OFd (Fig. 70C). OFv stains lighter than GrA in zinc preparations (Fig. 69E) and at similar intensities to OFd, although layer 4 of OFv is darker than layer of OFd

(Fig. 70D). In PV preparations, OFv stains moderately for PV immunopositive terminations, with a scattering of moderately stained PV immunopositive cell bodies in layers 3 and 4 (Fig. 70E). OFv stains darker in PV preparations than OFd, and lighter than OFm (Fig. 70E). In VGluT2 preparations, a moderately stained band is present in layer 4 and a lightly stained band is present in layer 6 of OFv (Fig. 70F). The band of staining in layer 4 of OFv is thinner than that of OFd and less intense than that of OFm (Fig. 70F).

Orbital frontal medial area (OFm). The orbital frontal medial area (OFm) is bordered laterally by OFv and dorsally by the medial frontal area (MF). OFm has a banded appearance in Nissl preparations, due to a moderately stained upper cortical layers populated with medium-sized cells in layer 3, a thin and pale granular layer 4, a thin and moderately stained layer 5 and a pale layer 6 (Fig. 70A). Of the three orbital frontal areas, OFm is the least densely myelinated and contains more horizontal fibers (Fig. 70B). Layers 3 and 4 of OFm stain darkly for CO (Fig. 70C). In zinc preparations, layers 1, 2, outer 3 and 5 are darkly stained, whereas layers 4 and 6 are lighter stained (Fig. 70D). Throughout the cortical layers, OFm stains darker than the adjacent OFv and MF in zinc preparations (Fig. 70D). OFm stains darkly for PV immunopositive terminations in layer 4 that extends to inner layer 3 (Fig. 70E). Moderately PV stained cell bodies are present in inner layer 3 and layer 4, and lightly PV stained cell bodies are present in layer 6 (Fig. 70E). A moderately stained band of VGluT2 terminations is present in layer 4 of OFm and extends up to inner layer 3 (Fig. 70F). OFm expresses higher levels of VGluT2 terminations than OFv and MF (Fig 70F). As OFm is dark in zinc, PV and VGluT2 preparations, it suggests that OFm receives proportionately more

corticocortical terminations that contain free ionic zinc, and more PV and VGluT2 immunopositive thalamocortical terminations than the adjoining OFv and MF.

Medial frontal area (MF). The medial frontal area (MF) is bordered dorsally by GrM and ventrally by OFm. In Nissl preparations, MF does not have a distinct granular layer 4 and has a thin layer 5 that is darkly stained and densely populated with cells (Fig. 70A). MF is moderately myelinated with a heterogeneous myelination pattern (Fig. 70B). Nearer to the GrM/MF border, MF is populated by myelination pattern is in a vertical orientation, whereas nearer to the MF/OFm border, the myelination pattern is in a horizontal orientation (Fig. 70B). This suggests that there may be further subdivisions in MF. In CO preparations, layer 4 of MF is moderately stained (Fig. 70C). The varying staining pattern of MF is present in zinc preparations as well (Fig. 70D). MF stains darker nearer to the GrM/MF border and lighter nearer to the MF/OFm border (Fig. 70D). In PV preparations, MF stains less intensely for PV immunopositive terminations than OFm and more intensely than GrM (Fig. 70E). Moderately PV stained cell bodies are present in layers 4 and 6 of MF (Fig. 70E). In VGluT2 preparations, a thin and moderately stained band is present in layer 4 and a thin and lightly stained band is present in layer 6 of MF (Fig. 70F). Throughout the cortical layers, MF expresses less VGluT2 immunopositive terminations than GrM and OFm (Fig. 70F).

Medial cortex

The medial wall of the galago neocortex can be divided into the rostral, middle and caudal regions. GrM, MF and OFm make up the rostral region of the medial cortex. The dorsal medial cortex includes parts of area 6, M1, area 3a, area 3b(S1) and area 1/2,

which have been described on previous pages. Ventral medial cortex consists of the paralimbic area (Para) and anterior cingulate, area 24. The caudal region of the medial cortex is largely occupied by area 17 at the caudal pole. Additionally, area 18, prostriata (PS), the medial area of the posterior parietal cortex (area 7m), the posterior cingulate (area 23), and the retrosplenial areas are located within the caudal region of the medial cortex. Areas 23, 24 and 30 follow the description of Brodmann (1909) for prosimian lemur.

Paralimbic area (Para). The paralimbic area (Para) largely corresponds to the rostral (CMAr) and caudal (CMAc) cingulate motor area (Wu et al., 2000). Para is bordered by the motor, premotor and somatosensory areas dorsally and by area 24 ventrally. In Nissl preparations, layer 4 of Para is not distinct and seems to merger with layer 3 to form a thick band populated with medium sized cells (Fig. 62A). Layer 5 of Para has a pale appearance and is more sparsely populated with cells than layer 5 of area 3b(S1)(Fig. 62A). Para is less densely myelinated than area 3b(S1) and more densely myelinated than area 24 (Fig. 62B). Furthermore, Para has a distinct outer band of Baillarger (Fig. 62B). In CO preparations, Para is less darkly stained than area 3b(S1) and stains at similar intensities to area 24 (Fig. 62C). Darkly CO stained cells are present in layer 5 of Para (Fig. 62C). In zinc preparations, Para is more darkly stained throughout the cortical layers than the adjoining areas 3b(S1) and 24 (Fig. 62D). A moderately stained band of PV immunopositive terminations is present in layer 4 of Para, and a second, fainter band is present in layer 6 (Fig. 62E). Para is also populated by moderately stained PV immunopositive cells (Fig. 62E). In VGluT2 preparations, layer 4 is moderately stained and layer 6 is faintly stained (Fig. 62F). Para expresses less VGluT2

immunopositive terminations in layers 4 and 6 than the corresponding layers in area 3b(S1)(Fig. 62F).

Area 24. In Nissl preparations, area 24 has a pale appearance with no obvious granular layer 4 (Fig. 62A; 65A). Area 24 is poorly myelinated with no distinct bands of Baillarger (Fig. 62B; 65B). A thin, moderately stained band of layer 4 in area 24 is present in CO preparations (Fig. 62C; 65C). The more rostral portions of area 24 stain paler in zinc preparations, especially in layers 4 and 5 (Fig. 62D). However, towards the caudal end, area 24 stains darker in zinc preparations (Fig. 65D). This hints at the possibility of subdivisions within area 24. This variation in staining pattern is present in PV preparations as well. There are two moderately PV-stained bands in layers 4 and 6 in the rostral portion of area 24 (Fig. 62E) that become faintly stained in the caudal portion (Fig. 65E). A scattered population of moderately stained PV immunopositive cell bodies is preset in area 24 (Fig. 62E; 65E). Area 24 has two VGluT2 stained bands; a thin, moderately stained band in layer 4 and a fainter band in layer 6 (Fig. 62F; 65F). Compared to area 3b(S1)(Fig. 65F) and Para (Fig. 62F), area 24 expresses lower level of VGluT2 staining.

Area 23. Area 23, the posterior cingulate area, is bordered dorsally by area 7m and ventrally by area 30. In Nissl preparations, the upper cortical layers of area 23 is paler than area 7m and the granular layer 4 of area 24 is thinner than that in area 7m. Furthermore, area 23 has a darker appearance than area 30 in Nissl stained sections. In myelin preparations, area 23 is less densely myelinated than the adjoining areas 7m and 30 (Fig. 54B). Area 23 is moderately stained in CO preparations, with a single stained band in layer 4 (Fig.54C). Compared to areas 7m and 30, area 23 is more lightly CO

stained (Fig. 54C). Area 23 is more darkly stained, especially inner layer 6, than area 7m in sections stained for free ionic zinc (Fig. 54D). Additionally, area 23 is more darkly stained throughout the cortical layers than area 30 (Fig. 54D). In PV preparations, area 23 is less intensely stained than both areas 7m and 30 (Fig. 54E). Layer 4 of area 23 stains less intensely for VGluT2 immunopositive terminations than layer 4 of area 7m and stains at similar intensity to layer 4 of area 30 (Fig. 54F). A pale, thin band of VGluT2 immunopositive terminations is present in layer 6 of area 23 as well (Fig. 54F).

Retrosplenial agranular area (RSag). The retrosplenial agranular area (RSag) in galagos is mostly buried within the calcarine sulcus. In Nissl preparations, RSag has a darkly stained layer 2, but otherwise is not well laminated. It has a paler appearance than the adjoining prostriata area (PS) due to a lowered cell packing density (Fig. 48A; 52A; 54A). RSag is moderately myelinated, and is more densely myelinated than PS and more sparsely myelinated than the retrosplenial granular area (RSg)(Fig. 48B; 52B; 54B). Layers 2 to 5 of RSag stain lightly for CO (Fig. 54C), and there is no distinct boundary between RSag and PS in CO preparations (Fig. 48C; 52C). In zinc preparations, RSag stains less intensely for corticocortical terminations that contain free ionic zinc compared to PS (Fig. 48D; 52D) and more intensely compared to RSg, especially in layer 2/3 (Fig. 48D; 52D). Layers 2/3, 4 and 6 of RSag stains with moderate intensity for PV immunopositive terminations, and layer 5 is lightly stained (Fig. 48E; 52E; 54E) RSag is populated by lightly stained PV immunopositive cell bodies (Fig. 48E; 52E; 54E). RSag stains darker than PS and lighter than RSg in PV preparations (Fig. 48E; 52E). In VGluT2 preparations, RSag is moderately stained (Fig. 52F), and is more lightly stained than both PS and RSg (Fig. 48F).

Retrosplenial granular area (RSg). The retrosplenial granular region in galagos is bordered dorsally by RSag, and is buried within the calcarine sulcus. RSg, like RSag, does not have well defined laminar properties. In Nissl preparations, layer 2/3 of RSg is darkly stained, marking the RSag/RSg boundary (Fig. 48A; 52A). In myelin preparations, RSg is more densely myelinated than RSag and has a distinct outer band of Baillarger (Fig. 48B). RSg stains darker than RSag in CO preparations, with a moderately stained band in layer 2/3 (Fig. 48C; 52C). Layer 2/3 of RSg stains poorly and upper layer 2, 5 and inner 6 stain darkly, as such RSg has a banded appearance in sections stained for free ionic zinc (Fig. 48D; 52D). In PV preparations, RSg stains darker than RSag, and has a band of PV immunopositive terminations in layer 2/3 and another in layer 5/6 (Fig. 48E; 52E). RSg stains darkly for VGluT2 immunopositive terminations, making a distinct RSag/RSg border (Fig. 48F).

Prostriata area (PS). The prostriata area (PS) is a more recently defined visual area (Rosa et al., 1997) that appears to be present in most mammals (Rosa and Krubitzer, 1999). PS runs along the ventromedial boundary of area 17 and is bordered rostrally by the retrosplenial areas. In Nissl preparations, the border between area 17 and PS is marked by the reduction in thickness of layer 4 in PS (Fig. 48A; 52A). The PS/RSag border is clearly demarcated as the thin and densely populated granular layer 4 in PS is absent in RSag (Fig. 48A; 52A). In myelin preparations, PS is poorly myelinated (Fig. 48B; 52B). PS stains moderately for CO, with a darker band in layer 4 and a lighter band in layer 6 (Fig. 48C; 52C). In CO preparations, PS is more lightly stained than area 17 and is more darkly stained than RSag (Fig. 48C; 52C). In zinc preparations, the almost white band in layer 4 of area 17 terminates at the area 17/PS border (Fig. 48D). PS stains

darker than RSag in sections stained for free ionic zinc (Fig. 48D; 52D). Layers 3/4 and 6 of PS stain moderately for PV immunopositive terminations and a scattering of lightly stained PV immunopositive cell bodies are present (Fig. 48E; 52E). In VGluT2 preparations, PS expresses two bands of VGluT2 immunopositive terminations, in layers 4 and 6 (Fig. 48F). PS is less intensely stained than area 17 and more intensely stained than RSag in sections stained for VGluT2 immunopositive terminations (Fig. 48F).

Remaining cortical areas – Perirhinal area (PRh)

In Nissl preparations, the perirhinal area (PRh) does not have a well developed granular layer 4, a darkly stained layer 2, and overall a darker appearance than the adjoining entorhinal cortex (Ent)(Fig. 57A; 58A). PRh is poorly myelinated compared to the surrounding cortical areas, such as TG (Fig. 57B) and ITc (Fig. 58B), and stains poorly in CO preparations (Fig. 57C; 58C). In zinc preparations, PRh is darkly stained throughout the cortical layers (Fig. 57D; 58D). The architectonic boundaries of PRh are clearly demarcated in zinc preparations as PRh stains darker than the surrounding cortical areas (Fig. 57D). PRh has low immunoreactivity for both PV (Fig. 57E; 58E) and VGluT2 (Fig. 57F; 58F).

Discussion

Galagos belong to the prosimian suborder, one of the three major branches of the primate order. They are of special interest as they have retained many anatomical features of early primates (Radinsky, 1977; Jerison, 1979), and as such their brains may have changed the least in primate evolution (Martin, 1990; Fleagle, 1999). Past architectonic

studies of galagos (e.g. (von Bonin, 1942; von Bonin, 1945; von Bonin and Bailey, 1961; Kanagasuntheram et al., 1966; Zilles et al., 1979; Preuss and Goldman-Rakic, 1991a) utilized a limited range of histological stains to characterize the cortical areas of galagos. In this study, we have used a battery of histological and immunohistochemical procedures to reveal and characterize the architectonic subdivisions of galago neocortex that have known or presumed functional significance. Some of these procedures give hint to the functional properties of a cortical area. For example, cortical areas with a layer 4 that is densely populated withVGluT2 and PV terminations, and few terminations containing free ionic zinc would suggest that the layer is dominated by thalamic rather than cortical inputs (Van Brederode et al., 1990; DeFelipe and Jones, 1991; Hackett et al., 1998; de Venecia et al., 1998; Latawiec et al., 2000; Fujiyama et al., 2001; Kaneko and Fujiyama, 2002; Wong and Kaas, 2008; Hackett and de la Mothe, 2009; Wong and Kaas, 2009a; Wong and Kaas, 2009b). Furthermore, areas that stain darkly for CO are typically sensory areas that have high metabolic activity (Wong-Riley et al., 1978; Wong-Riley, 1979). These procedures will provide improved overview of how the neocortex is organized in galagos. Our broader goal is to understand what features of cortical organizations are shared between prosimians and anthropoid primates, and features that may be different. Different features in cortical organizations between prosimian galagos and anthropoid primates may reflect functional specializations. As such, the present results are discussed in relation to previous architectonic studies of both prosimians and anthropoid primates.

Occipital cortex

Area 17. The occipital cortex of galagos consists of a large primary visual cortex (V1 or area 17) that occupies most of the caudal pole of the cerebral hemisphere. Extrastriate areas in the occipital lobe of galagos follow that of the primate visual system organization, sharing common cortical areas such as secondary visual cortex (V2 or area 18) that contains a second-order representation of the visual field (Rosa et al., 1997), and the third visual area, V3 (Lyon and Kaas, 2002a). Other proposed visual areas include the middle temporal visual area (MT)(Allman et al., 1973; Rosa et al., 1997; Collins et al., 2001; Kaskan and Kaas, 2007), the dorsomedial visual area (DM)(Rosa et al., 1997; Beck and Kaas, 1998a; Beck and Kaas, 1998b; Collins et al., 2001) and the dorsolateral visual area (DL)(Collins et al., 2001).

In galagos, the surface area of V1 is about 200mm^2, and is two to three times the surface area occupied by V1 of nocturnal nonprimates with similar body mass (Rosa et al., 1997), such as ferrets (Law et al., 1988) and hedgehogs (Kaas et al., 1970). Microelectrode recording studies have shown that V1 is retinotopically organized, with central vision represented on the anterolateral surface and peripheral vision represented on the medial wall, covering the banks of the calcarine sulcus (Rosa et al., 1997). V1 is co-extensive with the architectonically defined area 17 of Brodmann (1909). Area 17 has pronounced lamination pattern compared to adjoining area 18 that allowed it to be easily identified in early architectonic studies (e.g. von Bonin, 1942; von Bonin, 1945; von Bonin and Bailey, 1961; Kanagasuntheram et al., 1966; Zilles et al., 1979; Preuss and Goldman-Rakic, 1991a). Similar to primates and other mammals, layer 4 of area 17 is densely populated with granule cells in galagos. However, layer 4 of area 17 in galagos

corresponds to layers 4Cα and 4Cβ as identified in anthropoid primates by Brodmann (1909), and in most studies today. Hassler (1967) was one of the first to stress that Brodmann (1909) had misidentified layers in area 17 of anthropoid primates and that sublayers 4A and 4B of Brodmann were sublayers of layer 3. The laminar designations used here and previously for prosimian primates apply to all primates (e.g. Weller and Kaas, 1982; Diamond et al., 1985; Florence and Casagrande, 1987). Unlike area 17 in tree shrews (Lund et al., 1985; Wong and Kaas, 2009a), a cell poor cleft does not divides layer 4 into sublayers 4a and 4b in galagos. Layer 4 has been identified in previous architectonic studies of area 17 in galagos as in the present study (e.g. von Bonin, 1942; von Bonin, 1945; von Bonin and Bailey, 1961; Kanagasuntheram et al., 1966; Zilles et al., 1979; Preuss and Goldman-Rakic, 1991a). In terms of connections with the lateral geniculate nuclei, layer 4 of area 17 in galagos has similar connection patterns with that of monkeys (e.g. Hubel and Wiesel, 1972; Tigges et al., 1977; Hendrickson et al., 1978). Layer 4a of area 17 in galagos can be defined as the sublayer that receives projections from the magnocellular layers 1 and 2 of the lateral geniculate nucleus, whereas layer 4b is the sublayer that receives projections from the parvocellular layers 3 and 6 of the lateral geniculate nucleus (Glendenning et al., 1976; Diamond et al., 1985). In our preparations, layer 4 of area 17 in galagos is also characterized by dense expressions of PV and VGluT2 immunopositive terminations, reflecting dense inputs from the lateral geniculate nucleus of the sensory thalamus (Glendenning et al., 1976; Diamond et al., 1985). Furthermore, the poor zinc staining of layer 4 suggests that this layer is dominated by thalamic rather than cortical inputs.

Layer 3 of area 17 in galagos does not have the clear sublayers of many anthropoid primates. This layer is broad and has a heterogeneous architectonic appearance. This layer consists mainly of small pyramidal cells, with clusters of darkly stained cells that appear to co-localize with patches of PV-immunopositive terminations and CO rich patches known as CO blobs. In anthropoid primates, CO blobs are regions where processing of chromatic information takes place (Livingstone and Hubel, 1984; Hendrickson, 1985; Livingstone and Hubel, 1987; Tootell et al., 1988; Ts'o and Gilbert, 1988). Galagos do not have color vision (Petry and Hárosi, 1990). However, the distribution of CO blobs in galagos (Condo and Casagrande, 1990) is similar to that of diurnal anthropoid primates (Carroll and Wong-Riley, 1984; Livingstone and Hubel, 1984; Livingstone and Hubel, 1987). The CO blobs in galagos, as with the CO blobs in the nocturnal owl monkey (Ding and Casagrande, 1997), have been shown to be the target of projections from the koniocellular layers of the lateral geniculate nucleus (Lachica and Casagrande, 1992). Additionally, layer 3 of area 17 in galagos receives inputs from sublayers 4A and 4B (Casagrande et al., 1989) that converge within the CO blobs (Lachica et al., 1993). This has been observed in the diurnal anthropoid primates, macaques (Lachica et al., 1992) and squirrel monkeys (Lachica et al., 1993). The CO blobs in layer 3 of area 17 in galagos are also co-extensive with patchy callosal input to much of area 17 (Cusick et al., 1984). In addition to the intrinsic, callosal and thalamic projections to layer 3 of area 17 in galagos, layer 3 is the projection target of other extrastriate visual areas as well (Diamond et al., 1985; Cusick and Kaas, 1988; Krubitzer and Kaas, 1988; Krubitzer and Kaas, 1989; Beck and Kaas, 1998a; Collins et al., 2001; Lyon and Kaas, 2002c). The cortical projections to layer 3 of area 17 in galagos may

terminate in a patchy manner, as evidenced by the patchy distribution of synaptic zinc, which is found in corticocortical terminations (Danscher, 1982; Frederickson and Moncrieff, 1994; Frederickson et al., 2000; Ichinohe et al., 2003; Ichinohe and Rockland, 2004), in sections cut parallel to the artificially flattened cortex (Fig. 3). The patchy distributions of the zinc and VGluT2 stains may reflect a pattern of VGluT2-rich terminals of the lateral geniculate nucleus inputs, likely from the koniocellular layers 4 and 5, that are surrounded by walls of zinc-enriched terminals of projections from other visual cortical areas (Carey et al., 1979; Casagrande and De Bruyn, 1982; Diamond et al., 1985).

Area 18. Area 18 of this study corresponds to the second visual area, V2 (Rosa et al., 1997). V2 of galagos is a homologue of V2 that has been described in anthropoid primates (Allman and Kaas, 1974; Gattass et al., 1981; Rosa et al., 1988) and other mammals. The visuotopic organization of V2 in galagos (Rosa et al., 1997) is similar to that of anthropoid primates (e.g. Allman and Kaas, 1974; Gattass et al., 1981), with a complete representation of the visual field. However, galagos differ from anthropoid primates (Allman and Kaas, 1971a; Rosa et al., 1988) in that V2 of galagos does not completely surround V1 as V1 is bordered by area prostriata in the calcrine sulcus (Allman and Kaas, 1971a; Sanides, 1972; Gattass et al., 1987; Rosa et al., 1997). Furthermore, V2 of galagos is small and narrow, with a surface area of about 65mm^2 and a maximum width of about 3mm (Rosa et al., 1997). Area 18 of galagos has also been identified in previous architectonic studies (von Bonin, 1942; von Bonin, 1945; von Bonin and Bailey, 1961; Kanagasuntheram et al., 1966; Zilles et al., 1979; Preuss and Goldman-Rakic, 1991a) and closely corresponds to area occipitalis 2 of Zilles et al.

(1979). Architectonically, area 18 of galagos has lowered cell packing density in layers 4 and 6 than area 17 and the overall laminar pattern of area 18 is less distinct. Furthermore, area 18 expresses less PV and VGluT2 immunopositive terminations and more synaptic zinc in layers 4 and 6 than area 17. These observations suggest that area 18 receives proportionately less thalamocortical and more cortical inputs, including dense, topographically organized inputs from area 17 (Symonds and Kaas, 1978; Cusick and Kaas, 1988), and other extrastriate areas such as MT (Wall et a., 1982; Krubitzer, 1990a) and DM (Krubitzer and Kaas, 1993; Beck and Kaas, 1998a). In anthropoid primates, area 18 shows a distinct, regular periodic pattern of CO staining, with thick and thin CO stripes (Wong-Riley and Carroll, 1984; Tootell et al., 1985; Hendrickson, 1985; Livingstone and Hubel, 1987). Area 18 of galagos, however, only shows a weak pattern of patches or bands CO preparations (Condo and Casagrande, 1990; Kaskan and Kaas, 2007), and these were not apparent in the present preparations.

Area 19. Area 19 is used here to refer to the third visual area, V3, that was first defined in macaque monkeys based on the pattern of connections with V1 (Cragg, 1969; Zeki, 1969). More recently, V3 has been defined in several New World and Old World monkeys (Gattass et al., 1988; Sousa et al., 1991; Lyon and Kaas, 2001; Lyon and Kaas, 2002b; Lyon and Kaas, 2002c), and consists of the dorsal and ventral portions and a mirror reversal of the retinotopy of V2. In galagos, the dorsal and ventral portions of area 19 or V3 have not always been differentiated from the dorsomedial (DM) and dorsolateral (DL) visual areas (e.g. Rosa et al., 1997; Beck and Kaas, 1998a; Collins et al., 2001) because microelectrode mapping studies failed to provide compelling evidence for the presence of V3 (Allman and Kaas, 1975; Allman et al., 1979; Rosa et al., 1997)

and V3 did not have distinct enough staining characteristics to allow it to be differentiated from DM, DL or area 18 (von Bonin, 1942; von Bonin, 1945; von Bonin and Bailey, 1961; Kanagasuntheram et al., 1966; Zilles et al., 1979; Preuss and Goldman-Rakic, 1991a). As a result, the lack of a distinct architectonic area 19 in galagos may have affected the interpretation of the results in studies of connections. Some foci of label observed in previous studies of connections were within the dorsal and ventral portions of V3, but they were not differentiated from DM and DL. By placing injections of multiple tracers along the upper and lower field representations of V1, Lyon and Kaas (2002a) were able to provide clear connectional evidence for the existence of V3 in galagos. In sections from flattened cortex, V3 expressed more CO than V2 and was more myelinated, but these characteristics were similar to those in DM. V3 in galagos is narrower than V2 and likely to be discontinuous in the middle, such that the dorsal portion, containing the lower visual field representation, and the ventral portion, containing the upper visual field representation, are separate (Lyon and Kaas, 2002a). Further evidence for the existence of V3 comes from placements of tracers into MT of galagos that labeled neurons in the dorsal and ventral portions of V3 (Kaskan and Kaas, 2007).

The lack of distinct architectonic characteristics of area 19 has also lead to varying definitions of area 19. An early architectonic study of galago neocortex by von Bonin (1945) has an area 19 that is rather large and likely includes portions, if not all of, DM and DL. Using the cresyl-fast-violet stain for cell bodies, Zilles and colleagues (1979) identified a second visual area (Oc2) and rostrally adjoining parietal area 2 and temporal area 4, with no area 19, DM, nor DL. We observe that area 19 has a thin granular layer 4, moderate myelination density and CO expression. In zinc preparations,

area 19 expresses high levels of synaptic zinc compared to the adjoining area 18, DM and DL. Area 19 expresses moderate levels of PV and VGluT2 immunopositive terminations, and compared to the adjoining area 18, stains more darkly in PV and VGluT2 preparations. This suggests that area 19 receives proportionately more corticortical and thalamocortical terminations than area 18.

DM and DL. DM is a visual area first recognized in owl monkeys (Allman and Kaas, 1975), and it is at least roughly co-extensive with the area sometimes referred to as V3A (Van Essen and Zeki, 1978). DM of monkeys has connections with from V1, V2, MT and posterior parietal cortex (Wagor et al., 1975; Zeki, 1980; Burkhalter et al., 1986; Stepniewska and Kaas, 1996; Felleman et al., 1997; Gattass et al., 1997; Beck and Kaas, 1998a; Lyon and Kaas, 2002a). Similarly, DM of galagos has connections with V1, V2, MT and posterior parietal cortex (Rosa et al., 1997; Beck and Kaas, 1998a; Collins et al., 2001; Lyon and Kaas, 2002a). The cortical area defined as DM in earlier studies likely included the dorsal portion of V3, and as such, the findings that were reported for DM may also apply to the dorsal portion of V3 (For review see Kaas and Lyon, 2001; Lyon and Kaas, 2002a). DM as defined here is similar in location to area D of (Preuss and Goldman-Rakic, 1991a) and the caudal portion of Pa2 of Zilles and colleagues (1979). The rostral portion of cortex rostral defined as area 19 by von Bonin (1945) would include DM. Architectonically, DM has a thin, densely packed granular layer 4 and is moderately myelinated. In zinc preparations, DM expresses less synaptic zinc than the adjoining DL and area 19d. This indicates that DM receives proportionately less corticortical inputs than DL and area 19d. Compared to DL, DM also expresses more PV

immunopositive terminations and similar levels of VGluT2 immunopositive terminations, indicating that DM receives proportionately more thalamocortical inputs than DL.

DL, first described in owl monkeys (Allman and Kaas, 1974) and subsequently reduced in extent next to MT (Kaas and Morel, 1993) roughly corresponds to V4 (Stepniewska et al., 2005a), and is strongly interconnected with V2 and portions of the superior temporal lobe in monkeys (Tigges et al., 1974; Weller and Kaas, 1985; Cusick and Kaas, 1988; Steele et al., 1991; Stepniewska and Kaas, 1996; Gattass et al., 1997). In galagos, similar connection patterns are observed (Collins et al., 2001). As in monkeys, DL in galagos also has connections with V1 (Lyon and Kaas, 2002a), MT and MTc (Kaskan and Kaas, 2007). In previous architectonic studies, the region of DL was included within the rostroventral portion of area 19 of von Bonin (1945), the temporal areas 4 and 5 of Zilles et al. (1979) and the rostral portion of V4 or area D of (Preuss and Goldman-Rakic, 1991a). Architectonically, DL has a thin, moderately stained granular layer 4 and is less densely myelinated than the adjoining DM, MT and area 19. DL expresses more synaptic zinc and less PV and VGluT2 immunopositive terminations than the surrounding cortical areas. This indicates that DL receives proportionately more corticocortical and less thalamocortical terminations than the surrounding cortical areas.

Temporal cortex

MT. Visual associated areas in the temporal lobe of galagos include the middle temporal visual area (MT), the crescent surrounding MT (MTc), the middle superior temporal area (MST) and the fundus of the superior temporal area (FST). First described in owl monkeys (Allman and Kaas, 1971a), MT is now considered visual area common to

all primates (Kaas, 1997). MT is involved in visual motion processing and contains neurons that are selective for the direction of moving visual stimuli (Allman and Kaas, 1971a; Zeki, 1974; Van Essen et al., 1981; Rosa and Elston, 1998). There is a complete retinotopic representation of the visual hemifield in MT (Allman et al., 1973; Rosa et al., 1997; Collins et al., 2001; Kaskan and Kaas, 2007). In monkeys, MT receives direct corticocortical inputs from V1 and V2 (Allman et al., 1973; Rosa et al., 1997; Orban, 1997; Collins et al., 2001; Britten, 2003; Born and Bradley, 2005; Kaskan and Kaas, 2007), and some thalamocortical inputs from the lateral geniculate nucleus (Stepniewska et al., 1999; Sincich et al., 2004). The medial subdivision of the inferior visual pulvinar provides the major inputs (Lin and Kaas, 1980; O'Brien et al., 2001). Architectonically, MT of monkeys is characterized by dense myelination and dark staining in CO preparations (e.g. (Allman and Kaas, 1971b; Spatz and Tigges, 1972; Spatz, 1977; Van Essen et al., 1981; Tootell et al., 1985). Furthermore, MT of marmoset monkeys stains darkly in PV preparations (Bourne et al., 2007).

MT of galagos was first identified by Allman and colleagues (1973) as an oval region that has a surface area of approximately $18mm^2$ (Xu et al., 2004; Beck and Kaas, 1998a; Allman et al., 1973) and has similar corticocortical connection patterns to MT of monkeys (Cusick and Kaas, 1988; Krubitzer and Kaas, 1990a; Collins et al., 2001; Kaskan and Kaas, 2007). MT in galagos has a somewhat different connections with the inferior pulvinar compared to monkeys. In addition to receiving inputs from the medial nucleus of the inferior pulvinar like in monkeys, MT in galagos receives projections from the rest of the inferior pulvinar, the posterior and caudal subdivisions, as well (Wong et al., in press). The cortical area that we identify as MT corresponds to that of Preuss and

Goldman-Rakic (1991a) and is in a similar location, albeit smaller, to that identified by Zilles and colleagues (1979). von Bonin did not identify an area that may be in MT in the cortical map of galagos (1945). Architectonically, MT of galagos has a similar appearance to MT of monkeys, with dense myelination and high CO expression (Allman et al., 1973; Wall et al., 1982; Krubitzer and Kaas, 1990a; Collins et al., 2001; Kaskan and Kaas, 2007; Wong et al., in press). These previous findings are congruent with our current observations. In addition, the reduced zinc staining compared to surrounding cortex likely reflects the presence of dense thalamocortical inputs from the inferior pulvinar, while zinc staining that is present corresponds to corticocortical projections from cortical areas, such as V1 and V2 (Wall et al., 1982; Cusick and Kaas, 1988; Krubitzer and Kaas, 1990a; Collins et al., 2001; Kaskan and Kaas, 2007). The dark staining for PV and VGluT2 immunopositive terminations in layers 3 and 4 also reflects presence of strong projections from thalamic nuclei, such as the inferior pulvinar (Weller and Kaas, 1982).

MTc. Much of MT is bordered by a thin strip of cortex, MTc, first identified in New World owl monkeys (Kaas and Morel, 1993) and more recently in marmosets (Palmer and Rosa, 2006). In Old World macaques, part of this region had been previously identified as V4t (Ungerleider and Desimone, 1986). In monkeys (Ungerleider and Desimone, 1986; Kaas and Morel, 1993; Palmer and Rosa, 2006) and galagos (Kaskan and Kaas, 2007), MTc has connections with MT and the adjacent MST and FST areas, as well as with V1, V2, V3, DL and portions of the posterior parietal and inferior temporal cortex. Architectonically, MTc in galagos has a heterogenous appearance and is probably best observed in sections from artificially flattened cortex that was cut tangential to the

pia. In these sections stained for CO, MTc consists of a series of CO-dense puffs and CO-sparse surrounds (Kaskan and Kaas, 2007). Furthermore, MTc stains lighter for PV and VGluT2 immunopositive thalamocortical terminations and darker for synaptic zinc in corticocortical terminations compared to MT. This is likely to be due to the proportionately larger population of inputs from other cortical areas, such as MT, V1 and V2 (Kaskan and Kaas, 2007), and lower population of inputs from thalamic nuclei.

FST and MST. The fundal area of the superior temporal sulcus (FST) was first defined in macaque monkeys with a deep superior temporal sulcus (Desimone and Ungerleider, 1986). FST in monkeys has strong connections with both MT (Boussaoud et al., 1990; Krubitzer and Kaas, 1990a; Kaas and Morel, 1993; Palmer and Rosa, 2006) and MTc (Kaas and Morel, 1993). The medial superior temporal area (MST) was named as a projection target of MT in macaque monkeys by Maunsell and Van Essen (1983). Across primates MST receives projections from MT (Weller et al., 1984; Krubitzer and Kaas, 1990a; Rosa et al., 1993). FST of galagos is highly interconnected with MT as well (Krubitzer and Kaas, 1990a; Kaskan and Kaas, 2007). MST of galagos is a darkly CO stained oval that is located rostrally to MT (Kaskan and Kaas, 2007; present study), and is highly interconnected with MT (Kaskan and Kaas, 2007). Both FST and MST express proportionately more synaptic zinc and less PV and VGluT2 thalamocortical immunopositive terminations than MT. This indicates that a large proportion of inputs to FST and MST of galagos originate from surrounding cortical areas, such as MT (Krubitzer and Kaas, 1990a; Kaskan and Kaas, 2007).

Inferior temporal and remaining temporal areas. The inferior temporal cortex of galagos has previously been divided into at least two (von Bonin, 1945), to as many as

five (Preuss and Goldman-Rakic, 1991a) areas. Here, we have defined four areas in the inferior temporal cortex, the interior temporal rostral (ITr), inferior temporal caudal (ITc), temporopolaris (TG) and superior temporal dorsal areas (STd). ITr overlaps with TEm, and perhaps a portion of LMZ, of Preuss and Goldman-Rakic (1991a), and the caudal portion of Te2.2 and rostral portion of Te5 of Zilles and colleagues (1979). Architectonically, TEm has a well defined layer 4 (Preuss and Goldman-Rakic, 1991a). This is congruent with our observations on ITr. Additionally, ITr appears to have both a moderate population of corticocortical terminations, identified by the expression of synaptic zinc, and a moderate population of VGluT2 immunopositive thalamocortical terminations. ITc overlaps with TEc of Preuss and Goldman-Rakic (1991a) and Te5 of Zilles and colleagues (1979). This caudal portion of the inferior temporal cortex in galagos is moderately myelinated, as in macaques and owl monkeys (Preuss and Goldman-Rakic, 1991a; Fig. 12C). Additionally, ITc may receive a proportionately more PV and VGluT2 immunopositive thalamocortical terminations than synaptic zinc containing corticocortical terminations. In monkeys, a major input to ITc is from DL(V4)(see Stepniewska et al., 2005 for review), but there is only limited evidence for this from the cortical injections that involves DL in galagos (Wall et al., 1982; Collins et al., 2001; Kaskan and Kaas, 2007). In addition, injections in MTc labeled cells in ITr and ITc (Kaskan and Kaas, 2007). Furthermore, ITc has projections to V2 (Collins et al., 2001). The present TG is in a similar location to TG, and perhaps a portion of TEr, of Preuss and Goldman-Rakic (1991a) and Te6 of Zilles and colleagues (1979). Architectonically, TG is sparsely myelinated (Preuss and Goldman-Rakic, 1991a; present study). Additionally, there is evidence from the higher levels of free ionic zinc and lower

levels of VGluT2 expression that TG is receives proportionately more corticocortical terminations and proportionately less thalamocortical terminations than ITr. Our STd is in a similar location to STd of Preuss and Goldman-Rakic (1991a) and overlaps the rostral portion of Te2.2 of Zilles et al. (1979). Architectonically, STd has a thin layer 4 and broad layers 5 and 6, and is moderately myelinated (Preuss and Goldman-Rakic, 1991a; present study). Furthermore, STd expresses proportionately more synaptic zinc positive corticocortical terminations and proportionately less PV and VGluT2 immunopositive thalamocortical terminations than ITr and ITc.

Auditory areas. The auditory cortex of galagos contains at least two core sensory areas and a surrounding belt region (Kanagasuntheram et al., 1966; Brugge, 1982; Preuss and Goldman-Rakic, 1991a). Primary auditory cortex of galagos is located on the caudal bank of the lateral sulcus within the temporal lobe (Kanagasuntheram et al., 1966; Zilles et al., 1979; Brugge, 1982; Conley et al., 1991; Preuss and Goldman-Rakic, 1991a). In monkeys, two major core auditory fields, A1 and a rostral area (R) have been identified (Allman and Kaas, 1971b; Merzenich and Brugge, 1973; Imig et al., 1977) and receive inputs from the ventral subdivision of the medial geniculate nucleus (Morel et al., 1993; Kaas et al., 1999; Kaas and Hackett, 2000; de la Mothe et al., 2006). Two primary-like auditory areas have been identified in galagos as well, the koniocellular primary auditory cortex (A1), which receives projections from the ventral subdivisions of the medial geniculate nucleus in the thalamus (Conley et al., 1991), and the rostral auditory area (R) with similar architecture and likely similar thalamic inputs. An auditory responsive lateral belt, possibly consisting of at least two areas, was also identified (Brugge, 1982). The

lateral auditory belt has connections with the secondary, but not primary, subdivisions of the medial geniculate body (Conley et al., 1991).

The primary-like auditory fields A1 and R have similar architectonic appearances, and as such were described in this study as a single field, A. Area A has a koniocellular appearance with a densely packed layer 4 and is densely myelinated (Preuss and Goldman-Rakic, 1991a). These observations are congruent with our results. Furthermore, area A expresses more PV and VGluT2 immunopositive terminations, and less synaptic zinc than the surrounding areas. This suggests that area A receives denser inputs from the sensory thalamus, likely the ventral subdivision of the medial geniculate nucleus (Conley et al., 1991), and sparser inputs from other cortical areas compared to the adjoining areas. The lateral and medial belt areas that surround Area are less densely packed with cells and less myelinated than area A. The darker staining in zinc preparations suggests that both the lateral and medial Ab receives more corticocortical projections than area A. PV and VGluT2 immunopositive thalamic terminations are present in layer 4 of both lateral and medial Ab, although to a lesser extent than area A. Some of these thalamic projections are likely to originate from the secondary subdivisions of the medial geniculate body (Conley et al., 1991).

Parietal cortex

Area 3b(S1). In prosimian galagos, there are at least three cortical areas in the anterior parietal cortex, the primary somatosensory area, 3b(S1), 3a, and 1/2 (Sur et al., 1980; Carlson and Welt, 1980; 1981; Wu and Kaas, 2003). Area 3b(S1) has a topographic representation of the contralateral body surface that begins with the oral

cavity and face representations ventrally and proceeds medially to the hand, arm, trunk, and on the medial wall the hindlimb representation (Carlson and Welt, 1980; Sur et al., 1980; Wu and Kaas, 2003), as for monkeys (Kaas, 1983; Kaas and Pons, 1988; Kaas, 2007) and other mammals (for review, see Kaas, 1983). Area 3b(S1) of galagos corresponds to Pa1 of Zilles et al., (1979). As expected of primary sensory areas, area 3b(S1) of galagos has a koniocellular appearance with a layer 4 that is densely packed with granule cells (Kanagasuntheram et al., 1966; Preuss and Goldman-Rakic, 1991a; present study), is densely myelinated and metabolically active. Furthermore, layer 5 of area 3b(S1) in galagos contains large, elongated PV immunopositive pyramidal cells (Preuss and Kaas, 1996). Area 3b(S1) of galagos also expresses low levels of free zinc ions, and is densely populated with PV and VGluT2 immunopositive thalamocortical terminations. This suggests that layer 4 receives proportionately more inputs from the thalamus than from other cortical areas. Area 3b(S1) of galagos receives thalamic inputs from the ventroposterior nucleus, as in other mammals (Kaas, 1982; Burton and Carlson, 1986; see Kaas, 1983 for review). As in squirrels (Wong and Kaas, 2008) and tree shrews (Wong and Kaas, 2009a), architectonic features of area 3b(S1) are not uniform throughout, especially in layer 4, where the thickness varies throughout the extent of the cortical area (Fig. 16). The variable thickness of layer 4 in area 3b(S1) of galagos is likely to be related to discontinuities in the cortical representations of the cutaneous surface.

Area 3a. Area 3b(S1) of galagos is bordered rostrally by area 3a, a narrow strip of cortex where neurons are activated by taps to the body and noncutaneous stimuli, which suggests the activation of deep receptors in muscles and joints (Sanides and Krishnamurti, 1967; Kaas, 1983; Wu and Kaas, 2003). Movements can be evoked by

microstimulation of neurons in area 3a (Stepniewska et al., 1993; Wu and Kaas, 1999), and microelectrode stimulation studies have revealed a motor map in area 3a of galagos that is organized in a manner that is parallel to the somatotopic map in area 3b(S1) (Wu and Kaas, 2003). As in monkeys (Huerta and Pons, 1990; Huffman and Krubitzer, 2001), area 3a of galagos has connections to area 3b(S1), S2 and Pv (Wu and Kaas, 2003) that is similar to those of monkeys. Architectonically, area 3a of galagos has a thin layer 4 and larger pyramidal cells in layer 5 (Preuss and Goldman-Rakic, 1991a; Wu et al., 2000; present study). A subpopulation of the larger pyramidal cells in layer 5 of area 3a is PV immunopositive (Preuss and Kaas, 1996). Area 3a of galagos is also less densely myelinated and expresses less CO than area 3b(S1). Furthermore, area 3a has more synaptic free zinc ions, and less PV and VGluT2 immunopositive terminations. This suggests that area 3a receives proportionately more corticortical than thalamocortical projections. Area 3a in galagos is likely to be homologous to Poc2 of Zilles et al. (1979). The cortical connections with area 3b(S1), S2 and PV (Wu and Kaas, 2003) likely contribute to the dark staining of area 3a in zinc preparations. Area 3a in galagos is also likely to receive projections from the ventroposterior superior nucleus, as in monkeys (Cusick et al., 1985).

Area 1/2. The cortical area caudal to area 3b(S1), area 1/2, is an area that has topographic connections with area 3b(S1) and is likely to receive inputs from the ventral thalamus representing receptors mediating proprioception (Kaas and Pons, 1988; Wu and Kaas, 2003). Architectonically, area 1/2, which extends onto the medial cortical surface, is characterized by a moderately populated layer 4 and larger pyramidal cells in layer 5 compared to area 3b(S1)(Preuss and Goldman-Rakic, 1991a; Wu and Kaas, 2003; present

study), and reduced myelination with no distinct bands of Baillarger. In layer 4, area 1/2 expresses higher levels of free synaptic zinc and lower and lower levels of PV and VGluT2 immunopositive thalamocortical terminations than area 3b(S1). This suggests an increase in proportion of corticocortical over thalamocortical inputs. Some of these cortical inputs may be from area 3b(S1) (Wu and Kaas, 2003). Area 1/2 of galagos overlaps area 5 of Brodmann (1909), area 2-5 of Preuss and Goldman-Rakic (1991a) and the rostral portion of Pa2 of Zilles et al. (1979). Area 1/2 of galagos may be related to areas 1 and 2 of monkeys (Wu and Kaas, 2003). By location, architectonic and some connectional properties, area 1/2 of galagos is similar to the caudal somatosensory area, SC, of tree shrews (Remple et al., 2006; Remple et al., 2007; Wong and Kaas, 2009), and the parietal medial area of squirrels (Krubitzer et al., 1986; Slutsky et al., 2000; Wong and Kaas, 2008) and rats (Donoghue and Parham, 1983; Reep et al., 1990; Reep et al., 1994; Wang and Kurata, 1998).

S2 and Pv. Areas S2 and Pv lie posterior and ventral to area 3b(S1) and extend onto the upper bank of the lateral sulcus. These two areas have been identified in some species of monkeys (Cusick et al., 1989; Krubitzer et al., 1995; Qi et al., 2002) and other mammals (see Disbrow et al., 2000 for review) such as squirrels (Nelson et al., 1979; Wong and Kaas, 2008), rats (Walker and Sinha, 1972; Remple et al., 2003) and tree shrews (Remple et al., 2006; Wong and Kaas, 2009a). In galagos, S2 (Burton and Carlson, 1986; Wu and Kaas, 2003) and Pv (Wu and Kaas, 2003) have separate somatotopic representations that are organized such that the face representations of both S2 and Pv adjoin the face presentation in area 3b(S1)(Wu and Kaas, 2003). The neurons in S2 and Pv have a larger receptive field than the neurons in area 3b(S1)(Wu and Kaas,

2003). Both S2 and Pv of galagos, like most other mammals, have topographic connections with area 3b(S1)(Wu and Kaas, 2003). Furthermore, S2 and Pv are densely interconnected (Wu and Kaas, 2003). S2 of galagos has differing thalamocortical connections compared to other monkeys. In galagos, S2 receives dense inputs from the ventroposterior nucleus (Burton and Carlson, 1986; Garraghty et al., 1991), whereas in monkeys, S2 receives dense inputs from the ventroposterior inferior rather than ventroposterior proper nucleus (Garraghty et al., 1990; Krubitzer and Kaas, 1992). Architectonically, S2 and Pv have similar appearances (Wu and Kaas, 2003; present study). Both S2 and Pv have thinner granular layer 4 and are less densely myelinated than area 3b(S1). The increased expression of synaptic zinc in the corticocortical terminations in S2 and Pv compared to area 3b(S1) suggests that S2 and Pv receive proportionately more corticocortical inputs than area 3b(S1). Furthermore, S2 and Pv express lower levels of PV immunopositive thalamocortical terminations than area 3b(S1), suggesting a reduced population of thalamic projections to S2 and Pv. However, S2 and Pv express moderate levels of VGluT2 immunopositive thalamocortical terminations. These thalamocortical terminations are likely to originate from the ventroposterior nucleus (Burton and Carlson, 1986; Garraghty et al., 1991).

Posterior parietal cortex. In galagos, the posterior parietal cortex, which extends onto the medial cortical surface, is also known as Brodmann's area 7 (Brodmann, 1909) and overlaps with Pa2 of Zilles and colleagues (1979). We defined three areas, PPr, PPc and PPl, within the posterior parietal cortex, which has been divided into as many as six areas (Preuss and Goldman-Rakic, 1991a). The rostral portion of the posterior parietal cortex, area 7b in monkeys, is involved in higher-order processing of somatosensory

information (Kaas, 2004). In macaques, area 7b contains neurons that are responsive to visual and somatosensory stimulation (Hyvärinen and Shelepin, 1979; Robinson and Burton, 1980a; 1980b). Furthermore, area 7b of monkeys has connections with the premotor, prefrontal, caudal posterior parietal and superior temporal sulcus areas (Cavada and Goldman-Rakic, 1989; Lewis and Van Essen, 2000). The region defined as area 7b of galagos by Wu and Kaas (2003) corresponds in location to area 7b of macaques (Wu and Kaas, 2003). In galagos, the rostral portion of the posterior parietal cortex, PPr and PPl, or area 7b (Preuss and Goldman-Rakic, 1991a) has a crude map of complex behaviors that can be evoked by microstimulation (Stepniewska et al., 2005b). Furthermore, this rostral posterior parietal cortex region has connections with S2, Pv, M1 and premotor areas (Wu and Kaas, 2003; Fang et al., 2005; Stepniewska et al., 2005). Architectonically, PPr and PPl have similar appearances and possess the characteristics of association cortex. Both PPr and PPl of galagos have a thin layer 4 and are moderately myelinated. In zinc preparations, PPr and PPl express high levels of synaptic free zinc ions, with PPl staining more darkly than PPr. PPr expresses more PV immunopositive thalamocortical terminations than PPl and similar levels of VGluT2 thalamocortical terminations to PPl. Compared to the surrounding cortical areas, the dominant inputs to layer 4 of PPr and PPl are from other cortical areas. Thalamocortical inputs to layer This 4 of PPr and PPl may originate from the ventral lateral nucleus and the anterior pulvinar, as in monkeys (Kaas, 2004). Between PPl and PPr, the darker staining in zinc preparations and lighter staining PV preparations indicates that PPl receives proportionately more corticortical and less thalamocortical inputs than PPr.

PPc, within the caudal portion of the posterior parietal cortex overlaps with area 7a of Preuss and Goldman-Rakic (1991a). PPc has both visual and visuomotor functions (Kaas, 2004). Visual inputs to PPc of area 7a of monkeys include those from the superior temporal cortex (Maunsell and van Essen, 1983) and dorsal regions of the prelunate gyrus (May and Andersen, 1986). In galagos, PPc has connections with V2, V3, DM, DL, and MT (Beck and Kaas, 1998a; Collins et al., 2001; Lyon and Kaas, 2002; Kaskan and Kaas, 2007). Architectonically, PPc of galagos has a moderately populated granular layer 4. Compared to the surrounding cortical areas, PPc stains lighter for free ionic zinc, and darker for PV and VGluT2 immunopositive terminations. This suggests that layer 4 of PPc in galagos receives proportionately less corticocortical and more thalamocortical projections than the adjoining cortical areas MTc and area 7m. PPc may receive projections from the medial pulvinar, as in monkeys (Kaas, 2004).

Claustral cortex

We have retained the nomenclature from Zilles et al. (1979) and identified claustral cortex in galagos as the cortical areas that overlie the claustrum (Fig. 16). Claustral cortex in galagos is ventral to the somatosensory areas, and caudal to orbital frontal cortex. The claustral cortex of this study includes the insular and frontal parietal opercular areas of Preuss and Goldman-Rakic (1991a; 1991c). Claustral cortex in galagos is in a similar location to insular allocortex in another prosimian, the slow loris (Sanides and Krishnamurti, 1966, and to insular cortex in rodents (e.g. Zilles, 1990; Wong and Kaas, 2008) and in tree shrews (Zilles, 1978; Wong and Kaas, 2009a). Compared to monkeys, claustral cortex in galagos is in a similar location to precentral opercular

(PrCO) area (Preuss and Goldman-Rakic, 1991a) or proisocortical motor area (Cipolloni and Pandya, 1999) in Old World macaques. In macaques, PrCO or the proisocortical motor area may be responsible for initiating motor movements related to orofacial, head and neck structures (Cipolloni and Pandya, 1999). Architectonically, PrCO or proisocortical motor area in macaques has thin, granular layers 2 and 4 (Mesulam and Mufson, 1982). Studies of connections in macaques showed that proisocortical motor area has widespread cortical connections, including connections with the ventral granular frontal cortex (Preuss and Goldman-Rakic, 1989), area 3b(S1), and the secondary somatosensory, insula, premotor and cingulate areas (Cipolloni and Pandya, 1999; Disbrow et al., 2003). In galagos, claustral cortex, also identified as area 13 to 16 or insular cortex by Pritzel and Markowitsch (1982), has connections with the orbital frontal areas 9, 10 and 11 of Brodmann (1909) and area 6. There are two architectonically distinct areas within the claustral cortex, the dorsal and ventral areas. Architectonically, both areas, CLId and CLIv have a thin layer 4, as in PrCO of macaques (Mesulam and Mufson, 1982) and are sparsely myelinated. The border between CLId and CLIv are distinct in zinc and VGluT2 preparations. CLId stains darker for synaptic zinc and lighter for VGluT2 immunopositive terminations compared to CLIv. This suggests that CLId receives proportionately more corticocortical inputs and less VGluT2 immunopositive thalamocortical inputs than CLIv. It is possible that claustral cortex of galagos has similar connectivity to that in PrCO or prosiocortical motor area in macaques (Cipolloni and Pandya, 1999; Disbrow et al., 2003), in addition to having connections with the orbital frontal cortex and area 6 (Pritzel and Markowitsch, 1982).

Frontal cortex

Primary motor cortex. Primary motor cortex (M1) is about 2 to 3mm wide in galagos (Wu et al., 2000) and extends from the dorsal surface on to the upper portion of the medial surface (Zuckerman and Fulton, 1941). Electrical stimulation studies with microelectrodes have shown that M1 contains an complete body and orofacial map, with the orofacial regions represented laterally, the trunk centrally and hindlimb represented dorsally (Zuckerman and Fulton, 1941; Kanagasuntheram et al., 1966; Fogassi et al., 1994; Wu et al., 2000). This region is coextensive with the architectonically defined M1, also known as area 4 of Brodmann (1909), area F posterior of Fogassi et al. (1994) and is contained within the area praecentralis 1 of Zilles et al. (1979). M1 of galagos has strong connections with the ventrolateral nucleus of the thalamus (Fang et al., 2006) and with premotor areas (Fang et al., 2005). M1 of galagos has the general architectonic features of motor cortices, such as a poorly developed granular layer 4, a thick layer 5 that is populated with large pyramidal cells, and moderate myelination. Furthermore, the large pyramidal neurons in layer 5 of M1 in galagos are also SMI-32 immunopositive (Wu et al., 2000) and PV immunopositive (Preuss and Kaas, 1996). M1 stains darkly for synaptic zinc, poorly for PV immunopositive terminations and moderately for VGluT2 immunopositive terminations. From the dark zinc staining, it is likely that M1 receives proportionately more corticortical projections than the adjoining cortical areas. The presence of VGluT2, although not PV, immunopositive terminations in M1 are consistent with the evidence that M1 receive thalamic inputs (Fang et al., 2006) although proportionately less than the surrounding cortical areas.

Area 6. In galagos, area 6 consists of the premotor and supplementary motor areas (Preuss and Goldman-Rakic, 1991a; 1991c; Wu et al, 2000; Fang et al., 2005), and is within the area identified as Prc1 by Zilles and colleagues (1979). The premotor area has been further divided into the dorsal and ventral subdivisions (Wu et al., 2000; Fang et al., 2005), which respectively corresponds to area 6D and 6V of Preuss and Goldman-Rakic (1991a, 1991b, 1991c). The supplementary motor area (Wu et al., 2000; Fang et al., 2005) is in a similar location to area 6m of Preuss and Goldman-Rakic (1991a, 1991b, 1991c). These premotor areas typically contain neurons that require higher levels of current to evoke movements than those in M1 (Wu et al., 2000). The premotor areas have strong connections with M1, the prefrontal cortex and the spinal cord (Wu et al., 2000), and connections with the ventrolateral nucleus of the motor thalamus (Fang et al., 2006). Furthermore, a frontal eye field (FEF) has been described in galagos, where eye movements are evoked by when electrical stimulation with microelectrodes (Wu et al., 2000). These areas, defined by their neuron response properties and connection patterns, are included in the cortical maps in this study. However, the architectonic differences between these areas are subtle, and are described as a single field, area 6. Architectonically, area 6 have smaller pyramidal cells than M1 (Wu et al., 2000), and a moderately populated, thin layer 4. Area 6 stains lighter for synaptic zinc, and darker for PV and VGluT2 immunopositive terminations compared to M1. This indicates that area 6 receives proportionately less corticocortical and more thalamocortical inputs than M1.

Remaining frontal areas. We have divided the frontal pole of galagos into three main regions, the granular frontal, orbital frontal and medial frontal regions. The granular frontal area is further divided into three areas, the granular frontal anterior (GrA),

posterior (GrP), and medial (GrM) areas. These three areas are similar to GrA, GrP and GrM of Preuss and Goldman-Rakic (1991a; 1991c). GrA and GrP may contain more area, but we have not further subdivided GrA and GrP as the architectonic evidence for doing so is not strong in our material. The granular frontal areas are likely to have widespread connections with the rest of cortex, including the cingulate, insular, parietal, posterior parietal and inferior temporal cortices (Pritzel and Markowitsch, 1982; Preuss and Goldman-Rakic, 1991b). Furthermore, thalamocortical projections to the granular frontal areas may originate from the ventrolateral and ventroanterior nuclei (Pritzel and Markowitsch, 1982). Architectonically, the granular frontal areas have a distinct layer 4 and a layer 5 that is populated with darkly stained cells. All three areas are moderately myelinated with GrP showing a distinct outer band of Baillarger. GrP stains lighter, whereas GrA and GrM stain darker in zinc preparations, suggesting that GrP receives proportionately less corticocortical inputs than GrA and GrM. Furthermore, GrA receives proportionately less thalamocortical inputs than GrP, as GrA expresses less PV and VGluT2 immunopositive terminations. GrM does not have a homogenous appearance in PV preparations, hinting at the presence of a dorsal and ventral subdivision. Additionally, GrM receives proportionately more thalamocortical projections than GrP, as GrM stains darker for VGluT2 immunopositive terminations than GrP.

The orbital frontal region is further divided into three areas, the dorsal (OFd), ventral (OFv) and medial (OFm) areas. OFd is similar to area 13, OFv to area 14L and OFm to area 14M of Preuss and Goldman-Rakic (1991a, 1991c). These three areas are architectonically distinct from each other in the Nissl stain, where OFd has a distinct, moderately thick granular layer 4, OFv has a thin layer 4, and OFm has a thin and pale

layer 4. Of the three orbital frontal areas, OFm is the least densely myelinated and stains the darkest for synaptic zinc. OFv has the lowest and OFd has the highest expression of PV and VGluT2 immunopositive terminations of the three orbital frontal areas. These architectonic characteristics suggest that OFd receives the highest proportion of PV and VGluT2 immunopositive thalamocortical terminations, followed by OFm, and OFv receives the lowest proportion. OFm receives the highest proportion of corticocortical inputs, followed by OFv, and OFd receives the lowest proportion. Thalamocortical projections to the orbital frontal areas in galagos originate from the mediodorsal nuclei, and corticocortial projections to these areas originate from the insular cortex (Pritzel and Markowitsch, 1982).

The medial frontal (MF) area in galagos has been subdivided into the rostral and caudal areas (Preuss and Goldman-Rakic, 1991a; 1991c). We have left it as a single area, as architectonic subdivisions could not be reliably established in our material. Yet, a heterogeneous myelination pattern and variations in zinc staining within MF suggests the presence of subdivisions. The intense staining in zinc preparations and poor staining for PV and VGluT2 immunopositive terminations suggests that MF receives a higher proportion of corticocortical than thalamocortical projections. These corticocortical projections may originate from the cingulate and retrosplenial cortices (Pritzel and Markowitsch, 1982).

Medial cortex

*Medial area 7.*Medial area 7, 7m, in galagos approximate corresponds to area 7dm and 7vm of Preuss and Goldman-Rakic (1991a) and Pa2 of Zilles and colleagues

(1979). By location, it has been suggested that area 7m in galagos may have some homology to the medial parietal areas in macaque monkeys as both areas are located above the posterior cingulate area 23 (Preuss and Goldman-Rakic, 1991a). Architectonically, area 7m in galagos has a well developed granular layer 4 and is moderately myelinated. Area 7m of galagos stains darkly for synaptic zinc, moderately for PV and VGluT2 immunopositive terminations. This indicates that inputs to area 7m originate from other areas of cortex, as well as from nuclei in the thalamus.

Cingulate areas. In most mammals, the cingulate cortex surrounds the anterior portion of the corpus callosum and consists of at least the rostral, dorsal and ventral cingulate areas (e.g. Zilles, 1990; Vogt et al., 1992; Vogt et al., 2004; Wong and Kaas, 2008, 2009a, 2009b). The cingulate cortex is part of the limbic system and the Papez circuit (Vogt et al., 1992) and has architectonic features of both isocortex and allocortex (Zilles, 1990). The primate cingulate areas are involved in attention and memory, as evidenced by the presence of connections with the hippocampal cortex (Kobayashi and Amaral, 2007) and the frontal cortex (Kobayashi and Amaral, 2003). In addition, the primate cingulate areas mediate somatic and autonomic motor responses, and pain responses (Smith, 1945; Ward, 1948; Kaada, 1951; Barris and Schuman, 1953; Foltz and White, 1962; Foltz and White, 1968). In Old World macaque monkeys, the anterior cingulate (area 24) receives auditory inputs from areas around the superior temporal gyrus and multimodal inputs from the orbital frontal areas (Vogt and Pandya, 1987). Thalamic inputs to the anterior cingulate (area 24) in macaque monkeys include projections from the centrodensocellular, parafasicular, ventroanterior and mediodorsal nuclei (Vogt et al., 1987). The posterior cingulate (area 23) of macaque monkeys has

connections with area 19 (Vogt and Pandya, 1987), and with the anteromedial, lateroposterior and medial pulvinar nuclei of the thalamus (Baleydier and Mauguiere, 1985; Vogt et al., 1987).

We have retained the nomenclature of Preuss and Goldman-Rakic (1991a) for the cingulate areas in galagos, where cingulate cortex in galagos is divided into the paralimbic area (Para) that is part of the dorsal anterior cingulate cortex, area 24 that is part of the ventral anterior cingulate cortex, and area 23 that is part of the posterior cingulate cortex. These three cingulate areas are within the cingulate region defined by Zilles and colleagues (1979). Area 24 as identified here overlaps with a portion of the cingulate motor area (CMAc) that has connections with the spinal cord and M1 and contains neurons that causes movements of the forelimb, trunk and hindlimb with electrically stimulated by microelectrodes (Wu et al., 2000).

Architectonically, all three cingulate areas have poorly developed granular layer 4 and are poorly myelinated. In galagos, both Para, which approximately corresponds to area 24a of macaques by location (Vogt and Pandya, 1987; Vogt et al., 1987), and area 24, which is similar to area 24b and c of macaques by location (Vogt and Pandya, 1987; Vogt et al., 1987), express high levels of synaptic zinc, and lower levels of PV and VGluT2 immunopositive terminations. These staining patterns suggest that Para and area 24 of galagos receive proportionately high levels of corticortical inputs, possibly originating from the auditory and orbital frontal cortex as in macaques (Vogt and Pandya, 1987), and moderate levels of thalamocortical inputs, possibly originating from the centrodensocellular, parafasicular, ventroanterior and mediodorsal nuclei as in macaques (Vogt et al., 1987). The posterior cingulate area in galagos, area 23, has increased

staining for synaptic zinc and reduced staining for PV and VGluT2 immunopositive terminations, with the reduction being most pronounced for PV immunopositive terminations. This indicates that area 23 receives proportionately larger amounts of corticocortical projections and lower amounts of thalamocortical projections. Area 23 in galagos may have connections with areas 9 and 46 in the frontal cortex, the posterior parietal cortex (Kobayashi and Amaral, 2003) and areas around the superior temporal cortex (Seltzer and Pandya, 2009), as in macaques. Thalamocortical projections to area 23 in galagos may originate from anteromedial, lateroposterior and medial pulvinar nuclei, as in macaques (Vogt et al., 1987; Baleydier and Mauguiere, 1985).

Retrosplenial areas. In most mammals, the retrosplenial cortex surrounds the posterior portion of the corpus callosum and consists of at least the granular and agranular areas (e.g. Zilles, 1978; Palomero-Gallagher and Zilles, 2004, Wong and Kaas, 2008; 2009a; 2009b). The retrosplenial cortex plays a role in the processes of leaning and memory (van Groen and Wyss, 1990), as evidenced by the major inputs area 29 receives from the hippocampal and prefrontal cortices in monkeys (Kobayashi and Amaral, 2003). Area 30 of retrosplenial cortex in macaques have connections with the adjoining area 23 (Morris et al., 1999a; Morris et al., 1999b), as well as extrastriate visual areas, the mid-dorsolateral prefrontal cortex, areas in the superior temporal sulcus and the parahippocampal cortex (Morecraft et al., 2003; 2004; Seltzer and Pandya, 2009). Thalamic connections of area 30 in macaques include those with the lateroposterior, laterodorsal and anteroventral limbic nuclei (Morris et al., 1999a).

We have retained the nomenclature of Zilles et al., (1979) for galagos, where retrosplenial cortex is divided into the granular (RSg) and agranular (RSag) areas, which

respectively corresponds to areas 29 and 30 of Preuss and Goldman-Rakic (1991a). Architectonically, Both RSg and RSag of galagos do not have well defined lamination patterns. In galagos, RSg is characterized by a layer 2/3 that is densely packed with cells and by moderate myelination. RSag is characterized by low cell packing density and is more sparsely myelinated. RSg expresses less synaptic zinc than RSag, suggesting that RSg receives proportionately less corticocortical terminations than RSag. Furthermore, RSg expresses more PV and VGluT2 immunopositive terminations than RSag, suggesting that a larger proportion of inputs to RSg originates from nuclei in the thalamus than RSag. The parvalbumin distribution in the retrosplenial areas of galagos is similar to that of rhesus monkeys (Vogt et al., 2005).

Prostriata area. Area prostriata (PS), identified in primates by Sanides (1970), is part of the limbic cortex lying along the posteriomedial border of area 17 that is visual in function and contains a representation of the peripheral vision of the contralateral visual hemifield. PS has been identified in a number of mammals, including short-tailed opossums (Wong and Kaas, 2009b), gray squirrels (Wong and Kaas, 2008), tree shrews (Wong and Kaas, 2009a), and monkeys (Allman and Kaas, 1971a). In rats, the comparable region is known as the posteromedial visual area (Wang and Burkhalter, 2007), medial area 18b (Krieg, 1946; Caviness, 1975) and Oc2MM (Zilles and Wree, 1995). In cats, this area is known as the splenial visual area (see Rosa and Krubitzer, 1999, for review). PS in nonprimate mammals receives inputs from V1 and is responsive to visual stimuli (Kalia and Whitteridge, 1973; Tiao and Blakemore, 1976; Wagor et al., 1980; Olavarria and Montero, 1984; Law et al., 1988; Olavarria and Montero, 1990; Montero, 1993). In primates, PS has connections with visual areas such as V1, MST and

the cingulate motor cortex (Sousa et al., 1991; Rosa et al., 1993; Morecraft et al., 2000). Additionally, PS in nonprimates mammals is more expansive than primates (Rosa et al., 1997). In galagos, PS contains neurons that are responsive to visual stimuli (Rosa et al., 1997). Architectonically, PS of galagos resembles that of other mammals, including poor myelination, high expression of synaptic zinc, and moderate expression of PV and VGluT2 immunopositive terminations. The architectonic characteristics of PS in galagos suggest that this area is likely to have a larger proportion of corticocortical, rather than thalamocortical inputs. PS in galagos is relatively larger than in monkeys, which may be reflective of the ancestral state (Rosa et al., 1997).

Perirhinal area

The perirhinal area (PRh) in galagos is a narrow strip of cortex along the dorsal bank of the rhinal fissure and ventral to the temporal lobe. This area corresponds to area 35 of Brodmann (1909) and to area 35 in galagos identified by Preuss and Goldman-Rakic (1991a). As with most mammals, such as grey squirrels (Wong and Kaas, 2008), rats (Burwell, 2001; Palomero-Gallagher and Zilles, 2004), and tree shrews (Wong and Kaas, 2009a), PRh of galagos is poorly myelinated and lacks a well defined lamination pattern. Furthermore, PRh stains darkly for synaptic zinc and poorly for PV and VGluT2 immunopositive terminations. This suggests that PRh receives a large proportion of corticortical inputs and few thalamocortical inputs. In rats, PRh has connections with the hippocampal formation (Burwell and Amaral, 1998; Palomero-Gallagher and Zilles, 2004; Furtak et al., 2007) and is as such implicated in memory processes. Furthermore, PRh of rats receives projections from the anterior thalamic nuclei (Palomero-Gallagher,

and Zilles, 2004), the piriform, frontal, temporal, and insular cortices (Furtak et al., 2007). In macaque monkeys, PRh receives projections from visual areas in the temporal cortex, the parahippocampal cortex, and the insular cortex (Suzuki and Amaral, 1994) and has reciprocal connections with areas within the orbitofrontal cortex (Suzuki and Amaral, 1994; Kondo et al., 2005). It is probable that PRh in galagos, like most other mammals, has a role in memory processes, and has similar connection patterns to that in macaque monkeys.

Table 1: Abbreviations

3a	Dysgranular area
19d	Area 19 dorsal
19v	Area 19 ventral
3b(S1)	Primary somatosensory area
7m	Medial area 7
A	Primary auditory area
Ab	Auditory belt area
CGd	Cingulate dorsal area
CGv	Cingulate ventral area
CLI	Claustral cortex or area claustralis isocorticalis
CLId	Dorsal claustral area
CLIv	Ventral claustral area
CMAc	Caudal cingulate motor area
CMAr	Rostral cingulate motor area
CO	Cytochrome oxidase
DL	Dorsolateral visual area
DM	Dorsomedial visual area
Ent	Entorhinal cortex
FEF	Frontal eye field
FST	Fundus of the superior temporal area
GrA	Granular frontal anterior area
GrM	Granular frontal medial area
GrP	Granular frontal posterior area
IPS	Intraparietal sulcus
ITc	Inferior temporal caudal area
ITr	Inferior temporal rostral area
M1	Primary motor area
MF	Medial frontal cortex
MST	Middle superior temporal area
MT	Middle temporal visual area
MTc	Middle temporal cresent
OFd	Orbital frontal dorsal area
Ofm	Orbital frontal medial area
OFv	Orbital frontal ventral area
Para	Paralimbic area
PB	Phosphate buffer
PBS	Phosphate buffer with saline
Pirf	Piriform cortex

PMD	Premotor dorsal area
PMV	Premotor ventral area
PPc	Posterior parietal caudal area
PPl	Posterior parietal lateral area
PPr	Posterior parietal rostral area
PRh	Perirhinal area
PS	Prostriata
PV	Parvalbumin
Pv	Parietal ventral area
R	Rostral auditory area
RSag	Retrosplenial agranular area
RSg	Retrosplenial granular area
S2	Secondary somatosensory area
SMA	Supplementary motor area
STd	Superior temporal dorsal area
TG	Area temporopolaris
V1	Primary visual area
V2	Secondary visual area
VGluT2	Vesicle Glutamate Transporter 2

References

Allman JM and Kaas JH. 1971a. Representation of the visual field in striate and adjoining cortex of the owl monkey (Aotus trivirgatus). Brain Res 35(1):89-106.

Allman JM and Kaas JH. 1971b. A representation of the visual field in the caudal third of the middle tempral gyrus of the owl monkey (Aotus trivirgatus). Brain Res 31(1):85-105.

Allman JM and Kaas JH. 1974. The organization of the second visual area (V II) in the owl monkey: a second order transformation of the visual hemifield. Brain Res 76(2):247-265.

Allman JM and Kaas JH. 1975. The dorsomedial cortical visual area: a third tier area in the occipital lobe of the owl monkey (Aotus trivirgatus). Brain Res 100(3):473-487.

Allman JM, Campbell CB and McGuinness E. 1979. The dorsal third tier area in Galago senegalensis. Brain Res 179(2):355-361.

Allman JM, Kaas JH and Lane RH. 1973. The middle temporal visual area(MT)in the bushbaby, Galago senegalensis. Brain Res 57(1):197-202.

Baleydier C and Mauguiere F. 1985. Anatomical evidence for medial pulvinar connections with the posterior cingulate cortex, the retrosplenial area, and the posterior parahippocampal gyrus in monkeys. J Comp Neurol 232(2):219-228.

Barris RW and Schuman HR. 1953. [Bilateral anterior cingulate gyrus lesions; syndrome of the anterior cingulate gyri.]. Neurology 3(1):44-52.

Beck PD and Kaas JH. 1998a. Cortical connections of the dorsomedial visual area in prosimian primates. J Comp Neurol 398(2):162-178.

Beck PD and Kaas JH. 1998b. Thalamic connections of the dorsomedial visual area in primates. J Comp Neurol 396(3):381-398.

Born RT and Bradley DC. 2005. Structure and function of visual area MT. Annu Rev Neurosci 28:157-189.

Bourne JA, Warner CE, Upton DJ and Rosa MG. 2007. Chemoarchitecture of the middle temporal visual area in the marmoset monkey (Callithrix jacchus): laminar distribution of calcium-binding proteins (calbindin, parvalbumin) and nonphosphorylated neurofilament. J Comp Neurol 500(5):832-849.

Boussaoud D, Ungerleider LG and Desimone R. 1990. Pathways for motion analysis: cortical connections of the medial superior temporal and fundus of the superior temporal visual areas in the macaque. J Comp Neurol 296(3):462-495.

Britten KH. 2003. The middle temporal area: Motion processing and the link to perception. In The visual neurosciences, L.M. Chalupa, and J.S. Werner, eds. Cambridge, MA: MIT Press. 1203-1216.

Burkhalter A, Felleman DJ, Newsome WT and Van Essen DC. 1986. Anatomical and physiological asymmetries related to visual areas V3 and VP in macaque extrastriate cortex. Vision Res 26(1):63-80.

Burton H and Carlson M. 1986. Second somatic sensory cortical area (SII) in a prosimian primate, Galago crassicaudatus. J Comp Neurol 247(2):200-220.

Burwell RD and Amaral DG. 1998. Cortical afferents of the perirhinal, postrhinal, and entorhinal cortices of the rat. J Comp Neurol 398(2):179-205.

Burwell RD. 2001. Borders and cytoarchitecture of the perirhinal and postrhinal cortices in the rat. J Comp Neurol 437(1):17-41.

Carey RG, Fitzpatrick D and Diamond IT. 1979. Layer I of striate cortex of Tupaia glis and Galago senegalensis: projections from thalamus and claustrum revealed by retrograde transport of horseradish peroxidase. J Comp Neurol 186(3):393-437.

Carlson M and Welt C. 1980. Somatic sensory cortex (SmI) of the prosimian primate Galago crassicaudatus: organization of mechanoreceptive input from the hand in relation to cytoarchitecture. J Comp Neurol 189(2):249-271.

Carlson M, and Welt C. 1981. The somatosensory cortex SmI in prosimian primates. In Cortical sensory organisation. C.N. Woolsey, eds. Clifton, NJ: Humana Press. 1-27.

Carroll EW and Wong-Riley MT. 1984. Quantitative light and electron microscopic analysis of cytochrome oxidase-rich zones in the striate cortex of the squirrel monkey. J Comp Neurol 222(1):1-17.

Casagrande VA, and De Bruyn EJ. 1982. The galago visual system: Aspects of normal organization and developmental plasticity. In The lesser busybaby (Galago) as an animal model: Selected topics. D. Haines, eds. Boca Raton, Florida: CRC Press. 107-135.

Casagrande VA, and Kaas JH. 1994. The afferent, intrinsic, and efferent connections of primary visual cortex in primates. In Cerebral Cortex: Primary Visual Cortex in Primates, K.S. Rockland, and A. Peters, eds. New York: Plenum. 201-259.

Casagrande VA, Back PD and Lachia EA. 1989. Intrinsic connections of cytochrome oxidase (CO) blob and nonblob regions in area 17 of nocturnal primate. Soc. Neurosci. Abstr. 15, 1398.

Cavada C and Goldman-Rakic PS. 1989. Posterior parietal cortex in rhesus monkey: II. Evidence for segregated corticocortical networks linking sensory and limbic areas with the frontal lobe. J Comp Neurol 287(4):422-445.

Caviness VSJ. 1975. Architectonic map of neocortex of the normal mouse. J Comp Neurol 164(2):247-263.

Celio MR. 1986. Parvalbumin in most gamma-aminobutyric acid-containing neurons of the rat cerebral cortex. Science 231(4741):995-97.

Cipolloni PB and Pandya DN. 1999. Cortical connections of the frontoparietal opercular areas in the rhesus monkey. J Comp Neurol 403(4):431-458.

Collins CE, Stepniewska I and Kaas JH. 2001. Topographic patterns of v2 cortical connections in a prosimian primate (Galago garnetti). J Comp Neurol 431(2):155-167.

Conde F, Lund JS and Lewis DA. 1996. The hierarchical development of monkey visual cortical regions as revealed by the maturation of parvalbumin-immunoreactive neurons. Brain Res Dev Brain Res 96(1-2):261-276.

Condo GJ and Casagrande VA. 1990. Organization of cytochrome oxidase staining in the visual cortex of nocturnal primates (Galago crassicaudatus and Galago senegalensis): I. Adult patterns. J Comp Neurol 293(4):632-645.

Conley M, Kupersmith AC and Diamond IT. 1991. The organization of projections from subdivisions of the auditory cortex and thalamus to the auditory sector of the thalamic reticular nucleus in Galago. Eur J Neurosci 3(11):1089-1103.

Cragg BG. 1969. The topography of the afferent projections in the circumstriate visual cortex of the monkey studied by the Nauta method. Vision Res 9(7):733-747.

Cusick CG and Kaas JH. 1988. Surface view patterns of intrinsic and extrinsic cortical connections of area 17 in a prosimian primate. Brain Res 458(2):383-88.

Cusick CG, Steindler DA and Kaas JH. 1985. Corticocortical and collateral thalamocortical connections of postcentral somatosensory cortical areas in squirrel monkeys: a double-labeling study with radiolabeled wheatgerm agglutinin and wheatgerm agglutinin conjugated to horseradish peroxidase. Somatosens Res 3(1):1-31.

Cusick CG, Wall JT, Felleman DJ and Kaas JH. 1989. Somatotopic organization of the lateral sulcus of owl monkeys: area 3b, S-II, and a ventral somatosensory area. J Comp Neurol 282(2):169-190.

Danscher G and Stoltenberg M. 2005. Zinc-specific autometallographic in vivo selenium methods: tracing of zinc-enriched (ZEN) terminals, ZEN pathways, and pools of zinc ions in a multitude of other ZEN cells. J Histochem Cytochem 53(2):141-153.

Danscher G. 1982. Exogenous selenium in the brain. A histochemical technique for light and electron microscopical localization of catalytic selenium bonds. Histochemistry 76(3):281-293.

Danscher G. 1981. Histochemical demonstration of heavy metals. A revised version of the sulphide silver method suitable for both light and electronmicroscopy. Histochemistry 71(1):1-16.

DeFelipe J and Jones EG. 1991. Parvalbumin immunoreactivity reveals layer IV of monkey cerebral cortex as a mosaic of microzones of thalamic afferent terminations. Brain Res 562(1):39-47.

DeFelipe J. 1997. Types of neurons, synaptic connections and chemical characteristics of cells immunoreactive for calbindin-D28K, parvalbumin and calretinin in the neocortex. J Chem Neuroanat 14(1):1-19.

Diamond IT, Conley M, Itoh K and Fitzpatrick D. 1985. Laminar organization of geniculocortical projections in Galago senegalensis and Aotus trivirgatus. J Comp Neurol 242(4):584-610.

Ding Y and Casagrande VA. 1997. The distribution and morphology of LGN K pathway axons within the layers and CO blobs of owl monkey V1. Vis Neurosci 14(4):691-704.

Disbrow E, Litinas E, Recanzone GH, Padberg J and Krubitzer L. 2003. Cortical connections of the second somatosensory area and the parietal ventral area in macaque monkeys. J Comp Neurol 462(4):382-399.

Disbrow E, Roberts T and Krubitzer L. 2000. Somatotopic organization of cortical fields in the lateral sulcus of Homo sapiens: evidence for SII and PV. J Comp Neurol 418(1):1-21.

Donoghue JP and Parham C. 1983. Afferent connections of the lateral agranular field of the rat motor cortex. J Comp Neurol 217(4):390-404.

Fang PC, Stepniewska I and Kaas JH. 2008. Corpus callosum connections of subdivisions of motor and premotor cortex, and frontal eye field in a prosimian

primate, Otolemur garnetti. The Journal of Comparative Neurology 508(4):565-578.

Fang PC, Stepniewska I and Kaas JH. 2005. Ipsilateral cortical connections of motor, premotor, frontal eye, and posterior parietal fields in a prosimian primate, Otolemur garnetti. J Comp Neurol 490(3):305-333.

Fang PC, Stepniewska I and Kaas JH. 2006. The thalamic connections of motor, premotor, and prefrontal areas of cortex in a prosimian primate (Otolemur garnetti). Neuroscience 143(4):987-1020.

Felleman DJ, Burkhalter A and Van Essen DC. 1997. Cortical connections of areas V3 and VP of macaque monkey extrastriate visual cortex. J Comp Neurol 379(1):21-47.

Fleagle JG. 1999. *Primate adaptation and Evolution*. San Diego: Academic Press.

Florence SL and Casagrande VA. 1987. Organization of individual afferent axons in layer IV of striate cortex in a primate. J Neurosci 7(12):3850-868.

Fogassi L, Gallese V, Gentilucci M, Luppino G, Matelli M and Rizzolatti G. 1994. The fronto-parietal cortex of the prosimian Galago: patterns of cytochrome oxidase activity and motor maps. Behav Brain Res 60(1):91-113.

Foltz EL and White LE. 1962. Pain "relief" by frontal cingulumotomy. J Neurosurg 1989-100.

Foltz EL and White LE. 1968. The role of rostral cingulumotomy in "pain" relief. Int J Neurol 6(3-4):353-373.

Frederickson CJ and Moncrieff DW. 1994. Zinc-containing neurons. Biol Signals 3(3):127-139.

Frederickson CJ, Suh SW, Silva D and Thompson RB. 2000. Importance of zinc in the central nervous system: the zinc-containing neuron. J Nutr 130(5S Suppl):1471S-483S.

Fujiyama F, Furuta T and Kaneko T. 2001. Immunocytochemical localization of candidates for vesicular glutamate transporters in the rat cerebral cortex. J Comp Neurol 435(3):379-387.

Furtak SC, Wei SM, Agster KL and Burwell RD. 2007. Functional neuroanatomy of the parahippocampal region in the rat: the perirhinal and postrhinal cortices. Hippocampus 17(9):709-722.

Gallyas F. 1979. Silver staining of myelin by means of physical development. Neurol Res 1(2):203-09.

Garraghty PE, Florence SL, Tenhula WN and Kaas JH. 1991. Parallel thalamic activation of the first and second somatosensory areas in prosimian primates and tree shrews. J Comp Neurol 311(2):289-299.

Gattass R, Gross CG and Sandell JH. 1981. Visual topography of V2 in the macaque. J Comp Neurol 201(4):519-539.

Gattass R, Sousa AP and Rosa MG. 1987. Visual topography of V1 in the Cebus monkey. J Comp Neurol 259(4):529-548.

Gattass R, Sousa AP and Gross CG. 1988. Visuotopic organization and extent of V3 and V4 of the macaque. J Neurosci 8(6):1831-845.

Gattass R, Sousa AP, Mishkin M and Ungerleider LG. 1997. Cortical projections of area V2 in the macaque. Cereb Cortex 7(2):110-129.

Glendenning KK, Kofron EA and Diamond IT. 1976. Laminar organization of projections of the lateral geniculate nucleus to the striate crotex in Galago. Brain Res 105(3):538-546.

Hackett TA and de la Mothe LA. 2009. Regional and laminar distribution of the vesicular glutamate transporter, VGluT2, in the macaque monkey auditory cortex. J Chem Neuroanat

Hackett TA, Stepniewska I and Kaas JH. 1998. Thalamocortical connections of the parabelt auditory cortex in macaque monkeys. J Comp Neurol 400(2):271-286.

Hendrickson AE. 1985. Dots, stripes and columns in monkey visual cortex. Trends Neurosci 8:(4):404-410.

Hendrickson AE, Wilson JR and Ogren MP. 1978. The neuroanatomical organization of pathways between the dorsal lateral geniculate nucleus and visual cortex in Old World and New World primates. J Comp Neurol 182(1):123-136.

Hof PR, Glezer ,I, Conde F, Flagg RA, Rubin MB, Nimchinsky EA and Vogt Weisenhorn DM. 1999. Cellular distribution of the calcium-binding proteins parvalbumin, calbindin, and calretinin in the neocortex of mammals: phylogenetic and developmental patterns. J Chem Neuroanat 16(2):77-116.

Hubel DH and Wiesel TN. 1972. Laminar and columnar distribution of geniculo-cortical fibers in the macaque monkey. J Comp Neurol 146(4):421-450.

Huerta MF and Pons TP. 1990. Primary motor cortex receives input from area 3a in macaques. Brain Res 537(1-2):367-371.

Huffman KJ and Krubitzer L. 2001. Area 3a: topographic organization and cortical connections in marmoset monkeys. Cereb Cortex 11(9):849-867.

Hyvärinen J and Shelepin Y. 1979. Distribution of visual and somatic functions in the parietal associative area 7 of the monkey. Brain Res 169(3):561-64.

Ichinohe N and Rockland KS. 2004. Region specific micromodularity in the uppermost layers in primate cerebral cortex. Cereb Cortex 14(11):1173-184.

Ichinohe N, Fujiyama F, Kaneko T and Rockland KS. 2003. Honeycomb-like mosaic at the border of layers 1 and 2 in the cerebral cortex. J Neurosci 23(4):1372-382.

Imig TJ, Ruggero MA, Kitzes LM, Javel E and Brugge JF. 1977. Organization of auditory cortex in the owl monkey (Aotus trivirgatus). J Comp Neurol 171(1):111-128.

Jerison HJ. 1979. Brain, body and encephalization in early primates. J Hum Evol 8:615-635.

Kaada BR. 1951. Somato-motor, autonomic and electrocorticographic responses to electrical stimulation of rhinencephalic and other structures in primates, cat, and dog; a study of responses from the limbic, subcallosal, orbito-insular, piriform and temporal cortex, hippocampus-fornix and amygdala. Acta Physiol Scand Suppl 24(83):1-262.

Kaas JH and Hackett TA. 2000. Subdivisions of auditory cortex and processing streams in primates. Proc Natl Acad Sci U S A 97(22):11793-99.

Kaas JH and Lyon DC. 2001. Visual cortex organization in primates: theories of V3 and adjoining visual areas. Prog Brain Res 134:285-295.

Kaas JH and Morel A. 1993. Connections of visual areas of the upper temporal lobe of owl monkeys: the MT crescent and dorsal and ventral subdivisions of FST. J Neurosci 13(2):534-546.

Kaas JH. 2007. The evolution of somatosensory and motor systems in primates. In Evolution of primate nervous systems, J.H. Kaas, and T.M. Preuss, eds. London: Elsevier.

Kaas JH. 1982. The somatosensory cortex and thalamus in Galago. In The lesser busybaby (Galago) as an animal model: Selected topics. D.E. Haines, eds. Boca Raton, Florida: CRC Press. 169-181.

Kaas JH. 2004. Somatosensory system. In The human nervous system, G. Paxinos, and J.K. Mai, eds. New York: Elsevier Academic Press. 1059-1092.

Kaas JH. 1997. Theories of visual cortex organization in primates. In Cerebral cortex, J.H. Kaas, and K.S. Rockland, eds. New York: Plenum Press. 91-126.

Kaas JH. 1983. What, if anything, is SI? Organization of first somatosensory area of cortex. Physiol Rev 63(1):206-231.

Kaas JH, and Pons TP. 1988. The somatosensory system of primates. In Comparative primate biology, H.D. Steklis, and J. Erwin, eds. New York: Alan R. Liss. 421-468.

Kaas JH, Hackett TA and Tramo MJ. 1999. Auditory processing in primate cerebral cortex. Curr Opin Neurobiol 9(2):164-170.

Kaas JH, Hall WC and Diamond IT. 1970. Cortical visual areas I and II in the hedgehog: relation between evoked potential maps and architectonic subdivisions. J Neurophysiol 33(5):595-615.

Kaas JH, Nelson RJ, Sur M, Lin CS and Merzenich MM. 1979. Multiple representations of the body within the primary somatosensory cortex of primates. Science 204(4392):521-23.

Kalia M and Whitteridge D. 1973. The visual areas in the splenial sulcus of the cat. J Physiol 232(2):275-283.

Kanagasuntheram R, Leong CH and Mahran ZY. 1966. Observations on some cortical areas of the lesser busy baby (Galago senegalensis). J Anat 100:317-333.

Kaneko T and Fujiyama F. 2002. Complementary distribution of vesicular glutamate transporters in the central nervous system. Neurosci Res 42(4):243-250.

Kaskan PM and Kaas JH. 2007. Cortical connections of the middle temporal and the middle temporal crescent visual areas in prosimian galagos (Otolemur garnetti). Anat Rec (Hoboken) 290(3):349-366.

Kobayashi Y and Amaral DG. 2003. Macaque monkey retrosplenial cortex: II. Cortical afferents. J Comp Neurol 466(1):48-79.

Kobayashi Y and Amaral DG. 2007. Macaque monkey retrosplenial cortex: III. Cortical efferents. J Comp Neurol 502(5):810-833.

Kondo H, Saleem KS and Price JL. 2005. Differential connections of the perirhinal and parahippocampal cortex with the orbital and medial prefrontal networks in macaque monkeys. J Comp Neurol 493(4):479-509.

Krieg WJS. 1946. Connections of the cerebral cortex. I. The albino rat. A. Topography of the cortical areas. J Comp Neurol 84:221-275.

Krubitzer LA and Kaas JH. 1988. Cortical connections of MT and DL in the prosimian galago: Evidence that modular segregation of parallel pathways is a primitive feature in primates. Soc. Neurosci. Abstr. 14, 602.

Krubitzer LA and Kaas JH. 1989. Cortical integration of parallel pathways in the visual system of primates. Brain Res 478(1):161-65.

Krubitzer LA and Kaas JH. 1990a. Cortical connections of MT in four species of primates: areal, modular, and retinotopic patterns. Vis Neurosci 5(2):165-204.

Krubitzer LA and Kaas JH. 1990b. The organization and connections of somatosensory cortex in marmosets. J Neurosci 10(3):952-974.

Krubitzer LA and Kaas JH. 1993. The dorsomedial visual area of owl monkeys: connections, myeloarchitecture, and homologies in other primates. J Comp Neurol 334(4):497-528.

Krubitzer LA and Kaas JH. 1992. The somatosensory thalamus of monkeys: cortical connections and a redefinition of nuclei in marmosets. J Comp Neurol 319(1):123-110.

Krubitzer LA, Clarey J, Tweedale R, Elston G and Calford M. 1995. A redefinition of somatosensory areas in the lateral sulcus of macaque monkeys. J Neurosci 15(5 Pt 2):3821-839.

Krubitzer LA, Sesma MA and Kaas JH. 1986. Microelectrode maps, myeloarchitecture, and cortical connections of three somatotopically organized representations of the body surface in the parietal cortex of squirrels. J Comp Neurol 250(4):403-430.

de la Mothe LA, Blumell S, Kajikawa Y and Hackett TA. 2006. Thalamic connections of the auditory cortex in marmoset monkeys: core and medial belt regions. J Comp Neurol 496(1):72-96.

Lachica EA and Casagrande VA. 1992. Direct W-like geniculate projections to the cytochrome oxidase (CO) blobs in primate visual cortex: axon morphology. J Comp Neurol 319(1):141-158.

Lachica EA, Beck PD and Casagrande VA. 1993. Intrinsic connections of layer III of striate cortex in squirrel monkey and bush baby: correlations with patterns of cytochrome oxidase. J Comp Neurol 329(2):163-187.

Lachica EA, Beck PD and Casagrande VA. 1992. Parallel pathways in macaque monkey striate cortex: anatomically defined columns in layer III. Proc Natl Acad Sci U S A 89(8):3566-3570.

Latawiec D, Martin KA and Meskenaite V. 2000. Termination of the geniculocortical projection in the striate cortex of macaque monkey: a quantitative immunoelectron microscopic study. J Comp Neurol 419(3):306-319.

Law MI, Zahs KR and Stryker MP. 1988. Organization of primary visual cortex (area 17) in the ferret. J Comp Neurol 278(2):157-180.

Lewis JW and Van Essen DC. 2000. Corticocortical connections of visual, sensorimotor, and multimodal processing areas in the parietal lobe of the macaque monkey. J Comp Neurol 428(1):112-137.

Lin CS and Kaas JH. 1980. Projections from the medial nucleus of the inferior pulvinar complex to the middle temporal area of the visual cortex. Neuroscience 5(12):2219-2228.

Livingstone MS and Hubel DH. 1984. Anatomy and physiology of a color system in the primate visual cortex. J Neurosci 4(1):309-356.

Livingstone MS and Hubel DH. 1987. Psychophysical evidence for separate channels for the perception of form, color, movement, and depth. J Neurosci 7(11):3416-3468.

Luethke LE, Krubitzer LA and Kaas JH. 1989. Connections of primary auditory cortex in the New World monkey, Saguinus. J Comp Neurol 285(4):487-513.

Lund JS, Fitzpatrick D, and Humphrey AL. 1985. The striate visual cortex of the tree shrew. In Visual cortex, E.G. Jones, and A. Peters, eds. New York: Plenum Press. 157-205.

Lyon DC and Kaas JH. 2001. Connectional and architectonic evidence for dorsal and ventral V3, and dorsomedial area in marmoset monkeys. J Neurosci 21(1):249-261.

Lyon DC and Kaas JH. 2002a. Connectional evidence for dorsal and ventral V3, and other extrastriate areas in the prosimian primate, Galago garnetti. Brain Behav Evol 59(3):114-129.

Lyon DC and Kaas JH. 2002b. Evidence for a modified V3 with dorsal and ventral halves in macaque monkeys. Neuron 33(3):453-461.

Lyon DC and Kaas JH. 2002c. Evidence from V1 connections for both dorsal and ventral subdivisions of V3 in three species of New World monkeys. J Comp Neurol 449(3):281-297.

Martin RD. 2004. Palaeontology: Chinese lantern for early primates. Nature 427:22-23.

Martin RD. 1990. Primate origins and evolution. London: Chapman and Hall.

Maunsell JH and van Essen DC. 1983. The connections of the middle temporal visual area (MT) and their relationship to a cortical hierarchy in the macaque monkey. J Neurosci 3(12):2563-586.

May JG and Andersen RA. 1986. Different patterns of corticopontine projections from separate cortical fields within the inferior parietal lobule and dorsal prelunate gyrus of the macaque. Exp Brain Res 63(2):265-278.

Merzenich MM and Brugge JF. 1973. Representation of the cochlear partition of the superior temporal plane of the macaque monkey. Brain Res 50(2):275-296.

Mesulam MM and Mufson EJ. 1982. Insula of the old world monkey. I. Architectonics in the insulo-orbito-temporal component of the paralimbic brain. J Comp Neurol 212(1):1-22.

Montero VM. 1993. Retinotopy of cortical connections between the striate cortex and extrastriate visual areas in the rat. Exp Brain Res 94(1):1-15.

Morecraft RJ, Cipolloni PB, Stilwell-Morecraft KS, Gedney MT and Pandya DN. 2004. Cytoarchitecture and cortical connections of the posterior cingulate and adjacent somatosensory fields in the rhesus monkey. J Comp Neurol 469(1):37-69.

Morecraft RJ, Rockland KS and Van Hoesen GW. 2000. Localization of area prostriata and its projection to the cingulate motor cortex in the rhesus monkey. Cereb Cortex 10(2):192-203.

Morel A, Garraghty PE and Kaas JH. 1993. Tonotopic organization, architectonic fields, and connections of auditory cortex in macaque monkeys. J Comp Neurol 335(3):437-459.

Morris R, Pandya DN and Petrides M. 1999a. Fiber system linking the mid-dorsolateral frontal cortex with the retrosplenial/presubicular region in the rhesus monkey. J Comp Neurol 407(2):183-192.

Morris R, Petrides M and Pandya DN. 1999b. Architecture and connections of retrosplenial area 30 in the rhesus monkey (Macaca mulatta). Eur J Neurosci 11(7):2506-518.

Nelson RJ, Sur M and Kaas JH. 1979. The organization of the second somatosensory area (SmII) of the grey squirrel. J Comp Neurol 184(3):473-489.

O'Brien BJ, Abel PL and Olavarria JF. 2001. The retinal input to calbindin-D28k-defined subdivisions in macaque inferior pulvinar. Neurosci Lett 312(3):145-48.

Olavarria J and Montero V. 1990. Elaborate organization of visual cortex in the hamster. Neurosci Res 8(1):40-47.

Olavarria J and Montero VM. 1984. Relation of callosal and striate-extrastriate cortical connections in the rat: morphological definition of extrastriate visual areas. Exp Brain Res 54(2):240-252.

Orban GA. 1997. Visual processing in macaque area MT/V5 and its satellites. In Cerebral cortex: extrastriate cortex in primates, K.S. Rockland, and J.H. Kaas, eds. New York: Plenum Press.

Palmer SM and Rosa MG. 2006. Quantitative analysis of the corticocortical projections to the middle temporal area in the marmoset monkey: evolutionary and functional implications. Cereb Cortex 16(9):1361-375.

Palomero-Gallagher N, and Zilles K. 2004. Isocortex. In The Rat Nervous System. G. Paxinos, eds. London: Elsevier. 729-757.

Petry HM and Hárosi FI. 1990. Visual pigments of the tree shrew (Tupaia belangeri) and greater galago (Galago crassicaudatus): a microspectrophotometric investigation. Vision Res 30(6):839-851.

Preuss TM and Goldman-Rakic PS. 1989. Connections of the ventral granular frontal cortex of macaques with perisylvian premotor and somatosensory areas: anatomical evidence for somatic representation in primate frontal association cortex. J Comp Neurol 282(2):293-316.

Preuss TM and Goldman-Rakic PS. 1991a. Architectonics of the parietal and temporal association cortex in the strepsirhine primate Galago compared to the anthropoid primate Macaca. J Comp Neurol 310(4):475-506.

Preuss TM and Goldman-Rakic PS. 1991b. Ipsilateral cortical connections of granular frontal cortex in the strepsirhine primate Galago, with comparative comments on anthropoid primates. J Comp Neurol 310(4):507-549.

Preuss TM and Goldman-Rakic PS. 1991c. Myelo- and cytoarchitecture of the granular frontal cortex and surrounding regions in the strepsirhine primate Galago and the anthropoid primate Macaca. J Comp Neurol 310(4):429-474.

Preuss TM and Kaas JH. 1996. Parvalbumin-like immunoreactivity of layer V pyramidal cells in the motor and somatosensory cortex of adult primates. Brain Res 712(2):353-57.

Pritzel M and Markowitsch HJ. 1982. Organization of cortical afferents to the prefrontal cortex in the bush baby (Galago senegalensis). Brain Behav Evol 20(1-2):43-56.

Qi HX, Lyon DC and Kaas JH. 2002. Cortical and thalamic connections of the parietal ventral somatosensory area in marmoset monkeys (Callithrix jacchus). J Comp Neurol 443(2):168-182.

Raczkowski D and Diamond IT. 1978. Connections of the striate cortex in Galago senegalensis. Brain Res 144(2):383-88.

Radinsky LB. 1977. Early primate brains: facts and fiction. J Hum Evol 6:79-86.

Reep RL, Chandler HC, King V and Corwin JV. 1994. Rat posterior parietal cortex: topography of corticocortical and thalamic connections. Exp Brain Res 100(1):67-84.

Reep RL, Goodwin GS and Corwin JV. 1990. Topographic organization in the corticocortical connections of medial agranular cortex in rats. J Comp Neurol 294(2):262-280.

Remple MS, Henry EC and Catania KC. 2003. Organization of somatosensory cortex in the laboratory rat (Rattus norvegicus): Evidence for two lateral areas joined at the representation of the teeth. J Comp Neurol 467(1):105-118.

Remple MS, Reed JL, Stepniewska I and Kaas JH. 2006. Organization of frontoparietal cortex in the tree shrew (Tupaia belangeri). I. Architecture, microelectrode maps, and corticospinal connections. J Comp Neurol 497(1):133-154.

Remple MS, Reed JL, Stepniewska I, Lyon DC and Kaas JH. 2007. The organization of frontoparietal cortex in the tree shrew (Tupaia belangeri): II. Connectional evidence for a frontal-posterior parietal network. J Comp Neurol 501(1):121-149.

Robinson CJ and Burton H. 1980a. Organization of somatosensory receptive fields in cortical areas 7b, retroinsula, postauditory and granular insula of M. fascicularis. J Comp Neurol 192(1):69-92.

Robinson CJ and Burton H. 1980b. Somatic submodality distribution within the second somatosensory (SII), 7b, retroinsular, postauditory, and granular insular cortical areas of M. fascicularis. J Comp Neurol 192(1):93-108.

Rosa MG and Elston GN. 1998. Visuotopic organisation and neuronal response selectivity for direction of motion in visual areas of the caudal temporal lobe of the marmoset monkey (Callithrix jacchus): middle temporal area, middle temporal crescent, and surrounding cortex. J Comp Neurol 393(4):505-527.

Rosa MG and Krubitzer LA. 1999. The evolution of visual cortex: where is V2? Trends Neurosci 22(6):242-48.

Rosa MG, Casagrande VA, Preuss T and Kaas JH. 1997. Visual field representation in striate and prestriate cortices of a prosimian primate (Galago garnetti). J Neurophysiol 77(6):3193-3217.

Rosa MG, Soares JG, Fiorani M and Gattass R. 1993. Cortical afferents of visual area MT in the Cebus monkey: possible homologies between New and Old World monkeys. Vis Neurosci 10(5):827-855.

Rosa MG, Sousa AP and Gattass R. 1988. Representation of the visual field in the second visual area in the Cebus monkey. J Comp Neurol 275(3):326-345.

Sanides F and Krishnamurti A. 1967. Cytoarchitectonic subdivisions of sensorimotor and prefrontal regions and of bordering insular and limbic fields in slow loris (Nycticebus coucang coucang). J Hirnforsch 9(3):225-252.

Sanides F. 1970. Functional architecture of motor and sensory cortices in primates in the light of a new concept of neocortex evolution. In The primate brain. W. Montagna, eds. New York: Appleton-Century-Crofts. 137-208.

Sanides F. 1972. Representation in the cerebral cortex and its areal lamination patterns. In Structure and function of the nervous system. G.H. Boune, eds. New York: Academic Press. 329-453.

Seltzer B and Pandya DN. 2009. Posterior cingulate and retrosplenial cortex connections of the caudal superior temporal region in the rhesus monkey. Exp Brain Res 195(2):325-334.

Simons EL and Rasmussen T. 1994. A whole new world of ancestors: eocene anthropoids from Africa. Evol Anthropol 3128-139.

Sincich LC, Park KF, Wohlgemuth MJ and Horton JC. 2004. Bypassing V1: a direct geniculate input to area MT. Nat Neurosci 7(10):1123-28.

Slutsky DA, Manger PR and Krubitzer L. 2000. Multiple somatosensory areas in the anterior parietal cortex of the California ground squirrel (Spermophilus beecheyii). J Comp Neurol 416(4):521-539.

Smith WK. 1945. The functional significance of the rostral cingular cortex as revealed by its responses to electrical excitation. J Neurophysiol 8214-255.

Sousa AP, Piñon MC, Gattass R and Rosa MG. 1991. Topographic organization of cortical input to striate cortex in the Cebus monkey: a fluorescent tracer study. J Comp Neurol 308(4):665-682.

Spatz WB and Tigges J. 1972. Experimental-anatomical studies on the "middle temporal visual area (MT)" in primates. I. Efferent cortico-cortical connections in the marmoset Callithrix jacchus. J Comp Neurol 146(4):451-464.

Spatz WB. 1977. Topographically organized reciprocal connections between areas 17 and MT (visual area of superior temporal sulcus) in the marmoset Callithrix jacchus. Exp Brain Res 27(5):559-572.

Steele GE, Weller RE and Cusick CG. 1991. Cortical connections of the caudal subdivision of the dorsolateral area (V4) in monkeys. J Comp Neurol 306(3):495-520.

Stephan H, Frahm H and Baron G. 1981. New and revised data on volume of brain structures in insectivores and primates. Folia primatol 351-29.

Stepniewska I and Kaas JH. 1996. Topographic patterns of V2 cortical connections in macaque monkeys. J Comp Neurol 371(1):129-152.

Stepniewska I, Collins CE and Kaas JH. 2005a. Reappraisal of DL/V4 boundaries based on connectivity patterns of dorsolateral visual cortex in macaques. Cereb Cortex 15(6):809-822.

Stepniewska I, Fang PC and Kaas JH. 2005b. Microstimulation reveals specialized subregions for different complex movements in posterior parietal cortex of prosimian galagos. Proc Natl Acad Sci U S A 102(13):4878-883.

Stepniewska I, Preuss TM and Kaas JH. 1993. Architectonics, somatotopic organization, and ipsilateral cortical connections of the primary motor area (M1) of owl monkeys. J Comp Neurol 330(2):238-271.

Stepniewska I, Qi HX and Kaas JH. 1999. Do superior colliculus projection zones in the inferior pulvinar project to MT in primates? Eur J Neurosci 11(2):469-480.

Sur M, Nelson RJ and Kaas JH. 1980. Representation of the body surface in somatic koniocortex in the prosimian Galago. J Comp Neurol 189(2):381-402.

Suzuki WA and Amaral DG. 1994. Perirhinal and parahippocampal cortices of the macaque monkey: cortical afferents. J Comp Neurol 350(4):497-533.

Symonds LL and Kaas JH. 1978. Connections of striate cortex in the prosimian, Galago senegalensis. J Comp Neurol 181(3):477-512.

Tiao YC and Blakemore C. 1976. Functional organization in the visual cortex of the golden hamster. J Comp Neurol 168(4):459-481.

Tigges J, Spatz WB and Tigges M. 1974. Efferent cortico-cortical fiber connections of area 18 in the squirrel monkey (Saimiri). J Comp Neurol 158(2):219-235.

Tigges J, Tigges M and Perachio AA. 1977. Complementary laminar terminations of afferents to area 17 originating in area 18 and in the lateral geniculate nucleus in squirrel monkey. J Comp Neurol 176(1):87-100.

Tootell RB, Hamilton SL and Silverman MS. 1985. Topography of cytochrome oxidase activity in owl monkey cortex. J Neurosci 5(10):2786-2800.

Tootell RB, Switkes E, Silverman MS and Hamilton SL. 1988. Functional anatomy of macaque striate cortex. II. Retinotopic organization. J Neurosci 8(5):1531-568.

Ts'o DY and Gilbert CD. 1988. The organization of chromatic and spatial interactions in the primate striate cortex. J Neurosci 8(5):1712-727.

Ungerleider LG and Desimone R. 1986. Cortical connections of visual area MT in the macaque. J Comp Neurol 248(2):190-222.

Valente T, Auladell C and Perez-Clausell J. 2002. Postnatal development of zinc-rich terminal fields in the brain of the rat. Exp Neurol 174(2):215-229.

Van Brederode JF, Mulligan KA and Hendrickson AE. 1990. Calcium-binding proteins as markers for subpopulations of GABAergic neurons in monkey striate cortex. J Comp Neurol 298(1):1-22.

Van Essen DC, Maunsell JH and Bixby JL. 1981. The middle temporal visual area in the macaque: myeloarchitecture, connections, functional properties and topographic organization. J Comp Neurol 199(3):293-326.

van Groen T and Wyss JM. 1990. Connections of the retrosplenial granular a cortex in the rat. J Comp Neurol 300(4):593-606.

de Venecia RK, Smelser CB and McMullen NT. 1998. Parvalbumin is expressed in a reciprocal circuit linking the medial geniculate body and auditory neocortex in the rabbit. J Comp Neurol 400(3):349-362.

Vogt BA and Pandya DN. 1987. Cingulate cortex of the rhesus monkey: II. Cortical afferents. J Comp Neurol 262(2):271-289.

Vogt BA, Finch DM and Olson CR. 1992. Functional heterogeneity in cingulate cortex: the anterior executive and posterior evaluative regions. Cereb Cortex 2(6):435-443.

Vogt BA, Pandya DN and Rosene DL. 1987. Cingulate cortex of the rhesus monkey: I. Cytoarchitecture and thalamic afferents. J Comp Neurol 262(2):256-270.

Vogt BA, Vogt L, and Farber NB. 2004. Cingulate Cortex and Disease Models. In The Rat Nervous System. G. Paxinos, eds. London: Elsevier. 704-727.

Vogt BA, Vogt L, Farber NB and Bush G. 2005. Architecture and neurocytology of monkey cingulate gyrus. J Comp Neurol 485(3):218-239.

von Bonin G. 1942. The atriate area of primates. J Comp Neurol 77:405-429.

von Bonin G. 1945. The cortex of galago. Its relation to the pattern of the primate cortex. Urbana: University of Illinois Pr.

von Bonin G, and Bailey P. 1961. Pattern of the cerebral isocortex. In Primatologia II/2, A.H. Schultz, H. Hofer, and D. Starck, eds. Basel und New York: Karger.

Wagor E, Lin CS and Kaas JH. 1975. Some cortical projections of the dorsomedial visual area (DM) of association cortex in the owl monkey, Aotus trivirgatus. J Comp Neurol 163(2):227-250.

Wagor E, Mangini NJ and Pearlman AL. 1980. Retinotopic organization of striate and extrastriate visual cortex in the mouse. J Comp Neurol 193(1):187-202.

Walker C and Sinha MM. 1972. Somatotopic organization of Smll cerebral neocortex in albino rat. Brain Res 37(1):132-36.

Wall JT, Symonds LL and Kaas JH. 1982. Cortical and subcortical projections of the middle temporal area (MT) and adjacent cortex in galagos. J Comp Neurol 211(2):193-214.

Wang Q and Burkhalter A. 2007. Area map of mouse visual cortex. J Comp Neurol 502(3):339-357.

Wang Y and Kurata K. 1998. Quantitative analyses of thalamic and cortical origins of neurons projecting to the rostral and caudal forelimb motor areas in the cerebral cortex of rats. Brain Res 781(1-2):135-147.

Ward AA. 1948. The cingular gyrus. J Neurophysiol 23:1003-07.

Weller RE and Kaas JH. 1985. Cortical projections of the dorsolateral visual area in owl monkeys: the prestriate relay to inferior temporal cortex. J Comp Neurol 234(1):35-59.

Weller RE, and Kaas JH. 1982. The organization of the visual system in galago: Comparisons with monkeys. In The lesser busybaby (Galago) as an animal model: Selected topics. D.E. Haines, eds. Boca Raton, Florida: CRC Press. 108-135.

Weller RE, Wall JT and Kaas JH. 1984. Cortical connections of the middle temporal visual area (MT) and the superior temporal cortex in owl monkeys. J Comp Neurol 228(1):81-104.

Wong P and Kaas JH. 2008. Architectonic subdivisions of neocortex in the gray squirrel (Sciurus carolinensis). Anat Rec (Hoboken) 291(10):1301-333.

Wong P and Kaas JH. 2009a. Architectonic subdivisions of neocortex in the tree shrew (Tupaia belangeri). Anat Rec (Hoboken) 292(7):994-1027.

Wong P and Kaas JH. 2009b. An architectonic study of the neocortex of the short-tailed opossum (Monodelphis domestica). Brain Behav Evol 73(3):206-228.

Wong P, Collins CE, Baldwin MKL and Kaas JH. In press. Cortical connections of the visual pulvinar complex in prosimian galagos (*Otolemur garnetti)*. J Comp Neurol 517.

Wong-Riley M. 1979. Changes in the visual system of monocularly sutured or enucleated cats demonstrable with cytochrome oxidase histochemistry. Brain Res 171(1):11-28.

Wong-Riley MT and Carroll EW. 1984. Quantitative light and electron microscopic analysis of cytochrome oxidase-rich zones in V II prestriate cortex of the squirrel monkey. J Comp Neurol 222(1):18-37.

Wong-Riley MT, Merzenich MM and Leake PA. 1978. Changes in endogenous enzymatic reactivity to DAB induced by neuronal inactivity. Brain Res 141(1):185-192.

Wu CW and Kaas JH. 1999. Reorganization in primary motor cortex of primates with long-standing therapeutic amputations. J Neurosci 19(17):7679-697.

Wu CW and Kaas JH. 2003. Somatosensory cortex of prosimian Galagos: physiological recording, cytoarchitecture, and corticocortical connections of anterior parietal cortex and cortex of the lateral sulcus. J Comp Neurol 457(3):263-292.

Wu CW, Bichot NP and Kaas JH. 2000. Converging evidence from microstimulation, architecture, and connections for multiple motor areas in the frontal and cingulate cortex of prosimian primates. J Comp Neurol 423(1):140-177.

Xu X, Collins CE, Kaskan PM, Khaytin I, Kaas JH and Casagrande VA. 2004. Optical imaging of visually evoked responses in prosimian primates reveals conserved features of the middle temporal visual area. Proc Natl Acad Sci U S A 101(8):2566-571.

Zeki SM. 1969. Representation of central visual fields in prestriate cortex of monkey. Brain Res 14(2):271-291.

Zeki SM. 1974. Functional organization of a visual area in the posterior bank of the superior temporal sulcus of the rhesus monkey. J Physiol 236(3):549-573.

Zeki SM. 1980. The response properties of cells in the middle temporal area (area MT) of owl monkey visual cortex. Proc R Soc Lond B Biol Sci 207(1167):239-248.

Zilles K. 1990. Organization of the Neocortex of the rat. In The Cerebral Cortex of the Rat, B. Tees, and R.C. Kolb, eds. MIT Press. 21-34.

Zilles K, and Wree A. 1995. In Cortex: Areal and laminar structure. G. Paxinos, eds. Sydney: Academic Press. 649-685.

Zilles K, Rehkämper G, Stephan H and Schleicher A. 1979. A quantitative approach to cytoarchitectonics. IV. The areal pattern of the cortex of Galago demidovii (e. Geoffroy, 1796), (lorisidae, primates). Anat Embryol (Berl) 157(1):81-103.

Zuckerman S and Fulton JF. 1941. The motor cortex in Galago and Perodicticus. J Anat 75(Pt 4):447-456.

CHAPTER V

CONCLUDING REMARKS

Grey squirrels, tree shrews and galagos share several cortical areas, including the primary visual, somatosensory, auditory, motor, retrosplenial and perirhinal areas, that have similar architectonic characteristics in the preparations used in these studies. Furthermore, certain areas, such as the primary visual (Rosa and Krubitzer, 1999), somatosensory (Kaas, 1983; Johnson, 1990) and auditory (Ehret, 1997) areas have been identified in all mammals that have been examined (Krubitzer and Kaas, 2005). This adds support to the presence of a *Bauplan* of cortical organization from which modifications to it have given rise to the vast array of behavior and cognitive abilities in mammals.

Similarities and Differences in General Cortical Organization

The neocortical organization in grey squirrels, tree shrews and galagos are generally similar, sharing common areas such as area 17, A1, 3b(S1) and M1, with some differences (Fig. 71A, B). In all three mammals, area 17 or V1 occupies most of the caudal pole and extends onto the medial surface of the hemisphere. Area 17 in grey squirrels (Hall et al., 1971), tree shrews (Kaas, et al., 1972) and galagos (Weller and Kaas, 1982; Rosa et al., 1997) contains a complete representation of the visual field, with the lower visual hemifield represented dorsally and the upper visual hemifield

represented ventrally. In all three mammals, area 17 is bordered rostrally by area 18, a strip of less well myelinated cortex (Fig. 71B) that contains a mirror reversal of the contralateral visual hemifield and is topographically connected to area 17 (For grey squirrels, see Kaas et al., 1989; For tree shrews see Sesma et al., 1984; Lyon et al, 1998; For galagos, see Rosa et al., 1997), and caudally by area prostriata on the medial wall (Rosa and Krubitzer, 1999). Auditory cortex is located rostroventral to area 17, in the rostral extent of the temporal lobe, and contains at least two primary-like areas, A1 and R, surrounded by higher-order auditory processing, or belt areas (For grey squirrel, see Merzenich et al., 1976; Luethke et al., 1988; Wong and Kaas, 2008; For tree shrews, see Oliver and Hall, 1975; Casseday et al., 1976; Oliver and Hall, 1978; For galagos: Kanagasuntheram et al., 1966; Brugge, 1982; Preuss and Goldman-Rakic, 1991). Area 3b(S1) occupies most of the parietal cortex, and extends onto the medial surface of the hemisphere in galagos and tree shrews. As in other mammals (Kaas, 1983), area 3b(S1) of grey squirrels (Sur et al. 1978; Krubitzer et al., 1986; Slutsky et al., 2000), tree shrews (Lende, 1970; Sur et al., 1980a) and galagos (Carlson and Welt, 1980; Sur et al., 1980b; Wu and Kaas, 2003) has a topographic representation of the contralateral body surface. In the posterior parietal region, the parietal medial area in grey squirrels (Krubitzer et al., 1986; Slutsky et al., 2000), somatosensory caudal area in tree shrews (Remple et al., 2006, 2007) and area 1/2 in galagos (Wu and Kaas, 2003) all have dense connections with other somatosensory and motor areas. As such the strip of cortex that is caudal to area 3b(S1) in grey squirrels, tree shrews and galagos may be related. Primary motor cortex (M1) of all three mammals lies rostral to area 3b(S1), and is separated from area

3b(S1) by a strip of transitional, dysgranular area 3a. The presence of a motor cortex that is distinct from somatosensory cortex suggests that the neocortex in all three mammals

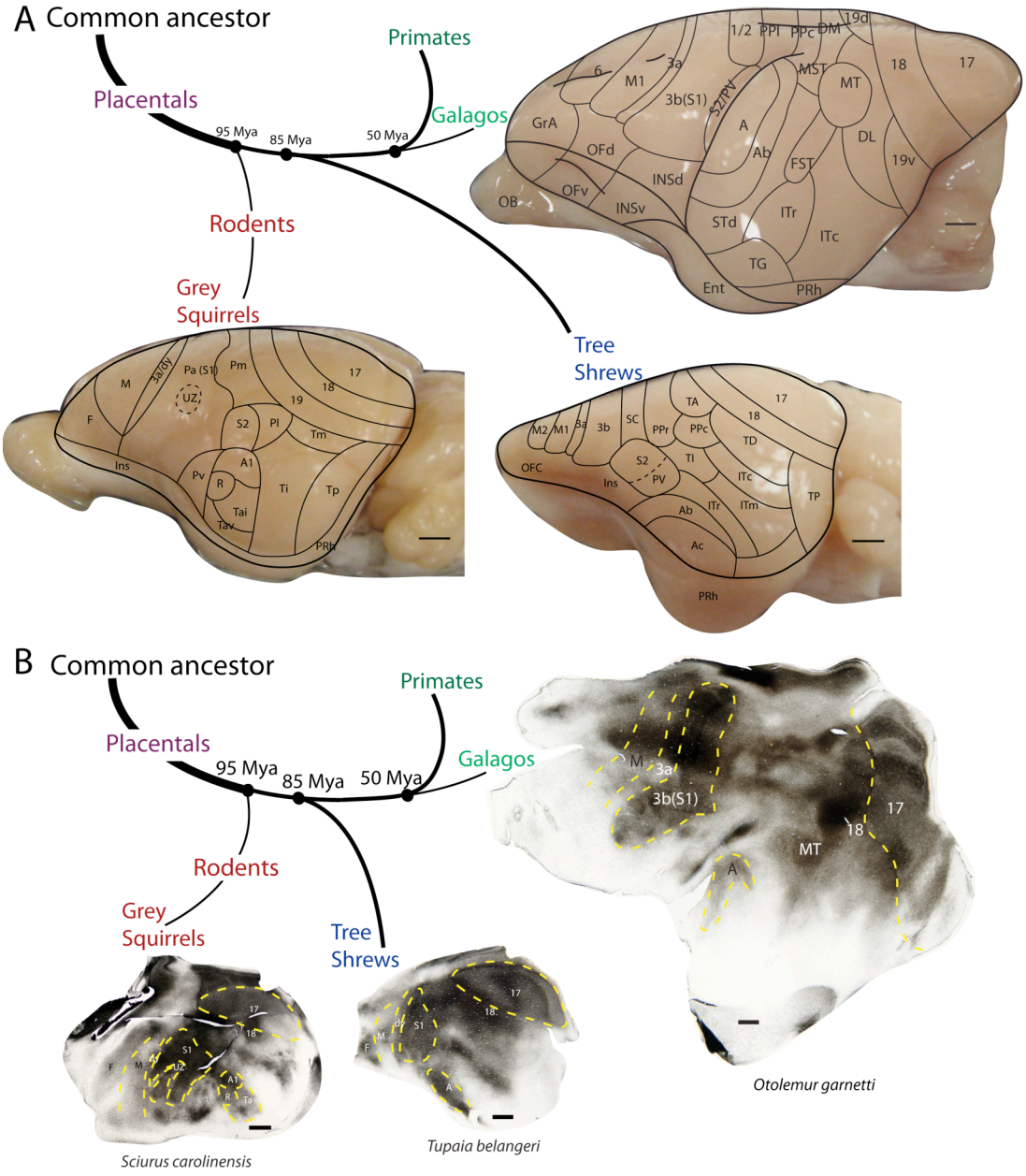

Figure 71. An evolutionary tree showing the phylogenetic relationship of grey squirrels, tree shrews and galagos. A. Proposed cortical areas are shown on a lateral view of the brains. B. Myelin stained preparations of tissue sectioned tangentially to the pia with the approximate borders of areas 17, 18, A, 3b(S1), 3a, M1 and F outlined with broken lines. Area MT is also indicated on the section from the galago. Scale bars = 2mm.

are evolutionarily more advanced than in mammals such as the short-tailed opossums (Catania et al., 2000; Wong and Kaas, 2009a), where the motor component is embedded within the somatosensory cortex. M1 of grey squirrels (unpublished results), tree shrews (Remple et al., 2007) and galagos (Zuckerman and Fulton, 1941; Kanagasuntheram et al., 1966; Fogassi et al., 1994; Wu et al., 2000) contains a complete map of the contralateral body movements. Medial cortex in grey squirrels, tree shrews and galagos are similar in that the rostral portion includes at least three cingulate areas, and the caudal portion includes the retrosplenial granular and retrosplenial agranular areas.

The three mammals differ in the organization and number of higher-order cortical areas. Galagos have a larger, more differentiated brain with more cortical areas than tree shrews and grey squirrels (Fig. 71A). Additionally, the galago brain is more convoluted than the smooth brains of grey squirrels and tree shrews. Like early primates, galagos have expanded temporal lobes compared to grey squirrels and tree shrews, a portion of which, such as the middle temporal visual area and surrounding areas, is devoted to visual processing (Kaas, 2006). Grey squirrels, unlike tree shrews and galagos, do not have a region of posterior parietal cortex that is separate from the parietal medial area. In the frontal cortex, grey squirrels have a single agranular architectonic field that corresponds to the primary motor area, with no obvious secondary or premotor area. Whereas tree shrews and galagos both have a secondary (M2) or premotor (area 6) that is rostral to M1 (Fig. 71A). The frontal cortex of galagos is more differentiated than that of grey squirrels and tree shrews, with at least two cortical areas on the dorsal surface of the hemisphere.

Similarities and Differences in Architectonic Appearances of Shared Cortical Areas

Area 17 is an architectonically distinct and easily identifiable area in almost all mammals that have been examined, including grey squirrels, tree shrews and galagos. In all three animals examined, area 17 has the characteristic koniocellular appearance of primary sensory cortices, is well myelinated and metabolically active. The densely-packed layer 4 stains darkly for PV and VGluT2 and poorly for synaptic in all three mammals. This indicates that terminations in layer 4 are predominantly from nuclei in the thalamus, such as the lateral geniculate nucleus and the pulvinar.

In spite of the similarities, there are differences in the sublamination patterns of area 17 in grey squirrels, tree shrews and galagos. Layer 4 of area 17 in of grey squirrels is a single layer. However, in tree shrews and galagos, layer 4 of area 17 contains two sublayers 4a and 4b. Furthermore, layer 4a and 4b of area 17 in tree shrews are separated by a cell-poor cleft. Layer 3 of area 17 in all three mammals contains sublayers. In tree shrews layer 3b shows patchy staining in zinc and VGluT2 preparations, reflecting a modular organization of terminations from the lateral geniculate nucleus, and in galagos, layer 3 contains the CO blobs, which are the target of projections from the koniocellular layers of the lateral geniculate nucleus (Lachica and Casagrande, 1992). However, layer 3 of area 17 in grey squirrels lacks distinct modular organization. This may reflect species specific differences in the pattern of terminations from the lateral geniculate nucleus.

The temporal lobe of grey squirrels, tree shrews and galagos are differently organized into areas. There are however, some similarities, including the primary auditory areas in the rostral portion of the temporal lobe. Within the temporal lobe, a

darkly myelinated region is present in all three mammals that has a well developed layer 4, and in comparison with the surrounding cortical areas, has reduced expression of synaptic zinc and increased expression of VGluT2 and PV immunopositive terminations. This is the temporal posterior (Tp) and temporal medial (Tm) areas in grey squirrels, the temporal dorsal (TD) area in tree shrews and the middle temporal visual (MT) area in galagos. These areas have connections with the pulvinar (Robson and Hall, 1977; Lyon et al., 2003; Wong et al., in press). Furthermore, TD in tree shrews (Sesma et al., 1984) and MT in galagos (Wall et al., 1982; Cusick and Kaas, 1988; Krubitzer and Kaas, 1990; Collins et al., 2001; Kaskan and Kaas, 2007) has connections with areas 17 and 18, although neither area Tp nor Tm in grey squirrels have connections with area 17 and at best have sparse connections with area 18 (Kaas et al., 1989). Microelectrode mapping studies have suggested the area Tm, much like area MT in primates (Allman and Kaas, 1971; Zeki, 1974; Van Essen et al., 1981; Rosa and Elston, 1998), contains directionally selective cells (Paolini and Sereno, 1998). However, more extensive studies on areas Tp and Tm in grey squirrels are required, to determine whether these areas contain a complete retinotopic representation of the visual hemifield and what their cortical connections are before any conclusions as to whether they are homologues of area MT in primates can be drawn. Based on the relative position and architectonic appearance of TD in tree shrews, it is possible that area TD is similar to the primate area MT (Sesma et al., 1984; Kaas and Preuss, 1993; Jain et al., 1994; Northcutt and Kaas, 1995; Wong and Kaas, 2009b).

Primary somatosensory cortex, 3b(S1), of all three mammals has the characteristics of koniocellular cortex, with thick, densely populated granular layer 4 and

dense myelination. As expected of primary sensory cortex, area 3b(S1) stains darkly in CO preparations as it is metabolically active. Layer 4 of area 3b(S1) stains darkly for VGluT2 immunopositive terminations as it receives inputs from the ventral posterior nuclei, in addition to containing a dense population of PV immunopositive terminations. Additionally, layer 4 of area 3b(S1) contains a low population of synaptic zinc in corticocortical terminations. In all three mammals, layer 4 of area 3b(S1) has non-uniform thickness, which is likely to be due to the presence of different representations of body parts. The forepaw and lip representation in area 3b(S1) of grey squirrels are subdivided into a number of barrel-like structures where each barrel represents one whisker on the upper and lower lips, and the glaborous skin on the forepaw. This specialized modular organization in area 3b(S1) of grey squirrels has been observed in other rodents as well (Woolsey et al., 1975), but has not been observed in tree shrews or galagos. As such, this specialized modular organization in area 3b(S1) of grey squirrels, and other rodents, may reflect different specialization for somatosensation in rodents than in primates.

Primary motor cortex (M1) in grey squirrels, tree shrews and galagos have similar architectonic characteristics, with a reduced granular layer 4 and less dense myelination compared to the surrounding cortical areas. Furthermore, layer 4 of M1 in all three mammals stain darker for synaptic zinc and lighter for PV and VGluT2 immunopositive terminations compared to adjoining cortical areas. Layer 5 of M1 in the grey squirrel (Wong and Kaas, 2008), tree shrew (Remple et al., 2007; Wong and Kaas, 2009b) and galagos (Wu et al., 2000) is thick and contains large SMI-32 immunopositive pyramidal cells.

The retrosplenial granular and agranular fields are easily identified in grey squirrels, tree shrews and galagos, as these two fields do not have well-defined laminar characteristics. RSG in grey squirrels, and RSg in tree shrews and galagos have merged layers 2 and 3 that are densely populated, and poorly developed granular layer 4. In grey squirrels, layer 6 is densely packed with darkly staining cells, whereas a darkly stained layer 6 is absent in tree shrews or galagos. As such, the retrosplenial granular area (RSG) in grey squirrels has a banded appearance in Nissl preparations, but the retrosplenial granular area (RSg) of tree shrews and galagos do not. In grey squirrels, RSG is poorly myelinated and does not have distinct bands of Baillarger. However, RSg in tree shrews and galagos is more densely myelinated, and has a distinct outer band of Baillarger. The upper cortical layers of the retrosplenial granular area in all three mammals stain poorly for synaptic zinc, and darkly for PV and VGluT2 immunopositive terminations. Additionally, RSG of grey squirrels and RSg of galagos have a banded appearance in PV and VGluT2 preparations because layer 5/6 stains darkly for PV and VGluT2 immunopositive terminations.

The retrosplenial agranular area in grey squirrels, tree shrews and galagos is poorly laminated, without a well developed granular layer 4, and has a lower cell packing density than the retrosplenial granular area. In grey squirrels and tree shrews, the retrosplenial agranular area is sparsely myelinated, and in galagos, the retrosplenial agranular area (RSag) is moderately myelinated. RSA of grey squirrels, and RSag of tree shrews and galagos stain more intensely for synaptic zinc compared to RSG, especially in layers 2 and 3. The retrosplenial agranular area in all three mammals stains less intensely for PV and VGluT2 immunopositive terminations compared to the retrosplenial granular

area. However, in galagos, RSag has a banded appearance in PV preparations, with layers 2/3, 4 and 6 showing moderate staining for PV immunopositive terminations.

The perirhinal (Prh) area in grey squirrels, tree shrews and galagos is easily identified due to similarities in architectonic appearances. Prh in all three mammals does not have a well-developed layer 4 and is sparsely populated with cells. Layer 2 of Prh in all three mammals is darkly stained and densely packed with cells. Prh is poorly myelinated, stains intensely for synaptic zinc and poorly for PV and VGluT2 immunopositive terminations in grey squirrels, tree shrews and galagos. This suggests that Prh in all three mammals receives a large population of corticocortical terminations and a small population of thalamocortical terminations.

Summary and Future Directions

Primary cortical areas such as area 17, area 3b(S1), A1 and M1 are easily identified in all three mammals as they have distinct architectonic characteristics. However, with the current histological and immnohistochemical methods used in these studies, some association areas have less characteristic architectonic appearances, and as such similar or homologous cortical areas across the three mammals are less easily defined. Other staining methods, such as the receptor-binding or RNA hybridization methods may help reveal more detailed architectonic characteristics of a cortical area. Using the receptor-binding method will establish a 'neurochemical fingerprint' of a cortical area, from which 'neurochemical families' of cortical areas with similar

‘neurochemical fingerprints’ may aid in the identification of homologous areas in different species.

References

Allman JM and Kaas JH. 1971. A representation of the visual field in the caudal third of the middle tempral gyrus of the owl monkey (Aotus trivirgatus). Brain Res 31(1):85-105.

Brugge JF. 1982. Auditory cortical areas in primates. In Cortical sensory organisation Clifton, NJ: Humana Press. 59-70.

Carlson M and Welt C. 1980. Somatic sensory cortex (SmI) of the prosimian primate Galago crassicaudatus: organization of mechanoreceptive input from the hand in relation to cytoarchitecture. J Comp Neurol 189(2):249-271.

Casseday HJ, Diamond IT and Harting JK. 1976. Auditory pathways to the cortex in Tupaia glis. J Comp Neurol 166(3):303-340.

Catania KC, Jain N, Franca JG, Volchan E and Kaas JH. 2000. The organization of somatosensory cortex in the short-tailed opossum (Monodelphis domestica). Somatosens Mot Res 17(1):39-51.

Collins CE, Stepniewska I and Kaas JH. 2001. Topographic patterns of v2 cortical connections in a prosimian primate (Galago garnetti). J Comp Neurol 431(2):155-167.

Cusick CG and Kaas JH. 1988. Surface view patterns of intrinsic and extrinsic cortical connections of area 17 in a prosimian primate. Brain Res 458(2):383-88.

Ehret G. 1997. The auditory cortex. j Comp Physiol 181547-557.

Fogassi L, Gallese V, Gentilucci M, Luppino G, Matelli M and Rizzolatti G. 1994. The fronto-parietal cortex of the prosimian Galago: patterns of cytochrome oxidase activity and motor maps. Behav Brain Res 60(1):91-113.

Hall WC, Kaas JH, Killackey H and Diamond IT. 1971. Cortical visual areas in the grey squirrel (Sciurus carolinesis): a correlation between cortical evoked potential maps and architectonic subdivisions. J Neurophysiol 34(3):437-452.

Jain N, Preuss TM and Kaas JH. 1994. Subdivisions of the visual system labeled with the Cat-301 antibody in tree shrews. Vis Neurosci 11(4):731-741.

Johnson JI. 1990. Comparative development of somatic sensory cortex.

Kaas JH. 2006. Evolution of the neocortex. Curr Biol 16(21):R910-14.

Kaas JH. 1983. What, if anything, is SI? Organization of first somatosensory area of cortex. Physiol Rev 63(1):206-231.

Kaas JH, and Preuss TM. 1993. Archontan affinities as reflected in the visual system. In Mammalian Phylogeny, F. Szalay, M. Novacek, and M. McKenna, eds. New York: Springer Verlag. 115-128.

Kaas JH, Hall WC, Killackey H and Diamond IT. 1972. Visual cortex of the tree shrew (Tupaia glis): architectonic subdivisions and representations of the visual field. Brain Res 42(2):491-96.

Kaas JH, Krubitzer LA and Johanson KL. 1989. Cortical connections of areas 17 (V-I) and 18 (V-II) of squirrels. J Comp Neurol 281(3):426-446.

Kanagasuntheram R, Leong CH and Mahran ZY. 1966. Observations on some cortical areas of the lesser busy baby (Galago senegalensis). J Anat 100:317-333.

Kaskan PM and Kaas JH. 2007. Cortical connections of the middle temporal and the middle temporal crescent visual areas in prosimian galagos (Otolemur garnetti). Anat Rec (Hoboken) 290(3):349-366.

Krubitzer L and Kaas J. 2005. The evolution of the neocortex in mammals: how is phenotypic diversity generated? Curr Opin Neurobiol 15(4):444-453.

Krubitzer LA and Kaas JH. 1990. Cortical connections of MT in four species of primates: areal, modular, and retinotopic patterns. Vis Neurosci 5(2):165-204.

Krubitzer LA, Sesma MA and Kaas JH. 1986. Microelectrode maps, myeloarchitecture, and cortical connections of three somatotopically organized representations of the body surface in the parietal cortex of squirrels. J Comp Neurol 250(4):403-430.

Lachica EA and Casagrande VA. 1992. Direct W-like geniculate projections to the cytochrome oxidase (CO) blobs in primate visual cortex: axon morphology. J Comp Neurol 319(1):141-158.

Lende RA. 1970. Cortical localization in the tree shrew (Tupaia). Brain Res 18(1):61-75.

Luethke LE, Krubitzer LA and Kaas JH. 1988. Cortical connections of electrophysiologically and architectonically defined subdivisions of auditory cortex in squirrels. J Comp Neurol 268(2):181-203.

Lyon DC, Jain N and Kaas JH. 1998. Cortical connections of striate and extrastriate visual areas in tree shrews. J Comp Neurol 401(1):109-128.

Lyon DC, Jain N and Kaas JH. 2003. The visual pulvinar in tree shrews II. Projections of four nuclei to areas of visual cortex. J Comp Neurol 467(4):607-627.

Merzenich MM, Kaas JH and Roth GL. 1976. Auditory cortex in the grey squirrel: tonotopic organization and architectonic fields. J Comp Neurol 166(4):387-401.

Northcutt RG and Kaas JH. 1995. The emergence and evolution of mammalian neocortex. Trends Neurosci 18(9):373-79.

Oliver DL and Hall WC. 1978. The medial geniculate body of the tree shrew, Tupaia glis. II. Connections with the neocortex. J Comp Neurol 182(3):459-493.

Oliver DL and Hall WC. 1975. Subdivisions of the medial geniculate body in the tree shrew (Tupaia glis). Brain Res 86(2):217-227.

Paolini M and Sereno MI. 1998. Direction selectivity in the middle lateral and lateral (ML and L) visual areas in the California ground squirrel. Cereb Cortex 8(4):362-371.

Preuss TM and Goldman-Rakic PS. 1991. Architectonics of the parietal and temporal association cortex in the strepsirhine primate Galago compared to the anthropoid primate Macaca. J Comp Neurol 310(4):475-506.

Remple MS, Reed JL, Stepniewska I, Lyon DC and Kaas JH. 2007. The organization of frontoparietal cortex in the tree shrew (Tupaia belangeri): II. Connectional evidence for a frontal-posterior parietal network. J Comp Neurol 501(1):121-149.

Robson JA and Hall WC. 1977. The organization of the pulvinar in the grey squirrel (Sciurus carolinensis). II. Synaptic organization and comparisons with the dorsal lateral geniculate nucleus. J Comp Neurol 173(2):389-416.

Rosa MG and Elston GN. 1998. Visuotopic organisation and neuronal response selectivity for direction of motion in visual areas of the caudal temporal lobe of the marmoset monkey (Callithrix jacchus): middle temporal area, middle temporal crescent, and surrounding cortex. J Comp Neurol 393(4):505-527.

Rosa MG and Krubitzer LA. 1999. The evolution of visual cortex: where is V2? Trends Neurosci 22(6):242-48.

Rosa MG, Casagrande VA, Preuss T and Kaas JH. 1997. Visual field representation in striate and prestriate cortices of a prosimian primate (Galago garnetti). J Neurophysiol 77(6):3193-3217.

Sesma MA, Casagrande VA and Kaas JH. 1984. Cortical connections of area 17 in tree

shrews. J Comp Neurol 230(3):337-351.

Slutsky DA, Manger PR and Krubitzer L. 2000. Multiple somatosensory areas in the anterior parietal cortex of the California ground squirrel (Spermophilus beecheyii). J Comp Neurol 416(4):521-539.

Sur M, Nelson RJ and Kaas JH. 1978. The representation of the body surface in somatosensory area I of the grey squirrel. J Comp Neurol 179(2):425-449.

Sur M, Weller RE and Kaas JH. 1980a. Representation of the body surface in somatosensory area I of tree shrews, Tupaia glis. J Comp Neurol 194(1):71-95.

Sur M, Nelson RJ and Kaas JH. 1980b. Representation of the body surface in somatic koniocortex in the prosimian Galago. J Comp Neurol 189(2):381-402.

Van Essen DC, Maunsell JH and Bixby JL. 1981. The middle temporal visual area in the macaque: myeloarchitecture, connections, functional properties and topographic organization. J Comp Neurol 199(3):293-326.

Wall JT, Symonds LL and Kaas JH. 1982. Cortical and subcortical projections of the middle temporal area (MT) and adjacent cortex in galagos. J Comp Neurol 211(2):193-214.

Weller RE, and Kaas JH. 1982. The organization of the visual system in galago: Comparisons with monkeys. In The lesser busybaby (Galago) as an animal model: Selected topics. D.E. Haines, eds. Boca Raton, Florida: CRC Press. 108-135.

Wong P and Kaas JH. 2008. Architectonic subdivisions of neocortex in the gray squirrel (Sciurus carolinensis). Anat Rec (Hoboken) 291(10):1301-333.

Wong P and Kaas JH. 2009a. An architectonic study of the neocortex of the short-tailed opossum (Monodelphis domestica). Brain Behav Evol 73(3):206-228.

Wong P and Kaas JH. 2009b. Architectonic subdivisions of neocortex in the tree shrew (Tupaia belangeri). Anat Rec (Hoboken) 292(7):994-1027.

Woolsey TA, Welker C and Schwartz RH. 1975. Comparative anatomical studies of the SmL face cortex with special reference to the occurrence of "barrels" in layer IV. J Comp Neurol 164(1):79-94.

Wu CW and Kaas JH. 2003. Somatosensory cortex of prosimian Galagos: physiological recording, cytoarchitecture, and corticocortical connections of anterior parietal cortex and cortex of the lateral sulcus. J Comp Neurol 457(3):263-292.

Wu CW, Bichot NP and Kaas JH. 2000. Converging evidence from microstimulation,

architecture, and connections for multiple motor areas in the frontal and cingulate cortex of prosimian primates. J Comp Neurol 423(1):140-177.

Zeki SM. 1974. Functional organization of a visual area in the posterior bank of the superior temporal sulcus of the rhesus monkey. J Physiol 236(3):549-573.

Zuckerman S and Fulton JF. 1941. The motor cortex in Galago and Perodicticus. J Anat 75(Pt 4):447-456.